



**Loughborough
University**

Bacterial Detection using an Anharmonic Acoustic Aptasensor

by

Shilpa Khobragade

A Doctoral Thesis

Submitted in partial fulfilment of the requirements for the award of
Doctor of Philosophy of Loughborough University

2018

© Shilpa Khobragade 2018

Abstract

Infectious diseases are currently, one of the greatest global challenges in medicine. Rapid and precise diagnosis and identification of pathogen is important for timely initiation of appropriate antimicrobial therapy. However, many patients with infectious diseases receive empirical treatment rather than appropriate pathogen-directed therapy. As a result antimicrobials have been overused and/or misused, which has ultimately led to antimicrobial resistance (AMR). AMR is broadly considered as the most significant public health threat facing the world today. Policy makers from all over the world have recognised the urgent need for rapid point-of-care (POC) diagnostics that would not only identify pathogens but also provide antimicrobial susceptibility profiles in meaningful timeframe to initiate appropriate antimicrobial therapy and thereby, prevent AMR. Traditional culture-dependent diagnostic methods are still considered as gold standard methods. But they are very slow and generally require 18 to 48 hours with further 8 to 48 hours to perform antibiotic susceptibility test. Among culture-independent methods, PCR and ELISA are label-based, costly, laborious and require specialised equipment and trained personnel to operate them. Lateral flow assays (LFAs) that are low-cost, simple, rapid and paper-based portable detection platforms are very popular, as they can be applied at the POC. However, it is difficult to integrate them with electronics and they also suffer from higher false-positive rates than PCR and ELISA. Optical, electrochemical and acoustic biosensor-based methods allow label-free, whole-cell bacterial detection. Among them, a relatively new technique called Anharmonic acoustic Detection Technique (ADT) is integrable and can be applied at the POC for rapid, label-free, low-cost, detection. ADT also allows detection with high specificity, which is lacking in most of the other methods; therefore, it was selected to explore its use for whole-cell bacterial detection. For the first time, ADT was integrated with specific multivalent DNA aptamers that bind whole bacterial cell for direct detection and quantification of viable *E. coli* (KCTC 2571) bacteria. This aptamer-based assay coupled with ADT constituted the anharmonic acoustic aptasensor. DNA aptamers were immobilised through biotin and streptavidin conjugation, onto the gold surface of quartz crystal resonator (QCR) to capture the target bacteria and the detection was accomplished by measuring the shift in the maximum value of magnitude of the transduced $3f$ signal (3 times the drive frequency) i.e. $\Delta|_{3f_{max}}$ upon binding, when driven at fundamental resonance frequency. This aptasensor provides a practical method for rapid, sensitive and quantitative on-site detection of bacteria confidently up to 2.5×10^4 (corresponding to 10^6 E.coli/mL) in 5 min, as compared to standard frequency shift (Δf_0) and dissipation shift (ΔD) measurements. Anharmonic acoustic aptasensor also demonstrated specificity by distinguishing between specific (*E.coli*) and non-specific (*S.typhi*) interactions. Linear quantitative correlation could be reliably achieved with $3f$ signal ($R^2 = 0.984$) for four concentrations of *E.coli* bacteria (10^5 - 10^8 cells/mL), than with Δf_0 and ΔD . Comparative performance of other bio-receptors of different size (anti-E.coli antibody) and different length (shorter linker with thiolated aptamer) was assessed against longer linker with biotinylated aptamer which gave the highest sensitivity and specificity than these two different receptors. To further enhance the sensitivity and specificity of this system, the same *E.coli*-binding aptamers were modified by introducing smart chemical moieties into their structure such that the newly configured aptamer sequences not only quantitatively detected bacteria but also gave characteristic signal, highly specific for that interaction. Thus, this anharmonic acoustic aptasensor can be applied for rapid, sensitive, specific and quantitative detection of whole-cell bacteria and thereby, can reduce diagnostic cycle and improve the appropriate prescribing of antimicrobial therapy and thus can be used to combat AMR.

Keywords: antimicrobial resistance, anharmonic detection, acoustic sensor, aptasensor, rapid point-of-care diagnostics.

Acknowledgements

I would like to express my deep gratitude to my supervisor Dr. Sourav Ghosh for his continuous support in PhD program. He was always there to listen and to give advice. He always encouraged me to explore my own ideas and gave me valuable suggestion when required. His valuable suggestion gave me a very good insight about the mathematics involved in my research problem and the physics behind it. His encouragement and useful suggestions made possible the successful completion of this thesis.

I am also grateful to my second supervisor Dr. Steve Christie and also Dr. Mark Platt for their guidance and support at all levels.

I am also indebted to Prof. David Williams for his guidance and support. His knowledge, patience, understanding made possible the successful completion of this thesis.

I wish to recognise Wolfson School of Mechanical, Electrical and Manufacturing Engineering of Loughborough University for providing the generous financial support without which my postgraduate studies would not have been possible.

I am also thankful to Dr. Igor Efimov and Victor Ostanin for their suggestions for experiments. I would also like to thank Dr. Niklas Sandstrom who designed the microfluidic flow-cell and kindly provided it for conducting experiments.

I would also like to thank Dr. Amit Chandra, Kulvinder Sikand, Tim Coles and Patricia Cropper for technical support.

I am also thankful to many of my colleagues especially Preeti Holland, Carlos Granja, Sam Swarbrick, Stavros Yika, Saba Meshksar and Arnab Guha for their support from Healthcare engineering research group.

Finally, I would like to thank my parents, sister and husband for their continual support during my post graduate years of study.

Abbreviations

ADE	:	Antimicrobial de-escalation
ADT	:	Anharmonic acoustic Detection Technique
AMR	:	Antimicrobial resistance
ASPs	:	Antimicrobial Stewardship Programs
AST	:	Antimicrobial Susceptibility Test
ATCC	:	American Type Culture Collection
BAW	:	Bulk Acoustic Wave
BRICS	:	Brazil, Russia, India, China and South Africa
BVD	:	Butterworth-Van Dyke
CDC	:	Centers for Disease Control and Prevention
COSHH	:	Control of Substances Hazardous to Health
DNA	:	Deoxyribonucleic Acid
ELFA	:	Enzyme-linked fluorescent assay
ELISA	:	Enzyme-Linked Immunosorbant Assay
EIA	:	Enzyme immunoassay
FDA	:	Food and Drug Administration
GAP	:	Global Action Plan
GDP	:	Gross Domestic Product
GLASS	:	Global Antimicrobial Resistance Surveillance System
HICs	:	High-income countries
HRP	:	Horseradish peroxidase
IDSA	:	Infectious Diseases Society of America
IgG	:	Immunoglobulin G
IMI	:	Innovative Medicines Initiative
IPA	:	Iso-propyl Alcohol

IUPAC	:	International Union of Pure and Applied Chemistry
IVD	:	In-vitro Diagnostics
KTH	:	Kungliga Tekniska högskolan
LAMP	:	Loop-mediated isothermal amplification
LFA	:	Lateral flow assay
LFI	:	Lateral flow immunoassay
LMICs	:	Low- and middle-income countries
LSPR	:	Localised Surface Plasmon Resonance
MALDI-TOF-MS	:	Matrix-assisted laser desorption/ionization time-of-flight mass spectrometry
µg	:	Microgram
µl	:	Microliter
µm	:	Micrometer
M	:	Molar
mcr-1	:	mobilised colistin resistance-1
MDR	:	Multidrug-resistant
min	:	Minute
ml	:	Milliliter
mm	:	Millimeter
mM	:	Millimolar
MHz	:	Mega Hertz
mPCR	:	multiplex Polymerase Chain Reaction
NASBA	:	Nucleic acid sequence-based amplification
NDM-1	:	New Delhi metallo-beta-lactamase 1
NDA	:	New drug application
nm	:	nanometer

PACCARB	:	Presidential Advisory Council on Combating Antibiotic-Resistant Bacteria
PBS	:	Phosphate Buffer Saline
PCR	:	Polymerase Chain Reaction
POC	:	Point-of-care
POCT	:	Point-of-care test
PQR	:	Piezoelectric Quartz Resonator
PSA	:	Potential Stripping Analysis
QCM	:	Quartz Crystal Microbalance
QCR	:	Quartz Crystal Resonator
qPCR	:	quantitative/real Polymerase Chain Reaction
REVS	:	Rupture Event Scanning
RI	:	Refractive index
RLC	:	Resistor, inductor, capacitor,
RNA	:	Ribonucleic acid
SAM	:	Self-Assemble Monolayer
SAW	:	Surface Acoustic Wave
SCPM	:	Streptavidin-Coated Polystyrene Microbeads
SDRI	:	Solutions to Drug-Resistant Infections
SELEX	:	Systemic Evolution of Ligands by Exponential Enrichment
SNR	:	Signal-to-Noise Ratio
SPR	:	Surface Plasmon Resonance
SYBR	:	Synergy Brands, Inc. (<i>stock symbol</i>)
TB	:	Tuberculosis
TSM	:	Thickness Shear Mode

UK	:	United Kingdom
URTIs	:	Upper respiratory tract infections
US	:	United States
VNBC	:	Viable but non-culturable
WHA	:	World Health Assembly
WHO	:	World Health Organization
XDR	:	Extensively drug-resistant
XPS	:	X-ray photoelectron spectroscopy

Publications

Khobragade, S., Swarbrick, S., Gruia, V., Efimov, I., Ispas, A., Ostanin, V., Bund, A. and Ghosh, S. (2017). Detection of flexibly bound adsorbate using the nonlinear response of quartz crystal resonator driven at high oscillation amplitude. *Electrochimica Acta*, 252, pp.424-429.

Khobragade, S., Sandstrom, N., Granja, C., Efimov, I., Ostanin, V., Wijngaart, W., Klenerman, D., and Ghosh, S. (2017). "Rapid, label-free, direct detection and quantification of *Escherichia coli* bacteria using nonlinear acoustic aptasensor," accepted for oral presentation in 19th International Conference on Nanobiotechnology and Biosensor, London, UK May 25-26, 2017 (peer-reviewed).

Table of Contents

Abstract.....	i
Acknowledgements	ii
Abbreviations	iii
Publications.....	vii
Table of Contents.....	viii
Chapter 1 Introduction.....	13
1.1 General Introduction	13
1.2 What is antimicrobial resistance?.....	13
1.2.1 The global problem of antimicrobial resistance	14
1.2.2 Emergence of antimicrobial resistance	19
1.2.3 Factors driving AMR.....	20
1.3 Global policy response to AMR.....	25
1.4 Tackling AMR through rapid diagnostics	27
1.5 Unmet diagnostic needs	28
1.6 Problem statement.....	30
1.6.1 Aim.....	30
1.6.2 Objectives	30
1.7 Dissertation Organization.....	31
Chapter 2 Literature review	33
2.1 Introduction.....	33
2.2 Background	33
2.3 Culture-dependent diagnostic methods.....	34
2.4 Culture-independent diagnostic methods.....	36
2.4.1 Nucleic acid-based methods.....	36
2.4.2 Immunological-based methods.....	38
2.4.3 Mass spectrometry-based methods.....	41
2.4.4 Biosensor-based methods.....	42

2.4.4.1	Transduction methods	44
2.4.4.2	Bio-receptors	53
2.5	Target bacteria.....	54
2.6	Summary	54
Chapter 3	Experimental considerations and methodology.....	56
3.1	Introduction.....	56
3.2	Transduction system: Concept and Experimental apparatus.....	56
3.2.1	Anharmonic acoustic Detection Technique (ADT)	56
3.2.2	Quartz crystal resonator (QCR) with gold electrodes.....	58
3.2.2.1	Energy trapping concept.....	62
3.2.2.2	Preparing the stepped (non-uniform) crystals	63
3.2.2.3	Demonstration of energy trapping with ADT	65
3.2.3	Transduction system check-up	67
3.2.4	Selection of mode of scan for experiments	70
3.2.5	Surface cleaning of gold electrodes.....	73
3.2.6	Experimental apparatus.....	80
3.2.6.1	Instrumental set-up.....	80
3.2.6.2	Microfluidic set-up	82
3.3	Linking bio-receptor with the transduction system.....	83
3.3.1	Formation of Self Assembled Monolayer (SAM) on gold electrode	83
3.3.2	Streptavidin Biotin interaction	85
3.3.3	Immobilisation of bio-receptor on the gold electrode.....	86
3.4	Stability of baseline measurements of transduction system	86
3.5	Summary	87
Chapter 4	Detection of bacteria using anharmonic acoustic aptasensor.....	88
4.1	Introduction.....	88
4.2	Background	88
4.3	Aptamers as bio-receptor.....	89
4.4	Aptamer for <i>E.coli</i> bacteria.....	94

4.5 Binding experiment	96
4.6 Linking the bio-receptor to the QCR	99
4.6.1 Cleaning the surface of gold electrode	99
4.6.2 Formation of self-assembled monolayer (SAM)	99
4.6.3 Deposition of Streptavidin.....	100
4.6.4 Immobilisation of bio-receptor on the gold electrode of QCR	100
4.7 Step-wise characterisation	100
4.8 Determination of drive amplitude.....	103
4.9 Detection of <i>E.coli</i> bacteria with anharmonic acoustic aptasensor	105
4.10 Quantitative analysis	111
4.11 Specificity analysis.....	112
4.10 Summary	113
 Chapter 5 Detection of bacteria using bio-receptors of different size and length integrated with ADT.....	
5.1 Introduction.....	115
5.2 Background	115
5.3 Comparison of aptasensor with immunosensor.....	116
5.4 Linking the antibodies to the QCR.....	116
5.4.1 Cleaning the surface of gold electrode	116
5.4.2 Formation of self-assembled monolayer (SAM)	116
5.4.3 Deposition of Streptavidin.....	117
5.4.4 Immobilisation of bio-receptor on the gold electrode of QCR	117
5.5 Determination of drive amplitude.....	118
5.6 Detection of <i>E.coli</i> bacteria with polyclonal antibodies	119
5.7 Comparison of the length of the linker (long vs short)	123
5.8 Linking the thiolated aptamer to the QCR	125
5.8.1 Cleaning the surface of gold electrode	125
5.8.2 Immobilisation of thiolated DNA aptamer.....	125
5.9 Determination of drive amplitude.....	127
5.10 Detection of <i>E.coli</i> bacteria with thiolated aptamer	128

5.11 Comparison of 3f signals with different bio-receptors	131
5.12 Summary	133
Chapter 6 Investigating novel mechanical designs of aptamer receptor for detection of bacteria using nonlinear acoustic biosensor	135
6.1 Introduction	135
6.2 Background	135
6.3 Modified aptamer sequences – novel mechanical designs.....	137
6.4 Hybridisation of aptamer sequences	139
6.6.1 Cleaning the surface of gold electrode	145
6.6.2 Formation of self-assembled monolayer (SAM)	145
6.6.3 Deposition of Streptavidin.....	145
6.6.4 Immobilisation of bio-receptor on the gold electrode of QCR.....	146
6.7 Determination of drive amplitude.....	146
6.9 Selection of aptamer configuration for <i>E.coli</i> detection.....	147
6.10 Detection of <i>E.coli</i> bacteria using aptamer configuration unzip	150
6.10 Summary	158
Chapter 7 Summary of conclusions and Future work	159
7.1 Introduction.....	159
7.2 Summary of contributions and conclusions of the work.....	159
7.2.1. Addressed the experimental challenges with the integrated biosensor assay	161
7.2.2. Anharmonic acoustic aptasensor enables detection of <i>E.coli</i> bacteria	163
7.2.3 Comparative performance of different bio-receptors integrated with ADT for detection of bacteria	165
7.2.4 Novel aptamer configurations enabling highly specific detection of bacteria	166
7.3 Potential impact through future research.....	167
7.3.1 Exploring detection of other pathogens	167
7.3.2 Exploring other diagnostic methods.....	167
7.3.3 Investigating QCRs with lower resonant frequency.....	167

7.3.4 Improving microfluidics for <i>in-situ</i> pathogen identification and AST.....	167
7.3.5 Modification of the aptamers to enable multiplex detection	168
7.4 Considerations for ‘Anharmonic acoustic aptasensor’ as POCT	168
References:.....	171

Chapter 1 Introduction

1.1 General Introduction

Infectious diseases continue to be a global public health problem, despite the advancement in knowledge of infectious diseases, improved sanitation, effective vaccines and antimicrobial drugs.^[1] Rapid and accurate identification of microbial cause is vital while caring for an individual patient with an infectious disease or even while responding to a worldwide pandemic. This improves clinical outcome, reduces recovery time and healthcare costs. Many patients with infectious diseases receive empirical treatment rather than appropriate therapy dictated by the rapid identification of the infectious agent. As a result antimicrobials have been overused and/or misused, which has ultimately led to antimicrobial resistance (AMR).^[2] AMR is a serious and ever-increasing threat to global public health that requires intensive and collective action across all government sectors and society.^[3] This chapter begins with description of the AMR problem and how it is endangering the global health, its emergence and also the factors driving AMR. This section is described in detail in order to give background information and motives for this research. Following this, the approach of policy makers from all over the world to this emerging problem of AMR is specified, recognising the urgent need for rapid point-of-care (POC) diagnostics to combat AMR. The role of rapid diagnostics in fighting AMR and their unmet needs are also listed, guiding the course of this research. Subsequently, the specific aim and objectives of this research are highlighted in the order in which the thesis chapters are presented. Finally, the chapter ends with the description of the thesis structure.

1.2 What is antimicrobial resistance?

The WHO defines AMR as a microorganism's (such as bacteria, fungi, viruses, and parasites) resistance to antimicrobial drugs (such as antibiotics, antifungals, antivirals, antimalarials, and anthelmintics) that were once able to treat an infection by that microorganism. AMR is a broader term and includes the more specific "antibiotic resistance", which applies only to bacteria becoming resistant to antibiotics.^[3]

1.2.1 The global problem of antimicrobial resistance

AMR is widely recognised as the most significant public health threat facing the world today. Many experts around the world have used appalling language in describing the range of challenges posed by AMR. But such a description is pertinent as AMR is a worldwide challenge associated with high morbidity and mortality, threatening the ability of modern medicine to treat common infectious diseases.^[4] In the words of England’s Chief Medical Officer, Prof Dame Sally Davies: “The world is facing an antibiotic apocalypse.” At the recent Solutions to Drug-Resistant Infections (SDRI 2017) conference, she warned that if antibiotics lose their effectiveness it will spell “the end of modern medicine” and urged world leaders to address the growing threat of AMR.^[5] Prior to this, in July 2014, a review on AMR was commissioned by the then Prime Minister of the United Kingdom (UK), who had asked economist Lord Jim O’Neill to analyse the global problem of rising drug resistance. This review estimated that if nothing is done to control AMR, there will be 10 million deaths a year and up to \$100 trillion lost to the global economy by 2050 (Fig. 1.1).^[6]

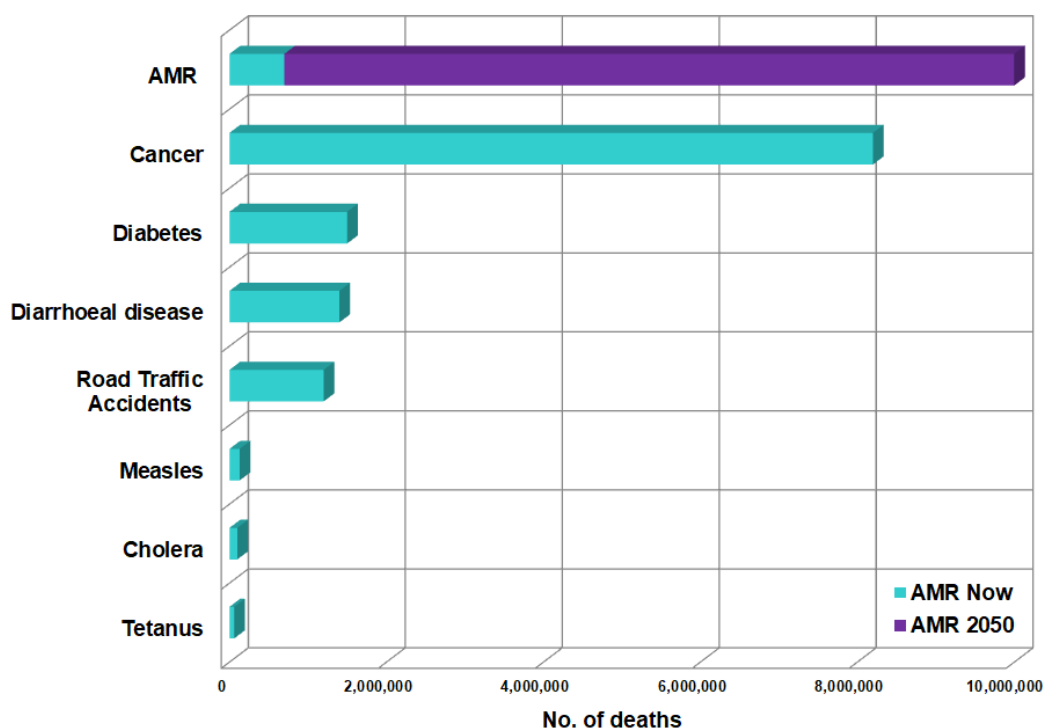


Fig. 1.1 - Deaths attributable to AMR every year compared to other major causes of death. Adapted and modified from ^[6,7].

It also predicted that if the current resistance rates increased by 40%, the region with the highest number of deaths attributable to AMR by 2050 would be Asia with 4.7 million followed by Africa with 4.1 million, while there would be 390,000 deaths in Europe and 317,000 in the United States (US) (Fig. 1.2).^[6,7] Although, the results from these burden reports were ridiculed as “broad brush estimates”, they highlighted the gravity of the incipient problem and the need for more comprehensive population-based AMR surveillance data.^[8] Nonetheless, another analogous report published by Centers for Disease Control and Prevention (CDC) estimated that in the US more than 2 million people acquire serious infections with antibiotic resistant microbes and at least 23,000 people die per year due to these infections. Even though, the total economic cost of AMR to the US economy has been difficult to calculate, CDC estimated direct costs of AMR to be \$20 billion, with a further \$35 billion in productivity costs.^[9] In Europe as well, AMR is estimated to be responsible for 25,000 deaths per year and about 700,000 deaths per year globally. In Europe alone, historical estimates from 2009 suggest a direct and indirect cost of €1.5 billion annually in healthcare costs and productivity losses.^[10]

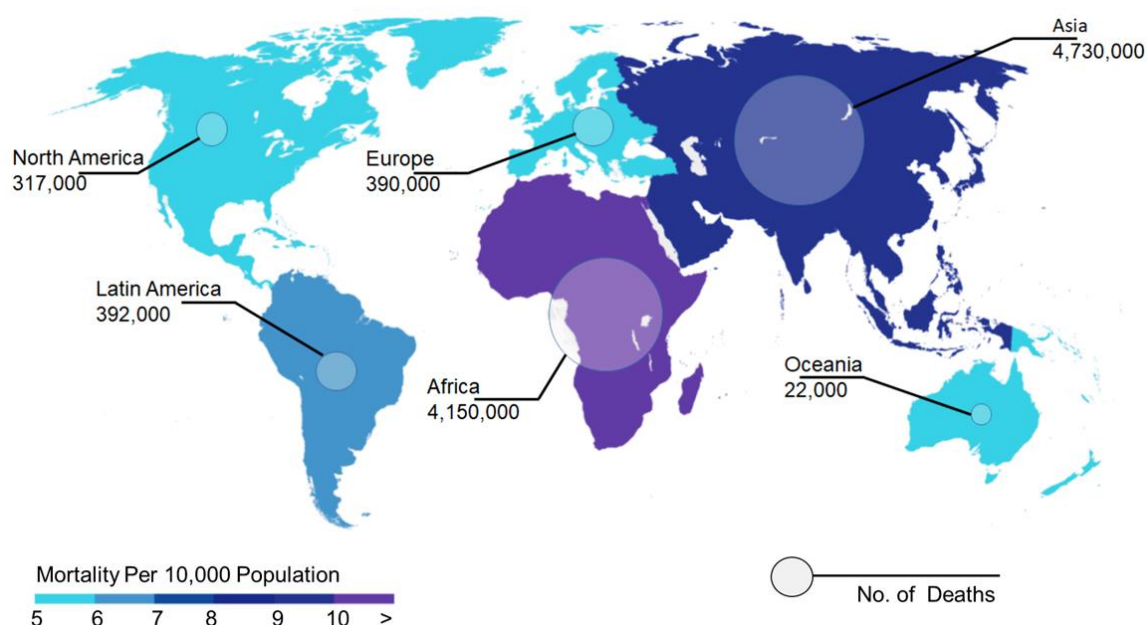


Fig. 1.2 – Estimated deaths attributable to AMR every year by 2050. Adapted and modified from ^[7].

According to a recent report by the World Bank Group, by 2050 AMR could cause global economic damage as large as the losses caused by the 2008 financial crisis. This report also projected that a high AMR-impact scenario could cause low-income countries to lose more than 5% of their Gross Domestic Product (GDP) and push up to 28 million people, mostly in developing countries, into poverty by 2050 (as shown in Fig. 1.3). Moreover, unlike the financial crisis of 2008, there would be no prospects for a cyclical recovery in the medium term, as the costly impact of AMR would persist.^[11] Also, the costs of some of the methods to contain AMR differ widely across countries, especially for infectious diseases like Tuberculosis (TB) which can become multidrug-resistant (MDR) or extensively drug-resistant (XDR) strains. MDR-TB and XDR-TB infections are far more expensive to treat than drug-susceptible TB. Figure 1.4 shows the cost variances in treating TB, with and without AMR. Because of the costs of medical personnel and supplies are much higher, it is much more expensive to cure infectious diseases in high-income countries (HICs) than in low- and middle-income countries (LMICs). Consequently, it costs 80 times more to treat one TB patient in the US than in India (Fig. 1.4).^[11]

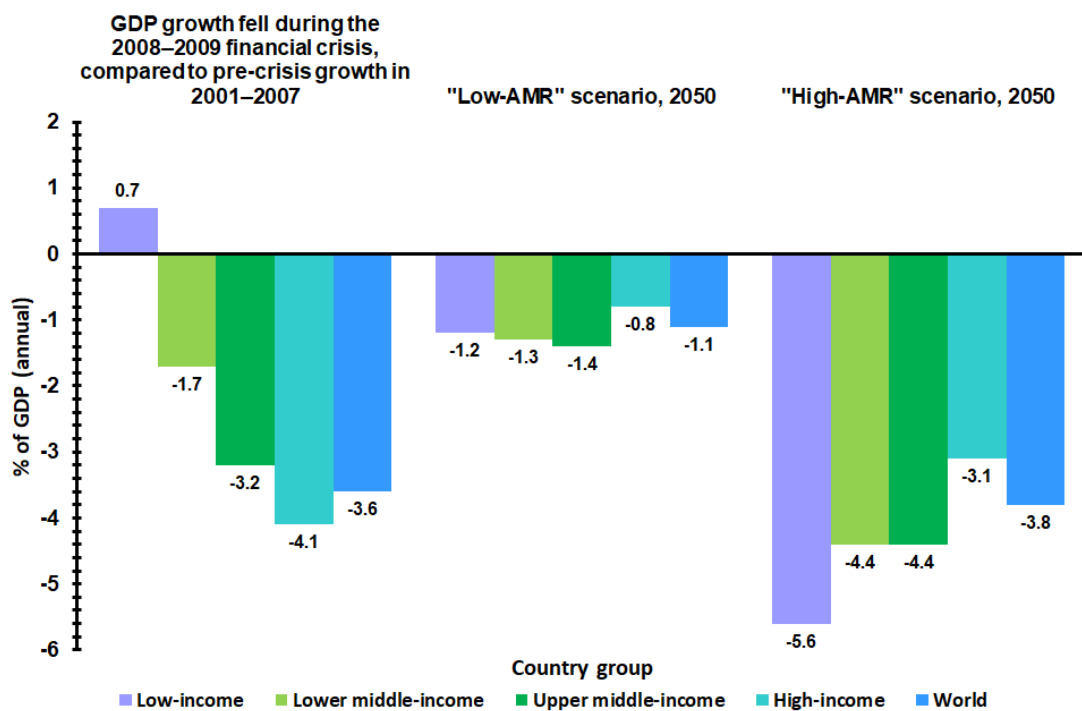
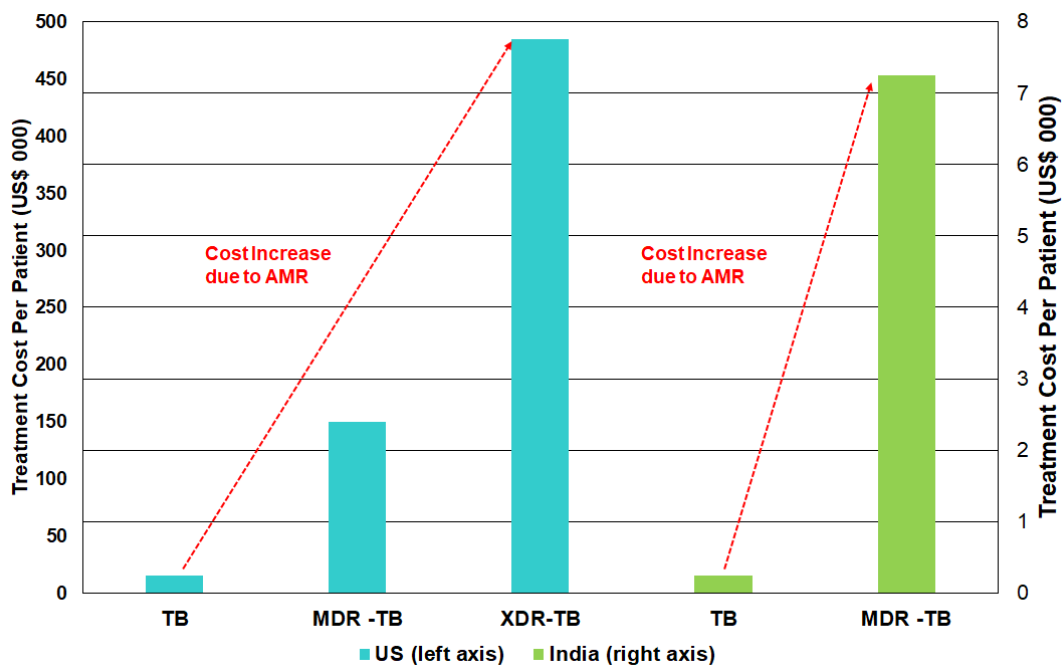


Fig. 1.3 – AMR-impact scenarios on GDP by 2050 (as projected by World Bank Group). Adapted and modified from ^[11].



TB = Tuberculosis (infectious disease caused by bacteria)
 MDR = Multidrug-resistant
 XDR = Extensively drug-resistant

Fig. 1.4 – AMR makes TB far costlier to treat. TB treatments costs are much higher in HICs than in LMICs (e.g., 80x higher for TB – and 20x higher for MDR-TB – in the US than in India. Adapted and modified from [11].

Recently, there has been an upsurge in global connectivity due to increasing global trade, growing human and animal populations, and technological developments. Consequently, there has been upward trend in rapid transport of antimicrobial resistant microbes and their resistant genes, thereby spreading AMR at an alarming rate. There is also impending danger of rapid rise in cases over a short timescale, if AMR may act as a compounding factor in a pandemic infection (e.g., influenza), it would then contribute to overall death and disability on a sudden and large scale.^[12] AMR phenomenon has thus become a global concern, as its impact on a pandemic infection may have catastrophic results. Moreover, microbes do not respect geographic borders, the rapidity with which new types of AMR can disseminate globally following their initial emergence or recognition is demonstrated by the novel carbapenemase New Delhi metallo-beta-lactamase 1 (NDM-1). The spread of NDM-1 (as presented in Fig. 1.5) demonstrates that AMR is a public health problem that surpasses national borders and will require international cooperation between health authorities if it

is to be controlled.^[7,13] Also, the emergence and spread of mobilised colistin resistance-1 (*mcr-1*) gene (Fig. 1.6) is a matter of concern as it confers resistance to colistin, a last-resort antibiotic used for treating Gram-negative infections.^[14] Also, the report issued by CDC on the case of a 70-year-old Nevada woman who died of an incurable infection in 2016, resistant to all 26 different antibiotics in the US, highlights the severity and magnitude of AMR problem.^[15]

Spread of NDM-1 (2009-2011)

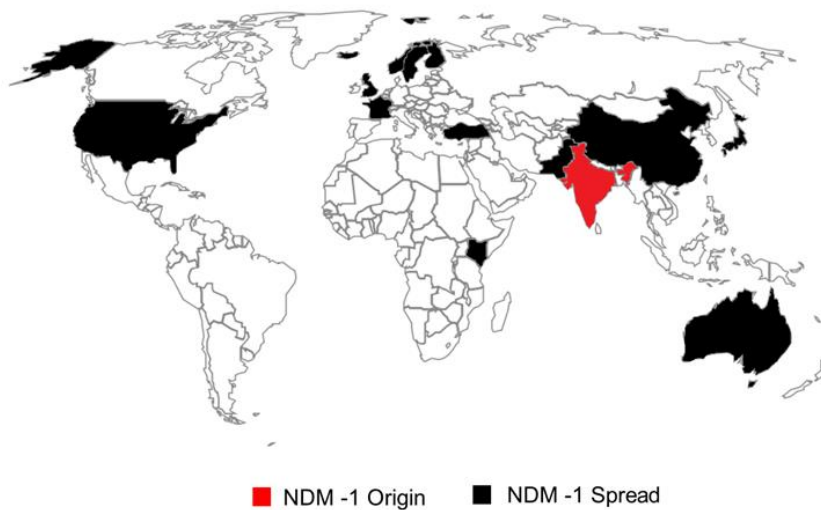


Fig. 1.5 - The spread of NDM-1 resistance across the world. Adapted and modified from ^[13].

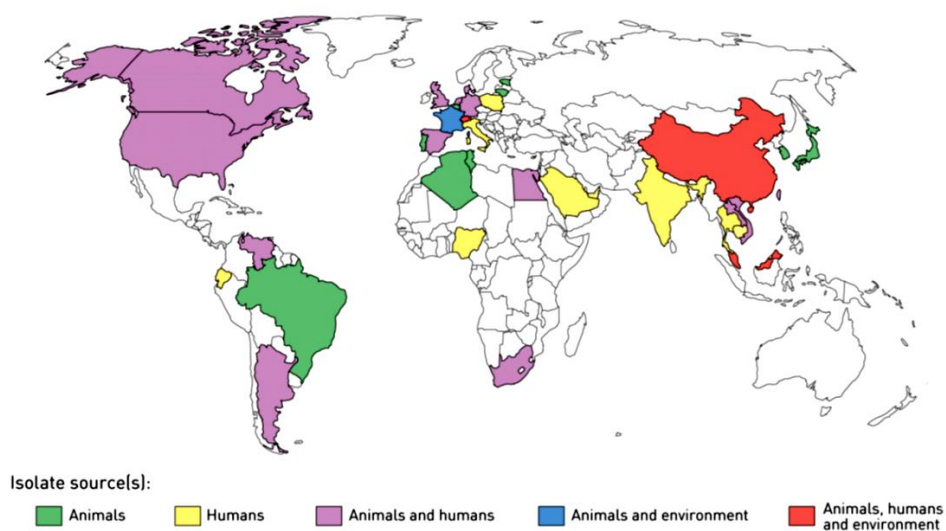


Fig. 1.6 - Countries reporting plasmid-mediated colistin resistance conferred by *mcr-1*. Adapted and modified from ^[14].

1.2.2 Emergence of antimicrobial resistance

Lately, AMR problem has been highly publicised with panic headlines using media-coined term “superbug” for the drug-resistant bacteria, but this problem itself is nothing new.^[16] AMR has a longer history than the modern use of antibiotics. It is a perception that exposure to antibiotics occurred in the modern “antibiotic era,” but research has revealed that the presence of antibiotic resistance genes dates back to between 10,000 and 2 billion years ago, as a response to the naturally occurring antibiotics in the environment.^[17] However, the beginning of so-called “antibiotic era” can be attributed to the period when the first antibiotic, “penicillin”, was serendipitously discovered by Sir Alexander Fleming in 1928.^[18,19]

Fleming was recognised for his achievements and he received the Nobel Prize for Physiology in 1945 along with his co-laureates, Sir Howard Florey and Dr. Ernst Chain, two Oxford based researchers who later devised a method of mass-production of this drug for commercial use. This discovery revolutionised the field of medicine and mankind believed that it had overcome the problem of bacterial infections. But Fleming had already predicted that penicillin would be used carelessly and over time become less effective at killing bacteria. At the end of his Nobel lecture he said, “There is the danger that the ignorant man may easily underdose himself and by exposing his microbes to non-lethal quantities of the drug make them resistant”.^[18]

Penicillin was successfully used in controlling bacterial infections among World War II soldiers.^[20] But true to Fleming’s prophecy, by the mid-1940s, after its introduction into clinical practice, penicillin resistance began to emerge because of its wide-scale use.^[21] This fostered development of new and better drugs in response to the inchoate AMR problem. The following period between 1950 and 1960 is often referred to as the golden era of antimicrobial discovery, and sometimes also as the halcyon years, when most of the antimicrobials used today were discovered.^[22]

But nearly all antimicrobial drugs developed so far were followed by the detection of resistance.^[23] Also, the triumphs in the golden era were soon followed by a considerable hiatus as there have been no successful discoveries

of novel agents after 1987, but only variations in existing drugs.^[24] This problem of “innovation gap” is further escalated by a discovery void in terms of antimicrobials with novel mechanisms of action that could primarily overcome resistance.^[24] Due to this imminent AMR problem, simple treatable infections pose a serious challenge for modern medicine, as they can soon be converted into untreatable deadly infections.^[25]

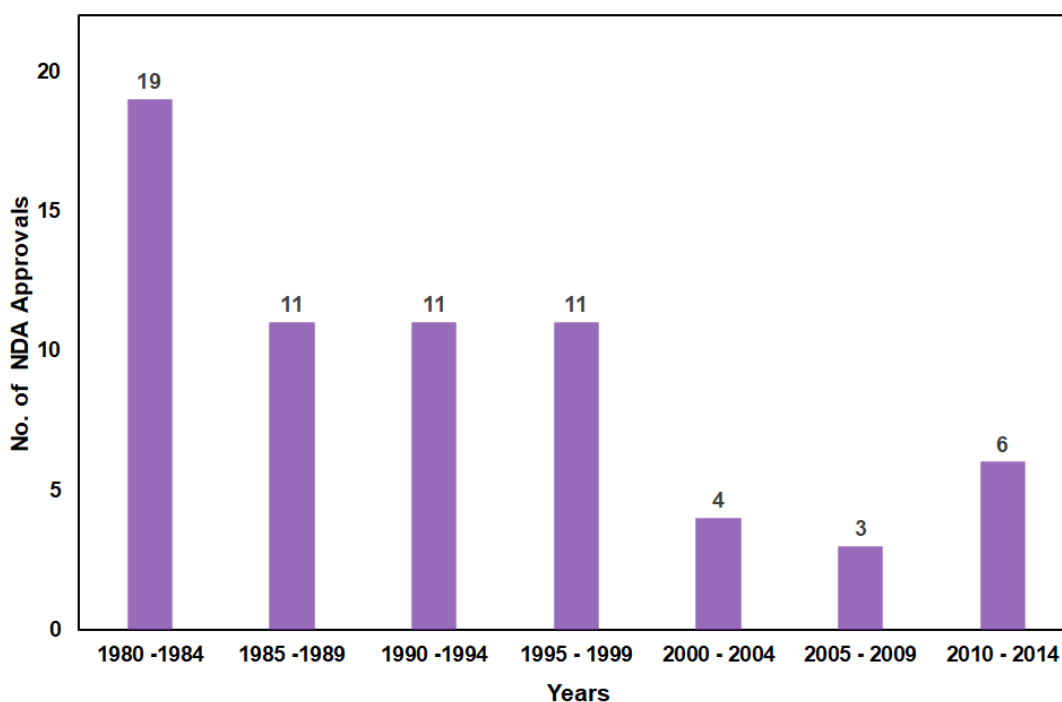
1.2.3 Factors driving AMR

To battle antimicrobial resistance, which is the biggest threat to human health, an understanding of its drivers is needed. There are several factors causing antimicrobial resistance, as outlined and described below:^[19,26,27]

- a. Lack of availability of new antimicrobial drugs
- b. Antimicrobial misuse or overuse
- c. Inappropriate prescription
- d. Sub-optimal diagnostics
- e. Patient perception and behaviour
- f. Poor-quality medicines
- g. Other factors

a. Lack of availability of new antimicrobial drugs

The number of new antimicrobial drugs developed and approved has decreased steadily over the past 30 years due to economic and regulatory barriers (Fig. 1.7), leaving fewer options to treat resistant bacteria.^[19] Many big pharmaceutical companies have given up antimicrobial research because of these obstacles, adversely affecting antimicrobial drugs pipeline.^[28] Antimicrobial resistance occurs as part of a natural evolution process in which microbe evolves, so the resultant AMR crisis can only be slowed but not stopped. Therefore, there is exigent need for new antimicrobial drugs as well as well as, new diagnostic tests to track the development of resistance.^[29]



*Antibacterial drugs are limited to systemic agents.

Fig. 1.7 - Number of Antibacterial New Drug Application (NDA) Approvals versus Year Intervals. Adapted and modified from ^[19].

b. Antimicrobial misuse or overuse

Livestock animals are frequently given antimicrobial drugs for disease prevention and growth promotion, which are ultimately transferred to the humans through meat, and even via their manure which is used as crop fertiliser. Antibiotic use in animals, agriculture and aquaculture, actually, account for about 80% of all in the US, so it's indisputably a *main* source of human antibiotic consumption (as shown in Fig. 1.8).^[30] Due to poor surveillance data in many other countries, the estimate of total global antibiotic consumption in agriculture vary, ranging from around 63,000 to over 240,000 tonnes, and is anticipated to increase by 67% from 2010 to 2030, with 99% increase amongst the BRICS countries (Brazil, Russia, India, China and South Africa) in that same time period.^[31] More than 70% of the antibiotics considered medically important for human health by the FDA and sold in the US (and >50% in most countries) are used in livestock. Antibiotics doses used in aquaculture are often higher than those in livestock and mostly remain in fish products as residues and also aquatic

environment. Amount of antibiotics used for crops is relatively lower than used in livestock, and does not require immediate attention, but the quantity of antibiotic use in the larger food chain needs close monitoring with mounting AMR concern. Also, a direct correlation between higher antibiotic consumption and prevalence of AMR has been seen in many studies conducted in industrialised countries.^[32,33]

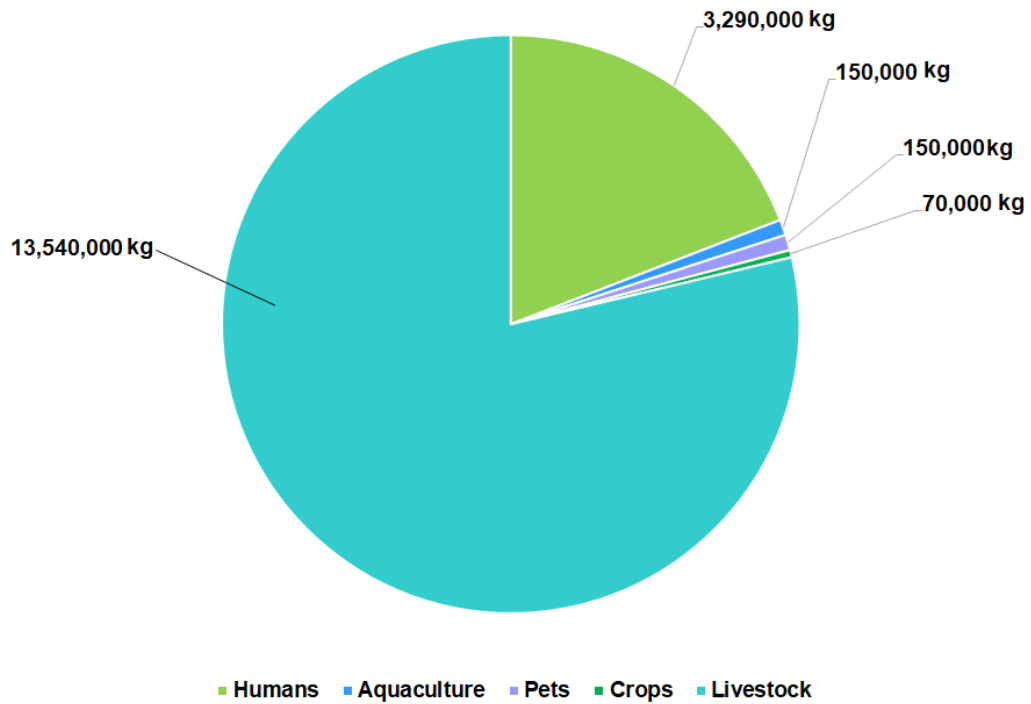


Fig. 1.8 - Estimated Annual Antibiotic Use in the United States. Adapted and modified from ^[30].

c. Inappropriate prescription

Antimicrobial drugs are among the most commonly prescribed drugs and almost half of them are not optimally prescribed.^[9] A review of patient data by CDC found that 30% of the prescriptions are unnecessary and huge amount of antimicrobial drugs are wasted globally.^[29] There are several factors that influence prescribing, including sociocultural, socio-economic factors, and cultural beliefs of both the physician and the patient.^[34] Inappropriate prescribing has been ascribed to a number of causes, including patient’s demand for antibiotics,^[35] unjustified prescription especially, for upper respiratory tract infections (URTIs) even though antibiotics are useless against viruses;^[36] under-prescription, for example, in

urinary tract infections; under-dosing, and short duration.^[37] Sub-inhibitory and sub-therapeutic antibiotic concentrations contribute to AMR by supporting genetic alterations in bacteria such as *Pseudomonas aeruginosa* and *Bacteroides fragilis*.^[19] The timing of initiation of antibiotic therapy is also important. Many times antibiotic therapy is initiated prematurely by physicians, in clinically stable patients. Also, in critically ill patients, antibiotic therapy is initiated by physicians mostly based on empirical diagnosis, due to lack of rapid diagnostic tools required for quickly arriving at definitive diagnosis. Moreover, broad-spectrum antibiotics are often prescribed by physicians as initial therapy, to cover a number of possible causative pathogens of that clinical presentation. Thus, in order to reduce AMR, it is important that physicians understand the difference between empiric and definitive therapy; identify opportunities to switch to narrow-spectrum antibiotics and diagnose accurately with the help of rapid diagnostic tools.^[38]

d. Sub-optimal diagnostics

Many experts consider sub-optimal diagnostics as the high driver of AMR. In spite of this, innovation in the field of diagnostics has been very slow, and many pharmaceutical companies have no interest in the advent of rapid diagnostics, that would decrease inappropriate prescription of antibiotics. As there is growing demand for diagnostic precision that can modify the widespread empiric antimicrobial use; there is need for development of rapid, reliable diagnostic methods for identifying the presence of infection, the specific infecting organism, and the susceptibility of the microbe to various therapeutic agents. It is well established that rapid diagnostic tests have a critical role to play, as they improve the efficiency of health care spending by guiding physician decision-making. They are also the foundation of disease surveillance and elimination. But, paucity of optimal diagnostics together with lack of interconnected diagnostic networks further augments the AMR problem.^[39,40]

e. Patient perception and behaviour

Knowledge about appropriate antibiotic prescription is lacking in most of the patients especially, for infections like URTIs.^[41] It is a common perception of patients that an antibiotic is a quick and effective antidote to most of their ailments. Consequently, physicians repeatedly experience pressure from patients to prescribe them.^[42,43] But treatment non-adherence to the prescribed antibiotic course is a shared trait of most of the patients and often the remaining unused pills of the course are “hoarded” by them for future use; thereby increasing the chances of misusing them later against non-susceptible organisms and consequent treatment failures.^[44] In many countries, multiple sources are sought by patients for the same illness and this problem is further escalated by the availability of wide variety of unregulated antibiotics without prescription, promoting overuse.^[44,45] The ability to purchase such antibiotics online has also made them available in countries where antibiotics are regulated.^[42] Also, there are many self-medicating patients that buy antibiotics over-the-counter (OTC) directly from pharmacists. Availability of new rapid diagnostics can facilitate pharmacists to provide a full and confident diagnosis at point of sale, without the need for a prescription from a physician.

f. Poor-quality medicines

Dissemination of poor-quality medicines including, falsified (i.e., intentional fraudulent manufacturing) or substandard (i.e., unintentional errors in manufacturing or degradation because of poor storage/handling) products pose a major obstacle to the treatment of many diseases.^[46,47] The inadvertent use of poor-quality medicines is likely to be one of the key factors contributing to AMR. By delivering sub-therapeutic drug concentrations, poor-quality medicines may promote the selection of drug resistance. Antimicrobials, particularly anti-malarial drugs, are susceptible targets and among the most common classes of drugs associated with quality concerns.^[48] Over 120,000 deaths among children younger than 5 years were reported, in 39 countries in sub-Saharan Africa, due to consumption of poor-quality anti-malarial medicines.^[49]

g. Other factors

Antimicrobial resistance selection process has been driven by antimicrobial exposure in health care setting and also the environment. Ongoing transmission of AMR is affected by many other factors such as, travel, migration, and standards of infection control, sanitation, and access to clean water, etc.

In a nutshell, of all the factors fuelling antimicrobial resistance, inappropriate use of antimicrobials is driving the emergence of AMR globally, and is also decreasing the usefulness of the few treatment options left to treat microbial illnesses. But lack of rapid POC diagnostic tests is the crux of the AMR problem, as unnecessary use of antibiotics is largely fostered by diagnostic uncertainty. Therefore, AMR problem can be controlled to great extent, if rapid diagnostic tests are made available for pathogen identification and also determination of their susceptibility to antimicrobials; as this will facilitate appropriate prescription and reduce the chances of development of drug-resistant or multidrug-resistant infectious diseases.

1.3 Global policy response to AMR

In April 2014, the WHO issued its first global report on AMR, in which they highlighted AMR as a “serious, global threat”.^[23] In July 2014, the UK Prime Minister commissioned an internationally renowned economist Lord Jim O’Neil to lead an independent review on AMR. This was co-founded and hosted by Wellcome Trust.^[6,7] Same year, in the month of September, US President signed an Executive Order and also declared 5 year plans to combat the AMR problem, both at national and international level.^[50] In October 2014, Europe’s Innovative Medicines Initiative (IMI) under its ‘New Drugs for Bad Bugs’ programme, a major public-private partnership effort, launched the DRIVE-AB project to promote responsible use of antibiotics and development of new economic models of antibiotic research and development.^[51]

The following year in Mar 2015, the White House in US published the “National Action Plan for Combating Antibiotic-Resistant Bacteria” and defined its number one goal as: “to slow the emergence of resistant bacteria through the judicious

use of antibiotics”.^[50] In May 2015, the World Health Assembly (WHA) of WHO endorsed a Global Action Plan (GAP) to tackle antimicrobial resistance, including antibiotic resistance, which is the most urgent drug resistance trend.^[52] A year later, in May 2016, Lord Jim O’Neil presented ten key elements to tackle AMR in a global way.^[6] In September 2016, global leaders met at the United Nations General Assembly in New York to commit to fighting antimicrobial resistance together; this boosted the worldwide action to control AMR. Meanwhile, the WHO continued to facilitate execution of the GAP through numerous meetings across the world in 2017.^[53] Also in May 2017, the US Presidential Advisory Council on Combating Antibiotic-Resistant Bacteria (PACCARB) held a two-day meeting discussing how labelling changes can be used to narrow the use of medically important antimicrobial drugs in food-producing animals.^[54] The National Action Plan that was initiated in 2015 released a report, emphasizing that strategies should ensure patients receive the “right antibiotic at the right time at the right dose for the right duration”. Based on this report, in 2017, Congress appropriated \$163 million for CDC to continue to fight AMR via the Antibiotic Resistance Solutions Initiative, which speaks to the seriousness of the problem.^[55] One of the main goals of the National Action Plan included development of Antimicrobial Stewardship Programs (ASPs) to primarily address inappropriate antimicrobial use and decrease drug resistance. The WHO has also developed the Global Antimicrobial Resistance Surveillance System (GLASS) to support the implementation of the GAP, which promotes and facilitates standardised AMR surveillance worldwide. The WHO *GLASS Manual for Early Implementation* provides details of the proposed approach and defines targets for the surveillance of resistance in common bacterial pathogens. As an accompaniment to the manual, a guide also has been developed to support the practice of robust microbiological diagnosis, including Antimicrobial Susceptibility Testing (AST), in patients presenting with clinical symptoms compatible with infectious diseases; a concept known as “diagnostic stewardship”. As part of a broader antimicrobial stewardship programs, diagnostic stewardship is aimed at reducing false-positive testing results, which can lead to overuse of antibiotics, and enhancing the detection of true-positive cases of infection for appropriate treatment. Effective ASP is closely related with

the ability to make correct and rapid diagnoses. Through careful diagnostic and antimicrobial stewardships, rapid diagnostics can be implemented successfully, revolutionizing the clinical care of patients.^[56,57]

1.4 Tackling AMR through rapid diagnostics

Antimicrobial de-escalation (ADE) has been widely accepted and recommended as an important strategy for addressing the global AMR crisis.^[58] ADE has been defined in numerous ways across studies, but in general it refers to the reduction in the use of broad-spectrum antibiotics through discontinuation of antibiotics or switching to a narrower spectrum agent when clinically possible, based on the sensitivity profile obtained from the antibiogram, thereby decreasing the risk of bacterial resistance.^[58] Although ADE is profoundly considered as key factor of controlling AMR, it is very challenging due to various reasons, including problem of comparability and reproducibility due to its inconsistent definition, overt reliability on clinical judgement, and lack of evidence supporting it.^[58,59] But above all, one of the main problems in creating reliable systems for ADE is due to the limitations with our current diagnostic testing. However, emerging technologies in the field of rapid diagnostics may augment ADE strategies and provide new prospects for stewardship programmes. Conventional pathogen identification can take up to 48 to 96 hours, followed by an additional 48 to 72 hours for AST from sample collection but with rapid diagnostics, it can be shortened to less than 24 hours, thereby supporting patient welfare.^[60,61] Main goals of stewardship programmes can be accomplished through rapid diagnostics - decreasing time to appropriate antibiotics, reducing unnecessary use of antibiotics, and facilitating decisions regarding ADE or discontinuation.^[62-64]

One of the ten points proposed in Jim O'Neill's Review on Antimicrobial Resistance is to transform antibiotic use through better use of rapid diagnostics.^[6] Global Action Plan of WHO on AMR also emphasised the need for "effective, rapid, low-cost diagnostic tools...for guiding optimal use of antibiotics in human and animal medicine".^[52] One of the main goals of US National Action Plan for Combating Antibiotic-Resistant Bacteria is also to advance the development and use of rapid and innovative diagnostic tests for

identifying and characterising resistant bacteria. Thus, the need for rapid diagnostics is not only the key component of ADE strategy but also the central theme of most of the recent policy initiatives taken to combat AMR.

1.5 Unmet diagnostic needs

Rapid diagnostics have the potential to change the drug paradigm and transform the fight against the superbugs. But in order to achieve that, diagnostics need to fulfil a variety of different roles in clinical practice and research. A number of professional groups like Infectious Diseases Society of America (IDSA, US), Jim O'Neill's AMR review group (UK) and Presidential Advisory Council on Combating Antibiotic-Resistant Bacteria (PACCARB, US) and have reviewed the established diagnostic methodologies and highlighted the following key unmet needs regarding diagnostic testing:^[2,64,65]

- Provide faster turnaround time compared with established culture methods,
- Diagnostic tests that rapidly identify pathogens with high sensitivity and high specificity and guide selection of appropriate antimicrobial agents and avoid unnecessary antibiotic use,
- Provide phenotypic drug-susceptibility results directly from clinical samples, thus guiding targeted antibiotic escalation or de-escalation from broad-spectrum to narrow-spectrum agents, and/or discontinuation of antimicrobial treatment,
- Diagnostic tests that distinguish between bacterial and viral infections to avoid or discontinue antibiotics for nonbacterial (viral, fungal, or parasitic) infections,
- Enable point-of-care testing for use in a variety of healthcare settings,
- Improve capabilities for AMR surveillance and outbreak investigation of drug-resistant pathogens.

Thus, rapid diagnostic test that meets the above criteria would ensure that patients receive effective treatment more quickly and also prevent infection “outbreaks”, as an infected patient can be rapidly isolated and infection control measures can be initiated promptly. This would also avoid wasting resources in unnecessary isolation. Patients, who are isolated as a precautionary measure

and waiting for their pending confirmatory diagnosis, could be quickly diagnosed and the use of costly resources could be averted. Thus, the rapid diagnostics can streamline and accelerate the initiation of the treatment regimens, improve patient outcomes and shorten duration of hospitalisation, thus freeing up hospital beds.^[66]

Traditional culture-dependent diagnostic methods identifying pathogens and also providing antimicrobial susceptibility profiles in microbial culture are still considered as gold standard methods. But these methods are very slow and also fail to fulfil most of the above mentioned criteria. Other culture-independent rapid diagnostic methods are reviewed in the light of the above mentioned unmet needs and discussed in chapter 2. Of all the culture-independent methods discussed in next chapter, label-free biosensors have the potential to combat AMR effectively through rapid pathogen identification at the point-of-care.

A biosensor is an analytical device comprised of 2 elements: a biological recognition element (e.g., nucleic acid, antibodies or aptamers) able to interact specifically with a target pathogen and a transducer that is able to convert the recognition of the pathogen into a measurable signal. Different transduction methods were reviewed (e.g. optical, electrochemical and acoustic) and among them Anharmonic acoustic Detection Technique (ADT) transduction method was selected for further investigation.

A transduction method however, requires means to enhance the capture of the target pathogen with sufficient efficiency for direct detection. This can be achieved through integration of an appropriate biological recognition element (or bio-receptor) with the transducer.

In chapters 4, 5 and 6, bio-receptors of different sizes and lengths are explored for direct, sensitive and specific detection of target *E.coli* bacteria.

1.6 Problem statement

1.6.1 Aim

The aim of research is to investigate the bio-affinity based platform for rapid point-of-care detection of bacteria by integrating a 'multivalent aptamer', binding whole bacterial cell as bio-receptor with the Anharmonic acoustic Detection Technique (ADT)* transduction method, that can be applied for rapid identification of the pathogen and subsequent determination of antimicrobial susceptibility.

(*ADT is applied for bacterial detection for the first time using multivalent aptamers in this work)

1.6.2 Objectives

The objectives of this research are:

O.1. To investigate the feasibility of detection of the target *E.coli* bacteria rapidly, sensitively and specifically using multivalent aptamer-based bioassay after integrating with ADT

O.1.1 To address the experimental challenges and develop a solution around the integrated biosensor assay and microfluidic flow-cell

O.2. To explore the comparative performance of different bio-receptors for whole-cell detection of *E.coli* bacteria coupled with ADT:

O.2.1 Compare multivalent aptamer with polyclonal antibody (a different receptor, one that is more common)

O.2.2 Compare aptamers with different linker lengths (long vs short)

O.3. To study the influence of structurally modified aptamers with designed nonlinearity in enhancing sensitivity and specificity of the anharmonic acoustic detection of *E.coli* bacteria; this includes introducing novel designs in the aptamers' molecular structures, two configurations were designed.

1.7 Dissertation Organization

The thesis incorporates seven chapters, summary of which is as follows:

Chapter 1 describes the problems related to infectious disease diagnosis, factors causing AMR and how rapid diagnostics can address these problems, unmet diagnostic needs and the aim and objectives of the research.

Chapter 2 deals with the literature review of various currently used rapid culture-independent diagnostic methodologies used at present. It highlights the potential advantages of Anharmonic acoustic Detection Technique (ADT) over other methods used for detection of whole-cell bacteria. In this chapter, the rationale to select *E.coli* bacteria as target microorganism is also discussed.

Chapter 3 describes materials and methods that were used and also deals with the experimental challenges that were addressed in relation to the biosensor assay to meet the research objective (O1.1): (a) increasing the sensitivity of the sensor through energy trapping; (b) identification of optimal method of measurement of $3f$ signal; (c) validation of surface cleaning method of gold electrodes of quartz crystal resonators (QCRs); (d) selection of suitable biosensor assay format; (e) addressing the problem of bubble formation with the microfluidic flow-cell; and (f) achievement of baseline stability.

Chapter 4 investigates the behaviour of the anharmonic acoustic response of a QCR for the rapid, sensitive and specific detection and quantification of *E.coli* bacteria through aptamer-based biosensor assay, for the first time. It describes the steps taken to meet the research object O.1. The developed anharmonic acoustic aptasensor response was observed for the different bacterial concentrations. Quantitative correlation was achieved with this new method and it was also compared with standard frequency and dissipation shift measurements.

Chapter 5 presents the experiments that explored the comparative performance of different bio-receptors (type and length) for whole-cell detection of *E.coli* bacteria using ADT transduction method. To meet the objectives O.2.1 and O.2.2, the multivalent *E.coli*-binding aptamer was first compared with

polyclonal anti-*E.coli* antibody and then with the same aptamer but of different linker length, respectively. The sensitivity and specificity of different assays were compared.

Chapter 6 is devoted for the experiments conducted to study the influence of novel structurally modified aptamers with designed nonlinearity in enhancing sensitivity and specificity of the anharmonic acoustic detection of *E.coli* bacteria. The *E.coli*-binding aptamer was further modified by introducing novel designs in the aptamers' molecular structures. Two different configurations were designed and explored to achieve the objective O.3.

Chapter 7 summarises the important contributions of this work and outlines the potential future directions.

Chapter 2 Literature review

2.1 Introduction

The aim of this chapter is to provide an overview of the rapid diagnostic methods that can be applied as point-of-care tests (POCTs) for detection and identification of pathogens. In this chapter, the limitations of the culture-dependent methods are discussed. Also, currently available various culture-independent diagnostic methods are reviewed that can quickly identify pathogens and reduce the length of the diagnostic cycle. Among the biosensor-based culture-independent diagnostic methods, the focus of this review was only on those methods that can be used for whole-cell bacterial detection. The rationale behind choosing *E.coli* bacteria as the target analyte is also discussed.

2.2 Background

Point-of-care testing is one of the most powerful tools available today in the fight against AMR. Lord O’Neil’s report is the first report that highlights the importance of rapid POC diagnosis in deterring the dissemination of AMR, this ground-breaking report also appeals the governments and regulators of HICs to promote the use of rapid POCTs among healthcare professionals.^[6,7,64] There are several definitions of POCT but no universally accepted definition.^[67] As per one textbook, POCT can be defined as the “provision of a test when the result will be used to make a decision and to take appropriate action, which will lead to an improved health outcome”.^[68] Regardless of the exact definition, the most important elements of POCT are rapid turn-around time that enables shortening of the diagnostic cycle; better decision-making at the point-of-prescription and preventing the unnecessary use of antimicrobials.^[69-71] POCTs play an important role in filling the gap between the centralised laboratory diagnostics and peripheral healthcare professionals.^[72] The important attributes of POCTs that distinguish them from conventional laboratory tests are: they do not require specialised laboratory infrastructure or trained personnel to use them; they deliver a rapid (i.e. within 1 hour) diagnosis and they are more cost-effective than conventional tests.^[73]

Presently, bacterial identification (ID) and antibiotic susceptibility testing (AST) are the well-established diagnostic methodologies. Pathogen isolation and identification from pure culture generally requires 18 to 48 hours with further 8 to 48 hours to perform AST and report the results. In case of infections with MDR organisms, AST results take almost 48 to 96 hours to reach the clinician and have very little effect on the ensuing therapy.^[60,61,64,74] For these kinds of serious infections, it is essential to get right drug in the first 24 hours of disease presentation so that there is a desired outcome.^[75-77] Phenotypic culture-based AST methods can be highly sensitive and more absolute, but suffer from a long turnaround time. Although, faster molecular AST methods are available^[78-80], but in addition to cost they have many limitations, like unable to detect unknown resistance mechanisms; unwarranted susceptibility, as they report only about the lack of resistance mechanism; cover narrow range of detectable resistance mechanisms; and limited information in comparison to phenotypic AST.^[81,82] Because of these limitations, molecular methods are better suited as an expensive add-on to current diagnostic cycle and cannot replace the conventional antibiogram.^[81] Since, it is unlikely to reduce the time required for phenotypic AST; if the initial pathogen identification step is shortened it will ultimately reduce the overall time of diagnostic cycle, and thus help clinicians to start appropriate antimicrobials at the same time as the clinical encounter.

2.3 Culture-dependent diagnostic methods

The conventional bacterial pathogen detection and identification methods are based on culturing the microbes on a selective medium followed by standard biochemical identification tests to confirm the presence of the target bacteria.^[83] These conventional methods are generally simple and economical but the major drawback of these methods is that they are time-consuming, as the microbes are required to be grown in different culture media such as pre-enrichment media, selective enrichment media and selective plating media. Typically conventional methods are laborious as they require the preparation of culture media, inoculation of plates and colony counting and may require several days for preliminary identification depending on the growth of the bacteria and more than a week for confirmation of the species of the pathogens.^[83,84] Additionally,

the sensitivity of conventional methods is low and sometimes they give false-negative results due to viable but non-culturable (VBNC) pathogens.^[85,86] Despite the fact that these conventional culture-dependent methods are still essential, recently different rapid culture-independent methods have been developed that overcome the limitations of culture-dependent methods for identification of pathogens. Figure 2.1 provides a comparison of culture-dependent and culture-independent detection methods.^[87]

Novel culture-independent methods are been developed with advances in terms of rapidity, sensitivity, specificity and distinction of the viable cells.^[84] However, each of these rapid culture-independent methods has its own advantages and limitations. Based on their main principle, these methods can be broadly classified into the following categories: nucleic-acid-based methods, immunological methods, mass spectrometry-based methods and biosensor-based methods.^[84] This review examines these rapid culture-independent diagnostic methods and their applications in combating AMR along with their advantages and limitations.

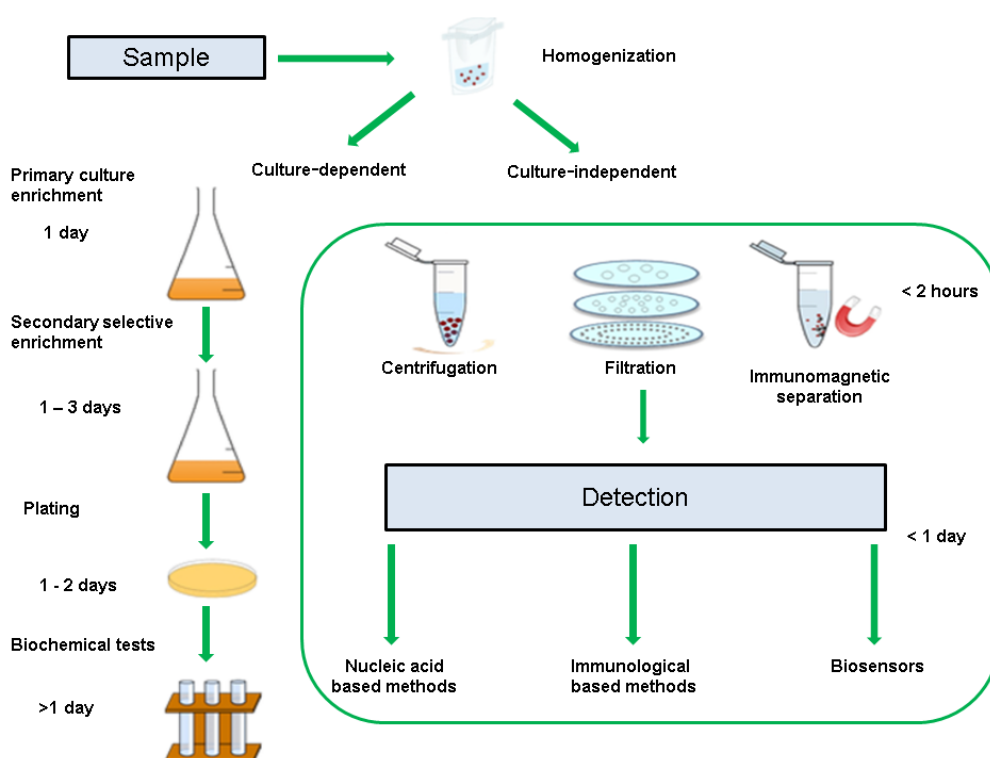


Fig. 2.1 - Culture-dependent methods vs Culture-independent methods. Adapted and modified from ^[87].

2.4 Culture-independent diagnostic methods

2.4.1 Nucleic acid-based methods

Nucleic acid-based detection methods comprise of two key techniques: nucleic acid hybridisation with probes or primers and nucleic acid amplification technique for pathogen identification.^[84] These methods include detection of species, strain, or serotype-specific DNA (deoxyribonucleic acid) or RNA (ribonucleic acid) sequences present in the target pathogen, by hybridising the target nucleic acid sequence to a synthetic oligonucleotide (probes or primers) which is complementary to the target sequence.^[84,87] The current nucleic acid-based methods are simple polymerase chain reaction (PCR), multiplex polymerase chain reaction (mPCR), real-time/quantitative polymerase chain reaction (qPCR), nucleic acid sequence-based amplification (NASBA), loop-mediated isothermal amplification (LAMP) and microarray technology.^[84]

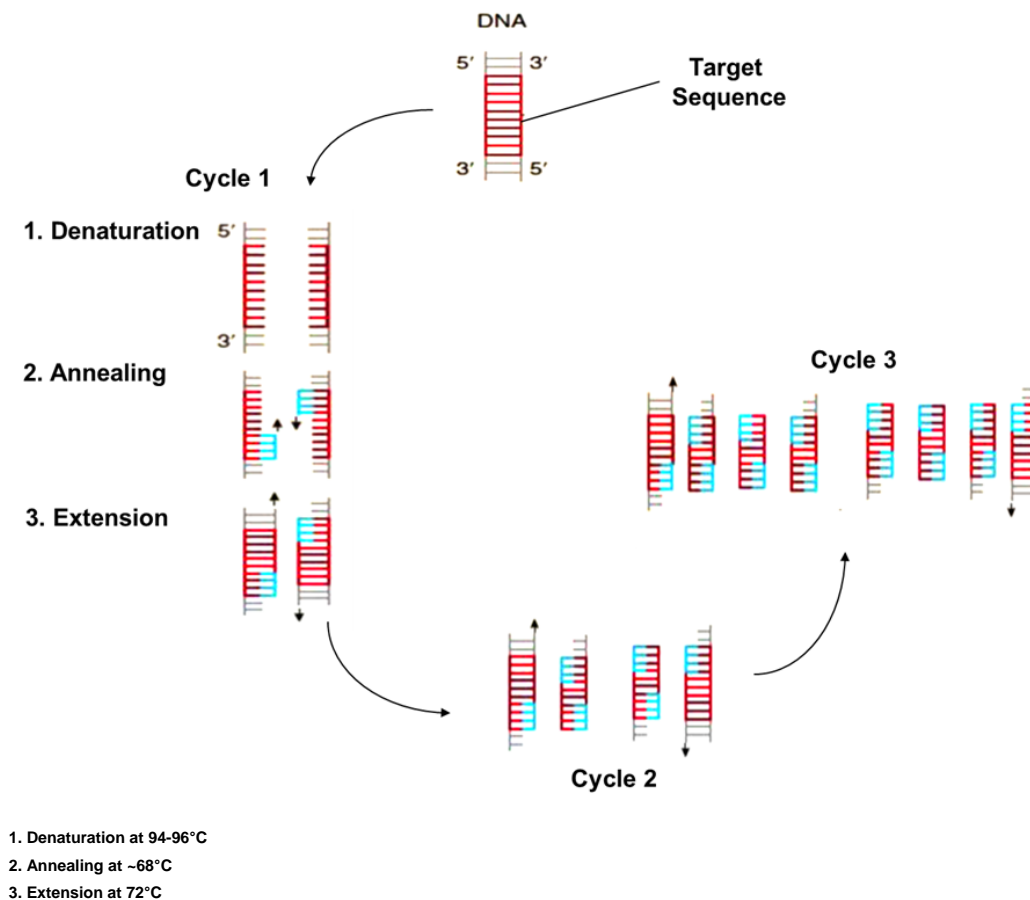


Fig. 2.2 – Schematic presentation of polymerase chain reaction (PCR). Adapted and modified from ^[88].

PCR was invented about 30 years ago and is one of the most commonly used nucleic acid-based methods for pathogen detection.^[89] The working principle of PCR is amplifying a specific target DNA sequence in a sample during a cyclic 3-step process (as shown in Fig. 2.2).^[83] Multiplex PCR also operates on a working principle similar to conventional PCR but comparatively, offers a more rapid detection. There are several commercial PCR-based systems for detection of antimicrobial resistance, already available in the market^[90], but they mostly focus on detecting Gram-positive bacteria and not Gram-negative bacteria due to the high intricacy of their resistance patterns.^[90,91] However, few PCR-based systems capable of detecting Gram-negative bacteria are in developmental stage, near to market.^[92-96] The PCR products are visualised on electrophoresis gel as bands by staining with ethidium bromide in simple PCR-based methods whereas in real-time PCR or quantitative PCR (qPCR) method, they are monitored by measuring the fluorescent signal produced by labelled probes or dyes.^[84] Thus, unlike simple PCR and multiplex PCR tests which are arduous and costly, qPCR allows high-throughput analysis and automation.^[97] Because of these advantages, various commercial qPCR kits for the detection of pathogens such as *Listeria monocytogenes*, *Escherichia coli*, *Salmonella*, and *Campylobacter*, etc. has been developed.^[98] NASBA also operates by amplifying nucleic acids but under isothermal conditions without thermocycling system needed for PCR.^[99] But, post-NASBA products are also detected using agarose gel electrophoresis or enzyme-linked gel assay, making it labour-intensive and costly.^[100] LAMP is a nucleic acid amplification method which is based on auto-cycling strand displacement DNA synthesis under isothermal conditions. Post-LAMP amplicons are also detected by agarose gel electrophoresis or SYBR Green I dye, making it expensive and laborious.^[84,100] However, different types of LAMP methods have been developed that use fluorescence assays to monitor amplicons, allowing high-throughput analysis but adding to the cost because of fluorescent labelling.^[100]

In general, all these nucleic acid-based methods do not allow isolating pathogens for further characterisation.^[2,61,78,101] In addition to the cost, the major limitation of nucleic acid-based methods is the incongruity between phenotype and genotype.^[90] Also, these genotypic tests for the detection of antimicrobial

resistance may generate false-negative results due to their inability to detect new resistance mechanisms or false-positive results, because they may detect inactive or incomplete resistance genes in a sample, which have not conferred resistance to the antimicrobial drug under test. A general disadvantage of PCR assays used for detection of bacterial pathogens is that the PCR amplification process will target DNA from both live and dead cells. Thus, PCR cannot distinguish between live and dead cells and hence providing more false-negative results.^[102] Therefore, though the nucleic-acid based tests are rapid, traditional culture-dependent methods are still considered as gold standard for pathogen identification.

2.4.2 Immunological-based methods

The detection of bacterial pathogens by immunological-based methods is based on antibody-antigen binding interactions, where a particular antibody will bind to a specific antigen. The sensitivity and specificity of these methods thus, depends on the binding strength of particular antibody to its antigen. The two major categories of immunological-based methods reported for the culture-independent detection of bacterial pathogens are enzyme-linked immunosorbent assay (ELISA) and lateral flow immunoassay (LFI).^[84]

ELISA is one of the most widely used immunological assays for pathogen detection, and is very precise and sensitive method for detecting antigens.^[103] Conventional ELISA normally includes chromogenic reporters and substrates that produce some kind of apparent colour change indicating the presence of antigen or analyte. Sandwich ELISA is the most effective form of ELISA whereby, the antigen to be measured is bound between two primary antibodies: the capture antibody and the detection antibody.^[84] In this method, the capture antibody is typically immobilised onto the walls of the microtiter plate wells. The target antigen binds to this primary antibody and the remaining unbound antigens are removed by washing step. After that, an enzyme-conjugated secondary detection antibody is introduced which binds to the antigen, thereby forming a complex. This complex can be detected by adding colourless substrate which changes colour in the presence of the conjugated enzyme (Fig. 2.3).^[100,104,109] Different types of enzymes are used in ELISA, for e.g.,

horseradish peroxidase (HRP), alkaline phosphatase and beta-galactosidase.^[105] Because it is sensitive and robust, many studies have used sandwich ELISA for rapid detection of pathogens like *Vibrio parahaemolyticus*,^[106] *Salmonella*, etc.^[107] Lately, high-throughput and automated ELISA systems that use enzyme-linked fluorescent assay (ELFA) such as VIDAS[®] (BioMerieux) and Assurance[®] EIA (BioControl) are available for the detection of pathogens.^[100,108] These systems are more sensitive and take about 45 mins to 2 h to complete an assay. However, ELISA is costly and requires specialised equipment and trained personnel to operate the system and use of fluorescent labelling in ELFA, makes it even more costly.^[84] Therefore, rapid, reliable and inexpensive, methods that can be conducted and interpreted at the point-of-care are still needed.

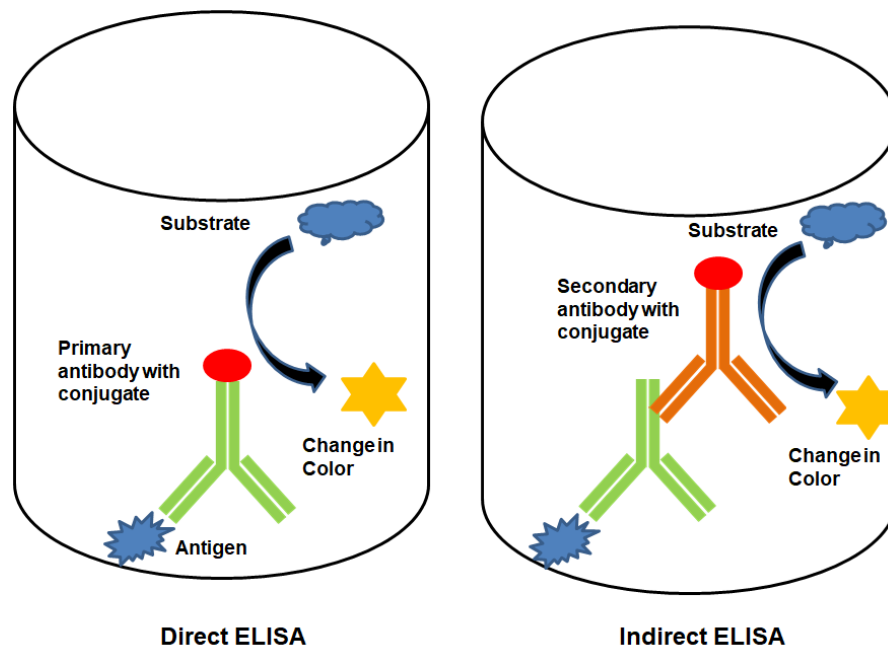


Fig. 2.3 - Principle of ELISA test: This test combines the specificity of antibodies with the sensitivity of simple enzyme assays, using antibodies or antigens coupled to an easily-assayed enzyme. Adapted and modified from ^[109].

Lateral flow immunoassays such as dipstick and immunochromatographic strips have been developed for rapid on-site detection of pathogens. This is a paper-based platform that is based on biochemical interaction of antigen-antibody. A lateral flow immunoassay is composed of four parts: a sample pad starting at the bottom, on which liquid sample is dropped; conjugate pad; reaction membrane containing test line and control line for target

antigen-antibody interaction; and absorbent pad, which reserves waste. The principle of LFI is very simple: a liquid sample (or its extract) containing the analyte of interest moves via capillary action through various zones of the strips. It travels through the conjugate release pad, which contains antibodies that are specific to the target analyte and are conjugated to coloured or fluorescent particles. Then the sample, together with the conjugated antibody bound to the target analyte, migrates along the strip to the nitrocellulose membrane, immobilised with antibody or antigen (as depicted in Fig. 2.4). The coloured or fluorescent particle can bind to the antibody or antigen immobilised at test line depending on the analytes present in the sample. The result can be visualised approximately 5 to 30 mins after the addition of sample.^[110] LFI employs different labels such as monodisperse latex, colloidal gold, carbon and fluorescent tags for pathogen detection.^[84] LFIs are designed for individual tests rather than high-throughput screening.^[110,111] Limitations of LFIs include: it is one-step assay so can be used only one time; obstruction of pores due to matrix components and restriction on total volume in a test gives a limit of sensitivity; test-to-test reproducibility is challenging; and also integration with on-board electronics and built-in quality control functions is challenging.^[110]

LFIs have advantages of low cost, long-term stability, minimum skill required and can be applied at the POC,^[110,111] but they have higher false-positive rates than ELISA and PCR.^[112] Also, growing demand for higher sensitivity is challenging the existing formats of this method.^[113] This is because most lateral flow assays employ antibodies to capture the analytes and there is an increasing concern about the specificity, sensitivity, and stability of these antibodies. This can be improved by using high-affinity aptamers instead of expensive antibodies in lateral flow assays.^[113]

Most lateral flow assays require a controlled temperature for storage which is largely a function of the stability of antibodies used in the system. Since aptamer have very high stability at high temperatures, it should be feasible to apply aptamer-based lateral flow tests to very low resource settings and highly sub-optimal field conditions with minimum performance loss. Also, protein-based antibodies show high sensitivity to denaturing agents, which limit their applications or require complicated sample pre-treatment. While, nucleic acid

aptamers show more resistance to different chemical buffers such as large ranges of pH, ion strength, and organic reagents. An additional advantage of using aptamers is the regeneration by heating or other methods. These advantages make aptamers appealing in the development of low-cost, reusable lateral flow assays.^[113]

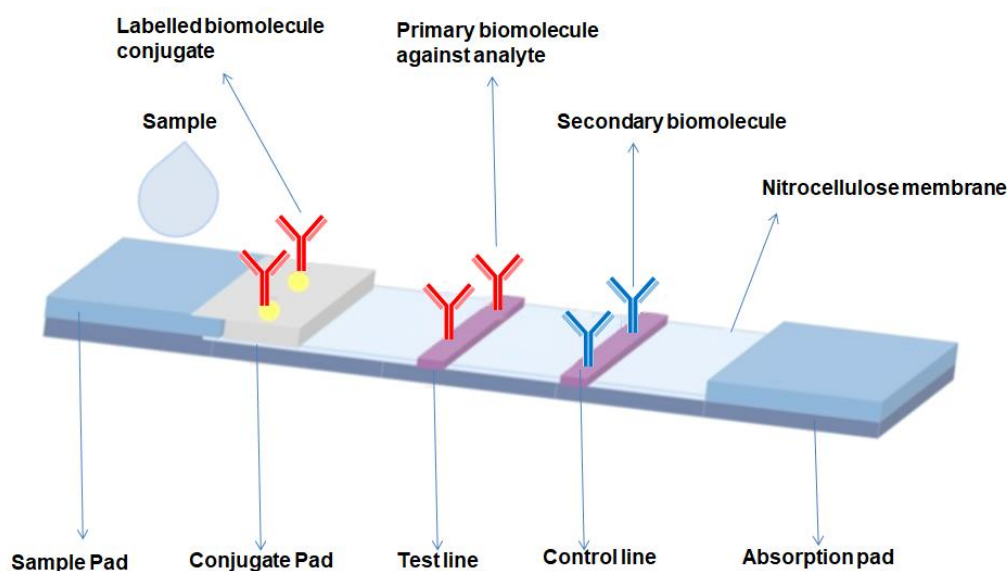


Fig. 2.4 – Pictorial representation of lateral flow immunoassay format. Adapted and modified from ^[114].

2.4.3 Mass spectrometry-based methods

Mass spectrometry-based method, such as matrix-assisted laser desorption/ionisation time-of-flight mass spectrometry (MALDI-TOF MS) utilizes lasers to ionise and accelerate bacterial and fungal molecules, which separate according to the mass-to-charge ratio, yielding a distinct signal. Its working principle is shown in Fig. 2.5.^[78,115] MALDI-TOF allows direct identification of organisms from positive blood-cultures and thus has reduced turnaround times by at least one working day. In two studies, it has been found that MALDI-TOF reduced the time to optimal antimicrobial therapy, hospital length of stay and hospitals costs by directly identifying pathogens from positive blood-cultures. But, in both the studies, direct MALDI-TOF identification was only one part of an intervention package, which also included rapid susceptibility testing from positive blood cultures and intensified antimicrobial stewardship measurements. Hence, it was difficult to assess the exact contribution of rapid pathogen

identification by MALDI-TOF in reducing the time to diagnosis.^[116,117] Moreover, MALDI-TOF-based identification of bacterial pathogens directly from positive blood-culture bottles is laborious, requires trained personnel to operate and is confined to the laboratory, difficult to use at the point-of-care.^[78]

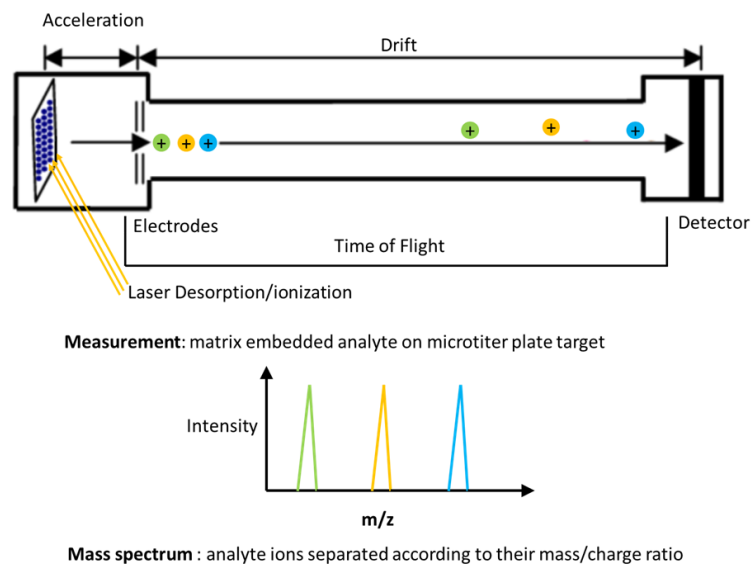


Fig. 2.5 - Principle of MALDI-TOF-MS: Target is embedded in surplus matrix molecules and the samples are prepared on a microtiter plate. The matrix and the analyte are evaporated into gas phase using a pulsed UV-laser. The matrix ionises the analyte molecules by proton transfer and also gives desorption support. The ions are then accelerated by an electrical field and enter the field-free flight tube of the mass spectrometer. By simple measurement of the TOF of the analyte ions, their mass to charge ratio can be determined. Adapted and modified from ^[118].

2.4.4 Biosensor-based methods

Biosensors have fomented a revolutionary breakthrough in the field of science and technology and are currently influencing all the areas of our life. Biosensors offer various advantages including small fluid volume manipulation, low energy consumption, portability, specificity, simplicity, high sensitivity, potential ability for real-time and on-site analysis coupled with the speed and low cost, etc. Therefore, they have been projected to have applications in controlling AMR.

Biosensors have been developed for many different analytes, which range in size from individual ions and small molecules to nucleic acids and proteins up to whole viruses and bacteria.^[119] Broadly, two types of biosensors have been developed: (i) those which involve sample processing steps for bacterial lysis in order to release the target bacterial component and (ii) processing-free methods which target whole bacterial cells. The main shortcoming of the first type of

biosensors that detect bacterial components (e.g., DNA, RNA, enzymes, exotoxins, etc.), is the requirement of extra reagents for sample processing, thus increasing both time and cost of these tests. Therefore, biosensors for the direct, reagent-less detection of whole bacterial cells are much more desirable for fast, cost-effective testing at the POC.^[120]

According to IUPAC definition, a biosensor is ‘a device that uses specific biochemical reactions mediated by isolated enzymes, immune-systems, tissues, organelles or whole cells to detect chemical compounds usually by electrical, thermal or optical signals’.^[121] A biosensor is different from a bio-analytical system, which requires additional processing steps, such as reagent addition and also from bio-probe which is disposable after one measurement, i.e. single use, and unable to continuously monitor the analyte concentration. Biosensor is a self-contained integrated device which is capable of providing specific quantitative or semi-quantitative analytical information using a biological recognition element (bio-receptor) which is in direct spatial contact with a transducer element.^[122] Thus, biosensor is an analytical device that consists of two main elements: a transducer and a bio-receptor (as shown in Fig. 2.6).

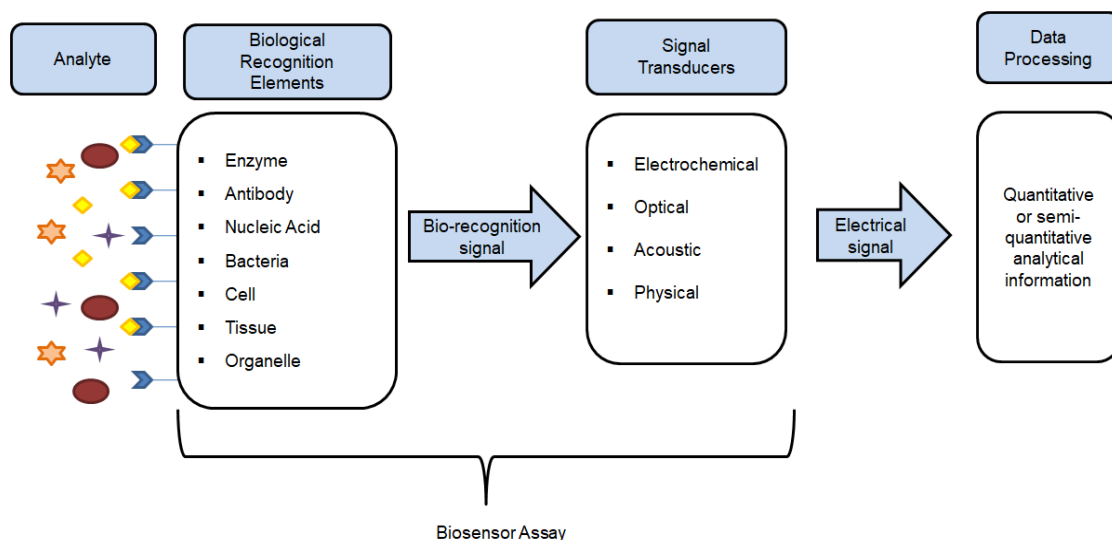


Fig. 2.6 - Principle of biosensor and main components: Biosensor is composed of two main elements viz. biological recognition element (or bio-receptor) and signal transducer. A bio-receptor is an immobilised sensitive biological element recognising the analyte. The biological response resulting from the interaction of the analyte with the bio-receptor is transformed to an electrical, optical or electrochemical signal by the transducer and then further processed, providing the information. Adapted and modified from ^[123].

2.4.4.1 Transduction methods

A transducer is used to convert (bio)chemical signal resulting from the interaction of the analyte with the bio-receptor into an electronic one. The intensity of generated signal is directly or inversely proportional to the analyte concentration. According to the transducing elements, biosensors can be classified as optical, electrochemical, acoustic, thermometric, micromechanical or magnetic sensors.^[84,89,100]

The focus of this review is only on the biosensors that are commonly used for the rapid detection of whole bacterial cells - optical, electrochemical and acoustic biosensors.

a. Optical transduction methods

Optical biosensors are the most commonly reported class of biosensors. The optical transduction method exploits the interaction of the optical field with a bio-receptor. There are two detection protocols that can be implemented in optical bio-sensing: label-based and label-free detection. In label-based sensing, the optical signal is detected through multiple methods like colorimetric, fluorescent or luminescent methods.^[124,125] In fluorescence-based detection, either target molecules or bio-receptors are labelled with fluorescent tags, such as dyes; the intensity of the fluorescence indicates the presence of the target molecules and the interaction strength between target and bio-receptors. In fiber-optic biosensors, optical fibers are employed for whole-cell bacterial detection. In this method, a source of light passes through the fibers that are immobilised with bio-receptors to a photon detector. After analyte binding event, appropriate labelling reagent is added which indicates change in signal at the detector. The label-based methods are very sensitive, for instance, fluorescent dye-loaded micelle approach could detect 15 bacteria/mL of *E.coli* bacteria,^[126] but these methods suffer from laborious labelling processes that may even interfere with the function of a bio-receptor. Also, there is signal bias as the number of fluorophores on each molecule cannot be accurately controlled making quantitative analysis difficult.^[127]

Most of the label-free detection mechanisms measure refractive index (RI) change induced by molecular interactions, which is related to the sample concentration or surface density, instead of total sample mass. Various optical structures have been investigated for sensitive label-free detection based on Surface Plasmon Resonance (SPR), interferometer, optical waveguide, optical ring resonator, optical fiber and photonic crystal biosensors. Most of these optical structures such as ring resonator and photonic crystal are in their infancy while others like SPR and waveguides are mature and have even been commercialised.^[124] SPR biosensors use surface plasmon waves (electromagnetic wave) to detect changes when the target analyte interacts with a bio-receptor immobilised on the sensor.^[124] The working principle of SPR is shown in Fig. 2.7. Different bio-receptors have been used along with these transduction methods for whole-cell bacterial detection, for e.g., antibodies, bacteriophages, and lectins. But there are two potential problems that limit their applications in whole-cell bacterial detection. First, the evanescent field in those basic SPR structures only penetrates into the surrounding medium for about 100 nm, and thus it is very difficult to detect the large target molecules like cells and bacteria. Second, there is similarity in RI between the bacterial cytoplasm and the aqueous medium.^[128] Thus, the performance of the SPR is weakened when detecting the target molecules in a complex solution, such as blood samples. Lately, nanoparticles have been used to enhance the sensitivity of the system through a process called Localised Surface Plasmon Resonance (LSPR), but this too have been reported to be less sensitive for detection of whole-cell bacteria. Additionally, there are other problems with optical biosensors like, lack of specificity,^[129] not suitable for studying small analytes, bulky size, high cost of instrumentation, technical difficulties for fabrication, etc. This emphasises that more research efforts are needed for developing optical biosensors that can be used as POCT for combating AMR.

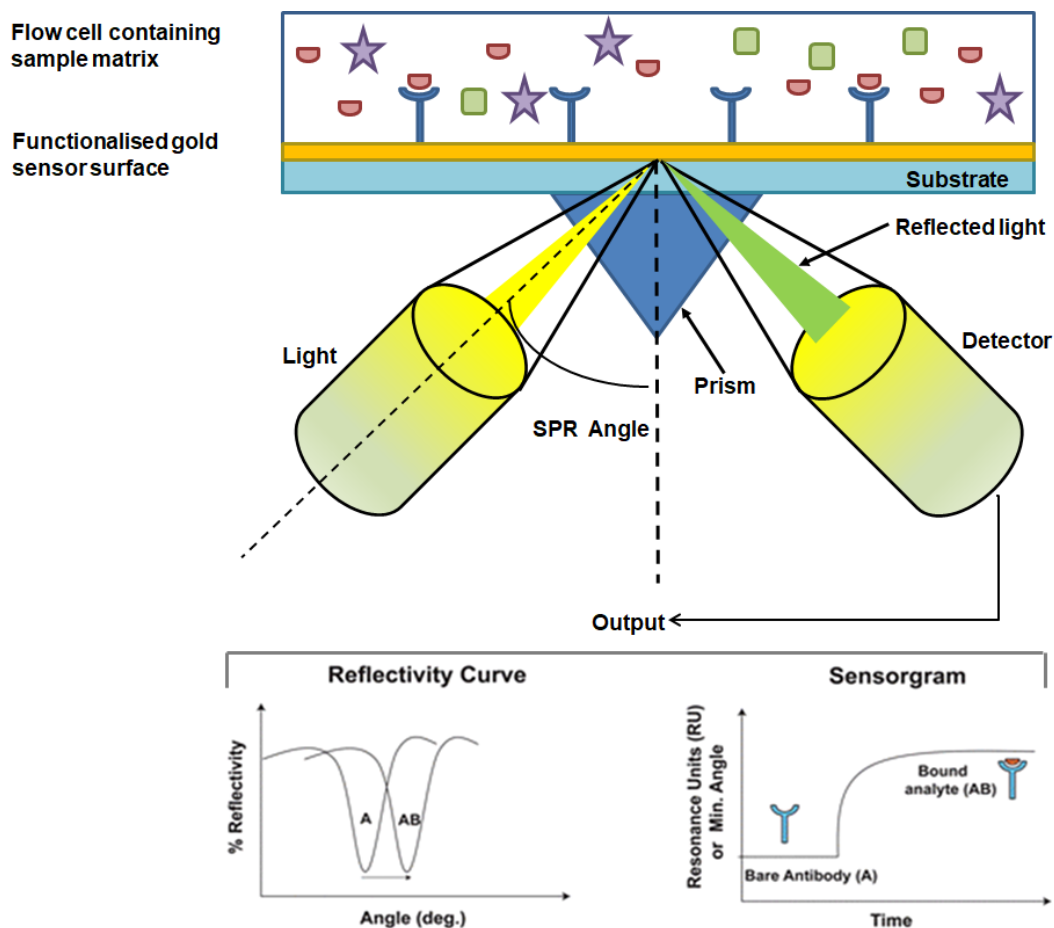


Fig. 2.7 - The principle of surface plasmon resonance (SPR): Polarized light is applied to the surface of the sensor chip and is reflected. The intensity of the reflected light is reduced at a certain incident angle, the SPR angle. Interacting substances near the surface of the sensor chip increase the refractive index, which alters the SPR angle. The optical detection unit detects position changes of the intensity dips in the wedge of the reflected light corresponding to the SPR angle. The signals produced are measured in resonance units (RU). Adapted and modified from ^[130].

b. Electrochemical transduction methods

The basic transduction principle for this class of biosensors is that chemical reactions between immobilised bio-receptor and target analyte produce or consume ions or electrons, which affects measurable electrical properties of the solution, such as electric current, potential, capacitance and electron transfer resistance across the working electrode.^[131] Based on this principle the electrochemical biosensors can be divided into three groups: potentiometric, amperometric, and impedimetric biosensors.

Potentiometric transduction method uses ion-selective electrodes to measure the change in potential that occurs upon recognition of analyte at

the working electrode. Though this method is widely used, but examples of its application for detection of whole bacterial cells are very few as potentiometric biosensors cannot provide specific and sensitive signals for larger analytes like bacteria. However, a chrono-potentiometric method called as Potential Stripping Analysis (PSA) was used to detect marine pathogenic bacteria. The detection range of PSA method was found to be good but it involved pre-incubation steps of bacterial processing, making it unsuitable for rapid and on-site detection methods.^[132]

Amperometric transduction methods involve direct measurement of the current generated by the oxidation or reduction of species produced in response to analyte and bio-receptor interaction. The measured current is directly proportional to the analyte concentration.^[133] These methods are very sensitive and easy but their limitations include low specificity as the signal depends on the applied potential. Also, its application in biological media is difficult as the other redox-active species may interfere with the signal at high potential and generate inaccurate results. The bio-receptor commonly employed for amperometric biosensors are enzymes, thus conferring it another limitation as the analyte of interest needs to be an enzymatic substrate. Because of these reasons, although amperometric biosensors are widely used their application for whole-cell bacterial detection is limited.^[134] An attempt was made to detect *E.coli* K-12 bacteria through bacteriophages which are viruses with the ability to infect and lyse specific bacterial strains. Bacteriophage-mediated cell lysis increased specificity and sensitivity but this bio-sensing system had the disadvantage of the need for pre-incubation of bacterial cells with enzyme enhancer and phage, thus increasing the duration of the test.^[135] Few other label-based amperometric methods have been tried for bacterial detection, but the system requiring labels again repudiates its POC utility.

Impedimetric transduction methods involve measurement of the change in capacitance and electron transfer resistance across a working electrode surface after analyte and bio-receptor interaction. They have advantage over amperometric biosensors as there is no need for the analyte to be an enzymatic substrate. Recently, many reports detailing the impedimetric

detection of whole bacterial cells have emerged. Most of these impedimetric biosensors have focused upon detection of the model organism *Escherichia coli*, although other bacteria have also been detected, including *Salmonella Typhimurium*, *Campylobacter jejuni*, and *Staphylococcus aureus*.^[120] Different amperometric methods are being employed to detect whole-cell bacteria, like bio-imprinting technique in which, bacterial cells can be deposited on a surface and then washed off, leaving their imprint on the surface.^[136] In another new method antibody-tagged bio-functional magnetic beads that were used to facilitate the migration of target bacteria to the sensor surface.^[137] Although, these methods are innovative but their set-up method is complicated and difficult to be translated at POCT. Additionally, the key disadvantages of amperometric transduction methods are variable reproducibility, high limits of detection, and problems with nonspecific binding which might raise false alarms, negating its application as POCT for fighting AMR.

c. Acoustic transduction methods

The application of acoustic transduction methods in the field of bacterial detection is generally lesser than electrochemical and optical biosensors.^[89,100] Acoustic transduction methods are so named because they apply an acoustic wave, as the sensing mechanism. Almost all acoustic biosensors use a piezo-electric quartz resonator (PQR) to generate acoustic waves. If the acoustic waves propagate on the surface of the material, the biosensors are classified as Surface Acoustic Wave (SAW)-based sensors and if they propagate through the bulk of the material then they are called as Bulk Acoustic Wave (BAW)-based sensors.^[138] SAW-based biosensors are mostly useful for chemicals sensing application and monitoring purposes rather than for physical measure and quantity determination with high absolute accuracy. Also, the performance of SAW-based biosensors, suffer from damping problems in the liquid phase. On the other hand, BAW-based biosensors were found to be suitable for measurement in liquid medium, as damping of oscillation is less than in SAW-based biosensors.^[139]

PQR are largely described as BAW devices. Other terms used for reference (i.e. name) or to describe these PQR or BAW crystals are: quartz crystal

microbalance (QCM) and thickness shear mode (TSM). The QCM term is often used because it describes the mass sensitivity of the crystal. TSM is used because it describes the motion of the crystal's vibration. In 1959, Sauerbrey demonstrated the dependence of quartz oscillation frequency on the change in surface mass.^[140] In fact, he coined the term quartz crystal microbalance in late 1950's and it was his work that led to the use of PQR as sensitive microbalances for thin films. He also developed an empirical equation showing that the frequency change of a quartz crystal TSM resonator was a linear function of absolute mass.^[141,142]

Thus, QCM sensors detect the resonance frequency change that results from increased mass on the sensor surface due to analyte binding (as depicted in Fig. 2.9). QCM sensors have been developed for the detection of whole bacterial cells, including *Escherichia coli*, *Salmonella enterica serovar Typhimurium*, *Campylobacter jejuni* and *Bacillus anthracis*.^[120] Micro-cantilever sensors also work on the same principle as of QCM. A change in resonant frequency of the cantilever is observed due to induced mechanical bending upon an increase in mass on the sensor surface. Micro-cantilever sensors have been developed for the detection of various whole-cell bacteria, including *E.coli O157:H7*, *Salmonella Typhimurium* etc. But the major disadvantage of micro-cantilever based method is that it needs to be operated in air as opposed to physiological media. Also, there are some other drawbacks that need to be overcome such as lack of specificity and sensitivity as well as excessive interference.^[120]

As per the equation given by Sauerbrey, the relationship between the mass and the frequency is linear but only, if the sensitive layer coated on the oscillator is rigid and the adsorbed analyte oscillates synchronously with PQR. But if the interaction between the sensitive layer and analyte is not rigid (flexibly/loosely bound analyte) it leads to free movement of the particles which then causes a positive frequency shift – anti-Sauerbrey behaviour. Also, if large sized analyte is bound to surface through weak bond then too positive frequency shift can be observed. Thus, positive and negative frequency shifts of QCM and micro-cantilever sensors depend on

the interaction strategies of the sensitive material with corresponding analyte, making them unreliable and imprecise.^[142]

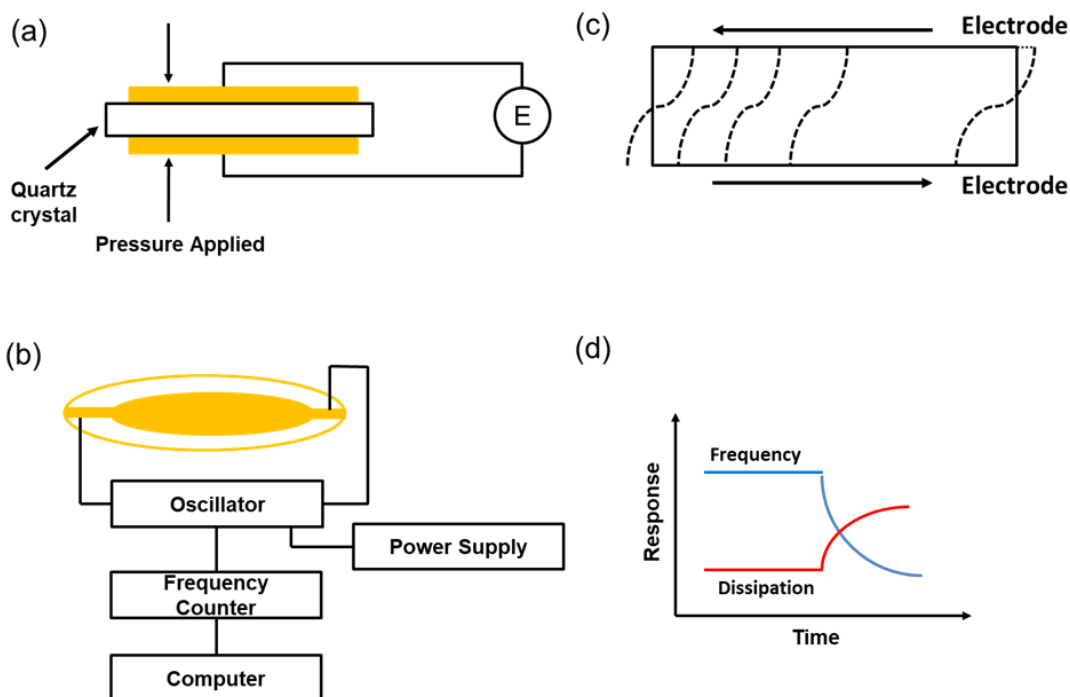


Fig. 2.9 – Principle of QCM: (a) Pressure exerted on a quartz crystal results in an electric field (E) between deformed surfaces. This is called piezoelectric effect. (b) Experimental setup of the quartz crystal microbalance (QCM). (c) Schematic representation of a QCR oscillating in the fundamental thickness shear mode. (d) Both, the frequency shift and the damping (dissipation) of the oscillation are captured with QCM. Adapted and modified from ^[143].

The positive frequency shift with increasing mass was also pointed by Dybwad. He postulated that positive frequency shift occurs if the PQR is put in contact with a very large sphere (representing analyte). He explained this phenomenon through a model termed as, “coupled-resonance model” (Fig. 2.10). In this model, the sphere is connected to the sensor via small bridge (or “point contact”) and it together with this contact forms a second resonator system of their own. Thus, the crystal and the sphere (analyte) form a coupled-resonator system with two different resonant frequencies ω and ω_s , respectively. The frequency shift of the coupled resonator relative to the unloaded crystal depends on whether ω_s is higher or lower than ω . In case of small mass tightly attached to the crystal, ω_s is much larger than the resonance frequency of the crystal, ω . So, this leads to negative frequency shift as the force exerted by the crystal does not move the sphere in space.

This is also called as “inertial loading”. But if large (micrometer-sized) spheres are attached to the crystal via weak bridges, ω_s , may be smaller than ω . In this case, positive frequency shift is observed that is proportional to the stiffness of the contact and independent of the sphere’s mass. This situation is termed as “elastic loading”. However, this model is applicable for spheres in dry state. The liquid leads to a strong coupling between the sphere and the crystal. In such situations, the frequency shift depends on the stiffness of the contact, rather than the size of the adsorbed object.^[144]

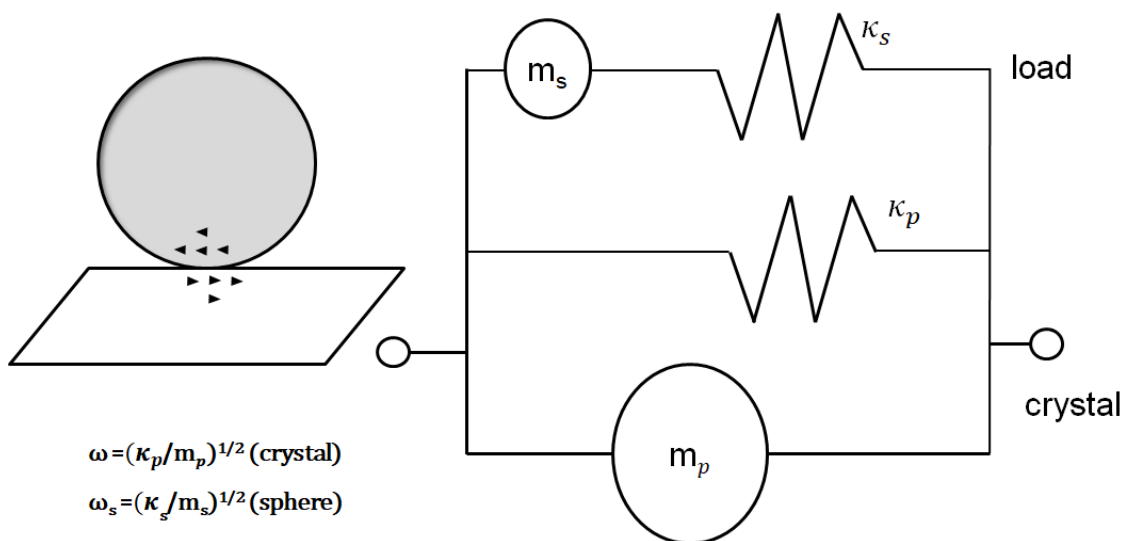


Fig. 2.10 Dybwad model: A sphere is shown adsorbed to the surface of a QCM. The sphere and the contact between the sphere and the surface constitute a resonating system of their own. Mechanical representation is shown on the right side. The crystal and the sphere form a system of coupled resonators with two resonance frequencies ω (crystal) and ω_s (sphere). The frequency shift of the composite resonator relative to the unloaded crystal depends on whether ω_s is higher or lower than ω . ω_s is high for small particles tightly attached to the crystal, which leads to Sauerbrey-type behavior (“inertial loading”). In the opposite limit, the sphere remains immobile in space due to inertia, but exerts a restoring force onto the crystal, thereby increasing the stiffness of the composite resonator (“elastic loading”). Adapted and modified from ^[144].

Another method that attempted to detect the affinity of interaction includes the bond rupture immunosensors, such as the rupture event scanning (REVS). In this technique, the sensor attached with the biological particles is driven close to its fundamental resonant frequency (f) by a pure sinusoidal oscillation at increasing amplitude. As the amplitude of oscillation increases, there is increasing acceleration of analytes adhered to the surface; which causes increase in force exerted by the surface on the analytes. This ultimately causes rupture of the bonds attaching the analytes to the surface. This rupture event is detected by measuring changes in the transduced electric signal recorded at

the third harmonic (3f). The signal indicated not only the presence of the analytes but also the number of analytes present and their affinity for a surface-bound receptor. However, this concept was not supported by theoretical explanation of the physical mechanism responsible for generation of the so called “rupture” signals, claimed to differentiate specific and non-specific interactions. It was also notified that it is challenging to reliably reproduce the rupture signal, especially when the concentration of adsorbents is low. Since the analyte detaches away from surface after a single measurement, the measurements are not repeatable with the same specimen.^[145]

Another acoustic transduction method, known as “Anharmonic acoustic Detection Technique (ADT)” employs a concept similar to that of Dybwad’s “coupled-resonance model”. ADT also explores the interaction between the surface of resonator and particle bound to the surface through a tether (or linker). Ghosh *et al.* postulated that anharmonic interaction forces could be responsible for the generation of the nonlinear signal. They developed a model to explain this phenomenon using a spring-mass model, where the particle was modelled as sphere and tether (or linker) as a spring (as shown in Fig. 2.11). In case of inertial loading, the sphere remains stationary but the resonator oscillates, this stretches the tether and this is transduced as nonlinear signal. The nonlinear signal thus depends upon the stiffness of the tether and also the angle it makes with the surface of resonator. This concept was validated by quantitative modelling of the interactions of a surface-bound particle with the oscillating surface for both physisorbed and specifically-bound cases, and the resulting nonlinear acoustic modulation of the oscillator was analysed. This technique demonstrated the ability to differentiate between specific (target) and non-specific (non-target) interactions, which is lacking in most of the sensing techniques. It also allows the measurement of activation energy or mechanical force-extension characteristics of a molecule. ADT has been previously established to selectively detect *Bacillus subtilis* spores and distinguished them from physisorbed SCPM (streptavidin-coated polystyrene microbeads), and can be further employed for detecting pathogens. ADT is ideal for application as rapid POC of diagnostic method, as it is entirely electronic; it is integrable and scalable and enables cost-effective, rapid and easy-to-use detection with minimal sample preparation.^[146-149]

Concept of Anharmonic acoustic Detection Technique

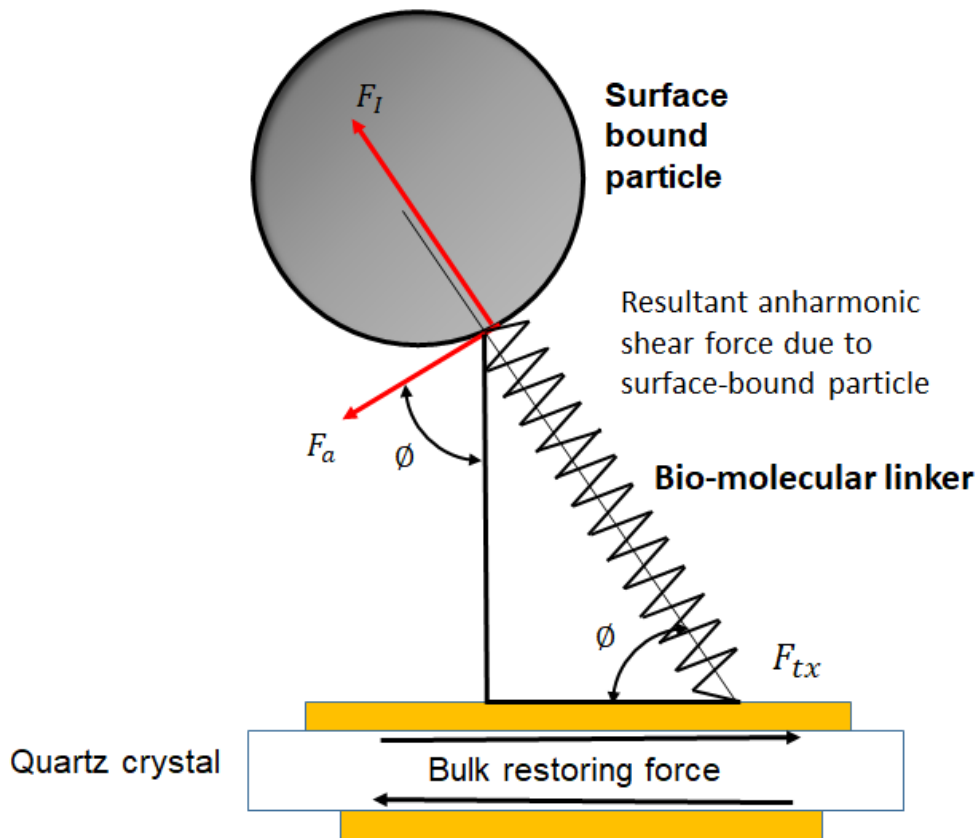


Fig. 2.11 - Concept of Anharmonic acoustic Detection Technique (ADT): Spring-mass model of a particle bound to an oscillating sensor surface via bio-molecular linker in liquid. The particle is modelled as a sphere, and the bio-molecular linker as an equivalent nonlinear spring of length (l). The force along the bio-molecular linker is given by F_l and the force perpendicular to the linker due to its angular stiffness is given by F_a and the horizontal component of the interaction force is given by F_{tx} . Adapted and modified from ^[146,147].

2.4.4.2 Bio-receptors

The bio-receptor responsible for recognising the target analyte can either be a:

- biological material: enzymes, antibodies, nucleic acids and cell receptors, or;
- biologically derived material: aptamers and recombinant antibodies, or;
- biomimic: imprinted polymers and synthetic catalysts.^[84,89,100]

Bio-receptors of different sizes and lengths have been explored that could be then integrated with ADT transducer for detection of target bacteria and are discussed in chapters 4, 5 and 6.

2.5 Target bacteria

ADT have been earlier used to sensitively detect *Bacillus subtilis* spores but not used for detecting pathogen as a whole. Hence, ADT technique has been used here for on-site detection of the *Escherichia coli* (*E.coli*) bacteria as a “model organism” because of the following reasons:

- a) *E.coli* bacteria are typically commensal bacteria of warm-blooded animals. They are often used as indicators for the presence of AMR in monitoring and surveillance programs, given the availability of simple and efficient isolation procedures.^[150,151]
- b) Easy handling in laboratory: *E.coli* has been widely studied for it is easy to maintain and breed in a laboratory setting owing to its particular experimental advantages.^[152]
- c) Indicator of water and food safety: It gets transmitted by the consumption of contaminated water and food. Even though most of the *E.coli* strains found in water or food are not virulent, the detection of *E.coli* is still crucial to the monitoring of water and food safety because the existence of *E.coli* indicates that microbial contamination is high.^[152]

2.6 Summary

Both pathogen identification and phenotypic AST should be fast to reduce the length of diagnostic cycle. As it is unlikely to shorten the time required to conduct phenotypic AST, the initial pathogen detection and identification step needs to be reduced, to abridge the overall time of the diagnostic cycle. This will help clinicians to initiate appropriate treatments quickly. Culture-dependent methods are very time-consuming and are currently considered obsolete. Therefore, in this chapter the most commonly used culture-independent rapid diagnostic methods were reviewed including, nucleic acid-based methods (PCR, mPCR, qPCR, NASBA, LAMP), immunological methods (ELISA, LFI), mass spectrometry-based method (MALDI-TOF-MS) and biosensor-based methods (optical, electrochemical and acoustic biosensors).

Detection of whole-cell bacteria is important so that they can be further utilised for subsequent determination of antibiogram. However, nucleic acid-based

methods are genotypic tests and do not permit isolating pathogens for further use. Immunological tests can detect whole-cell bacteria but in these methods also, bacteria cannot be recovered for AST. New method has been tried to identify lipid A directly on intact bacteria with MALDI-TOF mass spectrometry, but it is laborious. Optical and acoustic biosensors allow detection of whole-cell bacteria, but there are very few examples of application of electrochemical biosensors for detection of whole-cell bacteria. Furthermore, biosensor-based methods allow label-free detection of bacteria, except for optical label-based biosensors. Nucleic acid-based methods and immunological methods are also label-based and require laborious labelling processes, making them costly and this may also interfere with the function of the bio-receptor. Methods like PCR, ELISA or MALDI-TOF-MS also require specialised equipment and trained personnel to operate the system. Optical biosensors are bulky in size and the set-up method of electrochemical biosensors is very complicated, making them both difficult to be translated as POCT. Although, portable SPR biosensors have been fabricated the cost of instrumentation is very high. LFIs are cheap and can be employed at the point-of-care but it is difficult to integrate them with electronics. While, ADT is an easy-to-use, integrable, low-cost technology that can be miniaturised and applied as POCT. LFIs suffer from higher false-positive rates than PCR and ELISA. On the other hand, ADT could potentially address this problem because of its intrinsic ability to differentiate specific and non-specific interactions, making diagnosis more reliable and reproducible. Moreover, it is also possible to maintain suitable temperature and grow bacteria within the microfluidic device integrated with ADT, to investigate antibiotic action on slow growing pathogens. Therefore, as ADT is integrable and can be applied at the point-of-care for rapid, label-free, low-cost, detection with high specificity which is lacking in most of the other methods, this technology was selected to explore its use for whole-cell bacterial detection.

Also, for the first time, different bio-receptors of different sizes and lengths are integrated with ADT transduction method for sensitive and specific detection of whole-cell *E.coli* bacteria, which are covered in chapters 4, 5 and 6. *E.coli* bacteria were selected as target analyte, owing to its applicability in AMR surveillance program and easy handling procedure in laboratory.

Chapter 3 Experimental considerations and methodology

3.1 Introduction

In this chapter, experimental methodology and materials used are described. The principle and theoretical concept of ADT technique is also discussed. ADT together with the TSM AT-cut quartz crystal resonator constitute the 'transducer element' of the biosensor. This technique can detect the surface-bound particles and also has the ability to differentiate between specific (target) and non-specific (non-target) interactions, which is lacking in most of the sensing techniques. But, to achieve high sensitivity and specificity with this transduction technique, in this chapter several experimental considerations were addressed: exploration of different electrode geometry; choice of mode of scan for measurements; selection of suitable bioassay format; validation of gold electrode surface cleaning method and achievement of stable baseline, before performing experiments with the target *E.coli* bacteria.

3.2 Transduction system: Concept and Experimental apparatus

3.2.1 Anharmonic acoustic Detection Technique (ADT)

ADT is based on the anharmonic acoustic modulation of the oscillator caused by the nonlinear interactions between the attached particles and the surface. Ghosh *et al.* have hitherto, investigated the bio-molecular linker interaction forces in a biosensor through experimentation and also have validated the results by means of numerical modelling. They have used this technique and studied the nonlinear acoustic response from a TSM AT-cut quartz crystal resonator with specific antibodies functionalised on its surface, to selectively detect *Bacillus subtilis* spores and distinguish them from physically adsorbed SCPM (streptavidin-coated polystyrene microbeads). Their work unveiled the prospective benefits of ADT like, sensitive, quantitative and selective detection of surface-bound particles.^[146-149] Because of these advantages, this technique has potential to be further employed for detecting pathogens and/or biomarkers, which can be used for controlling AMR in due course.

Concept of ADT:

The concept of anharmonic acoustic detection technique has been explained through quantitative modelling; where a surface-bound particle attached to the sensor surface via bio-molecular linker (or tether), is modelled as a spring-mass system.^[146,147] Figure 3.1 shows this model along with the factors involved.

The sensor used here is thickness shear mode (TSM) AT-cut quartz crystal resonator which transduces charge by piezoelectric effect. When the sensor is driven by a harmonic force with a pure sinusoidal signal of frequency f_0 , which is typically its fundamental resonant frequency, the sensor surface oscillates in-plane. At higher frequencies, the particles bound to the surface through linkers are apparently static due to inertia effects or partially follow the displacement of the sensor surface. As a result, the oscillation stretches the bio-molecular linker and opposing forces act along the linker, which are then passed onto the sensor. These forces due to surface-particle interaction alter the acoustic response of the sensor to an anharmonic one, which is then transduced into an electrical signal.

These forces acting on the sensor surface were investigated and a mathematical function was derived for the amplitude of the forces. Fourier analysis was applied to analyse this function and expressed as a Fourier series which contains harmonics with n times the excitation frequency, where n is an odd and non-zero number. The relative deviation in first harmonic ($1f$) is negligible.

Also, the amplitude of the harmonics decreases with increase in harmonic number [as shown in Fig. 3.1 (B)]. Therefore, among the higher odd harmonics, the shift in amplitude of the third harmonic ($3f$) was selected as a parameter for measurement of the anharmonicity of the consequent response.

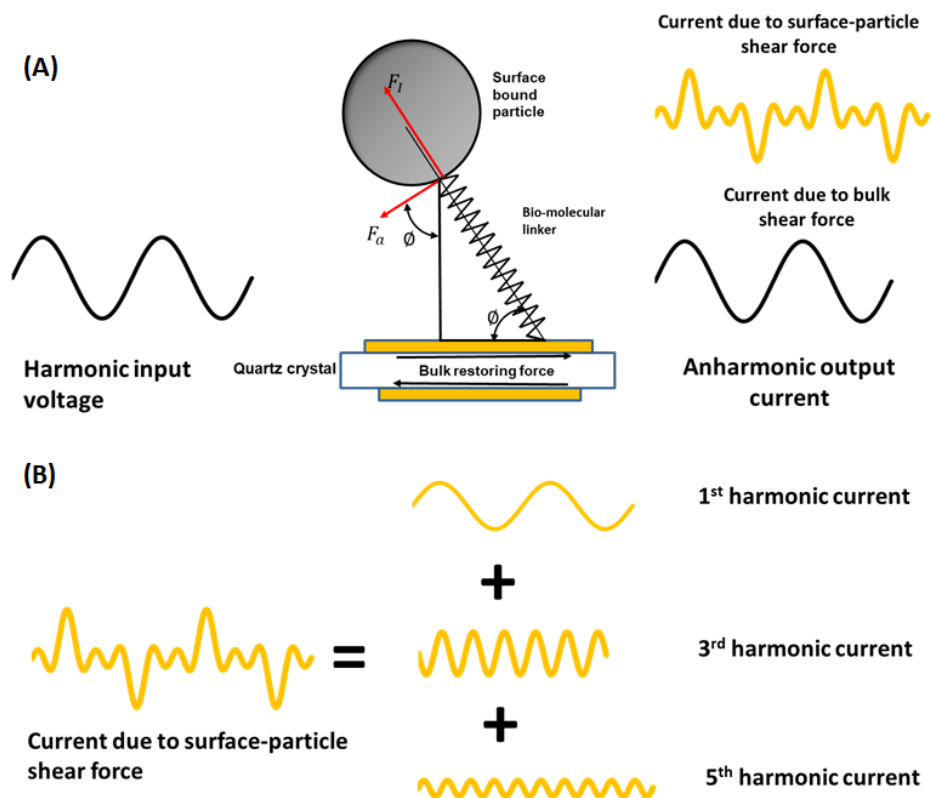


Fig. 3.1 – Concept of ADT: (A) Anharmonic output current comprised of current due to bulk shear force and surface-particle shear force and (B) Fourier analysis of current due to surface-particle shear force. Adapted and modified from ^[146,147].

3.2.2 Quartz crystal resonator (QCR) with gold electrodes

QCRs have been extensively used as TSM acoustic wave devices for detecting changes occurring on the surfaces of the quartz crystal. For many years, QCRs were used for mass measurement in vacuum^[140,141] and in gas-phase experiments and were called as quartz crystal microbalance (QCM), however; recently scientists realised that they can be used in contact with liquids and viscoelastic deposits. When the QCR comes in contact with a solution, there is a decrease in frequency that is dependent upon the viscosity and the density of the solution. For proper analysis and elucidation of experimental results, it is important to understand the behaviour of the QCR operating under total liquid immersion. This problem was first treated by Glassford, and later by Kanazawa and Gordon.^[153] They demonstrated that QCR measurements can be performed in liquid, in which case a viscosity related decrease in the resonant frequency will be observed as:

$$\Delta f = -fu^{3/2}[(\rho L \times nL)/(\pi \times \rho q \times \mu q)]^{1/2} \quad \text{Eqn. (1)}$$

Where,

f_u - frequency of oscillation of unloaded crystal,

ρq - density of quartz – 2.648 g . cm⁻³,

μq - shear modulus of quartz- 2.947.10¹¹ g.cm⁻¹.s⁻²,

ρL - density of the liquid in contact with the electrode, and

ηL - viscosity of the liquid in contact with the electrode.

There is decrease in resonant frequency as a result of damping of the resonant oscillation due to viscous coupling of the liquid medium onto the oscillating crystal surface. Thus, since the resonant frequency is affected by both mass and liquid loading, measurement of the resonant frequency alone cannot distinguish changes in surface mass from changes in solution properties. The viscous loss results in increase in resonance resistance, R, of the QCR. Thus, both Δf and ΔR measurements are typically used as independent indicators of mass loading and viscosity at the crystal-liquid interface of the QCR.^[153]

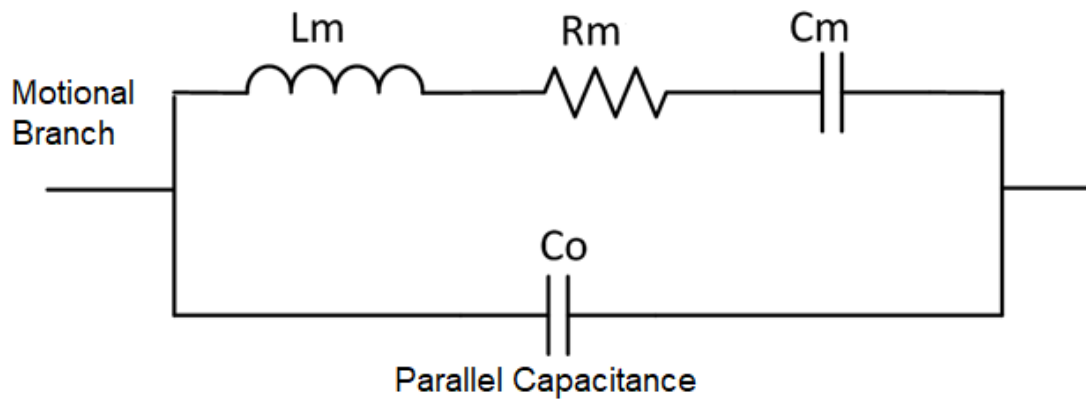


Fig. 3.2 - Butterworth Van-Dyke Model for a Piezoelectric Resonator: Equivalent circuit for a QCM under mass loading including parasitic capacitance (C_o). Adapted and modified from ^[154].

The electrical behaviour of the QCR is often described using an equivalent circuit model. The Butterworth-Van Dyke (BVD) equivalent circuit routinely used to describe the unperturbed (without mass or liquid loading) QCR as shown in Fig. 3.2. The BVD electrical model consists of two arms.

The “motional arm” has three series components modified by the mass and viscous loading of the crystal: (1) R_m (resistor) represents energy dissipated during oscillation, (2) C_m (capacitor) represents energy stored during oscillation (3) L_m (inductor) corresponds to the inertial component of the oscillation, which is related to the mass displaced during the vibration. Making electrical contact to a quartz crystal is done through electrodes on each face of the crystal. These electrodes introduce additional “static arm” capacitance (C_0) in parallel with the series RLC, as shown in the Fig. 3.2. It has not been meticulously demonstrated that the BVD circuit model is an appropriate description for the loaded QCR, but it has been used extensively by many researchers, as the impedance measurements made on liquid-loaded QCRs could be fitted well with this model.

The mechanical interactions between the QCR and the contacting liquid influence the electrical characteristics of QCR, especially near its resonance, where the amplitude of the oscillation is maximum. To evaluate the electrical characteristics of QCR, the electrical admittance is used, which is defined as the ratio of current flow to applied voltage. For analyses purposes, the measured admittance data was fitted to the BVD model to extract the values of three equivalent circuit parameters Q (quality factor), R_m (motional resistance), and f_0 (resonance frequency).

Martin *et al.* have also applied BVD circuit model, to derive a linear relationship between the change in series resonance resistance, ΔR , of the quartz oscillator and $(\rho L \cdot \eta L)^{1/2}$ under liquid loading, which is given by following equation:^[154]

$$\Delta R = \left[n \cdot \omega_s \cdot \frac{L_u}{\pi} \right] \cdot \left[\frac{2 \cdot \omega_s \cdot \rho L \cdot \eta L}{\rho q \cdot \mu q} \right]^{1/2} \quad (\text{Eqn. 2})$$

Where,

ΔR - change in series resonance resistance, in Ω ,

n - Number of sides in contact with liquid,

ω_s - angular frequency at series resonance(=2.π.f_s, where f_s is the oscillation frequency in solution in Hz), and

L_u - Inductance for the unperturbed (i.e. dry) resonator, usually in mH.

Dimensions of QCR with gold electrodes

TSM quartz crystal resonators used were 8.3 mm in diameter and 112 μm in thickness with fundamental resonant frequency range of 14.275 -14.325 MHz (Lap-Tech Inc., Bowmanville, Ontario, Canada). They were made from optically polished AT-cut quartz, cut at an angle of $35^\circ 15.0 \pm 1'$ to the crystal optical axis. The crystals had excellent frequency stability with operating temperature range between 20°C to 40°C . The quartz substrate was sandwiched between evaporated layers of gold keyhole-styled electrodes of 165 nm uniform thickness, with 5 mm and 4 mm diameters, respectively, as shown in Fig. 3.3.

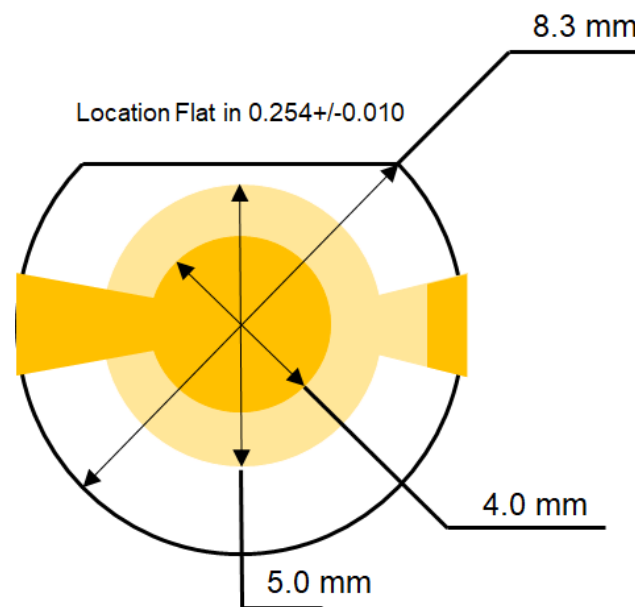


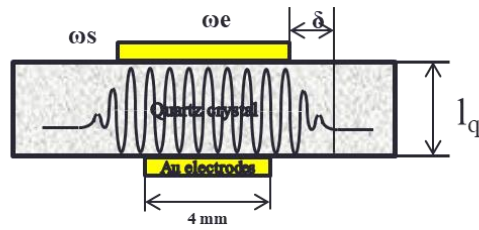
Fig. 3.3 – Schematic of Quartz Crystal Resonator with gold electrodes obtained from Lap-Tech Inc., Canada.

For all applications that require use of QCR, it is important to reduce or eliminate the unwanted spurious responses; this can be achieved by improving the electrode geometry, thereby, improving the performance of QCR. Shockley *et al.* had postulated that to obtain a strong resonance and to suppress these unwanted spurious responses, energy trapping by partial loading (deposition of extra mass) is vital.^[155] Energy trapping has been known and used for a long time in TSM quartz crystal resonators and its basic theory is discussed in next section.

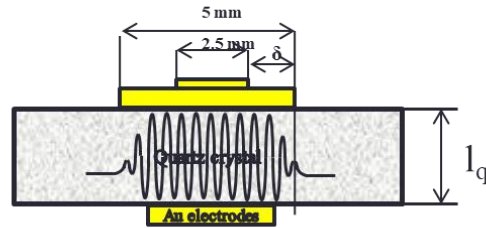
3.3.2.1 Energy trapping concept

The concept of energy trapping was first introduced by Mortley in 1946,^[156-158] but it remained relatively unknown and its significance was not recognised, until his results were rediscovered independently by Shockley *et al.* in 1967.^[154] They applied the energy trapping theory to a simplified model of a TSM AT-cut quartz crystal (or wafer), by partially loading it with extra mass. They also gave an approximate mathematical theory to explain the phenomenon of energy trapping in rectangular crystals, where the thickness-shear vibrations in a partially electroded quartz crystal can be confined to the area under and close to the electroded region of the crystal.^[155]

This concept was also applied to the circular AT-cut quartz crystals by Efimov *et al.*, where they even investigated the variation in sensitivity of QCR in response to energy trapping effect. They reiterated that “energy trapping” means the total inner reflection of the acoustic wave generated in the electroded area from the boundary with the non-electroded part of the crystal. Moreover, they further focussed the oscillation energy by partially loading the gold electrode of QCR with extra copper deposits in the centre as well as, at controlled locations.^[159] They observed that the central copper deposit (as shown in Fig. 3.4) not only shifted the resonant frequency of the QCR but also changed the shape and magnitude of the sensitivity curve. The sensitivity decreased near the boundary of the electrode and the quartz, but increased close to the copper deposit, to a peak at the centre that is higher than the value for the unloaded gold electrode.^[159] Thus, it was observed that the energy trapping effect not only suppresses the spurious modes but also increases the sensitivity of the QCR by confining the oscillations to the region of additional loading. Hence, this effect was further explored in terms of anharmonic acoustic detection technique and the electrode geometry was modified to stepped (non-uniform) crystals, by loading the gold electrodes of QCR with central gold deposits.



(a) Uniform crystal



(b) Stepped (non-uniform) crystal – Energy trapping

Fig. 3.4 – Schematic representation of spatial distribution of oscillation at a QCR with thickness (l_q) in case of: (a) uniform crystal (b) stepped (non-uniform) crystal. The distance δ represents exponential decay of the oscillation from the edge of: (a) the electrode area and (b) the localised metal deposit. Adapted and modified from ^[159].

3.2.2.2 Preparing the stepped (non-uniform) crystals

The QCRs with stepped electrodes were prepared by following three steps: (1) Preparing the substrates for gold sputtering, (2) Gold sputtering, and (3) Thickness measurements.

Preparing the substrates for gold sputtering:

The area of the gold electrode of QCR that was not supposed to be coated with gold was masked. But, the central circular area with diameter of 2.5 mm (to be coated with gold) was left unmasked (as depicted in Fig. 3.5). The substrates thus prepared, were then sputtered with gold using Q150T ES System.

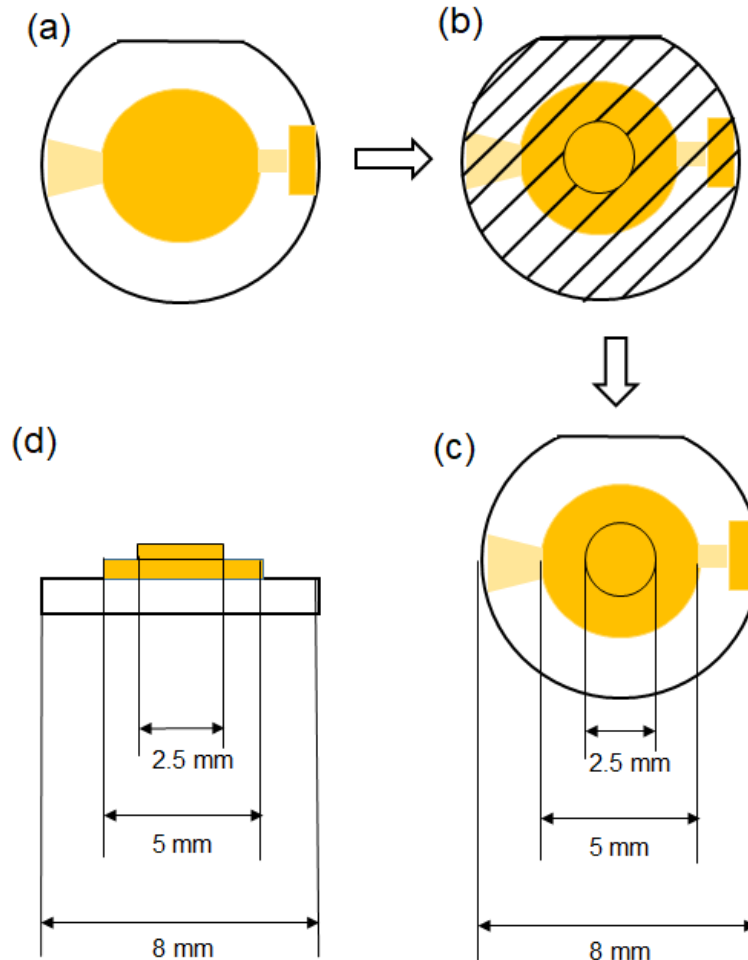


Fig. 3.5 – Preparation of stepped (non-uniform) crystals: (a) Top view of gold electrode of quartz crystal (b) Central circular area of gold electrode (diameter 2.5 mm) left unmasked (c) Top view and (d) Side view of stepped (non-uniform) crystals after gold sputtering.

Gold sputtering:

Q150T ES System was used for sputtering the gold electrodes with another layer of gold in centre. The coating thickness is proportional to the square of the distance between the stage height and the rods (loaded with small quantity of gold to be evaporated). Also, the thickness of the gold to be deposited can be controlled by changing the property of current and the time for which it is passed. With a current of 20 mA, a deposition rate 20 nm/min is typically achieved. So after setting material to gold and passing 20 mA current for ~180 milliseconds, gold deposition of thickness ranging from 60 nm to 70 nm was achieved on the substrates.

Thickness measurement:

The thickness of the sputtered crystals was measured using Zygo NewView 5000. The Zygo NewView 5000 is a non-contact 3D surface profiler that uses scanning white light interferometry to image and measure the microstructure and topography of surfaces. It provides graphic images and high-resolution numerical analysis to accurately characterise the surface structure of test parts. Figure 3.6 shows vertical step height measured of typical stepped (non-uniform) crystal using Zygo NewView 5000.

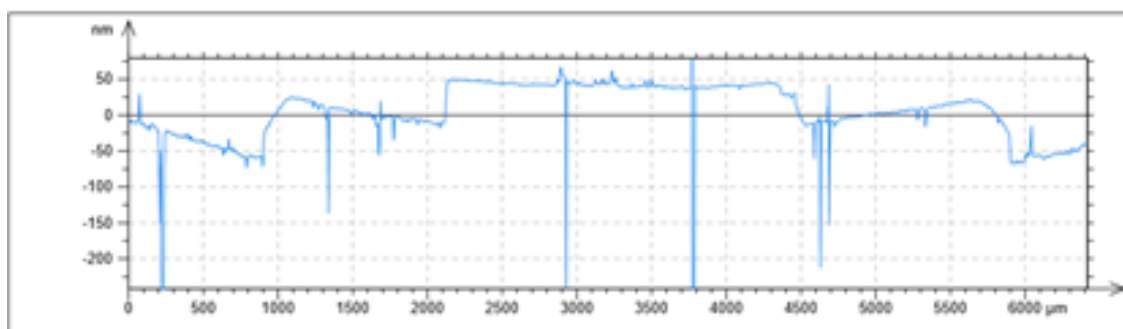


Fig. 3.6 - Vertical step height measured of stepped crystal using Zygo NewView 5000.

3.2.2.3 Demonstration of energy trapping with ADT

To demonstrate the energy trapping effect on the ADT signal, pilot experiments were performed, where QCRs with the uniform and stepped electrodes were used to detect the streptavidin-coupled beads. The anharmonic acoustic response from both the sensors was compared.

Experimental procedure:

QCRs with the uniform and stepped (~ 65 nm height) electrodes were cleaned as per procedure given in section 3.3.5 (c). Then, both the cleaned quartz crystals were immersed in about 250 μL of 1mM ethanolic solution of mixture of thiols [biotin terminal group (10%), and methoxy terminal group (90%)] and left overnight for formation of a self-assembled monolayer (SAM). Next day, the crystals were then washed with ethanol in a well 3 times, followed by flowing de-ionised (DI) water. Phosphate buffer saline (PBS) solution was then flowed over the surface of each crystal at the flow rate 10 $\mu\text{L}/\text{min}$ and

then baseline measurements were taken over 20 mins. Streptavidin-coupled Dynabeads[®] (Thermo Fisher Scientific, UK) with 2.8 μm diameter were used as analyte, at concentration 10^7 beads per mL of PBS. 100 μL of beads were flowed over the surface at 10 $\mu\text{L}/\text{min}$ flow rate for further 15 mins.

Resonant frequency (f_0) was determined with frequency sweep and the sensor was then driven by a pure sinusoidal oscillation at f_0 in amplitude mode scan. Three successive 1s AMS scans were taken every 5 mins after stopping the flow for baseline measurement and similarly after flowing streptavidin-coupled beads. The maximum (terminal) values of the $3f$ current were plotted as seen in the Fig. 3.7, for both the crystals with uniform and stepped electrodes.

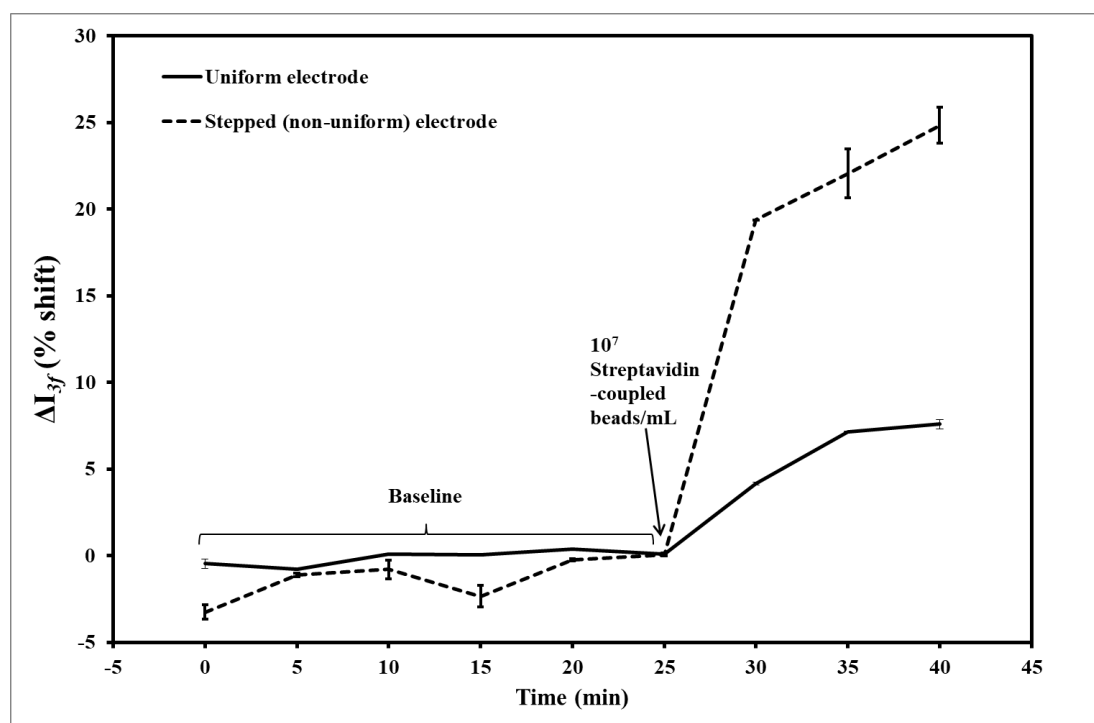


Fig. 3.7 – Last values of $3f$ current plotted for detecting streptavidin-coupled beads using QCR with uniform and stepped (non-uniform) electrodes (Surface – 10% Biotin thiol and 90% OCH₃ thiol / AMS scan 0.5 amp /1s scan).

Results and discussion:

The terminal values of modulus of $3f$ current for all the scans are plotted in Fig. 3.7. The baselines were recorded for both QCRs with uniform and stepped electrodes over 20 mins, with %CoV as -4.1% and -1.0%, respectively. A shift of 7.6% was seen in $3f$ signal after passing streptavidin-coupled beads over QCR with uniform electrode. However, almost three times shift of 24.8% was recorded after passing the beads over stepped (non-uniform) crystal. Thus, it was observed that the sensitivity of the QCR increased dramatically by loading it with central gold deposit (~ 65 nm height) and concentrating the oscillations to loaded area through energy trapping effect. Thus, QCRs with central gold deposits i.e. stepped crystals were used for all further experiments.

3.2.3 Transduction system check-up

It is a good practise to test the sensor parameters, in order to optimize equipment performance or to detect faults at an early stage; because an erroneous parameter characterisation can lead to misinterpretation of the data measured during the experiment. Operation at increasing glycerol concentrations is an excellent test of a QCR experimental setup, and should provide predictable results up to more than 70% glycerol. Therefore, the effect of the variation of the density of the glycerol and water mixture (% w/w) in contact with the surface of the QCRs with stepped (non-uniform) electrode was compared to that with uniform electrode. A comparison was made against the theoretical predictions of equations 1 and 2. Thus, both frequency shift in Hz (Fig. 3.8 and 3.9) and resistance shift in ohms (Fig. 3.10 and 3.11) were measured and compared with the values calculated from the equations.

In both the crystals (uniform and stepped), an agreement between measured and expected values was within +/- 25% which is generally considered acceptable for glycerol concentrations up to 70%. Although, slight deviation from the equations was observed after introducing 70% glycerol/water mixture (% w/w) over the surfaces, as glycerol becomes inhomogeneous after 70% in water.^[160] Thus, the QCRs with stepped electrodes were validated for

experimental use with ADT technique, as their behaviour in liquid medium is similar to that with uniform electrodes.

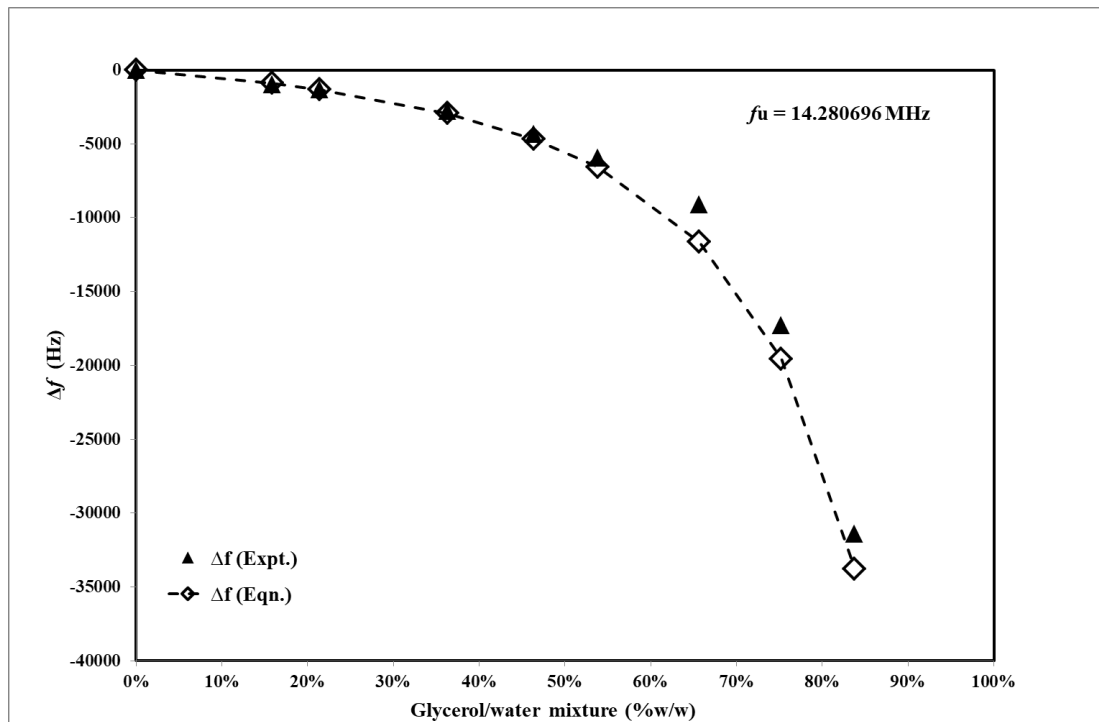


Fig. 3.8 - Frequency shift (Hz) after loading the Uniform crystal ($f_u = 14.280696$ MHz) with titrations of glycerol/water (%w/w).

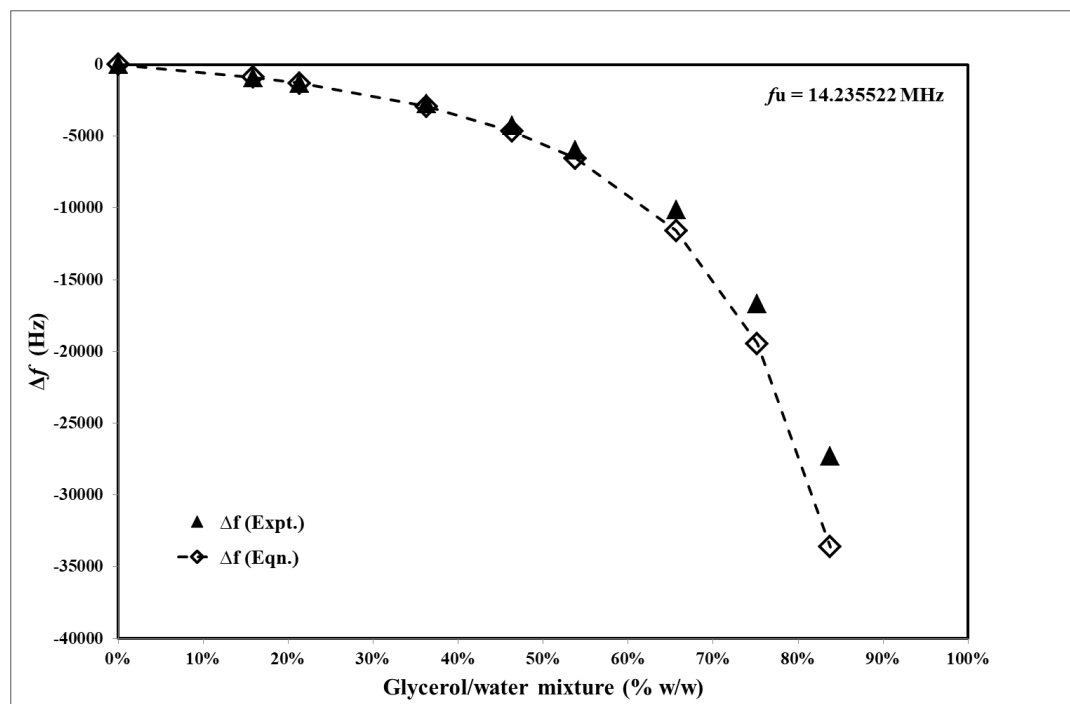


Fig. 3.9 - Frequency shift (Hz) after loading the Stepped (non-uniform) crystal ($f_u = 14.235522$ MHz) with titrations of glycerol/water (%w/w).

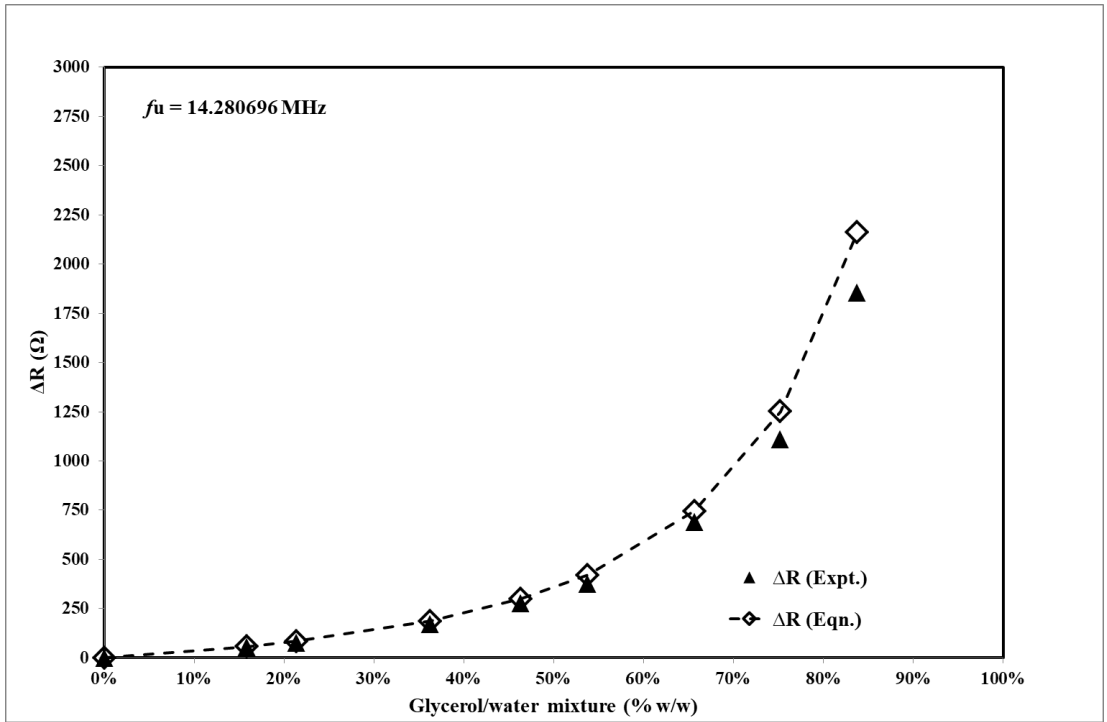


Fig. 3.10 - Resistance shift in ohms (Ω) after loading the Uniform crystal ($f_u = 14.280696 \text{ MHz}$) with titrations of glycerol/water (%w/w).

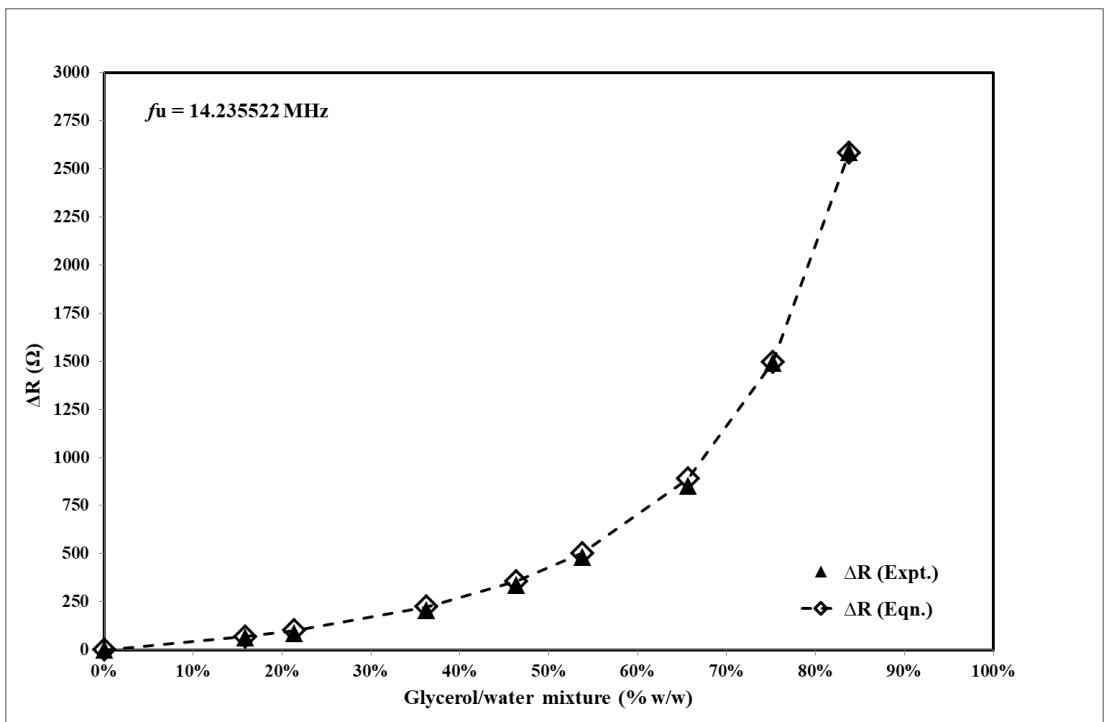


Fig. 3.11 - Resistance shift in ohms (Ω) after loading the Stepped (non-uniform) crystal ($f_u = 14.235522 \text{ MHz}$) with titrations of glycerol/water (%w/w).

3.2.4 Selection of mode of scan for experiments

ADT allows measurements of response on fundamental resonance and higher harmonics to the signal of varied amplitude applied to fundamental resonance only. There are generally two modes of scans used for measurements:

(1) Frequency mode scan (FMS scan): In this mode, the sensor is driven at a fixed frequency (the resonant frequency) and amplitude, for specified time span. The frequency span could be varied between 0 and 200 kHz.

(2) Amplitude mode scan (AMS scan): In this mode, the sensor is driven at a fixed frequency (which is equal to the fundamental resonant frequency obtained from preceding FMS scan), for specified amplitude ramp (start and finish value, amplitude linearly increasing with time) and for specified time span. The highest amplitude applied is 0.5 Standard Units (SU), which equals an excitation voltage of 15 Volts (1 SU equals 30 Volts).

In both the modes, shift in the peak (or maximum) values of $3f$ current (I_{3f}) is measured, as an anharmonic response for quantitative detection of analytes (at different concentrations) after binding with corresponding bio-receptor. Both FMS and AMS scans are preceded by FMS scans at 0.02 SU to determine resonant frequency (f_0). However, for AMS scans it is imperative to determine f_0 values before each scan to get maximum response. Consequently, real-time measurements are difficult to obtain with AMS mode scan, as the driving frequency needs to be reset to resonant frequency before each scan. Thus, both the scan modes were tested to determine whether the relative shift in I_{3f} values are affected or not, if the driving frequency is not reset to f_0 . Titrations of glycerol and water were flowed over the surface of QCR and corresponding I_{3f} values were obtained in both AMS and FMS mode scan.

In AMS mode scan, the driving frequencies were selected at f_0 and varied around it: from f_0-3 kHz to f_0+3 kHz with amplitude ramp of 0.5 SU, as shown in Figure 12. The corresponding maximum values of I_{3f} after passing titrations of glycerol/water (% w/w), are plotted in Fig. 3.13. Similarly, FMS scans were taken at fixed f_0 (with span 200 kHz) and amplitude of 0.5 SU; and the

corresponding peak values of I_{3f} curves are plotted in Fig. 3.14. The resonant frequency (f_0) shifted by ~ 0.5 kHz and ~ 1 kHz with 20% and 30% Glycerol/water mixtures, respectively. In Fig. 3.13, the I_{3fmax} on 20% Glycerol/water curve (b') corresponds with the resonant frequency after resetting the driving frequency to f_0 (-0.5 kHz). While the I_{3fmax} corresponding to 0 kHz which is initial driving frequency f_0 for 10% Glycerol/water mixture, is less than that observed at -0.5 kHz i.e. $b' > b$. Same is the case, with 30% Glycerol/water curve, where $c' = I_{3fmax}$ at -1kHz (after resetting) and $c = I_{3fmax}$ at 0 kHz (without resetting) and $c' > c$. Thus, with AMS scans if the driving frequency is not reset to resonant frequency, the true maximum values are not captured, as it does not take into account the lateral (resonant frequency f_0) and vertical (amplitude of I_{3f}) shift after viscous loading, as shown in Fig. 3.13. So, there is need to reset the driving frequency to f_0 before each measurement, which adds one more step to experiment making real-time measurements difficult. However, with FMS scan as depicted in Fig. 3.14, both the shifts in amplitude of I_{3f} as well as in resonant frequency f_0 are accounted for and the peak values give the precise extent of change in signal without resetting the driving frequency to f_0 after each measurement.

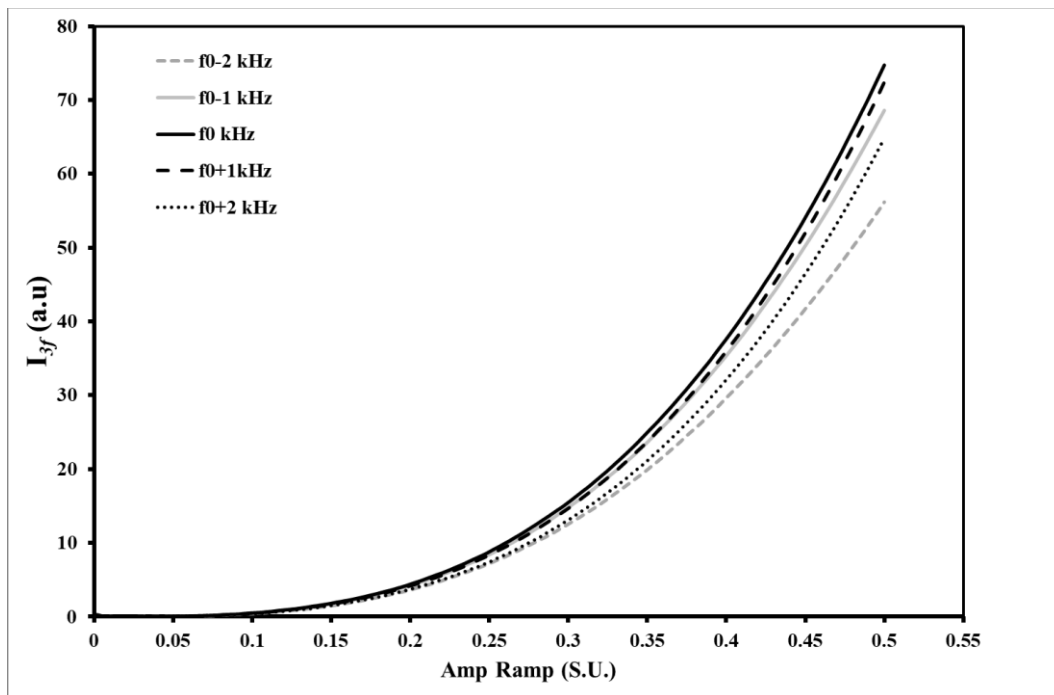


Fig. 3.12 – Graph showing AMS scans (0.5 SU) taken at resonant frequency (f_0) and from $f_0 - 2$ kHz to $f_0 + 2$ kHz after flowing 10% Glycerol/water mixture (% w/w).

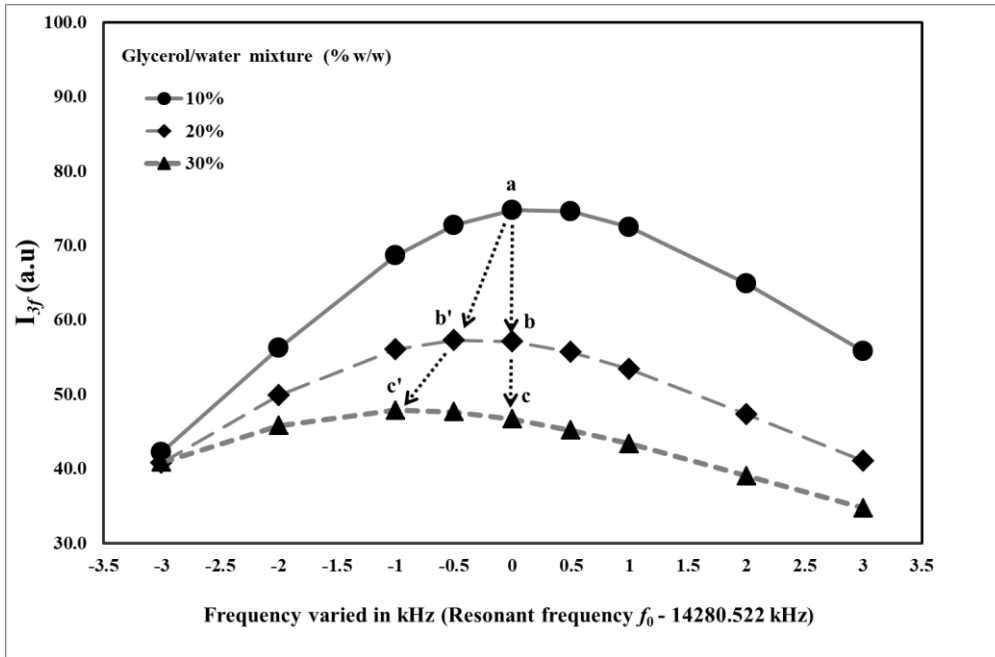


Fig. 3.13 – Graph showing last (maximum) values of I_{3f} with AMS scans (0.5 SU) after flowing titrations of Glycerol/water (% w/w) – (a) I_{3fmax} for 10%; (b) & (c) I_{3fmax} for 20% and 30% without resetting the driving frequency to f_0 ; and (b') & (c') I_{3fmax} for 20% and 30% after resetting the driving frequency to f_0 .

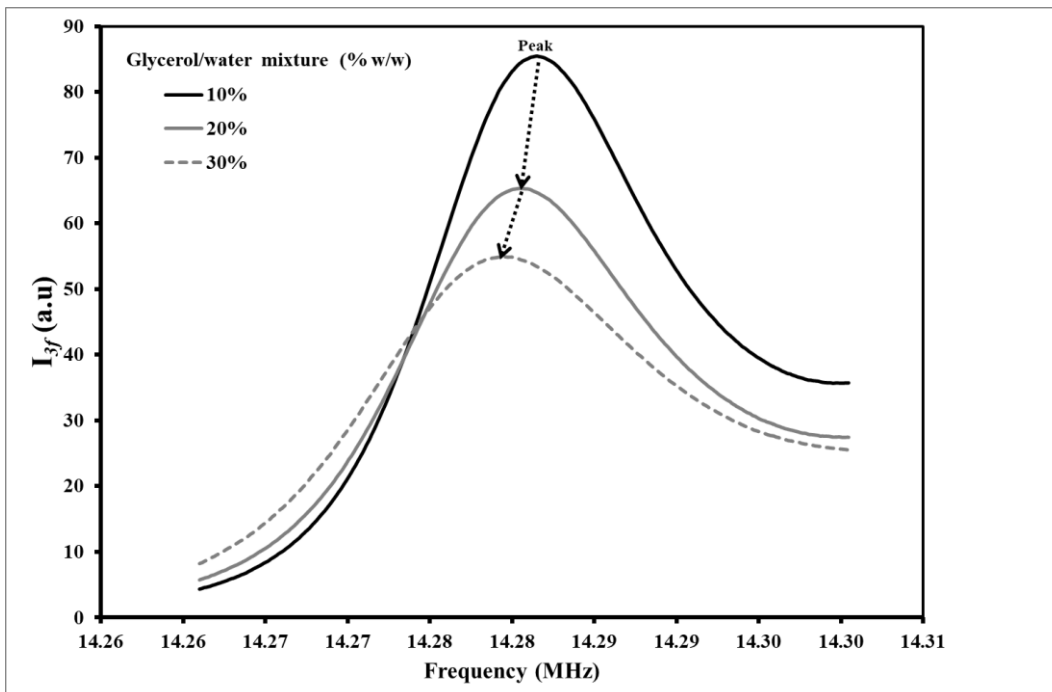


Fig. 3.14 – Graph showing I_{3f} curves with FMS scans (0.5 SU) after flowing titrations of Glycerol/water (% w/w). The arrows point towards the peaks of the curves (I_{3fmax}).

3.2.5 Surface cleaning of gold electrodes

Over the last two decades, there has been growing interest in surface science to design surfaces with tailored properties; as this has application predominantly in biosensor studies. Molecular level of control over surface can be achieved through controlled grafting of monolayers. The main route to achieve this level of control over surface modification is to use self-assembled monolayer (SAM).^[161] It is important that monolayer forming molecules should align on the surface with exactly the same orientation and also to avoid defects there should be perfect packing of the monolayer. For this, the substrate on which the monolayer is formed should be clean and devoid of contamination layer. The gold electrodes of QCR were used as substrate for all the experiments.

The properties of an alkanethiolate SAM formed on gold primarily depends on the immersion time, the solvent used, and purity of the thiol and on the quality of the gold substrate.^[162] The roughness and cleanliness of the immersed substrate is of crucial importance for the quality of the monolayer. There are a variety of techniques for cleaning the surface before depositing the SAM. These include exposure to a powerful oxidising mixture of concentrated sulphuric acid and hydrogen peroxide (Pirahna solution),^[162] and the less aggressive solution comprising of hydrogen peroxide, ammonium and water,^[163] electrochemical potential cycling, UV photo-oxidation,^[164] ozonolysis,^[165] thermal desorption,^[166] and dry cleaning methods include UV/ozone treatment, and etching in oxygen or argon plasma. The sensitive nature of the metal (gold) surfaces requires avoidance of harsh cleaning procedures. Therefore lately, there has been growing importance of plasma cleaning as surface treatment. Thus for the experiments, the substrates used i.e. gold electrodes of QCR were first treated with organic solvents and then cleaned with argon plasma. To arrive at optimal cleaning procedure, the surfaces were characterised by measuring contact angles and with X-ray photoelectron spectroscopy (XPS) measurements.

Chemicals and materials used: All solvents and chemicals were of reagent quality and were used without further purification. For cleaning quartz crystals

acetone, isopropyl alcohol (IPA) and ultra-pure 200-proof ethanol (Sigma-Aldrich, USA) were used.

Substrate preparation: Cleaning procedures were investigated by preparing the substrates under different conditions, described as follows:

- a) **As received (AR):** QCR with gold electrodes, as received from Lap-Tech Inc., Bowmansville, Ontario, Canada were used.
- b) **Organic solvent treatment (OST):** The substrates were cleaned with acetone for 5 mins; then with IPA by ultra-sonication process for 5 mins. After that they were dried with nitrogen gas and then stored in a well of clean 24-well tissue culture plate, containing 250 μL of ethanol.
- c) **Organic solvent plus Argon plasma treatment (OST+APT):** After cleaning the substrates with OST, they were further cleaned with argon plasma for 1 min in a Harrick Plasma cleaner. They were then stored in a well of clean 24-well tissue culture plate covered with plastic film.
- d) **Organic solvent, Argon plasma plus Ethanol treatment (OST+APT+ET):** After cleaning the substrates with OST+APT, they were then stored in a well of clean 24-well tissue culture plate, containing 250 μL of ethanol.

Contact angle measurements:

The substrates were prepared as described above and then carried to the LMCC Analysis suite in Chemical Engineering Building to measure surface contact angle. Contact angles measurements were determined by sessile drop technique at ambient temperature in atmospheric conditions, where a droplet of liquid was placed on the solid surface using a syringe or a micropipette.

For each type of surface two drop sizes were used viz. 1 μL and 2.5 μL and the apparent contact angles were measured using a microscope equipped with an instrument. All reported contact angles are the average of at least three measurements taken at different locations on the substrate for three different crystals and have a maximum error of $\pm 4^\circ$.

The static contact angles measured were more or less same for the two drop sizes used viz. 1 μL and 2.5 μL (volume). It was observed that substrates with AR, were borderline hydrophobic with static contact angles as $90.56^\circ (\pm 4.23^\circ)$ for 1 μL and $94.02^\circ (\pm 0.32^\circ)$ for 2.5 μL drop sizes, indicating that they had contamination layer over the surfaces.^[167,168]

Also, the substrates treated with only OST were slightly contaminated as the static contact angles measured were $87.72^\circ (\pm 3.70^\circ)$ for 1 μL and $88.94^\circ (\pm 1.75^\circ)$ for 2.5 μL drop sizes. The static contact angles for the substrates cleaned with OST+AT were $<40^\circ$ viz. $33.07^\circ (\pm 0.45^\circ)$ and $39.00^\circ (\pm 0.41^\circ)$ for 1 and 2.5 μL drop sizes, respectively. But when the substrates were further immersed in ethanol, the contact angles increased to $62.33^\circ (\pm 0.75^\circ)$ and $71.64^\circ (\pm 0.83^\circ)$ for 1 and 2.5 μL drop sizes, respectively. Thus, the crystals treated with OST+APT were more hydrophilic and clean than the ones immersed in ethanol OST+APT+ET; possibly due to contamination, to a much lesser extent, upon exposure of the cleaned surface to ethanol and ambient conditions. The results from the static-contact-angle measurements versus droplet volume for all the surfaces of the different substrates cleaned with different treatments are given in Table 3.1.

X-ray photoelectron spectroscopy (XPS) measurements

XPS measurements were carried out with a Thermo Scientific K-Alpha spectrometer using a monochromatic Al K α X-ray source (Ion Gun Operating range: 100 eV - 4 keV) with a spot size of 400 μm . The survey spectra were collected over a range of -10 to 1350 eV with pass energy of 200 eV. The high resolution spectra over the Au 4f, C1s, O1s, S2p, and N1s regions were acquired with pass energy of 50 eV.

The substrates were prepared as described above (AR, OST, OST+APT and OST+APT+ET) and then carried to the LMCC Analysis suite in Chemical Engineering Building where the Thermo Scientific K-Alpha spectrometer equipment is located.

In XPS, the surfaces of the substrates were irradiated with X-rays. This excited photoemission from the core levels of the atoms present on the

surface and the resulting photoelectrons emerging from the surface were collected and their energy was analysed. The kinetic energy of a photoelectron depends on the binding energy of electrons in the core levels from which photoemission is excited and each element gives rise to a set of peaks at characteristic energies. Thus, the following Figure 3.15 showing photoelectron spectrum for the different substrates allows identification of the elements present on their surfaces.




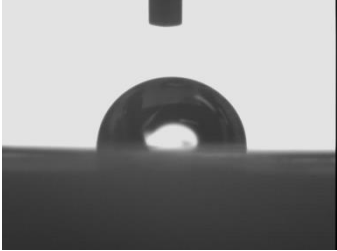
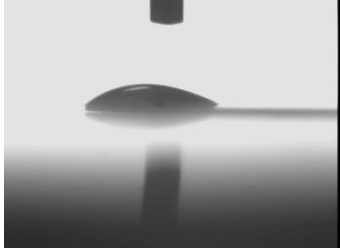
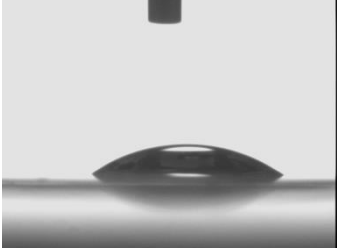
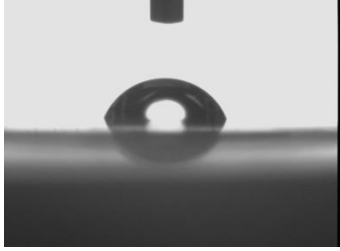
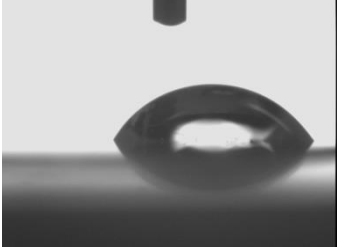
The XPS spectra showing surveys of entire surface for AR and OST+APT are almost overlapping each other with high peaks for gold indicating no contaminants on the surface. For substrates treated with OST+APT+ET the gold peak was comparatively lower, suggesting contamination to lesser extent, as confirmed from the high resolution spectra for Au 4f (Fig. 3.16).

High resolution spectra over Au 4f (Fig. 3.16) demonstrated that the peaks were higher for relatively cleaners surfaces – AR and OST+APT. Also, the high resolution spectra over C1s and O1s (Fig. 17 and 18) showed that peaks were high for substrates treated with OST and OST+APT+ET, but comparatively, lower for OST+APT. However, the peak for O1s for OST+APT was slightly higher than for AR. For substrate treated with organic solvent, there is no peak for gold but high peaks for C1s and O1s as seen in Fig. 17 and 18 showing high contamination.

Contact angle measurements provide an easy tool for the routine control of surface contamination on metals. Although, they give no direct information on the chemical composition of the contaminant, however correlating these measurements with XPS survey data provided accurate characterisation of the contaminants.

The substrates treated with organic solvent and then with argon plasma (OST+APT) were found to be hydrophilic and cleaner with comparatively less contaminants on the surface, as confirmed from XPS measurements. Further immersing in ethanol contaminated them to a lesser extent. Therefore, for all the experiments the substrates were cleaned with organic solvents first and then with Argon plasma for 1 min; and subsequently immersed them into the thiol solution directly rather than in ethanol to avoid contamination.

Table 3.1 – Static contact angles

Substrates	Static contact angles	
	1 μ L drop	2.5 μ L drop
AR	 90.56° (\pm 4.23°)	 94.02° (\pm 0.32°)
OST	 87.72° (\pm 3.70°)	 88.94° (\pm 1.75°)
OST+APT	 33.07° (\pm 0.45°)	 39.00° (\pm 0.41°)
OST+APT+ ET	 62.33° (\pm 0.75°)	 71.64° (\pm 0.83°)

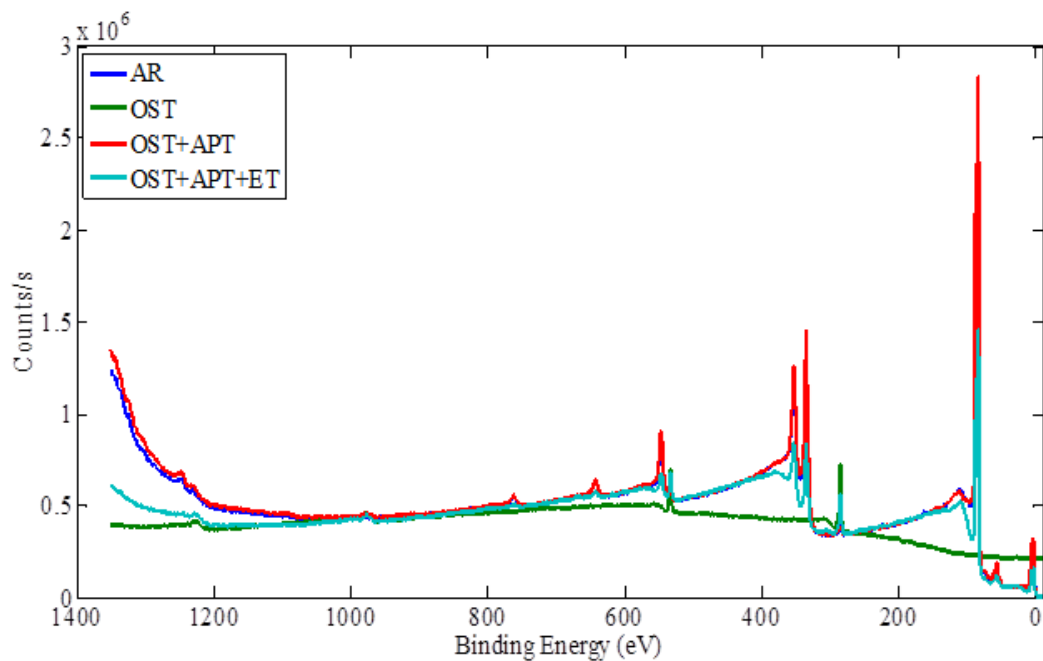


Fig. 3.15 - XPS spectra showing comparison of surveys for different substrates – As received (AR), Organic solvent treatment (OST), Organic solvent plus Argon plasma treatment (OST+APT) and Organic solvent, Argon plasma plus ethanol treatment (OST+APT+ET).

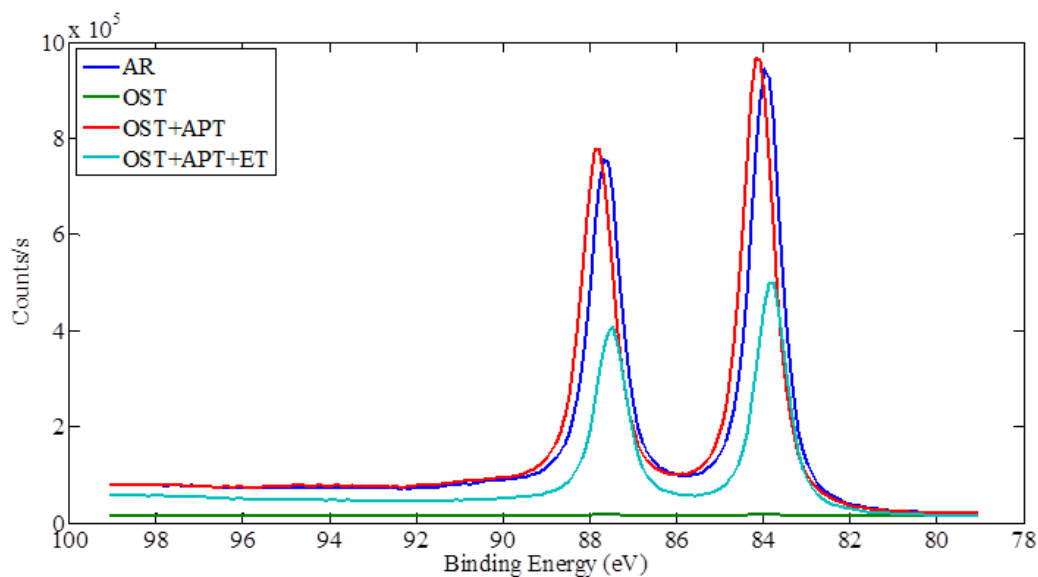


Fig. 3.16 - High resolution spectra over the Au 4f for different substrates – As received (AR), Organic solvent treatment (OST), Organic solvent plus Argon plasma treatment (OST+APT) and Organic solvent, Argon plasma plus Ethanol treatment (OST+APT+ET).

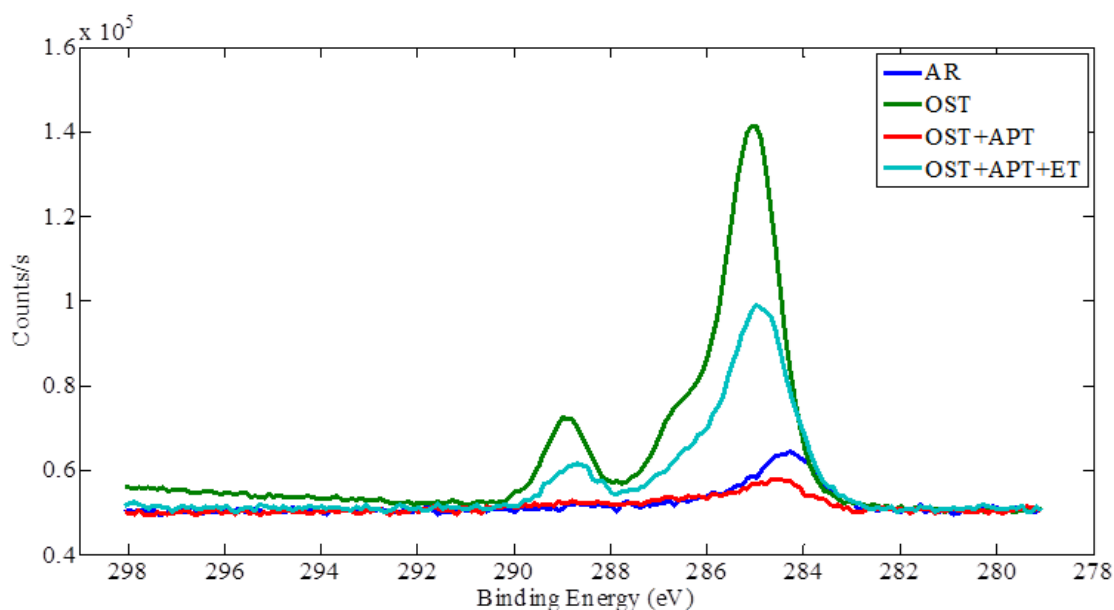


Fig. 3.17 - High resolution spectra over the C1s for different substrates – As received (AR), Organic solvent treatment (OST), Organic solvent plus Argon plasma treatment (OST+APT) and Organic solvent, Argon plasma plus Ethanol treatment (OST+APT+ET).

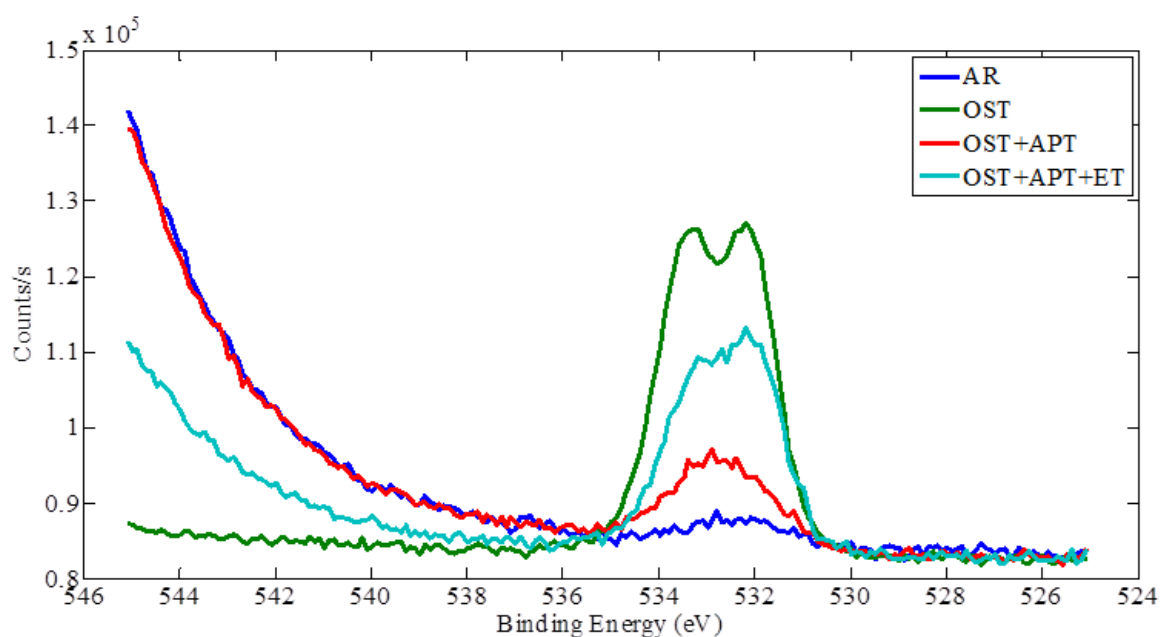


Fig. 3.18 - High resolution spectra over the O1s for different substrates – As received (AR), Organic solvent treatment (OST), Organic solvent plus Argon plasma treatment (OST+APT) and Organic solvent, Argon plasma plus Ethanol treatment (OST+APT+ET).

3.2.6 Experimental apparatus

3.2.6.1 Instrumental set-up

ADT instrumental set-up consists of following components:

- (a) Signal generator and amplifier
- (b) SensAND ADT machine (Nonlinear Network Analyzer)
- (c) Printed Circuit Board (PCB) cartridge on which QCR is mounted (RAPP-ID project, KTH, Sweden)
- (d) Computer with SensAND control software

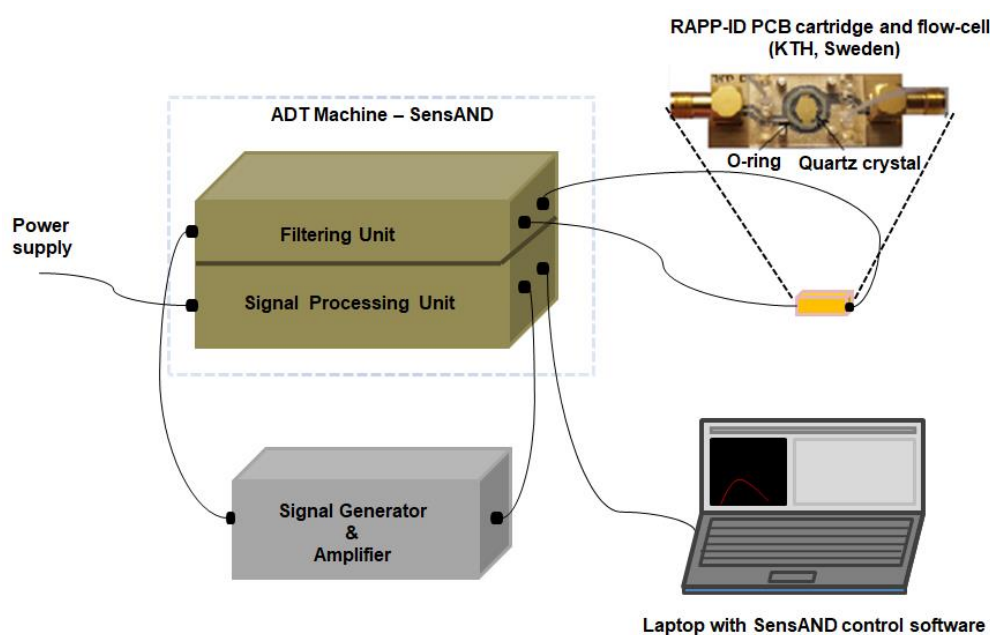


Fig. 3.19 – Schematic view of connections.

A dedicated electronic instrument, which may be described as a “Nonlinear Network Analyzer”, has been designed, built and used for ADT experiments.^[146-149] It is referred to as SensAND ADT machine here, consisting of a filtering unit and a signal processing unit, which are connected to each other through connections not visible externally. Figure 3.19 gives a schematic view at the connections between the components of ADT instrumental setup. This instrument is capable of driving a large variety of piezoelectric oscillators at a range of amplitude (0 up to 40V) at Radio Frequencies (RF 100 kHz to 300MHz), and recording complex (real and imaginary) electrical signal (current and voltage) at three frequencies

synchronously and sensitively (noise $\sim 1\mu\text{V}/\text{Hz}^{1/2}$) using 12 heterodyne receivers.

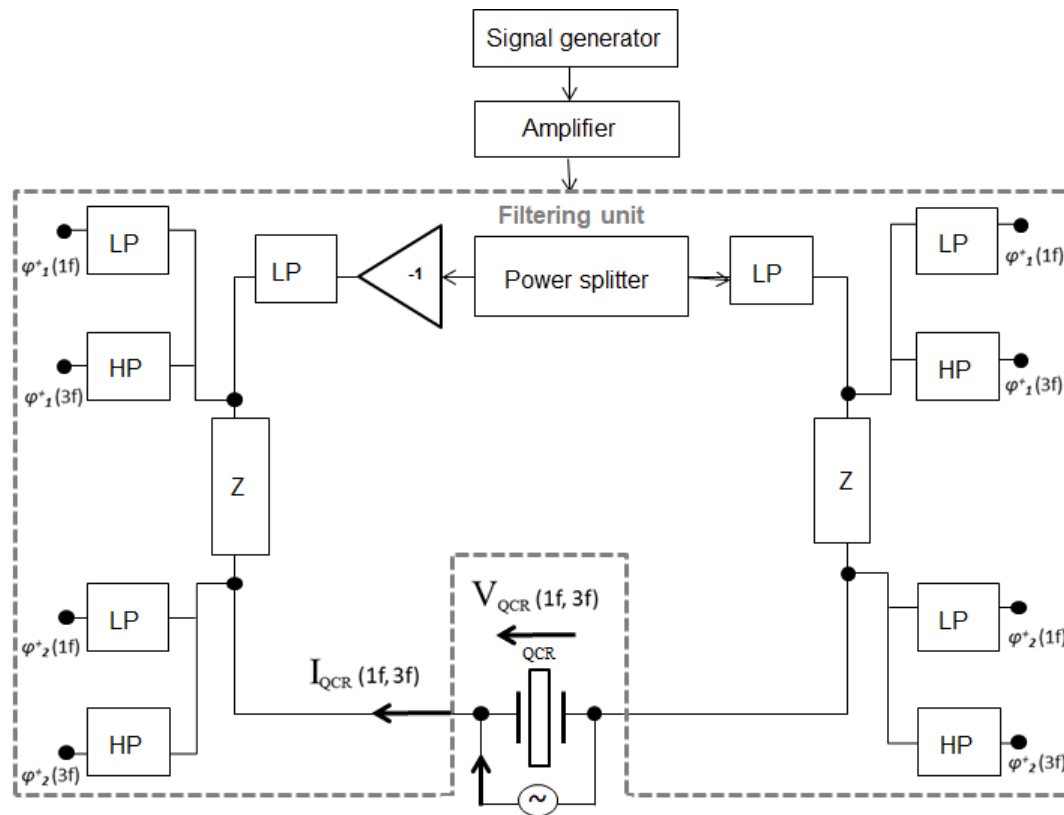


Fig. 3.20 – Schematic circuit of filtering unit. The input signal provided by the signal generator, is amplified and conducted to the filtering unit. Power splitter then splits the input signal into two signals which are filtered through low pass filters. Due to potential difference V_{QCR} , a current I_{QCR} starts flowing. The potential measurement points are designated with a ϕ . The values measured at these points are passed over to the signal processing unit.^[169]

In ADT experiments, the complex current and voltage signals were recorded at the drive frequency (first Fourier harmonic 1f) and three times the drive frequency (third Fourier harmonic 3f). The piezoelectric quartz oscillator acts as an actuator and a microphone at the same time. The driving and pickup electrodes are the same, i.e. only two electrodes used, as in a QCM. The microvolt-level third harmonic signals were separated from the powerful drive signal applied at the fundamental resonance by appropriate highly linear passive filtering network. Fig. 3.20 shows the schematic circuit of the signals within the filtering unit.

For convenience, the experimental data is reported in terms of normalised or scaled units, where 1 unit on the applied voltage scale corresponds to 30 V. SensAND control software is used to display transduced output signal. The recorded data was analysed using Wolfram Mathematica software.

3.2.6.2 Microfluidic set-up

A sample delivery system must ensure that the sensor is efficiently exposed to the sample. Earlier experiments with ADT machine done by Ghosh *et al.* were done using simple batch method, wherein a droplet of sample was placed on the sensor surface.^[148,149] However, in all the experiments for this PhD project, a microfluidic flow-cell (Fig. 3.21) was used for sample delivery. The microscale features of the microfluidic flow-cell ensured laminar flow and very little mixing. This microfluidic flow-cell was procured from KTH, Sweden where it was specifically designed for use with PCB cartridge (RAPP-ID project, KTH, Sweden) on which QCRs were mounted.

However, the performance of this microfluidic flow-cell was frequently challenged with the problem of bubble formation, which apparently affected the signal acquired. The problem was identified to be at the entry point of tubes into the flow-cell. The tubes had to be cut diagonally to fit in the flow-cell. Due to the difference in the diameter of the tubes and inlet/outlet of flow-cell bubbles were formed. Potential site of bubble formation is shown in Fig. 3.22 (A). This problem was resolved by increasing the diameter of both inlet and outlet and inserting small piece of softer tube having internal diameter same as the outer diameter of the harder tubes connected to sample reservoir (as shown in Fig. 3.22 (B) and (C)). Thus, introducing the softer tube at the inlet and outlet eliminated the problem of bubble formation as the harder tubes could be inserted directly without cutting them diagonally.

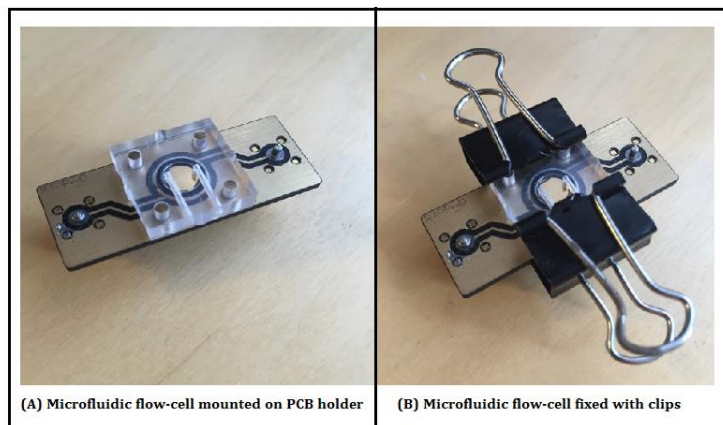


Fig. 3.21 – Microfluidic flow-cell (A) mounted on PCB holder (B) fixed with clips.

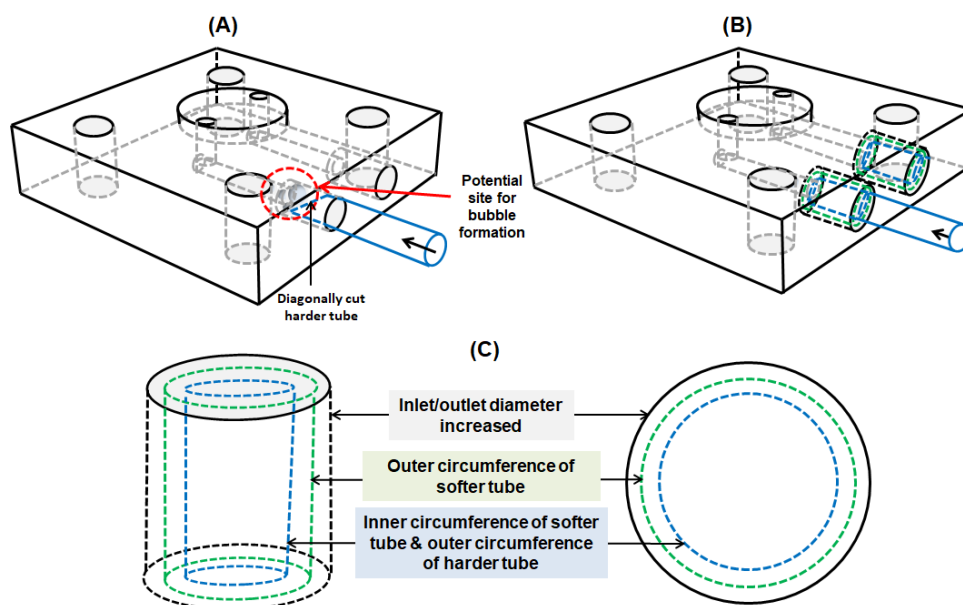


Fig. 3.22 – Microfluidic flow-cell inlet and outlet modified to solve problem of bubble formation. Microfluidic flow-cell (3D view) showing: (A) Potential site for bubble formation due to insertion of diagonally cut harder tube into the inlet; (B) Inlet diameter increased to incorporate softer tube (outer) into which harder tube (inner) is inserted, (C) Cut section of inlet showing circumferences of outer softer tube and inner darker tube. Inner circumference of softer tube is same as outer circumference of harder tube.

3.3 Linking bio-receptor with the transduction system

3.3.1 Formation of Self Assembled Monolayer (SAM) on gold electrode

Self-assembled monolayer is a highly ordered film, exactly one molecule thick that forms on a solid support. The experimental conditions more often

implemented for preparing SAMs yield organic interfaces having reproducible and desired functional behaviours. Molecules that form SAM (Fig. 3.23) usually have one group that binds to the substrate, a “chain” in the middle that helps them pack tightly by van der Waals forces, and a head group that endows the modified surface various desirable properties (e.g., hydrophobicity or hydrophilicity, chemical reactivity, bio-specificity or biological resistance). Thus, the selection of surface terminal group depends on the preferred properties required for immobilising the target analyte. Thiols and disulphides form SAMs on various metals including gold which is the mostly widely used substrate. Figure 3.24 depicts the steps used for adsorption of alkane thiols on the surface of gold electrode.^[170] Since biotin terminal group was chosen for experiments, the cleaned gold electrodes of the QCRs were immersed in about 250 μl of 1mM ethanolic solution of mixture of thiols [biotin terminal group (10%), and methoxy terminal group (90%)] and left overnight for formation of a mixed self-assembled monolayer (SAM) with good monolayer packing.

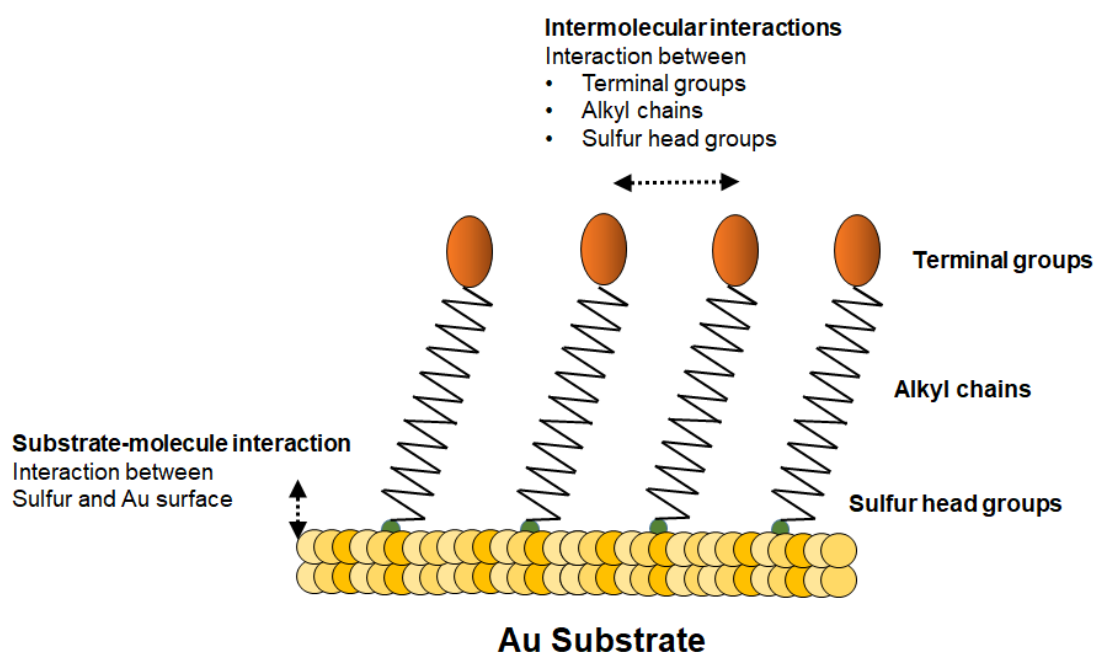


Fig. 3.23 – Self-assembled monolayers (SAMs) formed by adsorption of alkanethiols, $X(\text{CH}_2)_n\text{SH}$, onto gold substrate. Adapted and modified from ^[171].

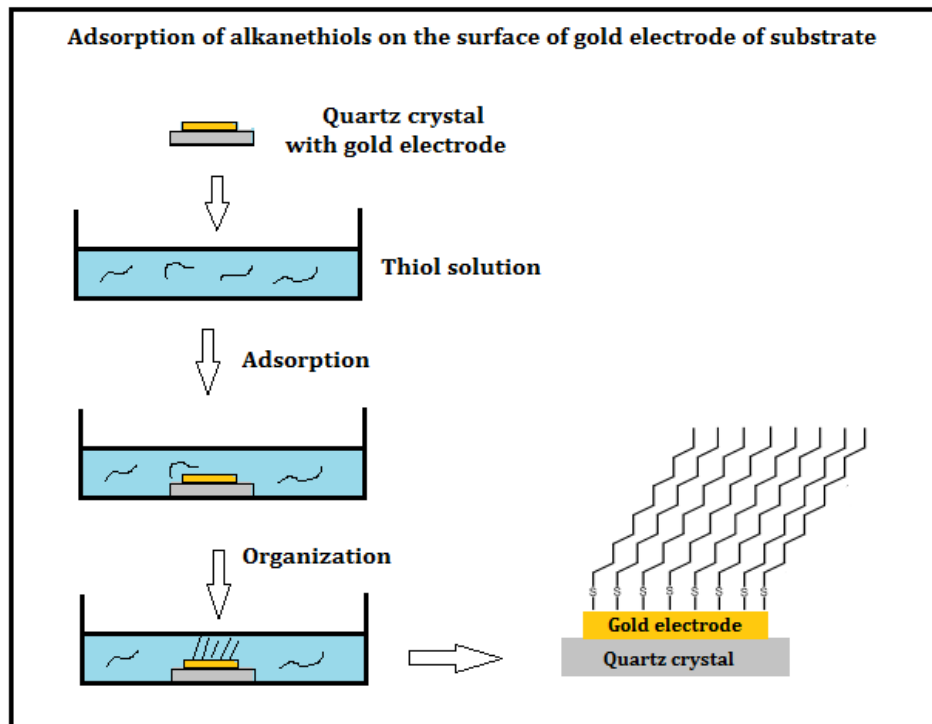


Fig. 3.24 – Adsorption of alkanethiols on the surface of gold electrode. Adapted and modified from ^[172].

3.3.2 Streptavidin Biotin interaction

Streptavidin is a basic tetrameric protein isolated from *Streptomyces avidinii*. It binds tightly to biotin, a small vitamin ligand. The association constant between biotin and streptavidin is about 10^{15} , highest known in biochemistry. A combination of high affinity, binding capacity, reproducibility, and chemical resistance makes the biotin streptavidin system ideal for sensor-based bioassays.^[173] Moreover, biotin-group can be incorporated into oligonucleotides sequences and these biotinylated bio-receptors are easily available.

Optimum orientation of the bio-receptor can also be achieved through the streptavidin biotin interaction that can enhance biosensor performance, as the recognition sites are not sterically hindered.^[174] Thus, streptavidin was selected as bio-molecule of choice to be linked to the other end of the thiol through biotin

3.3.3 Immobilisation of bio-receptor on the gold electrode

The bio-receptor immobilisation step is critical in the development of any kind of biosensor. After coating the surfaces with streptavidin, biotinylated bio-receptors (antibodies and aptamers) were immobilised on the surfaces of gold electrodes. Immobilisation steps of different bio-receptors are described in respective chapters.

3.4 Stability of baseline measurements of transduction system

Baseline measurements are taken before introducing target analyte on the sensor functionalised with corresponding bio-receptor. For the comparability purposes, it is imperative that baseline is measured under the same conditions as that after passing analyte. Baseline values essentially represent the noise in the system. Therefore, baseline stability is important to get better signal-to-noise ratio after introduction of the target analyte.

To achieve baseline stability following measures were taken. Before any experiment, the QCR was warmed up for at least 30 mins. For the QCR to warm up, the PCB cartridge had to be plugged into the machine, and the crystal had to be mounted on the PCB. After ensuring proper clamping and no bubble in the system, the surface was acoustically cleaned by flowing PBS buffer at high flow rate (~100 $\mu\text{L}/\text{min}$) and by taking intermittent constant amplitude scans at 0.5 SU for 30 seconds. By following the above steps, a stable baseline could be achieved.

Sometimes conducting liquids can provide a short circuit between the QCR electrodes; if not prevented, the QCR stability can be severely degraded. Hence, simple solution was applied, to dry the bottom surface of the crystal before placing the crystal on the PCB shielded from the solution on the top surface of the QCR. Changes in hydrostatic pressure due to turbulence while withdrawing liquids using syringe can also cause unwanted signal variations due to crystal stress and sometimes degrade QCR baseline stability. Hence, a syringe pump procured from Harvard Apparatus (UK) was used to withdraw fluids at steady flow rate to minimize variances in these effects.

3.5 Summary

Linking suitable bio-receptor to the transduction system of choice is the most critical step determining the performance parameters of the biosensor assembly. In this chapter, before linking the bio-receptor to the QCR that vibrates in thickness shear mode and transduces anharmonic acoustic signal, optimal experimental procedures were achieved and objective O.1.1 was attained. Energy trapping effect was explored to obtain sensitive ADT signal by loading the QCR with central gold deposit. The Kanazawa response of this QCR with loaded (stepped) electrode was validated. Different modes scan were tested i.e. AMS and FMS, out of which FMS mode scan was selected for further measurements. Also, the QCR was integrated with microfluidic set-up and the problem related to bubble formation that affected the ADT signal was resolved. The interface between the transducer and the bio-receptor plays important role, influencing the generation of anharmonic acoustic signal. Biotin-streptavidin bioassay format was selected to ensure optimum orientation of the bio-receptor, thereby, enhancing the performance of the biosensor assay. The surface cleaning method of gold electrodes was validated and measures to achieve baseline stability were identified, before performing experiments with *E.coli* bacteria which are described in next chapters.

Chapter 4 Detection of bacteria using anharmonic acoustic aptasensor

4.1 Introduction

Rapid and conspicuous detection of specific pathogens is regarded as the greatest challenge to combat AMR. Target detection in biosensor-based diagnostic methods relies on successful bio-recognitions. Ligands having high affinity and specificity make diagnosis exact and efficient.^[175] In biosensor-based diagnostic methods, it is vital to identify appropriate bio-receptor targeting bacteria, which can be then potentially coupled with the transducer. The right combination would then expedite diagnosis and thus decreasing the time between culture collections to specific antimicrobial treatment. Antibodies have been commonly used as ligands in diagnostics due to their target specificities and affinities.^[176] However, their intrinsic properties as proteins confer a number of shortcomings, such as, production via animal immunization, labour-intensive and time-consuming production process, expensive, inter-batch variation, sensitivity to temperature, irreversible denaturation, and limited shelf-life, etc.^[177] Therefore, aptamers have been developed that can be used instead of antibodies. Aptamers are composed of single-stranded oligonucleotides (ssDNA or ssRNA), and exhibit highly selective and specific binding affinities for target molecules.^[178] While aptamers are analogous to antibodies in their range of target recognition and variety of applications, they possess several key advantages over their protein counterparts. Therefore, in this chapter for the first time 'aptamer' as bio-recognition element, have been coupled with anharmonic acoustic transduction technique for detection of target *E.coli* bacteria.

4.2 Background

The biosensor-based diagnostic methods exploit the distinctive properties of a biological recognition event on a transducing device. Bio-receptor is the distinguishing feature of a biosensor and comprises recognition system of the sensor toward target analyte. Antibody-based detection methodologies are still considered the standard assays in environmental, food and clinical analysis.

But, though very commonly used, antibodies are posed with lot of limitations like, batch-to-batch variation in the production of antibody, and difficulty in generating even specific monoclonal antibodies, especially against non-immunogenic molecules. These drawbacks has lead several groups to consider using other recognition molecules like artificial DNA or RNA sequences as the screening ligand. However, these new single-stranded oligonucleotides (DNA or RNA molecules) work in an entirely different manner compared to earlier DNA or RNA microarrays, in that the ligand binding capacity is the result of the oligonucleotides' three-dimensional conformation, not nucleotide base–base complementarity.^[179]

4.3 Aptamers as bio-receptor

These new synthetic ssDNA or ssRNA ligands, known as aptamers, have been defined in the Encyclopaedia of Analytical Chemistry as artificial nucleic acid ligands that can be generated against amino acids, drugs, proteins and other molecules.^[179,180] Aptamers are usually 20–80 nucleotides with 6–30 kDa molecular weights, that can fold into unique three-dimensional conformations characterised by stems, loops, bulges, hairpins, pseudoknots, triplexes, or quadruples as shown in below Fig. 4.1.^[181] Based on their three-dimensional structures, aptamers can well-fittingly bind to a wide variety of targets from single molecules to complex target mixtures or whole organisms.

Aptamers are mostly unstructured in solution, but they fold upon associating with their target into three-dimensional structures as shown in Fig. 4.2. Similar to conformational recognition that mediates antibody–antigen recognition and complex formation, aptamers bind to their targets using high-specificity and high-affinity through van der Waals forces, hydrogen bonding, electrostatic interactions, stacking of flat moieties and shape complementarity. Thus, aptamers are also referred to as “chemical antibodies”.^[182]

In 1990, two labs independently identified nucleic acids (aptamers) specifically binding to their targets. Gold lab used the term SELEX for their process of selecting RNA ligands against T4 DNA polymerase; and the Szostak lab, coined the term *in-vitro* selection, selecting RNA ligands against various

organic dyes. The Szostak lab also coined the term aptamer (from the Latin, apto, meaning 'to fit') for these nucleic acid-based ligands.^[183-185] Since then, a variety of aptamers have been generated against number of targets. Aptamers can be used to detect any target ranging from simple small molecules such as dyes^[186], ATP^[187], metal ions^[188], to complex protein^[189-192] to whole organism.^[193-195]

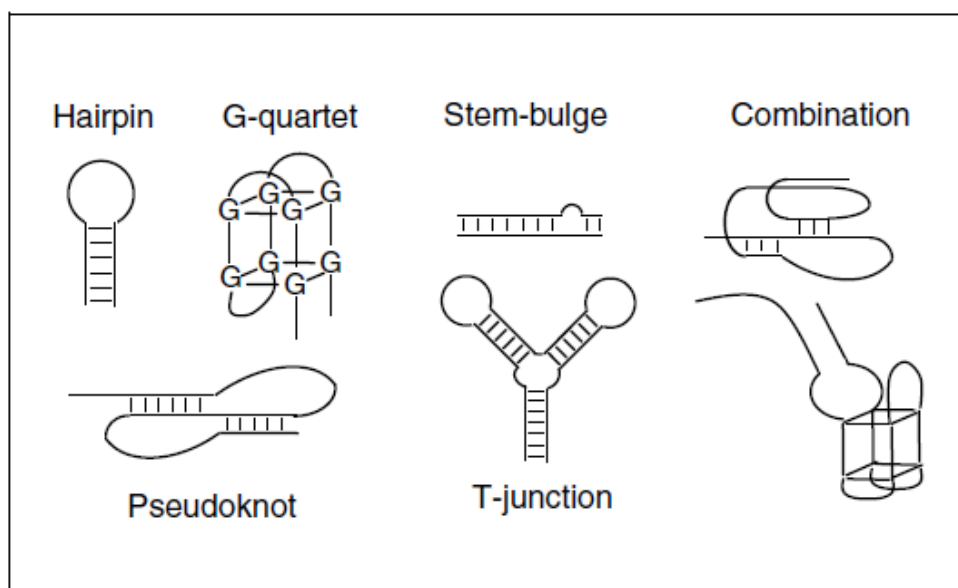


Fig. 4.1 – Tertiary structures of aptamers adopted after binding to their target molecules. Adapted and modified from ^[181].

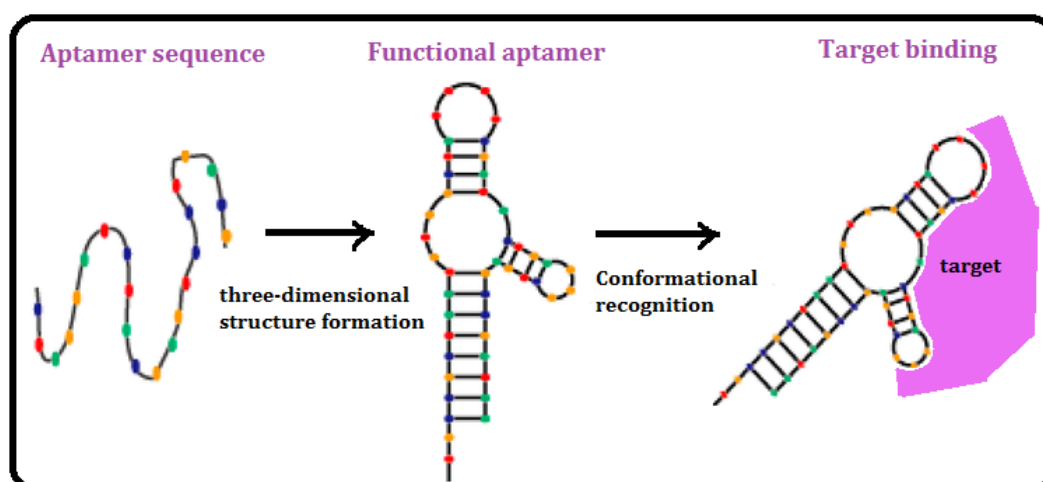


Fig. 4.2 - Schematic diagram of aptamer conformational recognition of targets to form an aptamer-target complex. Adapted and modified from ^[182].

SELEX method

Systematic Evolution of Ligands via Exponential Enrichment (SELEX) is the gold-standard methodology for developing specific aptamers. In principle, the conventional SELEX process includes multiple rounds of exponential amplification and enrichment, which allows evolution of aptamers with high target-specific affinity from a random oligonucleotide pool.^[182]

The steps involved in SELEX process to successfully generate target-specific aptamers are as follows (Fig. 4.3): First a single-stranded DNA or RNA oligonucleotide pool or library is carefully designed and chemically synthesised. The pool or library is comprised of 10^{14} – 10^{15} random sequences, with a centralised random sequence (35–50 nucleotides long) flanked by fixed sequences at either end which served as primer binding domain during PCR^[183-185]; the random sequences prepared in the initial pool fold into different secondary and tertiary structures.

They are then then incubated with targets (immobilised or free) under optimal conditions to form aptamer-target complexes; unbound sequences are separated from target-bound sequences through different methods, such as membrane filtration, affinity columns, magnetic beads, or capillary electrophoresis; target-bound sequences are then amplified by PCR, and reaction products are used as a new aptamer sub-pool for the next selection round; the enriched aptamer sequences are identified by high-throughput sequencing methods.

Several negative-target selections (counter-selections) are added to the process that can eliminate nonspecific sequences generated by their binding to non-target moieties. Specific aptamers can be obtained after 8–20 rounds of selection, with the entire process taking weeks to months. Thus, aptamers can be selected using a relatively rapid *in-vitro* selection process and can be inexpensively synthesized.

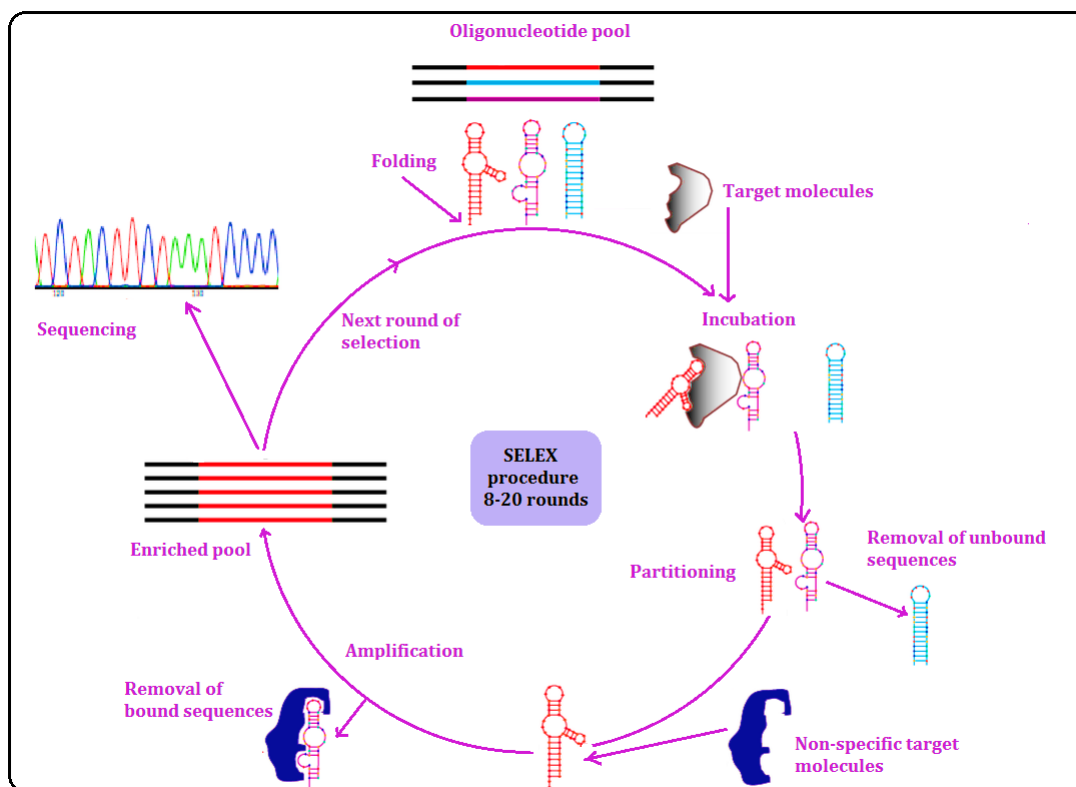


Fig. 4.3 - Schematic diagram of the SELEX process to generate target-specific aptamers. Adapted and modified from [182].

Although, both DNA and RNA aptamers can adapt a three dimensional structure, and give rise to binding pockets for their respective targets,^[196] RNA aptamers are versatile and have generally superior binding affinity and specificity than DNA aptamers due to the frequent occurrence of modified nucleotides within their structure, their base pairing properties and their tendency to form intricate three-dimensional structures.^[197,198] But the production of RNA aptamers is very expensive as the SELEX process requires the synthesis of random oligonucleotide libraries which is costly. Therefore, an *in-vitro* transcription step is introduced in the SELEX procedure to obtain the initial RNA pool. As opposed to this, the selection procedure for DNA aptamers is simpler and inexpensive pools (libraries) of DNA oligonucleotides can be chemically synthesized and contain only single-stranded sequences as opposed to the initial double-stranded pool of DNA sequences required for the *in-vitro* transcription step used for RNA-based aptamer selection. Furthermore, reverse transcription is not required and an asymmetric PCR step is sufficient to recover the sub-library of

ligand-binding aptamers needed to proceed to the next round of selection.^[199] Also, RNA aptamers are more susceptible to nuclease degradations than DNA aptamers. Some researchers have tried to stabilise the RNA aptamers by modifying them but it had negative impact on their binding affinities.^[200,201] For these reasons, ssDNA aptamers were chosen to be used as bio-recognition element to be coupled with ADT for detection of *E.coli* bacteria.

Advantages over antibodies

Single-stranded DNA aptamers have high affinity and specificity toward their targets that is comparable to antibodies. Additionally, they have several advantages over antibodies. Aptamers can be easily generated by chemical synthesis, which not only excludes any batch-to-batch variations but also reduces the cost and the time needed for production.^[202] Aptamers can be identified even for non-immunogenic targets, as the SELEX process can be performed completely *in-vitro* and independent of living, contrary to antibodies which are limited to physiologic conditions by animal immunisation. Also, antibodies undergo irreversible denaturation at room temperature or higher, while aptamers are more thermostable can reform to their original conformations when optimal temperature is restored.^[203] Likewise, aptamers have dissociation constants that can reach as low as the picomolar–femtomolar range.^[204-206]

As they are nucleic acids, different functional groups (e.g., thiol or amino) can be easily incorporated onto the 3' and/or 5' ends of oligonucleotides during synthesis and employed for immobilisation on substrates. In the same way, variety of labelling molecules (e.g., biotin, fluorescent tags) can also be covalently attached and serve as reporters in bio-sensing applications.^[203,207] Moreover, aptamers are very specific as they can discriminate even between highly similar molecules, such as theophylline and caffeine, which differ by only a methyl group.^[208,209] Therefore, due these attractive features, aptamers are very suitable to be used in bio-sensing applications.

Application of aptamers as 'aptasensors'

When aptamers are used as biological recognition element for specific target analyte to form a stable complex, the device together with transducer is called aptasensor. Thus, the so-called aptasensors (aptamer-based biosensors) are expected to be one of the most promising devices in bio-sensing applications.^[210] Similar to immunoassays, aptamer-based bioassays can adopt different assay configurations to produce a clear signal and are suitable for nearly all antibody-based designs. Since, aptamers can be generated against range of targets, many aptamer-based bioassays have been developed for application in medical diagnostics, food and environmental analysis, etc.^[211-214] Aptasensors have also been developed, in which aptamers are immobilised on the substrate and different biosensing techniques are used for detecting target-binding, for e.g., electrochemical or optical systems such as fluorescence^[215], surface plasmon resonance^[216], quartz crystal microbalance^[217], or cantilever.^[218,219] Efficient immobilisation at high density is also possible due to their small size and versatility, which is essential for multiplexing for miniaturized systems.^[220] Aptamers are chemically stable and confer greater stability which is one of the important aspects for biosensor development. However, aptamer technology in biosensors remains in an early phase of development. As a result, there remains a need to combine aptamers and their potential biosensors to tackle the numerous challenges of the currently limited conventional diagnostic methods. Therefore, for the first time 'aptamer' was coupled with the ADT technique (advantages discussed in chapter 2), to harness the benefit of this unique combination for detection of target bacteria.

4.4 Aptamer for *E.coli* bacteria

Escherichia coli (*E.coli*) bacteria is part of large family of gram-negative bacteria viz. *Enterobacteriaceae* and is referred to as entero-bacteria or "enteric bacteria", as several members live in the intestines of people and animals. It has been reported that gram-negative bacteria possess a negatively-charged outer membrane that can repel nucleic-acid molecules due to which it is difficult to generate aptamers that bind to the surface

molecules of bacterial cells. Moreover, bacteria have short generation times leading to rapid changes in protein expression and high surface variation between cultures and colonies. Such variation can hinder consistent measurement of aptamer binding.^[221]

Nevertheless, some ssDNA aptamers against *E.coli* bacteria have recently been reported. Peng *et al.* enriched ssDNA library specific for *E.coli* K88 bacteria.^[222] This group further isolated ssDNA with high affinity and specificity against K88 fimbriae protein, selected after 11 rounds.^[223] Bruno and co-workers have selected DNA aptamers against the endotoxin lipopolysaccharide (LPS) and the outer membrane protein of *E.coli* bacteria.^[224,225] Savory *et al.* identified ssDNA with high specificity and affinity for an uro-pathogenic strain of *E.coli* bacteria.^[226] Wu *et al.* reported the development of aptamer-based biosensors (aptasensors) based on label-free aptamers and AuNPs for the detection of *E.coli* O157:H7 and *S.typhimurium*, with the aim of establishing a preliminary method to evaluate the utility of aptamer-AuNPs assay for enteropathogenic bacteria.^[227]

Single-stranded DNA aptamers targeting bacteria can be classified into two general categories, (1) targeting whole cells with known or unknown molecular targets and (2) targeting predefined bacteria cell surface targets or bacteria spores.^[228] Whole-living cell SELEX conserves two major advantages: (1) selection without a prior purification of the targets and (2) conservation of membrane proteins in their native conformation similar to the *in-vivo* conditions. It is also well-known that there is difference in the bacterial cell membrane because they express different sets of molecules at different growth states. This impedes with the consistent measurement of the aptamer binding as detection of bacteria based on the single surface molecule or protein might omit the positive bacteria which happen to negatively express specific molecules or express mutated ones.^[229] Consequently, it was decided to obtain polyvalent ssDNA aptamers targeting whole cells of *E.coli* bacteria.

To obtain ssDNA aptamers targeting whole bacterial cells, whole-cell SELEX method is used. It was beyond the scope of this project to perform whole-cell SELEX method to get ssDNA aptamers for *E.coli* bacterial cells. Therefore,

alternative option was to use the already reported aptamer sequences in literature for capturing *E.coli* bacteria.

Kim *et al.* had isolated four sequences of ssDNA aptamers against *E.coli* bacteria using a whole bacterial cell–SELEX process and characterised their affinity and selectivity to other *E.coli* strains and faecal coliform bacteria cells.^[220,230] They performed 10 rounds of selection against a faecal strain of *E.coli* along with multiple negative selections against other species of bacteria. They identified four candidate sequences with high affinity for the target strain.

All four candidates were highly selective against negative target bacteria. Out of them the one with strong fluorescent intensity at the saturation point was selected to be coupled with ADT transduction method. The ssDNA aptamer consists of a central random region of 45 nucleotides flanked by two different constant sequences at the 3' and 5' ends: 5'-GCAATGGTACGGTACTTCC-N45-CAAAGTGACGCTACTTTGCTAA-3' (88-mer) with fluorescein (FITC) at 5' end [5'-fluorescein-GCAATGGTACGGTACTTCC-3' (19-mer)] and Biotin TEG at 3' end [CAAAGTGACGCTACTTTGCTAA-3'- Biotin TEG (24-mer)].

4.5 Binding experiment

Binding of ssDNA sequence to *E.coli* (*KCTC 2571*) bacterial strain were assessed by measuring fluorescence intensity.

Bacterial strain and culture conditions:

E.coli (*KCTC 2571*) strain reported to bind the selected ssDNA aptamer, was procured from Microbial Resource Centre, Korean Collection for Type Culture (KCTC), Korea Research Institute of Bioscience and Biotechnology. The *E.coli* (*KCTC 2571*) strain cultures were supplied by KCTC in lyophilised powder form which was further re-activated and cultured at 37°C. *E.coli* (*KCTC 2571*) strain lyophilised cultures were re-activated by breaking open the ampoule containing them by following steps showed in Fig. 4.4. The lyophilised powder was added to nutrient broth media and was cultured overnight in incubator with mild shaking. Next day, the colonial growth

(18 – 24 hours) of pure culture was inoculated with cryopreservative in Microbank™ cryovials and stored in freezer at -80°C.

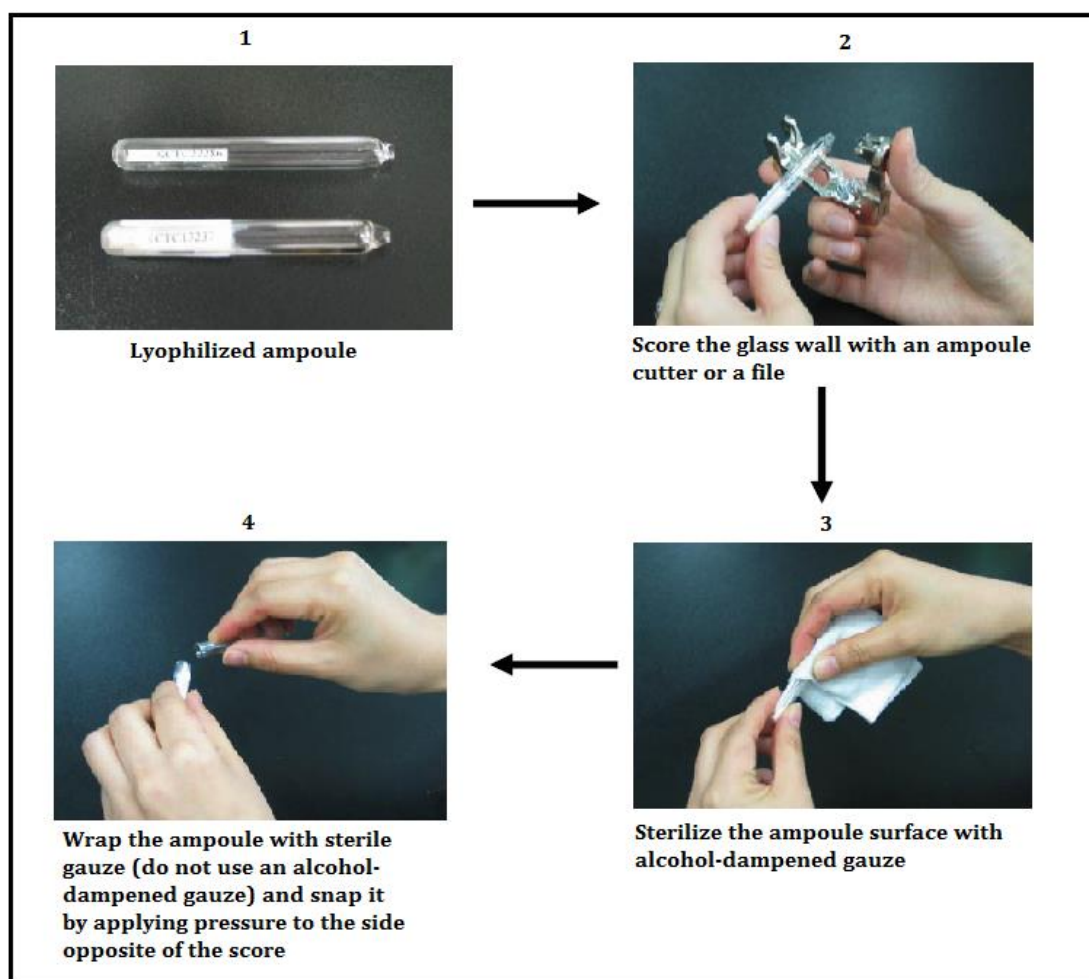


Fig. 4.4 – Procedure for breaking open the ampoule and re-activating lyophilized cultures of *E.coli* (KCTC 2571) bacterial strain.

Reagents:

- a) Binding buffer was prepared with 0.1 mg/ml salmon sperm DNA, 1% bovine serum albumin [BSA], 1× phosphate-buffered saline [PBS], and 0.05% [v/v] Tween 20.
- b) Washing buffer was prepared with 1× PBS and 0.05% [v/v] Tween 20.

Method:

Microplate wells were first washed with 150 µL of 5% BSA in PBS overnight at 4°C and next day washed with washing buffer. *E.coli* (KCTC 2571) was

cultured in nutrient broth to middle growth phase (OD600 of 0.45) and centrifuged at 13,000 rpm for 10 mins to remove the media. Subsequently, bacterial cells at concentration 10^7 E.coli/mL were incubated with different amounts of both the fluorescein-labelled ssDNA aptamers (0, 5, 12.5, 25, 500, 125, and 250 nM as final concentrations) in 1 ml of binding buffer for 45 mins at 25 °C with mild shaking. Cells were washed two times to remove unbound ssDNA aptamers from cells by centrifugation (13,000 rpm for 10 mins) and were re-suspended in 1 ml of washing buffer. Finally, the fluorescence intensity of each sample was measured with BMG FLUOstar Omega microplate reader (at excitation 485 nm and emission 520 nm wavelengths). The fluorescence intensity was compensated by subtraction with the fluorescence intensity of blank and then by division with respective gains.

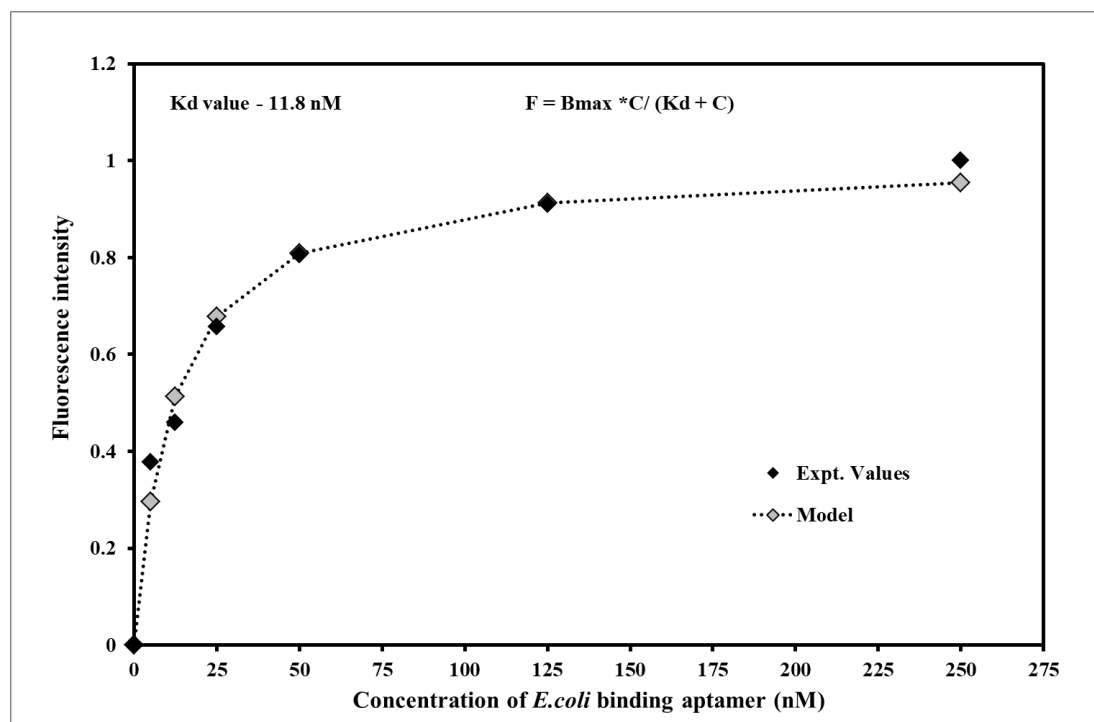


Fig. 4.5 – Binding saturation curve obtained by fluorescence analysis for *E.coli* binding aptamer with Kd value of 11.8 nM obtained by nonlinear regression model.

Results and discussion:

Fluorescent intensities of each sample of *E.coli* (*KCTC 2571*) strain bacteria mixed with different concentrations of fluorescein-labelled ssDNA (0, 5, 12.5, 25, 500, 125, and 250 nM as final concentrations) were measured. Binding of

ssDNA sequences to *E.coli* (KCTC 2571) strain were assessed. To estimate the affinity of the selected ssDNA to target cells, the fluorescence intensity versus the added ssDNA concentration was plotted. The resultant saturation curve was then fitted by nonlinear regression analysis, and the dissociation constant was calculated. The dissociation constants (K_d) was estimated to be 11.8 nM (as shown in Fig. 4.5), which was found to be close to the K_d value of 12.4 nM, as reported in literature.^[230] Thus, binding of the reported ssDNA aptamer to the target *E.coli* (KCTC 2571) bacteria was confirmed by measuring fluorescence intensity.

4.6 Linking the bio-receptor to the QCR

4.6.1 Cleaning the surface of gold electrode

AT-cut stepped (non-uniform) quartz crystals were used with fundamental resonant frequency range of 14.23 -14.25 MHz (Lap-Tech Inc., Bowmansville, Ontario, Canada). The surfaces of gold electrodes of quartz crystals were cleaned with acetone for 5 mins and then with isopropanol (IPA) by ultra-sonication process for 5 mins. Then after drying with nitrogen gas, they were placed in plasma cleaner to remove impurities and contaminants from the surface using inert argon gas for 1 min in a Harrick Plasma cleaner. They were then stored in a well of clean 24-well tissue culture plate covered with plastic film.

4.6.2 Formation of self-assembled monolayer (SAM)

The cleaned quartz crystals were then immersed in about 250 μ l of 1mM ethanolic solution of mixture of thiols [biotin terminal group (10%), and methoxy terminal group (90%)] and left overnight for formation of a SAM. Thiols with biotin terminal group HS-C11-(EG)6-Biotin (th004-m11.n6-0.005) and methoxy terminal group HS-C11-(EG)3-OCH₃ (th006-n3) were obtained from Prochimia Surfaces, Poland. The following day, the gold surfaces of quartz crystals were rinsed three times with ultra-pure ethanol (Sigma-Aldrich, UK) for removing the non-adsorbed thiols and then both sides of crystal were dried with a stream of nitrogen gas. After making sure that the

electrode on bottom side was completely dried, the crystal was mounted on PCB cartridge and sealed with “O-ring” of microfluidic flow-cell with only one face exposed to the solution. The gold surfaces were then rinsed with de-ionized (DI) water to remove ethanol followed by phosphate buffer saline (PBS) with physiological pH 7.4.

4.6.3 Deposition of Streptavidin

PBS buffer solution (100 μL) was then flowed over the substrate at the continuous flow rate of 10 $\mu\text{L}/\text{min}$ and baseline measurements were taken for 15 mins at 5 min interval (Fig. 4.6 Step-1). This was followed by about 150 μL of Streptavidin (10 $\mu\text{g}/\text{mL}$) for 15 mins at the flow rate of 10 $\mu\text{L}/\text{min}$; thus forming a strong bond with the biotin terminal group of the alkane thiol. Measurements were taken under flow for 15 mins at 5 min interval (Fig. 4.6 Step-2).

4.6.4 Immobilisation of bio-receptor on the gold electrode of QCR

After depositing streptavidin, PBS buffer solution (500 μL) was then flowed over the substrate at the continuous flow rate of 100 $\mu\text{L}/\text{min}$ for 5 mins, to remove the unbound streptavidin. Then the surface was functionalised with biotinylated *E.coli*-binding ssDNA aptamer, by passing over the surface for 15 mins (Fig. 4.6 Step-3). The excess aptamers were removed by flowing PBS solution and then baseline measurements were taken every 5 minutes over 30 minutes under a continuous flow of PBS at flow rate of 5 $\mu\text{L}/\text{min}$.

After this, in order to detect *E.coli* (KCTC 2571) bacteria by direct assay, different concentrations of bacteria were spiked into the sample over the prepared sensor surface at a flow rate of 5 $\mu\text{L}/\text{min}$ for further 60 mins (Fig. 4.6 Step-4).

4.7 Step-wise characterisation

When aptamers i.e. single stranded oligonucleotides are used as biological recognition element for specific analytes (antigens) to form a stable complex, the device together with transducer is called ‘aptasensor’. Here, for the first

time the anharmonic acoustic transducer ADT was coupled with aptamers as bio-receptor for detection of *E.coli* bacteria. The resultant aptasensor was characterised step-by-step (as depicted in Fig. 4.6) with the admittance analysis.

To determine the viscoelastic properties of the bound surface mass on QCR surface, the measured admittance data points were fitted to the BVD model to extract the values of the three equivalent circuit parameters Q (quality factor), R_m (motional resistance), and f_0 (Resonance frequency). Out of these, frequency (Δf) and dissipation (ΔD) spectra of the same quartz crystal were monitored that were subjected to different treatments as shown in Fig 4.6.

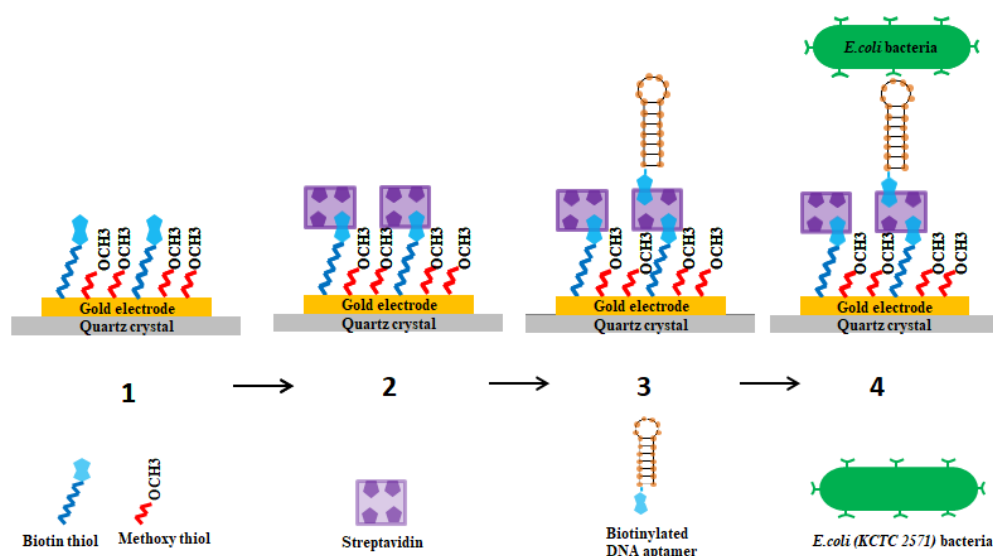


Fig. 4.6 - Functionalisation steps – (1) Mixed SAM with 10% biotin thiol and 90% methoxy thiol, (2) Streptavidin layer, (3) Biotinylated ssDNA aptamer and (4) final step of flowing the *E.coli* (KCTC 2571) bacteria.

The frequency shift is reported in Hz whereas the dissipation shift is plotted in terms of arbitrary units (a.u). When streptavidin is injected into the flow-cell, frequency shift of Δf (~ 150 Hz) and dissipation (a.u) shifts are observed (Fig. 4.6 Step-2). Large Δf (~ 275 Hz) and ΔD (a.u) are observed during the biotinylated aptamer immobilisation step due to the more mass going on the surface. Following aptamer binding, any unbound aptamer was removed from the flow-cell by rinsing with PBS. After taking baseline measurements, the bio-interface was used for detection of the target bacteria. When *E.coli* (KCTC 2571) bacteria are spiked and it enters the flow chamber and

binds to the immobilised aptamers (Fig. 4.6 Step-4), an increase in the resonance frequency and a corresponding increase in the dissipation signal of the functionalised sensor crystal are observed. The positive frequency shift is conceivably due to flexible binding of bacteria to immobilised ssDNA aptamer. It has been reported earlier by Olsen *et al.* that when attachment is flexible, as observed for bacteria, the sensor signals are inversely proportional to additional mass, and is probably determined by interfacial viscoelasticity and acoustic and electro-magnetic coupling.^[231] Pomorska *et al.* have also reported that the QCR most likely probes the contact strength, rather than the mass of the particle.^[232] The *E.coli*-binding ssDNA aptamer used here have been isolated by whole bacterial cell–SELEX process and its possible binding targets on *E.coli* surface may be the components of outer cellular membrane of *E.coli* such as LPS, outer membrane proteins, and flagella. The flexibility can perhaps be attributed to the binding of aptamer to target 'flagella' on the surface of *E.coli* bacteria. The bacteria thus have a high degree of freedom and the displacements of crystal particles may not be in phase with the displacements of the bacteria. This causes stretching of the bonds and thus causing a positive frequency shift (anti-Sauerbrey effect).

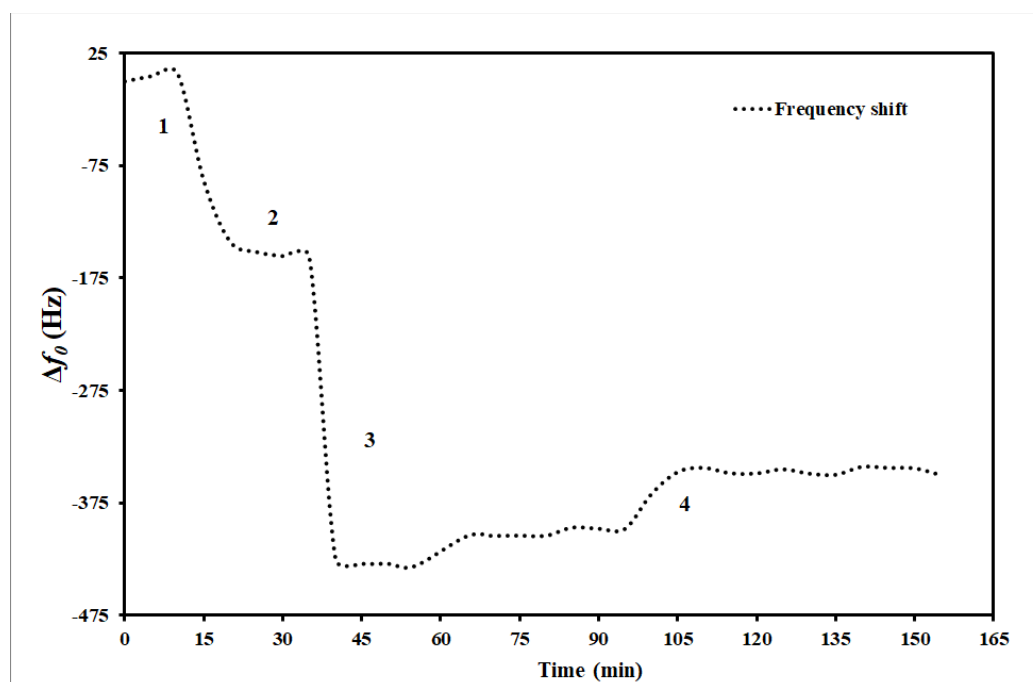


Fig. 4.7 – Resonant frequency (Δf) spectra of the QCR monitored that was subjected to the stepwise treatment as shown in fig. 4.6

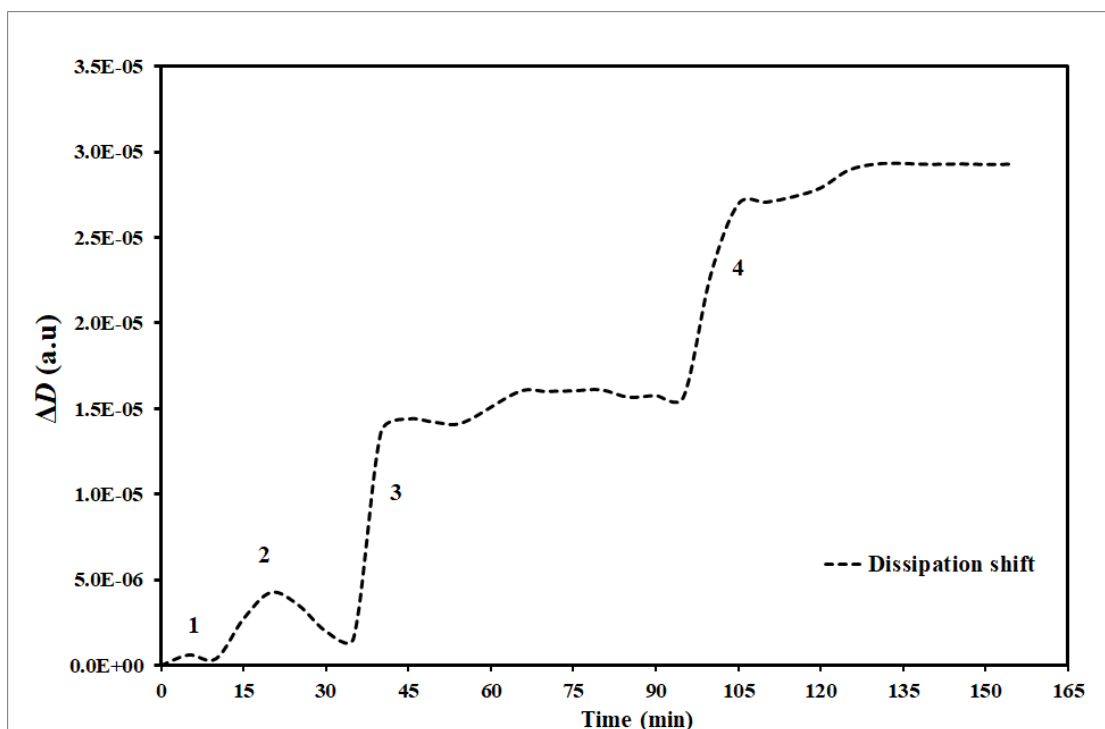


Fig. 4.8 - Dissipation (ΔD) spectra of the QCR monitored that was subjected to the stepwise treatment as shown in fig. 4.6

4.8 Determination of drive amplitude

The surfaces of the QCR were functionalised with *E.coli*-binding aptamers, and then rinsed with PBS buffer. After taking baseline measurements, 10^7 *E.coli*/mL (as final concentrations) were spiked into the sample and passed over the prepared sensor surface at a flow rate of 5 μ l/min for 60 mins. Resonant frequency (f_0) was determined with frequency sweep and the sensor was then driven by a pure sinusoidal oscillation at f_0 in frequency mode scan, at different amplitudes ranging from 0.1 to 0.5 SU. The complex values (in-phase and quadrature) of current and voltage were recorded at $1f$ and $3f$ simultaneously using the ADT machine. The percentage shift in the peak values of the corresponding $3f$ signal (I_{3fmax}) from baseline, are plotted over time (Fig. 4.9) and at 60 mins (Fig. 4.10). Maximum shift was observed at 0.1 SU which corresponds to excitation voltage of 3 Volts and 7.5 nm of oscillation amplitude at surface.^[233,234] But the value of oscillation amplitude seems to have inverse relation with corresponding $3f$ signal. At 0.2 SU (6 Volts) $3f$ signal dropped despite increase in oscillation amplitude. Thus, 0.1 SU was selected for further measurements as it gave maximum $3f$ signal.

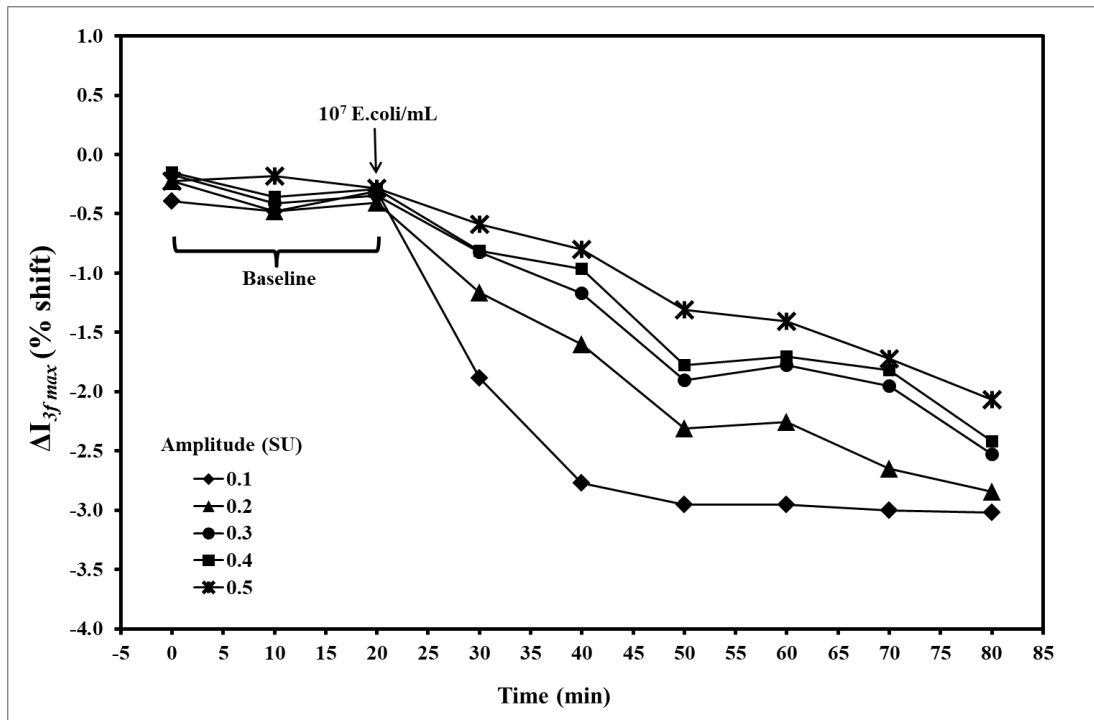


Fig. 4.9 - $I_{3f \max}$ shift (%) measured at different amplitudes – 0.1 to 0.5 SU over 60 mins, after passing 10^7 E.coli/mL on the surface functionalised with aptamers.

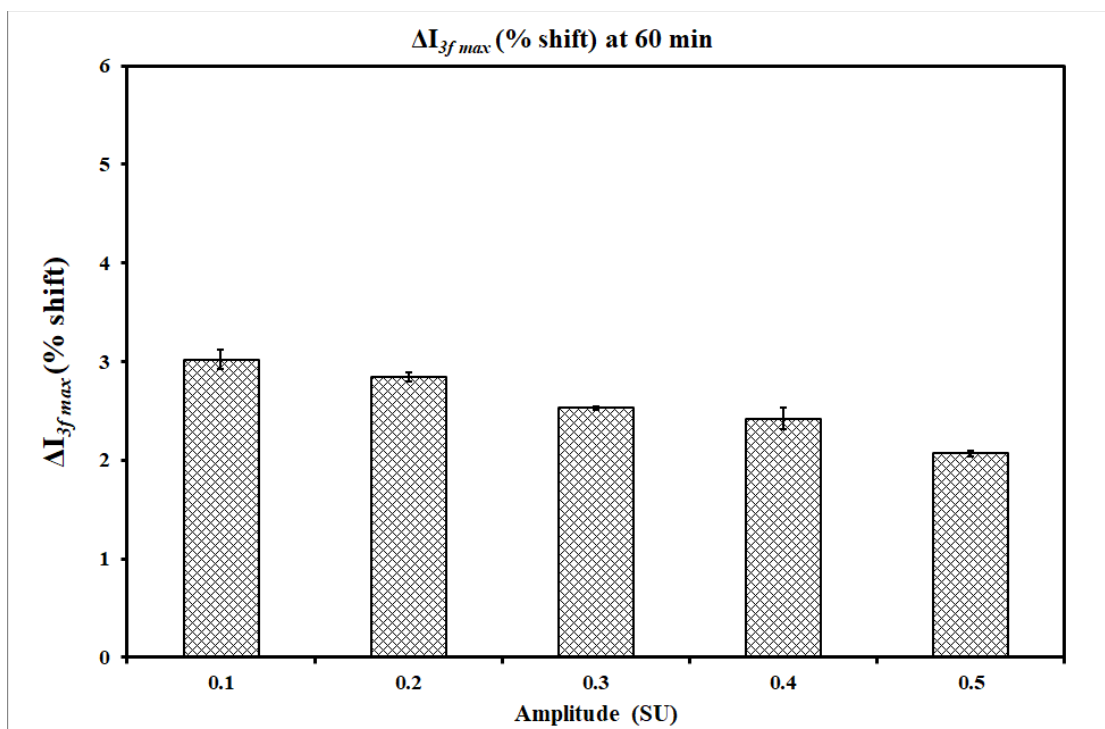


Fig. 4.10 - $I_{3f \max}$ shift (%) measured at different amplitudes – 0.1 to 0.5 SU at 60 mins, after passing 10^7 E.coli/mL on the surface functionalised with aptamers.

4.9 Detection of *E.coli* bacteria with anharmonic acoustic aptasensor

After determining the optimal drive amplitude, triplicate sets of experiments were carried out with a range of *E.coli* bacterial concentrations. In order to detect *E.coli* (KCTC 2571) by direct assay, different concentrations of bacteria were spiked into the sample (10^5 - 10^8 cells/mL as final concentrations) over the prepared sensor surface at a flow rate of 5 μ L/min for further 60 mins. A total of 3×10^4 , 3×10^5 , 3×10^6 & 3×10^7 bacterial cells were therefore injected over 60 mins, respectively. To check specificity of the sensor, *S.typhi* bacterial samples were also used at 10 times the concentration of *E.coli* bacteria. Thus, 10^8 cells/mL as final concentrations of *S.typhi* bacteria were also spiked into the sample over the prepared sensor surface at a flow rate of 5 μ L/min for further 60 mins. As a control, only PBS buffer solution was also flowed and baseline measurements were taken. Frequency mode scans were taken at 0.02 SU and 0.1 SU (0.1s period) and Δf_0 , ΔD and $\Delta I_{3f_{max}}$ were simultaneously monitored in real time during streptavidin and aptamer immobilisation and *E.coli* detection using a quartz crystal nonlinear network analyzer. All the measurements were taken in continuous flow mode.

Relative decrease in peak values of $\Delta I_{3f_{max}}$ (% shift) from baseline are plotted over 60 mins for which the *E.coli* bacteria were flowed over the sensor surface after achieving the baselines, as shown in the Fig. 4.13. This relative decrease in $\Delta I_{3f_{max}}$ was compared with the increase in resonant frequency (Δf_0) and the relative increase in dissipation values ΔD . Fig. 4.11 and Fig. 4.12 depict the frequency shift and dissipation shift over 60 mins after introducing the *E.coli* bacteria over the surface functionalised with *E.coli*-binding aptamers.

It was observed that the measurements were less noisy with lower coefficient of variation for $\Delta I_{3f_{max}}$ compared to Δf_0 and ΔD measurements over time. Also, the signal-to-noise ratio was comparatively higher for $\Delta I_{3f_{max}}$ compared to Δf_0 and ΔD measurements.

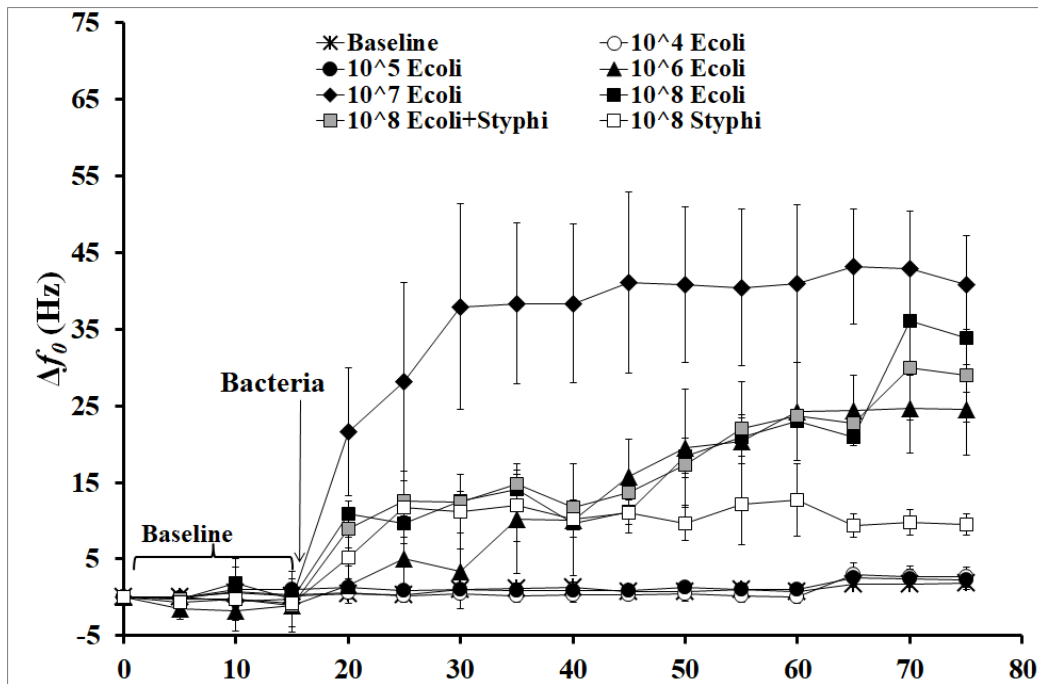


Fig. 4.11- Frequency shift (Hz) as a function of time with bacterial suspension of different concentrations (cells/mL) over the surface functionalised with aptamers.

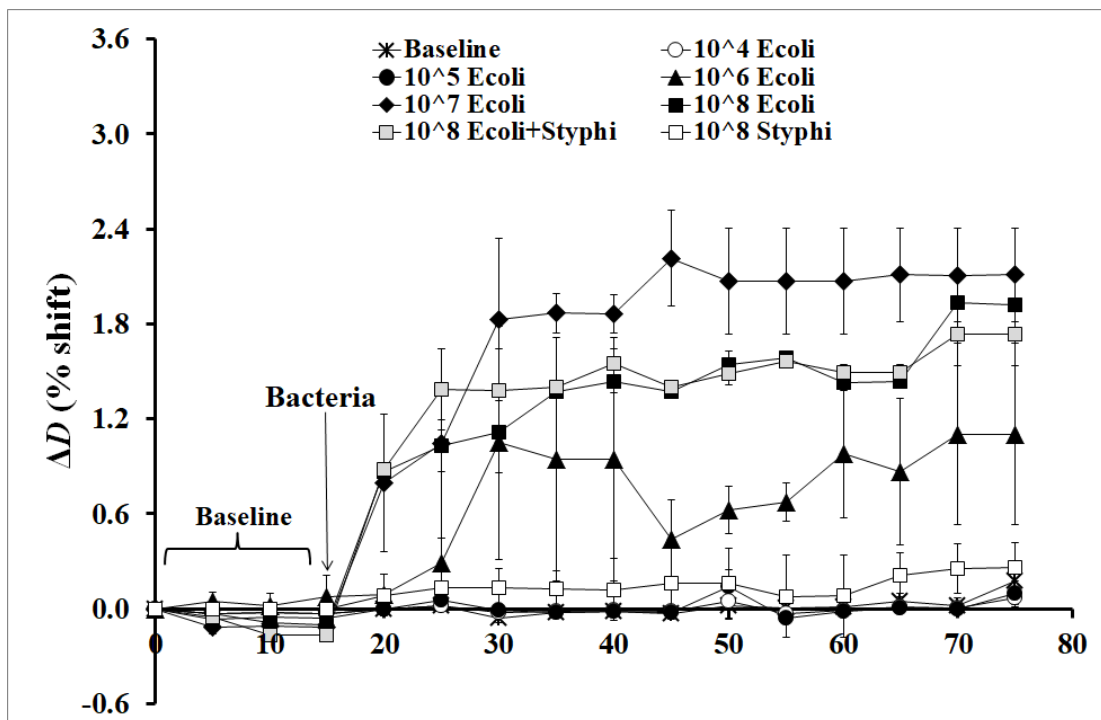


Fig. 4.12 - Dissipation shift (%) as a function of time with bacterial suspension of different concentrations (cells/mL) over the surface functionalised with aptamers.

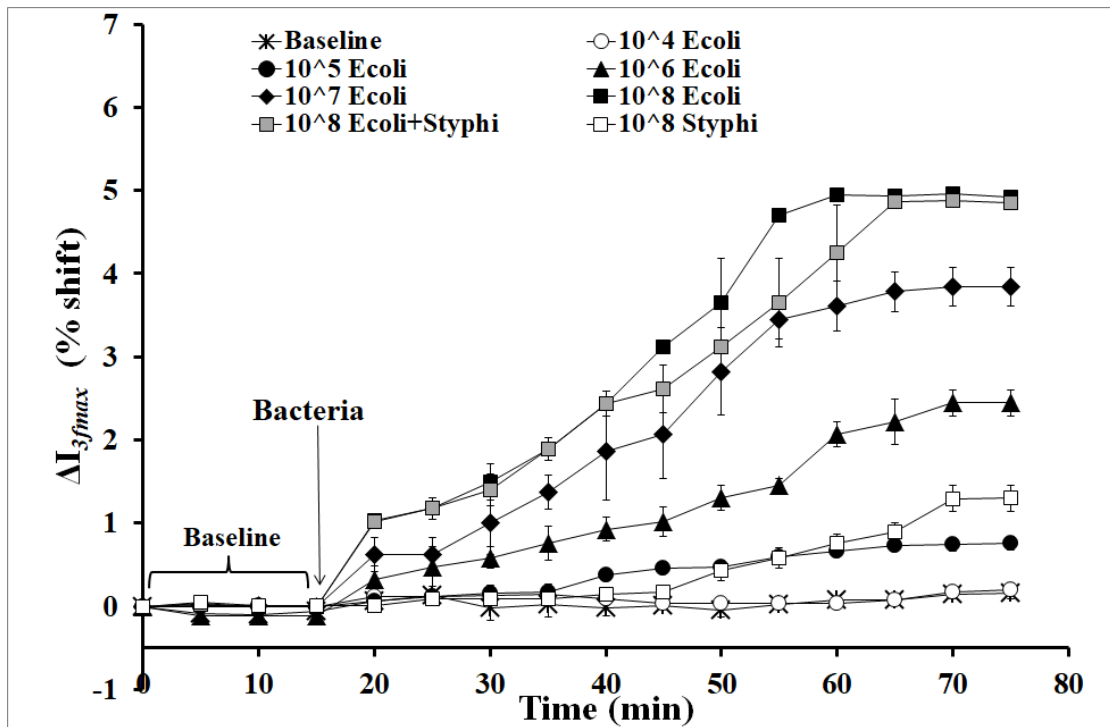


Fig. 4.13 – I_{3fmax} shift (%) as a function of time with bacterial suspension of different concentrations (cells/mL) over the surface functionalised with aptamers.

For all the three parameters, shift in the respective values are plotted at 5 mins (please see Fig. 4.14, 4.16 and 4.18) and 30 mins (please see Fig. 4.15, 4.17 and 4.19). Also, the shifts measured at 60 mins at the end of the experiment are given in the table 4.2 for all the three parameters with mean values and standard deviations. About 10^6 E.coli/mL bacteria could be reliably and rapidly detected with 3f signal (ΔI_{3fmax}) at 5 mins (i.e. 2.5×10^4 bacteria) than with Δf_0 and ΔD ; as the 3f signal was much higher (x 250.228) than that observed for 100 times the concentration of *S.typhi* bacteria at 5 mins. Signal observed with Δf_0 (x 0.315) and ΔD (x 1.029) was comparatively much less at 5 mins for 10^6 E.coli/mL bacteria with respect to 10^8 *S.typhi*/mL. Quantitative correlation could be also achieved with only I_{3fmax} . Thus, ADT technique enables reliable and rapid quantitative detection of bacteria as compared to standard frequency shift and dissipation shift measurements.

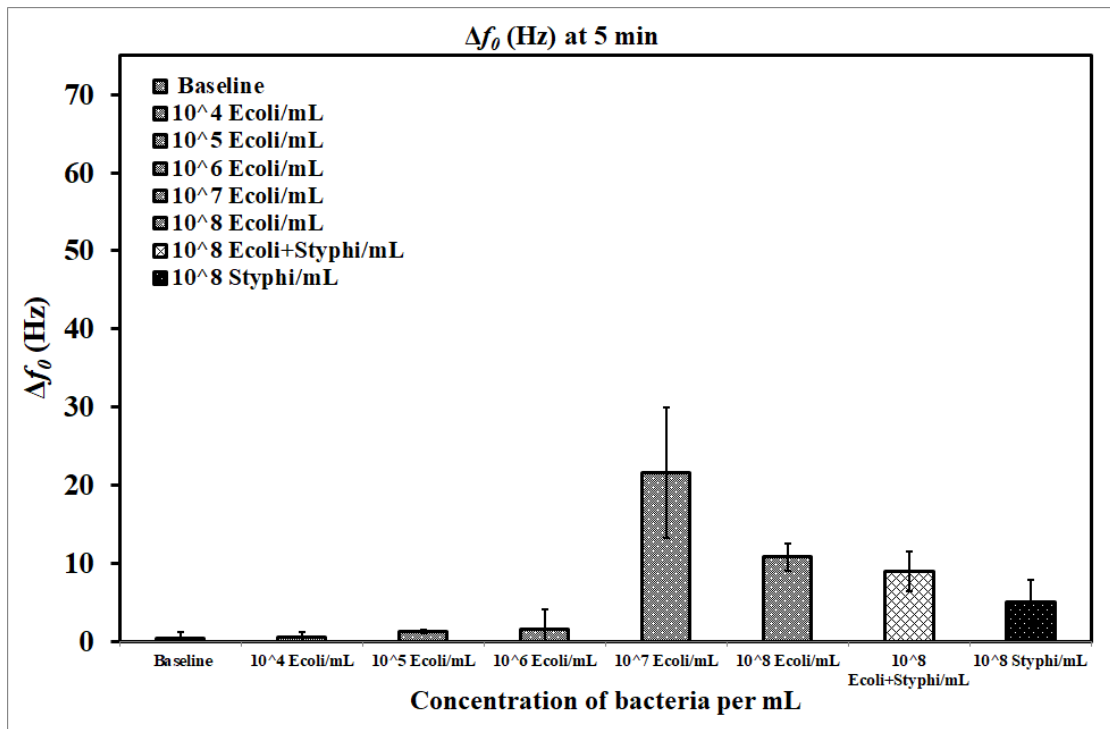


Fig. 4.14 - Frequency shift (Hz) at 5 mins with *E.coli* bacterial suspension of different concentrations (cells/mL) over the surface functionalised with aptamers.

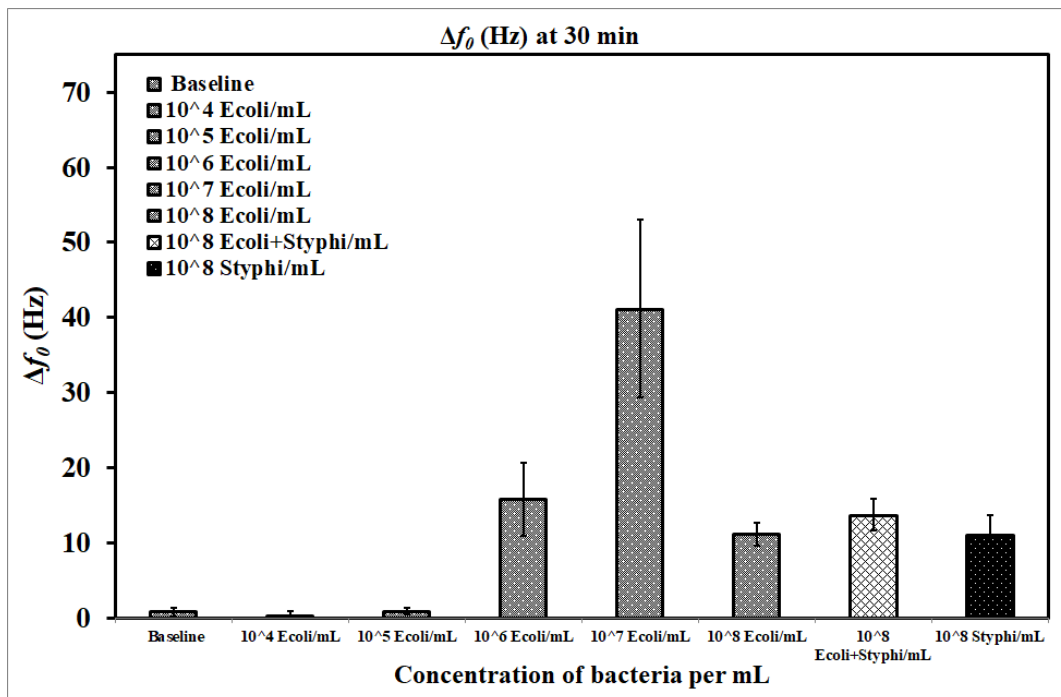


Fig. 4.15- Frequency shift (Hz) at 30 mins with *E.coli* bacterial suspension of different concentrations (cells/mL) over the surface functionalised with aptamers.

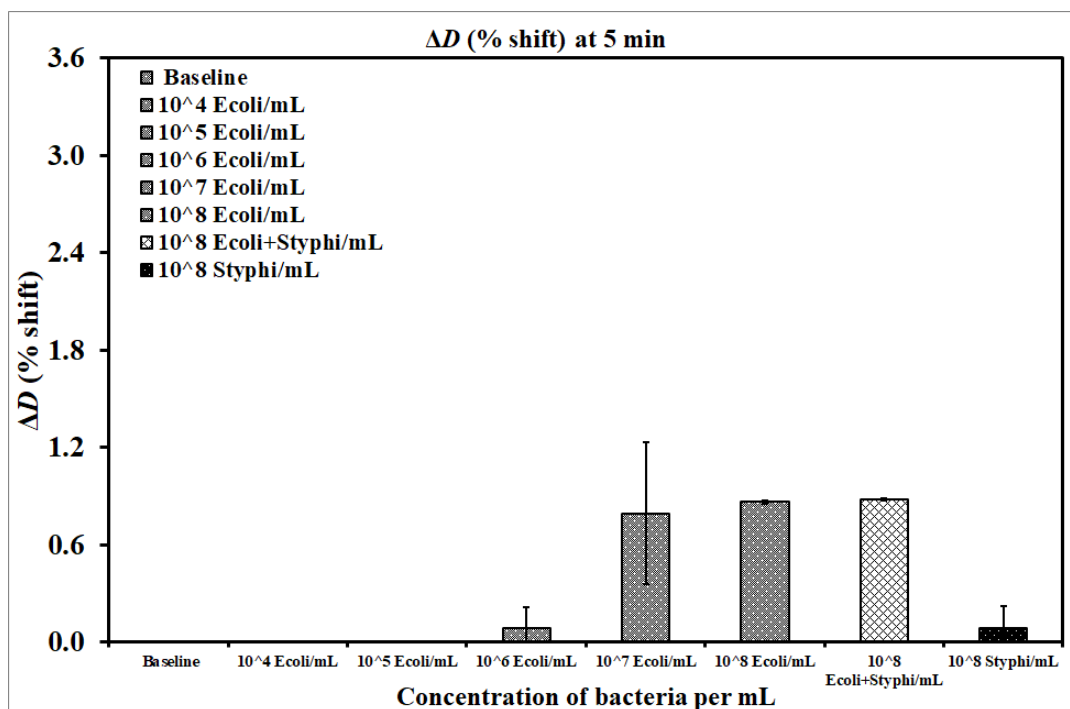


Fig. 4.16 - Dissipation shift (%) at 5 mins with E.coli bacterial suspension of different concentrations (cells/mL) over the surface functionalised with aptamers.

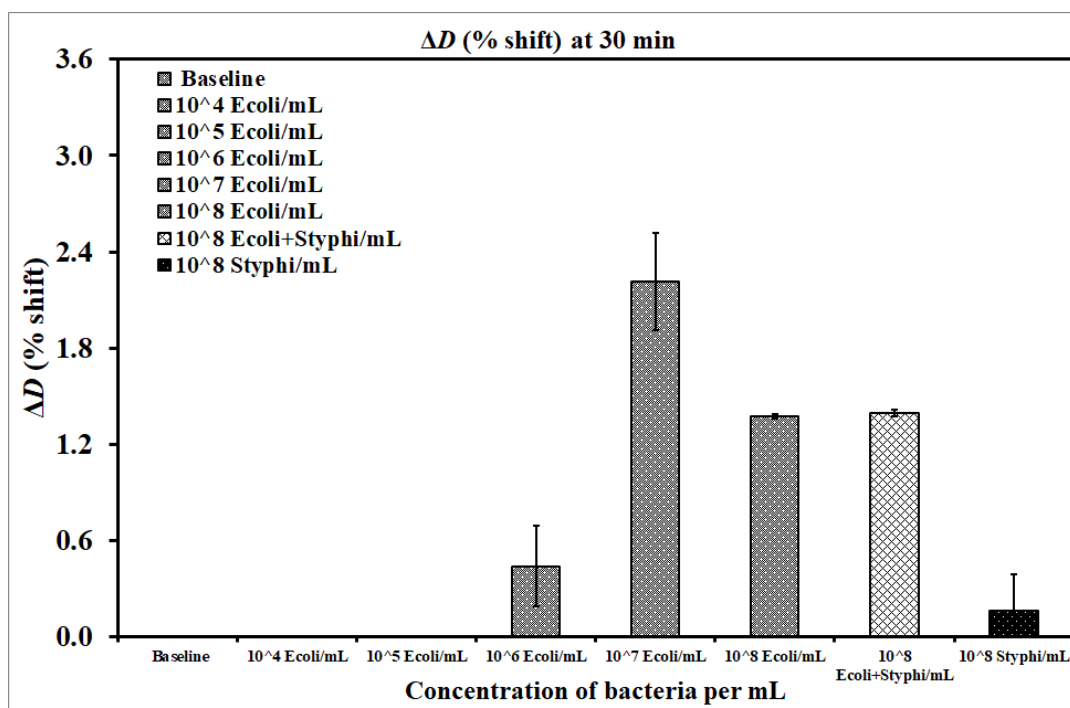


Fig. 4.17 - Dissipation shift (%) at 30 mins with E.coli bacterial suspension of different concentrations (cells/mL) over the surface functionalised with aptamers.

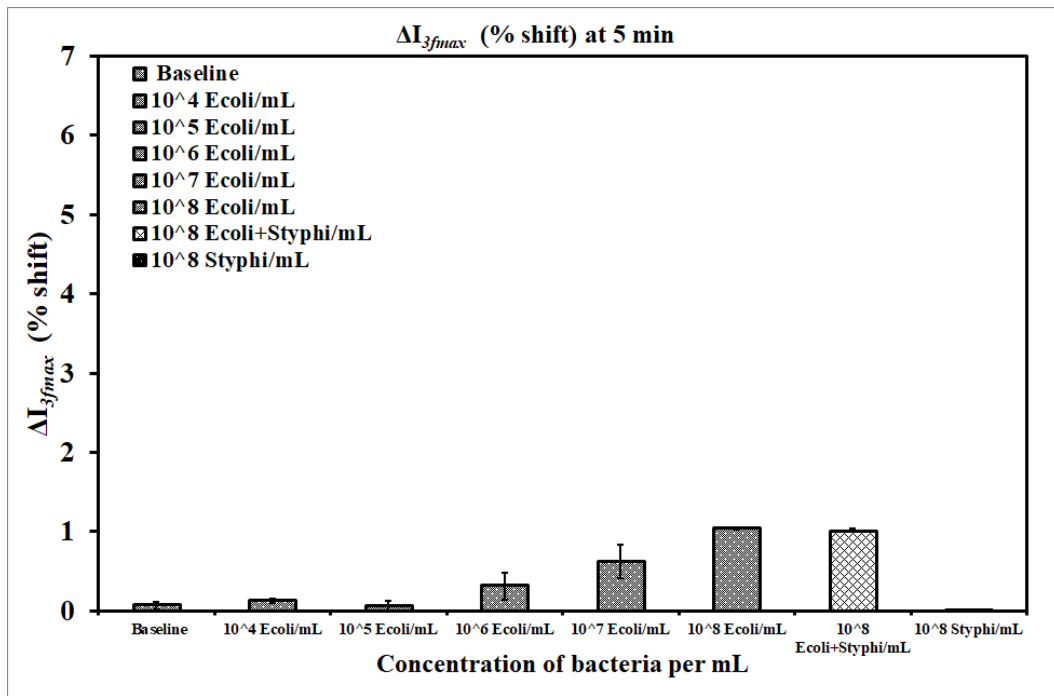


Fig. 4.18– I_{3fmax} shift (%) at 5 mins with *E.coli* bacterial suspension of different concentrations (cells/mL) over the surface functionalised with aptamers.

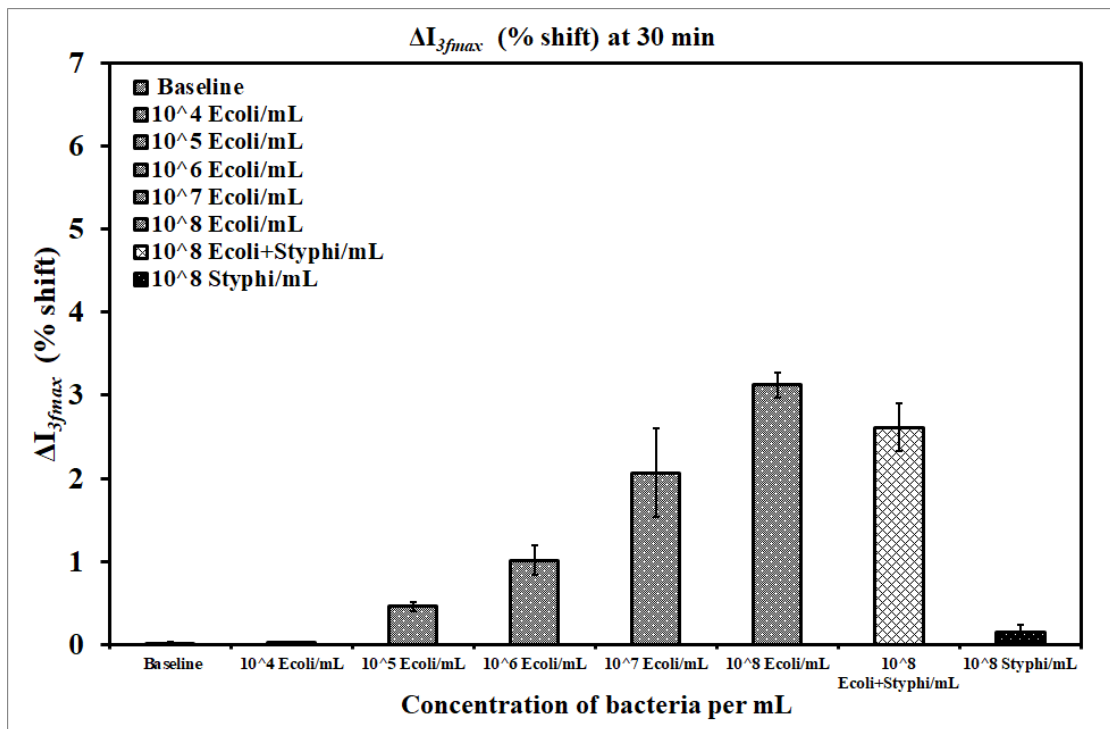


Fig. 4.19 - I_{3fmax} shift (%) at 30 mins with *E.coli* bacterial suspension of different concentrations (cells/mL) over the surface functionalised with aptamers.

Table 4.2 – Mean values and standard deviations measured after 60 mins*						
At 60 mins	Δf_0		ΔD		ΔI_{3fmax}	
	Mean	S.D	Mean	S.D	Mean	S.D
Baseline	1.833	0.907	0.176	0.179	0.158	0.110
10^4 Ecoli/mL	2.667	2.307	0.068	0.078	0.204	0.126
10^5 Ecoli/mL	2.233	2.155	0.095	0.142	0.761	0.137
10^6 Ecoli/mL	24.500	10.221	1.105	0.992	2.444	0.282
10^7 Ecoli/mL	40.800	11.012	2.111	0.509	3.836	0.402
10^8 Ecoli/mL	33.833	12.154	1.919	0.372	4.927	0.002
10^8 Ecoli+Styphi/mL	28.933	10.450	1.736	0.34	4.857	0.126
10^8 Styphi/mL	9.500	2.390	0.261	0.276	1.297	0.263

* Triplicate set of experiments were performed for each concentration of bacteria.

4.10 Quantitative analysis

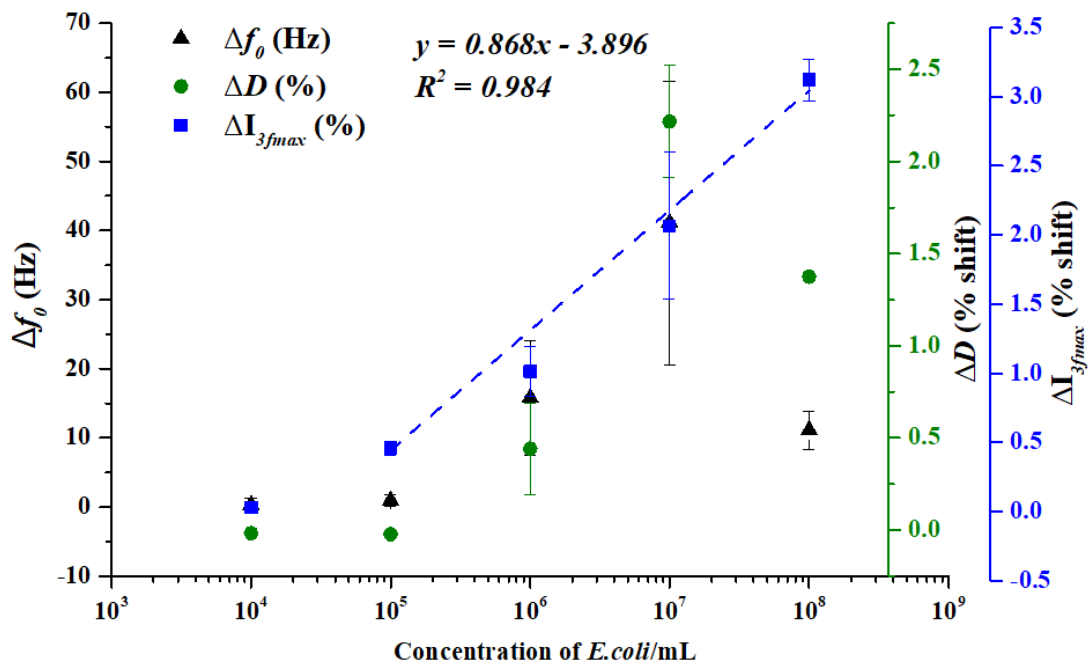


Fig. 4.20 – Signal response for different concentrations of *E.coli* bacteria (cells/mL) showing: (a) Frequency shift, Δf (Hz); (b) Dissipation shift, ΔD (% shift); and (c) $3f$ signal, I_{3fmax} (% shift).

A strong linear correlation was observed for four concentrations of *E.coli* bacteria (10^5 - 10^8 cells/mL) with ΔI_{3fmax} ($R^2 = 0.984$) than for three concentrations of *E.coli* (10^5 - 10^7 cells/mL) with Δf_0 ($R^2 = 0.955$) and ΔD ($R^2 = 0.826$); excluding higher concentration 10^8 cells/mL. For the highest concentration of *E.coli* of 10^8 cells/mL, negative frequency and dissipation shifts were observed. This could be due to increase in mass going on the surface, underlining the need for washing step with these methods. Linear quantitative correlation could be achieved for *E.coli* concentrations with ΔI_{3fmax} , from the fit and this does not require washing step, as the $3f$ signal corresponds to the number of bacteria attached to the surface and not their mass.

4.11 Specificity analysis

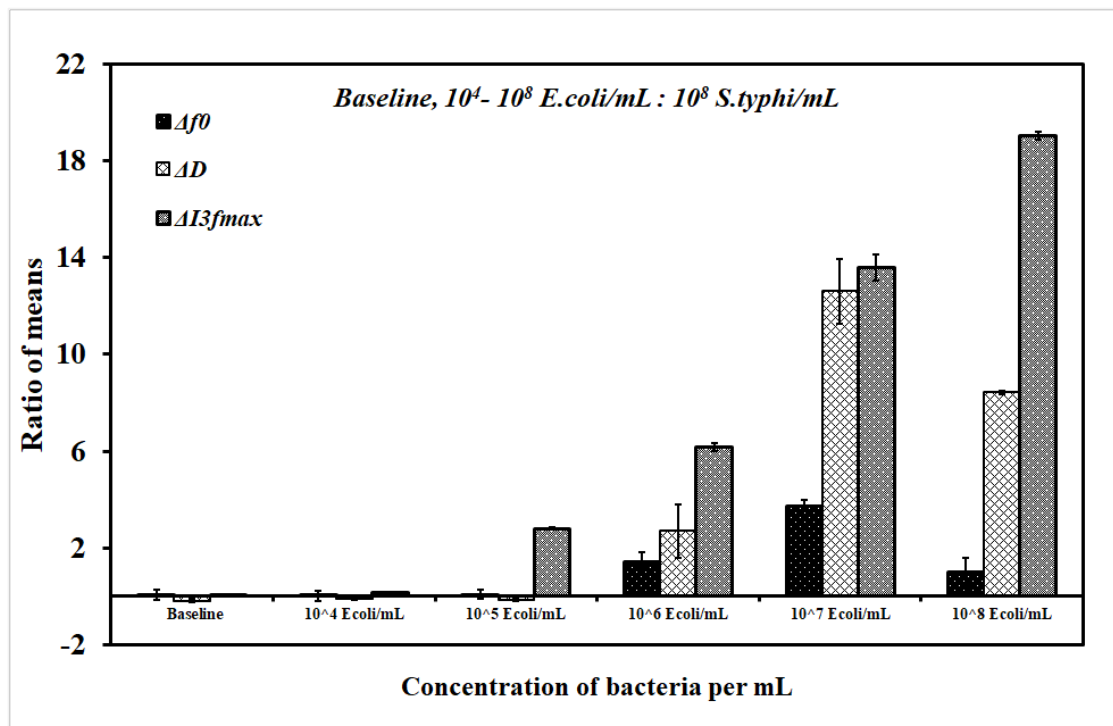


Fig. 4.19 – Comparison of specificity: ratio of mean values of Δf_0 , ΔD and ΔI_{3fmax} for baseline and different concentrations of *E.coli*/mL and 10^8 *S.typhi*/mL.

Mean values of the triplicate sets of experiments conducted with each concentration of *E.coli* bacteria (10^5 - 10^8 cells/mL) and *S.typhi* bacteria (10^8 cells/mL) recorded at 30 mins, were calculated and their ratios were compared. These ratios for Δf_0 , ΔD and ΔI_{3fmax} measurements are plotted in

Fig. 4.19. For same concentrations of *E.coli* and *S.typhi* bacteria (10^8 cells/mL), the ratio values were, 1.01 for Δf_0 , 8.42 for ΔD and highest 19.02 for ΔI_{3fmax} . Thus, the increase in resonant frequency and the relative increase in dissipation were found to be lower by 18.83 and 2.26 times than the relative decrease in 3f signal (I_{3fmax}). Thus, ADT technique enables reliable specific detection of bacteria as compared to standard frequency shift and dissipation shift measurements.

4.10 Summary

This work investigated the behaviour of the nonlinear acoustic response of a QCR in the rapid detection and quantification of *E.coli* (KCTC 2571) bacteria through aptamer-based assay. In this investigation, the fabricated 'anharmonic acoustic aptasensor' on gold surface of QCR electrodes was successful in rapid, sensitive, specific and quantitative detection of *E.coli* bacteria and met the first objective O.1 of this thesis. The response of this sensor was observed for the bacterial suspensions ranging from 10^5 - 10^8 cells/mL and this sensor enabled the following:

Rapid and sensitive detection of viable whole-cell *E.coli* bacteria: The results show that the 3f signals (I_{3fmax}) allow rapid, sensitive and quantitative detection of 2.5×10^4 viable *E.coli* bacteria in 5 mins, as compared to standard frequency shift (Δf_0) and dissipation shift (ΔD) measurements.

Quantitative detection of viable whole-cell *E.coli* bacteria: Linear quantitative correlation could be reliably achieved with 3f signal (I_{3fmax}) ($R^2 = 0.984$) for four concentrations of *E.coli* bacteria (10^5 - 10^8 cells/mL), than with Δf_0 and ΔD .

Specific detection of viable whole-cell *E.coli* bacteria: To determine specificity, *S.typhi* bacteria were used as control sample. For the same concentrations of *E.coli* and *S.typhi* bacteria (10^8 cells/mL), the ratio values were, 1.01 for Δf_0 , 8.42 for ΔD and highest 19.02 for ΔI_{3fmax} . Thus, the increase in resonant frequency and the relative increase in dissipation were found to be lower by 18.83 and 2.26 times than the relative decrease in 3f signal (I_{3fmax}).

Reproducible detection of viable whole-cell *E.coli* bacteria: Triplicate set of experiments were performed to validate reproducibility after achieving stable baseline each time.

To sum up, this anharmonic acoustic aptasensor which allows fast, sensitive quantitative detection of viable target bacteria with high specificity and reproducibility not only saves time but also allows subsequent AST by sparing intact bacteria for further characterisation. Thus, this could be applied to reduce the diagnostic cycle and prevent AMR.

Chapter 5 Detection of bacteria using bio-receptors of different size and length integrated with ADT

5.1 Introduction

In biosensors, the interaction forces between the ligand and the bio-receptor are very important as they determine the characteristics of the output signal. In chapter 4, anharmonic acoustic aptasensor detected *E.coli* bacteria sensitively and specifically due to the high affinity of the polyvalent aptamers towards the target bacteria and the level of selectivity of the ADT technique. In the ADT technique, for a given drive frequency (f), the $3f$ signal is dependent on the force-extension characteristic of the molecular tether, its length, and also the size of the particles. Hence, in this chapter, bio-receptors of different size i.e. anti-*E.coli* antibodies and different length i.e. thiolated *E.coli*-binding aptamer are investigated for detection of *E.coli* bacteria and compared with the *E.coli*-binding aptamer with long linker length (biotinylated aptamer).

5.2 Background

It has been demonstrated earlier that the deviation of the $3f$ signal depends on the mechanical characteristics of the linker and also its length.^[146-149] In the previous chapter, the nonlinear acoustic response of QCR was probed with functionalised specific DNA aptamers that are multivalent and bind whole bacterial cell for direct detection and quantification of viable *E.coli* KCTC 2571 bacteria. This anharmonic acoustic aptasensor could directly detect 10^7 cells/mL target bacteria within 5 mins and had high specificity towards *E.coli* (KCTC 2571) bacteria as compared to same concentration of *S.typhi* bacteria. Aptamers are smaller in size in comparison to antibodies (8–25 kDa nucleic acids vs ~150 kDa antibodies). As ADT signal is influenced by the linker characteristics, polyclonal antibodies which are larger than aptamers were investigated with the same bioassay parameters used for detection of *E.coli* bacteria. Also, for the length of the linker same *E.coli* binding aptamers were employed, but instead of using biotin-streptavidin interface, thiolated aptamers were used that would directly bind to the sensor surface.

5.3 Comparison of aptasensor with immunosensor

Polyclonal antibodies (pAb) are very commonly used as bio-receptor in lot of immunosensor-based assays for bacterial detection. They are typically raised in rabbits, goats or sheep.^[235] Polyclonal antibodies raised against specific bacterial strains are the most commonly used bio-receptors for whole bacterial cell detection, where the binding targets on the cell envelope are usually unknown.^[120] To increase the specificity and sensitivity of the sensor, isolated surface epitopes can be used to produce monoclonal antibodies.^[236] However, since the aptamers used for *E.coli* detection are also polyvalent, polyclonal anti-*E.coli* antibodies were selected for comparison purpose.

5.4 Linking the antibodies to the QCR

5.4.1 Cleaning the surface of gold electrode

AT-cut stepped (non-uniform) quartz crystals were used with fundamental resonant frequency range of 14.23 -14.25 MHz (Lap-Tech Inc., Bowmansville, Ontario, Canada). The surfaces of gold electrodes of quartz crystals were cleaned with acetone for 5 mins and then with isopropanol (IPA) by ultra-sonication process for 5 mins. Then after drying with nitrogen gas, they were placed in plasma cleaner to remove impurities and contaminants from the surface using inert argon gas for 1 min in a Harrick Plasma cleaner. They were then stored in a well of clean 24-well tissue culture plate covered with plastic film.

5.4.2 Formation of self-assembled monolayer (SAM)

The cleaned quartz crystals were then immersed in about 250 μ l of 1mM ethanolic solution of mixture of thiols [biotin terminal group (10%), and methoxy terminal group (90%)] and left overnight for formation of a SAM. Thiols with biotin terminal group HS-C11-(EG)6-Biotin (th004-m11.n6-0.005) and methoxy terminal group HS-C11-(EG)3-OCH₃ (th006-n3) were obtained from Prochimia Surfaces, Poland. The following day, the gold surfaces of quartz crystals were rinsed three times with ultra-pure ethanol (Sigma-Aldrich, UK) for removing the non-adsorbed thiols and then both sides

of crystal were dried with a stream of nitrogen gas. After making sure that the electrode on bottom side was completely dried, the crystal was mounted on PCB cartridge and sealed with “O-ring” of microfluidic flow-cell with only one face exposed to the solution. The gold surfaces were then rinsed with de-ionized (DI) water to remove ethanol followed by phosphate buffer saline (PBS) with physiological pH 7.4.

5.4.3 Deposition of Streptavidin

PBS buffer solution (100 μL) was then flowed over the substrate at the continuous flow rate of 10 $\mu\text{L}/\text{min}$ and baseline measurements were taken for 15 mins at 5 min interval. This was followed by about 150 μl of Streptavidin (10 $\mu\text{g}/\text{mL}$) for 15 mins at the flow rate of 10 $\mu\text{L}/\text{min}$; thus forming a strong bond with the biotin terminal group of the alkane thiol. Measurements were taken under flow for 15 mins at 5 min interval.

5.4.4 Immobilisation of bio-receptor on the gold electrode of QCR

After depositing streptavidin, PBS buffer solution (500 μL) was then flowed over the substrate at the continuous flow rate of 100 $\mu\text{L}/\text{min}$ for 5 mins, to remove the unbound streptavidin.

Then the surface was functionalised with biotinylated polyclonal anti-*E.coli* antibodies, by passing over the surface for 15 mins. The excess antibodies were removed by flowing PBS solution and then baseline measurements were taken every 5 minutes over 30 minutes under a continuous flow of PBS at flow rate of 5 $\mu\text{l}/\text{min}$. Rabbit polyclonal anti-*E.coli* antibodies (biotin) Ab68451 (Abcam, Cambridge, UK), were used. Aliquots of pAbs were prepared and stored at -20°C or -80°C to avoid repeated freeze / thaw cycles.

The steps followed to link the biotinylated polyclonal anti-*E.coli* antibodies to the surface of gold electrodes of QCR, are depicted in Fig. 5.1.

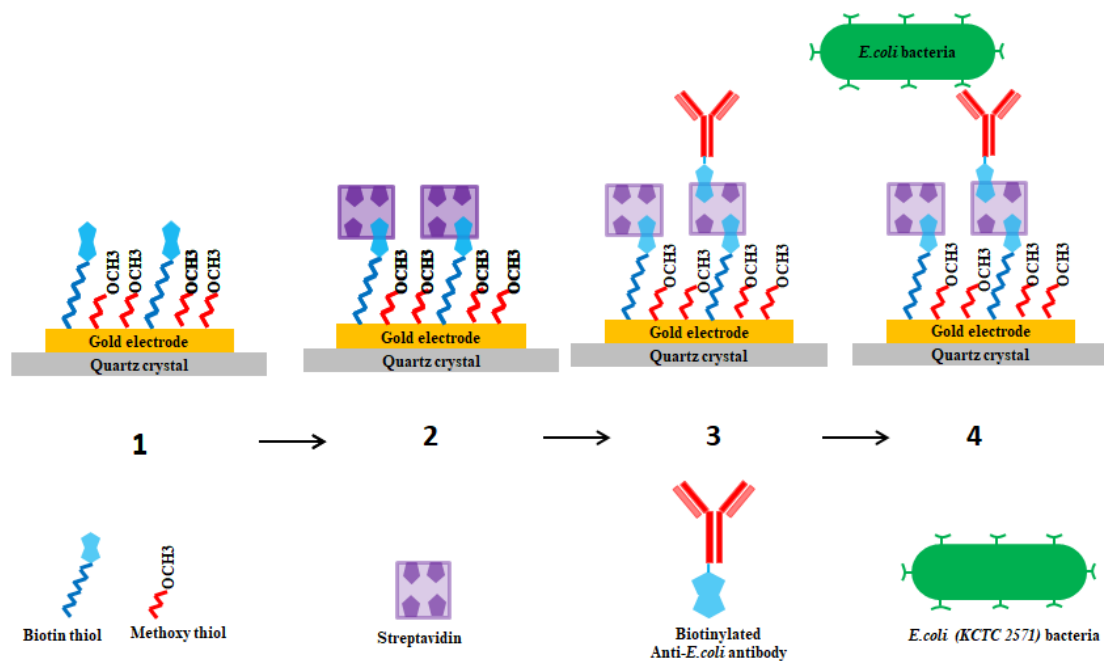


Fig. 5.1 - Functionalisation steps: (1) Mixed SAM with 10% biotin thiol and 90% methoxy thiol, (2) Streptavidin layer, (3) Biotinylated Anti-*E.coli* antibody and (4) final step of flowing the *E.coli* (KCTC 2571) bacteria.

After functionalising the surface with anti-*E.coli* antibodies, in order to detect *E. coli* (KCTC 2571) by direct assay, 10^7 cells/mL of bacteria were spiked into the sample (as final concentrations) over the prepared sensor surface at a flow rate of $5 \mu\text{l}/\text{min}$ for further 60 mins. A total of 3×10^6 bacterial cells are therefore injected over 60 mins, respectively. Frequency scans were taken at 0.02 SU and 0.1 SU (0.1s period) and Δf and ΔD were simultaneously monitored in real time during *E.coli* detection steps using a quartz crystal nonlinear network analyzer. All the measurements were taken in continuous flow mode.

5.5 Determination of drive amplitude

To determine the optimal drive amplitude, the surfaces of the QCR were functionalised with polyclonal anti-*E.coli* antibodies, and then rinsed with PBS buffer. After taking baseline measurements, 10^7 *E.coli*/mL (as final concentrations) were spiked into the sample and passed over the prepared sensor surface at a flow rate of $5 \mu\text{l}/\text{min}$ for 60 mins.

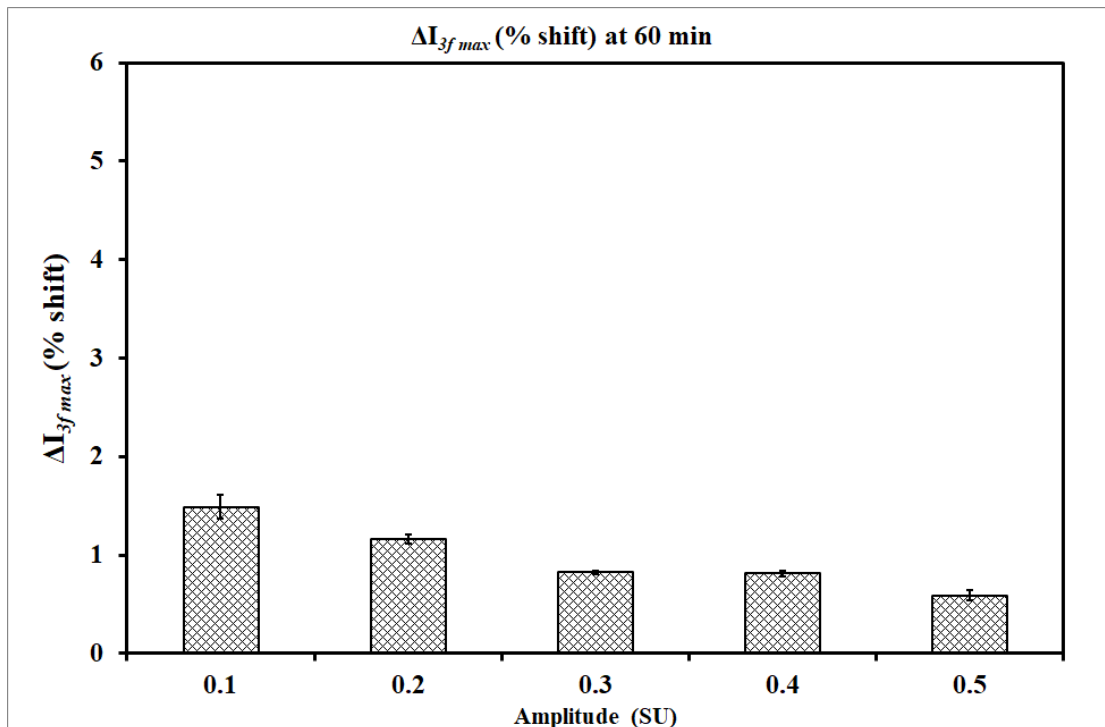


Fig. 5.2 - $I_{3f_{max}}$ shift (%) measured at different amplitudes – 0.1 to 0.5 SU at 60 mins, after passing 10^7 *E.coli*/mL on the surface functionalised with polyclonal antibodies (pAbs).

Resonant frequency (f_0) was determined with frequency sweep and the sensor was then driven by a pure sinusoidal oscillation at f_0 in frequency mode scan, at different amplitudes ranging from 0.1 to 0.5 SU. The complex values (in-phase and quadrature) of current and voltage were recorded at $1f$ and $3f$ simultaneously using the ADT machine. The percentage shift in the peak values of the corresponding $3f$ signal ($I_{3f_{max}}$) from baseline, are plotted at 60 mins (Fig. 5.3). Maximum shift was observed at 0.1 SU which corresponds to excitation voltage of 3 Volts and 7.5 nm of oscillation amplitude at surface.^[233,234] But the value of oscillation amplitude seems to have inverse relation with corresponding $3f$ signal. At 0.2 SU (6 Volts) $3f$ signal dropped despite increase in oscillation amplitude. Thus, 0.1 SU was selected for further measurements as it gave maximum $3f$ signal.

5.6 Detection of *E.coli* bacteria with polyclonal antibodies

After determining the optimal drive amplitude, triplicate sets of experiments were carried out with two concentrations of *E.coli* bacteria. In order to detect

E.coli (KCTC 2571) by direct assay, different concentrations of bacteria were spiked into the sample ($10^6 - 10^7$ cells/mL as final concentrations) over the prepared sensor surface at a flow rate of 5 μ l/min for further 60 mins. A total of 3×10^5 & 3×10^6 bacterial cells are therefore injected over 60 mins, respectively. To check specificity of the sensor, *S.typhi* bacterial samples were also used at 10 times the concentration of *E.coli* bacteria. Thus, 10^8 cells/mL as final concentrations of *S.typhi* bacteria were also spiked into the sample over the prepared sensor surface at a flow rate of 5 μ l/min for further 60 mins. Frequency scans were taken at 0.02 SU and 0.1 SU (0.1s period) and Δf_0 , ΔD and ΔI_{3fmax} were simultaneously monitored in real time during streptavidin and polyclonal antibody immobilisation and *E.coli* detection using a quartz crystal nonlinear network analyzer. All the measurements were taken in continuous flow mode.

Comparison of sensitivity

The shifts in the respective values of I_{3fmax} are plotted at 5 mins, 30 mins and 60 mins (as shown in Fig. 5.5, 5.6 and 5.7, respectively). The signals with 10^6 *E.coli*/mL and 10^7 *E.coli*/mL were much higher at 5 mins, 30 mins and 60 mins when compared to the signal obtained with 10^8 *S.typhi*/mL bacteria.

Relative decrease in peak values of ΔI_{3fmax} from baseline are plotted over 60 mins for which the *E.coli* and *S.typhi* bacteria were flowed over the sensor surface after achieving the baselines, as shown in the Fig. 5.4.

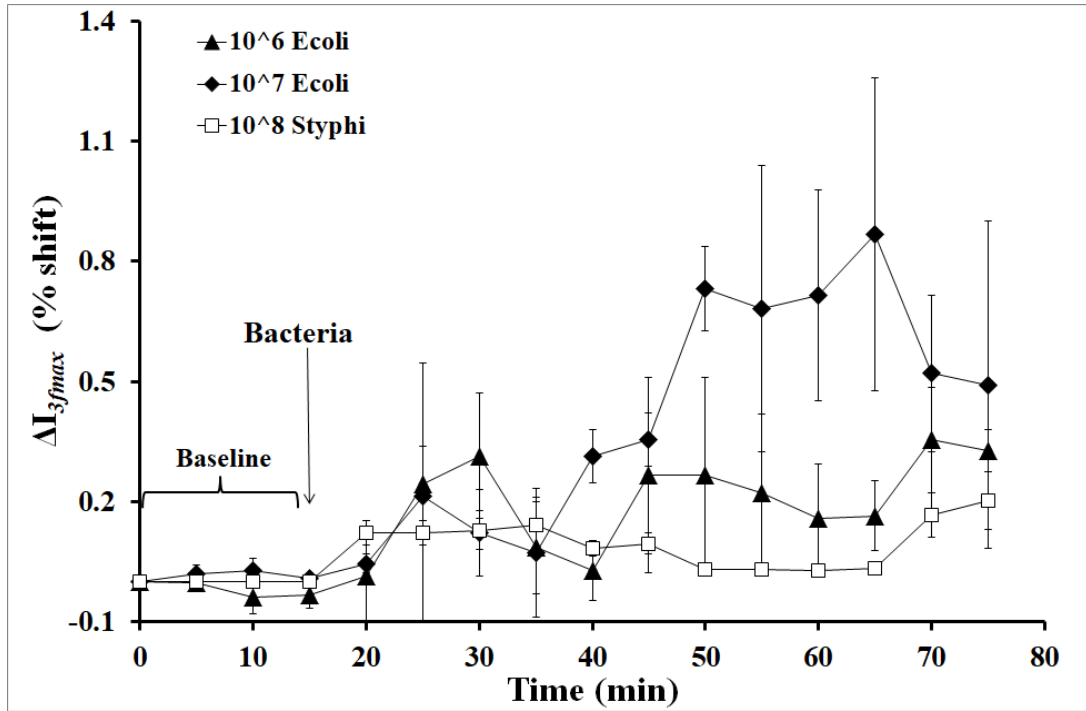


Fig. 5.3 - I_{3fmax} shift (%) as a function of time with 10^6 , 10^7 E.coli/mL and 10^8 S.typhi/mL over the surface functionalised with polyclonal antibodies.

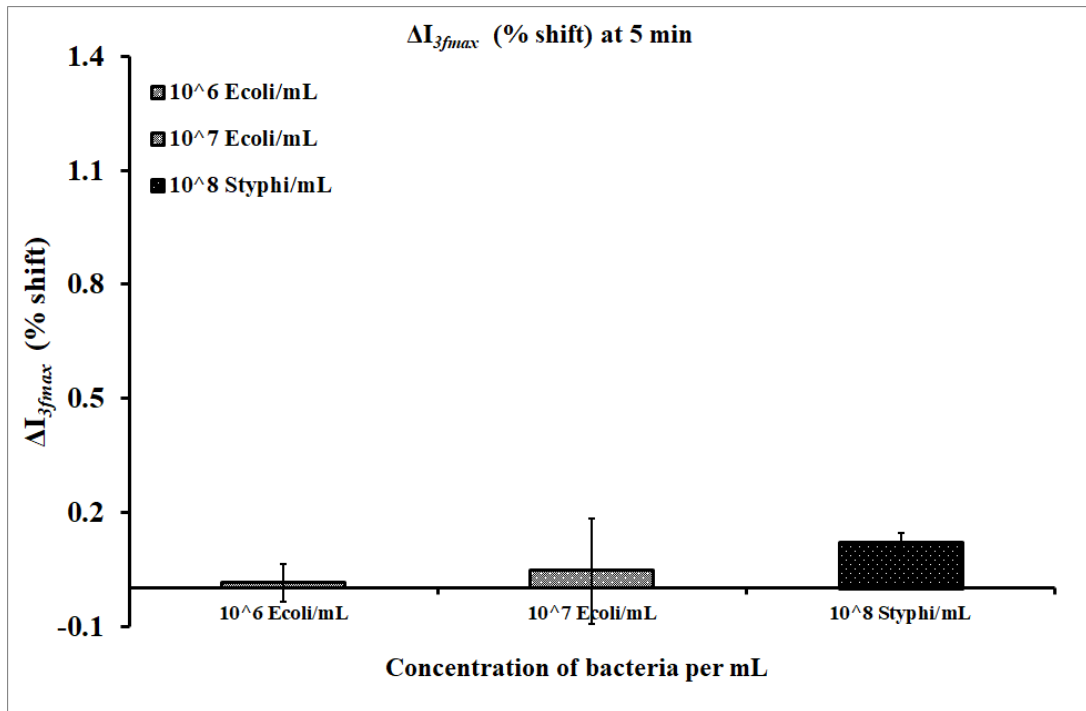


Fig. 5.4 - I_{3fmax} shift (%) at 5 mins with with 10^6 , 10^7 E.coli/mL and 10^8 S.typhi/mL over the surface functionalised with polyclonal antibodies.

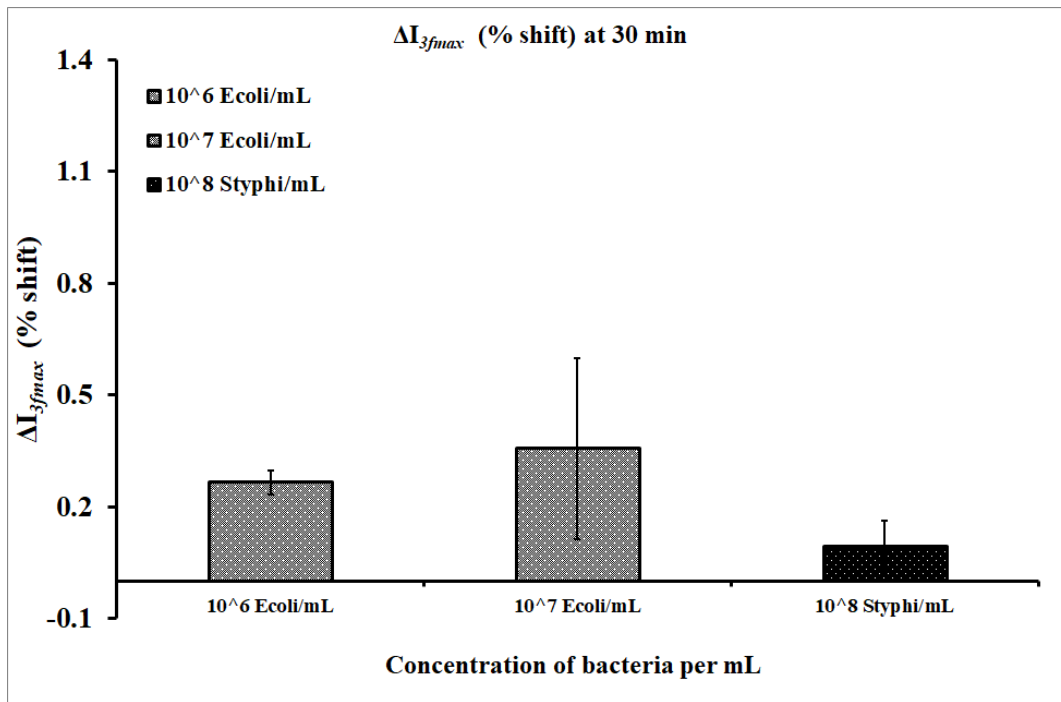


Fig. 5.5 - I_{3fmax} shift (%) at 30 mins with 10^6 , 10^7 E.coli/mL and 10^8 S.typhi/mL over the surface functionalised with polyclonal antibodies.

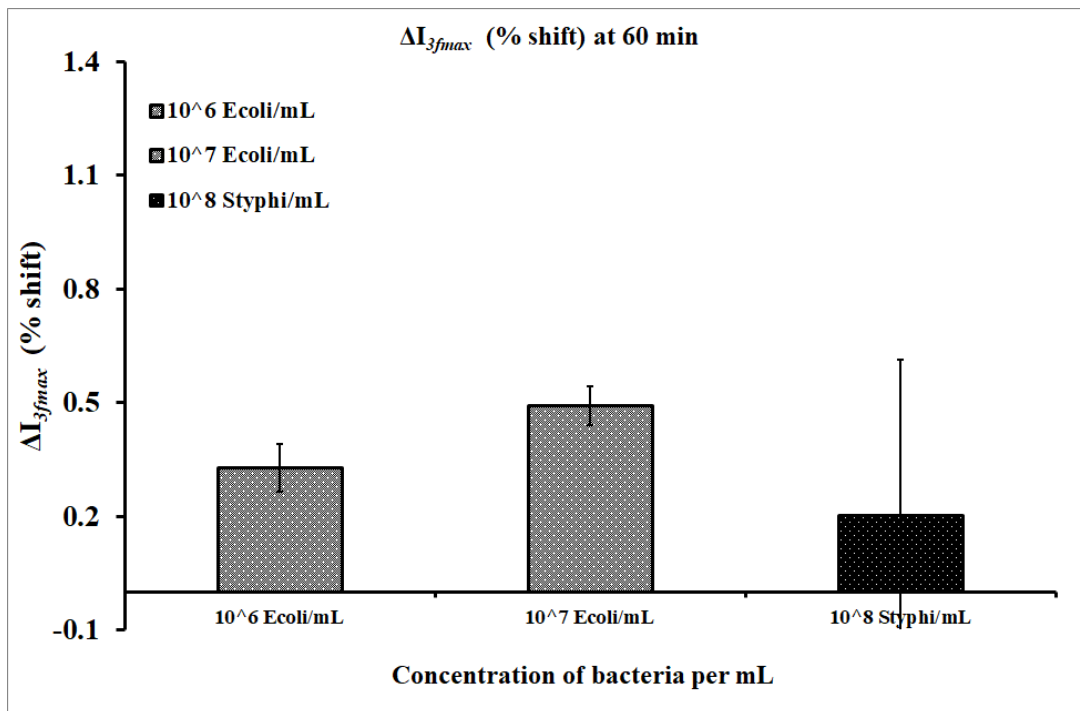


Fig. 5.6 - I_{3fmax} shift (%) at 60 mins with 10^6 , 10^7 E.coli/mL and 10^8 S.typhi/mL over the surface functionalised with polyclonal antibodies.

Comparison of specificity

Mean values of the triplicate sets of experiments conducted with each concentration of *E.coli* bacteria (10^6 - 10^7 cells/mL) and *S.typhi* bacteria (10^8 cells/mL) recorded at 30 mins, were calculated and their ratios were compared. These ratios for ΔI_{3fmax} measurements are plotted in Fig. 5.7. For 10 times lower concentration of *E.coli* than *S.typhi* bacteria, the ratio values was 3.71. This value was found to be lower than that observed with aptamer as bio-receptor for same bacterial concentrations (as shown in Fig. 5.17).

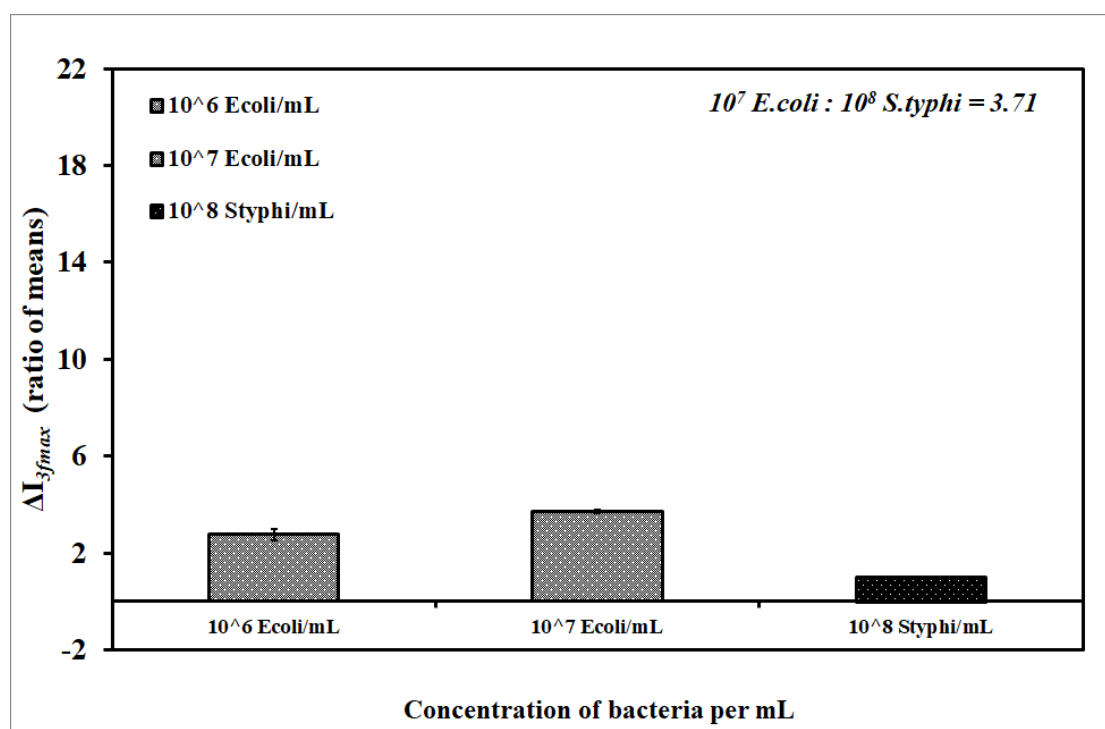


Fig. 5.7 - Comparison of specificity: ratio of mean values of I_{3fmax} shift for different concentrations of *E.coli*/mL and 10^8 *S.typhi*/mL.

5.7 Comparison of the length of the linker (long vs short)

Linkers with different lengths were investigated by Ghosh *et al.*, where the ADT signal varied with the linker length.^[146-149] It was found that with the longer linker the percentage elongation is less and also the inclination is less, resulting in lower $3f$ response compared to a short linker. Based on this, the linker length was investigated for detection of *E.coli* bacteria. Before the *E.coli* binding aptamers were immobilised on the surface of the sensor through

biotin-streptavidin assay which comprised of biotin thiol, streptavidin and then the biotinylated aptamer. This allowed three-dimensional folding of the aptamer providing functional aptamer-immobilised surface. The bacteria were then bound to the surface through this chain of molecules acting as biomolecular linker. To compare linker with shorter length, to the same aptamer sequence a thiol group was added to the 3' end instead of biotin. Introduction of terminal thiol groups allowed for the straight-forward immobilisation of DNA aptamers on gold surfaces.

Chemisorption of thiols to elemental gold is a well-known mechanism resulting in stable self-assembled monolayers (SAMs). Immobilisation of thiolated DNA to gold is widely used.^[237] Aptamer could be immobilised in a highly controlled orientation, i.e. via this thiol group. This controlled orientation facilitates high binding activity by avoiding a loss of functionality resulting from immobilisation in random orientation. However, several factors influencing aptamer folding have to be carefully considered during the immobilisation of aptamers on to the sensor surfaces. For this, the gold electrode is first incubated with thiol-modified aptamer (ssDNA) and then subsequently exposed to 6-mercaptohexanol (MCH) solution. This treatment of the gold layer with MCH, blocks access of analyte and buffer components to the gold surface (causing unspecific adsorption), and on the other hand, supports the vertical orientation of the aptamers when conjugated to the surface (by preventing interaction of aptamer and gold surface, thereby enhancing functional structures).^[238]

Mixed SAMs are commonly formed by the simultaneous co-immobilisation of different components. However, MCH is also used only to backfill after DNA aptamer immobilisation, to displace non-specific interactions between the aptamer and gold and to cause the aptamer to stand up from the surface. The inclusion of MCH during thiolated aptamer immobilisation may prevent non-specific adsorption of aptamer during aptamer immobilisation, forcing the aptamer to stand up from the surface and allowing a greater aptamer loading of the surface than when only thiolated DNA aptamer is immobilised.

5.8 Linking the thiolated aptamer to the QCR

5.8.1 Cleaning the surface of gold electrode

AT-cut stepped (non-uniform) quartz crystals were used with fundamental resonant frequency range of 14.23 -14.25 MHz (Lap-Tech Inc., Bowmansville, Ontario, Canada). The surfaces of gold electrodes of quartz crystals were cleaned with acetone for 5 mins and then with isopropanol (IPA) by ultra-sonication process for 5 mins. Then after drying with nitrogen gas, they were placed in plasma cleaner to remove impurities and contaminants from the surface using inert argon gas for 1 min in a Harrick Plasma cleaner. They were then stored in a well of clean 24-well tissue culture plate covered with plastic film.

5.8.2 Immobilisation of thiolated DNA aptamer

Thiolated DNA aptamers were purchased from Sigma-Aldrich, UK. 6-mercaptohexanol (MCH), tris(2-carboxyethyl)phosphine hydrochloride solution (TCEP), sodium chloride, and magnesium chloride were all procured from Sigma-Aldrich, UK. Ethylenediaminetetraacetic acid disodium salt dehydrate (EDTA), tris-EDTA buffer (TE Buffer), and 10 mM phosphate buffer saline solution (PBS) were procured from Fisher Scientific, UK, and used for surface cleaning and functionalisation. Immobilisation buffer was 1xTE buffer, 1 M NaCl, 50 mM MgCl₂ and 10 mM EDTA. Thiolated DNA aptamer was reduced with 0.5M TCEP in a 1:1 (v/v) ratio for 1-2 hours at room temperature. After reduction, the DNA was diluted to 1 μ M with immobilisation buffer.

1 μ M reduced thiolated DNA aptamer solution was immobilised on the gold electrode. After immobilisation, the gold electrodes were sequentially rinsed in immobilisation buffer and then washed three times in PBS to remove any remaining Mg²⁺. To ensure complete thiol coverage of the gold surface, the electrodes were backfilled with MCH using immersion in 1mM in DI water for 30 mins. The gold electrodes were then washed three times with PBS.

Immobilisation of the thiolated DNA aptamer on the surface was confirmed by simultaneously measuring the frequency shift. After achieving baseline,

introduction of 1 μM reduced thiolated DNA aptamer caused frequency shift (Δf_0) of ~ 300 Hz. A positive frequency shift (Δf_0) of ~ 100 Hz was observed due to introduction of an aqueous solution of MCH (as shown in Fig. 5.9).

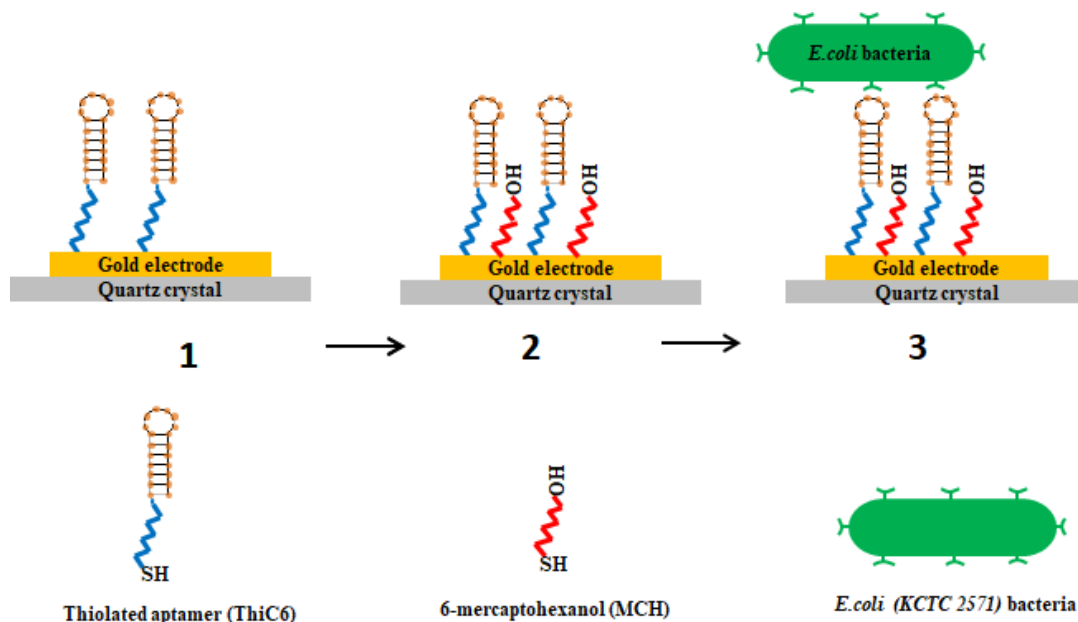


Fig. 5.8 - Functionalisation steps: (1) Thiolated aptamer (ThiC6), (2) backfilling with 6-mercaptohexanol (MCH), (3) final step of flowing the *E. coli* (KCTC 2571) bacteria.

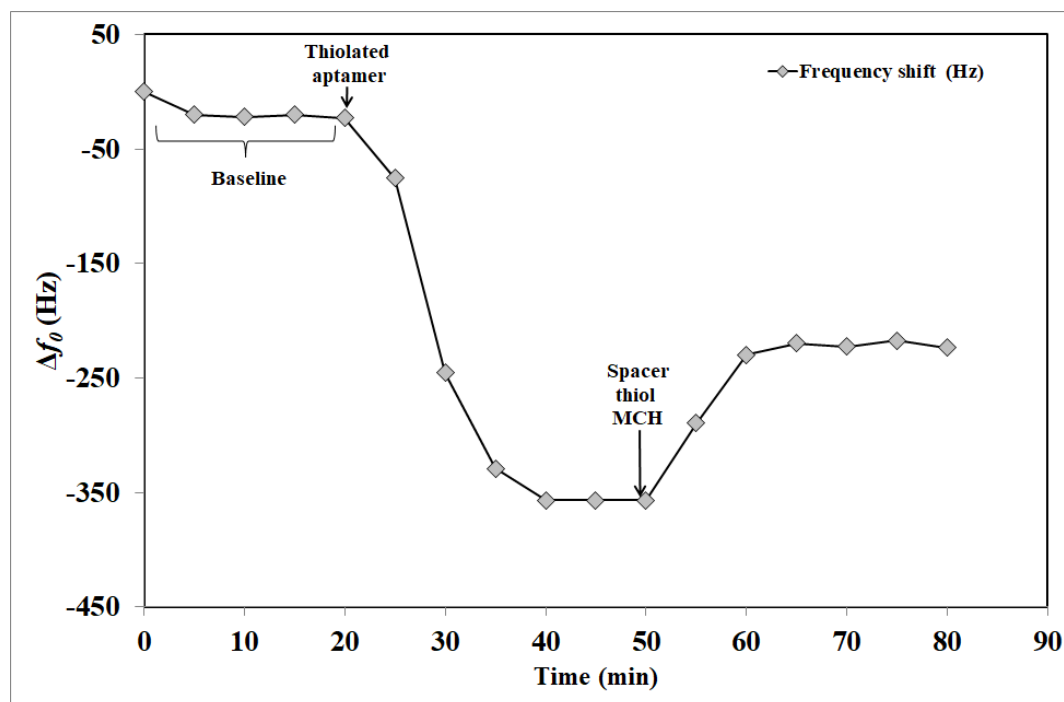


Fig. 5.9 - Frequency shift measured after immobilising: (a) thiolated DNA aptamer (b) aqueous solution of spacer thiol MCH.

5.9 Determination of drive amplitude

The surfaces of the QCR were functionalised with thiolated *E.coli* binding DNA aptamer, and then rinsed with PBS buffer. After taking baseline measurements, 10^7 *E.coli*/mL (as final concentrations) were spiked into the sample and passed over the prepared sensor surface at a flow rate of $5 \mu\text{l}/\text{min}$ for 60 mins. Resonant frequency (f_0) was determined with frequency sweep and the sensor was then driven by a pure sinusoidal oscillation at f_0 in frequency mode scan, at different amplitudes ranging from 0.1 to 0.5 SU. The complex values (in-phase and quadrature) of current and voltage were recorded at $1f$ and $3f$ simultaneously using the ADT machine. The percentage shift in the peak values of the corresponding $3f$ signal (I_{3fmax}) from baseline, are plotted at 60 mins (Fig. 5.10).

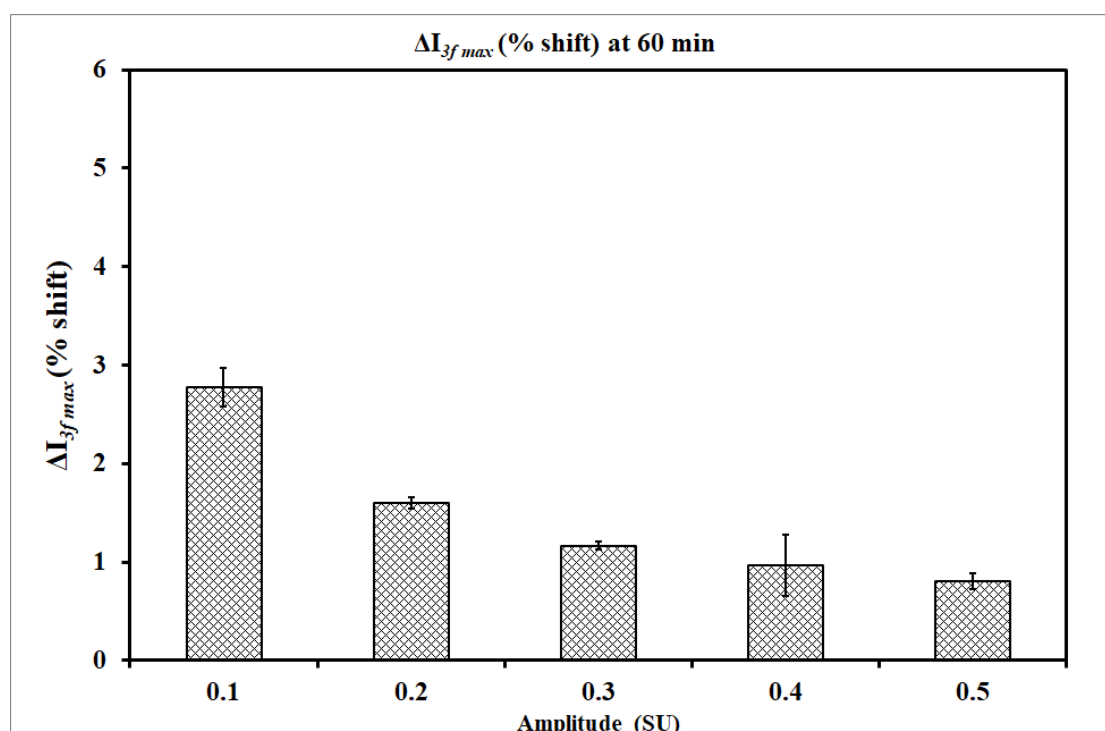


Fig. 5.10 - I_{3fmax} shift (%) measured at different amplitudes: 0.1 to 0.5 SU at 60 mins, after passing 10^7 *E.coli*/mL on the surface functionalised with thiolated DNA aptamers.

Maximum shift was observed at 0.1 SU which corresponds to excitation voltage of 3 Volts and 7.5 nm of oscillation amplitude at surface.^[233,234] But the value of oscillation amplitude seems to have inverse relation with

corresponding $3f$ signal. At 0.2 SU (6 Volts) $3f$ signal dropped despite increase in oscillation amplitude. Thus, 0.1 SU was selected for further measurements as it gave maximum $3f$ signal.

5.10 Detection of *E.coli* bacteria with thiolated aptamer

After determining the optimal drive amplitude, triplicate sets of experiments were carried out with a range of *E.coli* bacterial concentration. In order to detect *E.coli* (KCTC 2571) by direct assay, bacteria were spiked into the sample (10^7 cells/mL as final concentrations) over the prepared sensor surface at a flow rate of 5 μ l/min for further 60 mins. A total of 3×10^6 bacterial cells are therefore injected over 60 mins, respectively. To check specificity of the sensor, *S.typhi* bacterial samples were also used at 10 times the concentration of *E.coli* bacteria. Thus, 10^8 cells/mL as final concentrations of *S.typhi* bacteria were also spiked into the sample over the prepared sensor surface at a flow rate of 5 μ l/min for further 60 mins. Frequency scans were taken at 0.02 SU and 0.1 SU (0.1s period) and Δf_0 , ΔD and ΔI_{3fmax} were simultaneously monitored in real time during streptavidin and thiolated aptamer immobilisation and *E.coli* detection using a quartz crystal nonlinear network analyzer. All the measurements were taken in continuous flow mode. Relative decrease in peak values of ΔI_{3fmax} from baseline are plotted over 60 mins for which the *E.coli* and *S.typhi* bacteria were flowed over the sensor surface after achieving the baselines, as shown in the Fig. 5.11.

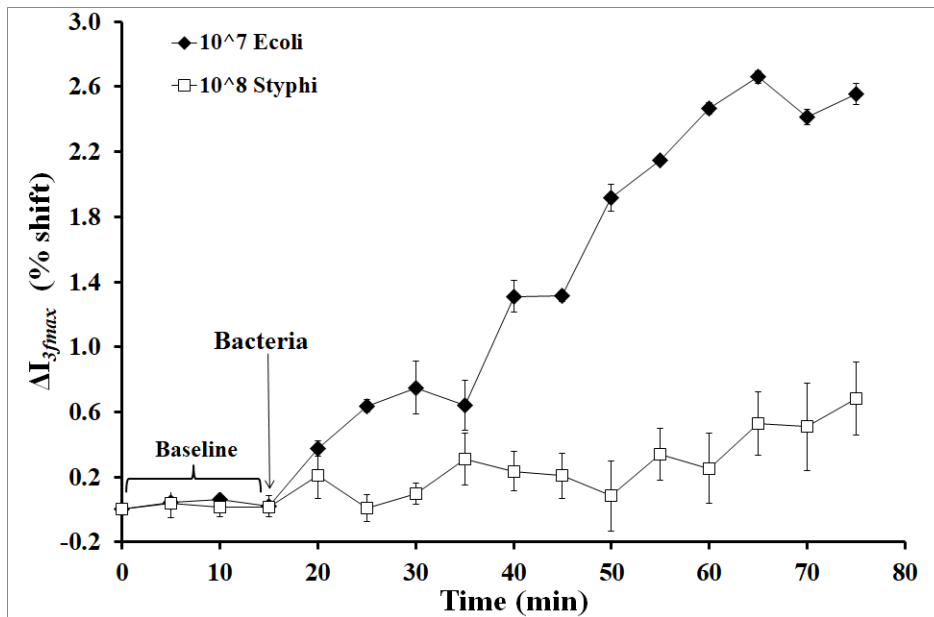


Fig. 5.11 - I_{3fmax} shift (%) as a function of time with bacterial suspension of different concentrations (cells/mL) over the surface functionalised with thiolated aptamers.

Comparison of sensitivity

The shifts in the respective values of I_{3fmax} are plotted at 5 mins, 30 mins and 60 mins (please see Fig. 5.12, 5.13 and 5.14, respectively). The signal with 10^7 E.coli/mL was much higher at 5 mins, 30 mins and 60 mins when compared to the signal obtained with 10 times the concentration of *S.typhi* bacteria.

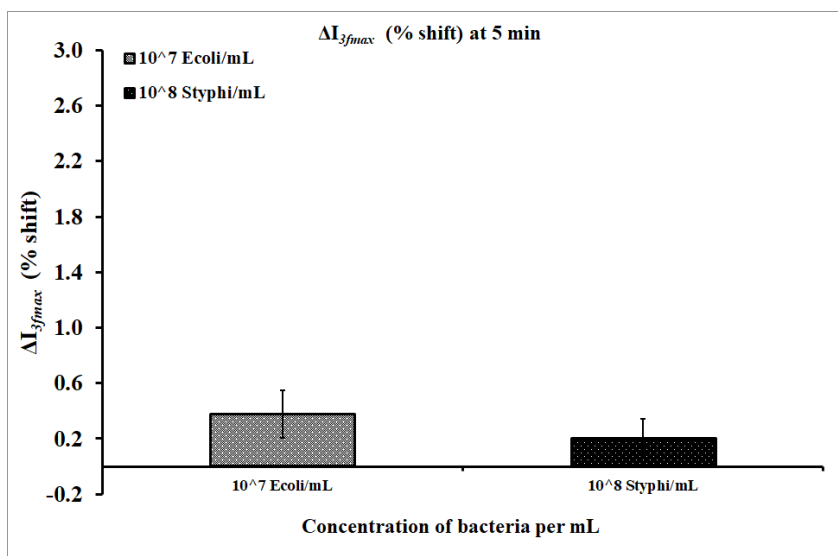


Fig. 5.12 - I_{3fmax} shift (%) at 5 mins with 10^7 E.coli/mL and 10^8 S.typhi/ over the surface functionalised with thiolated aptamer (shorter linker length).

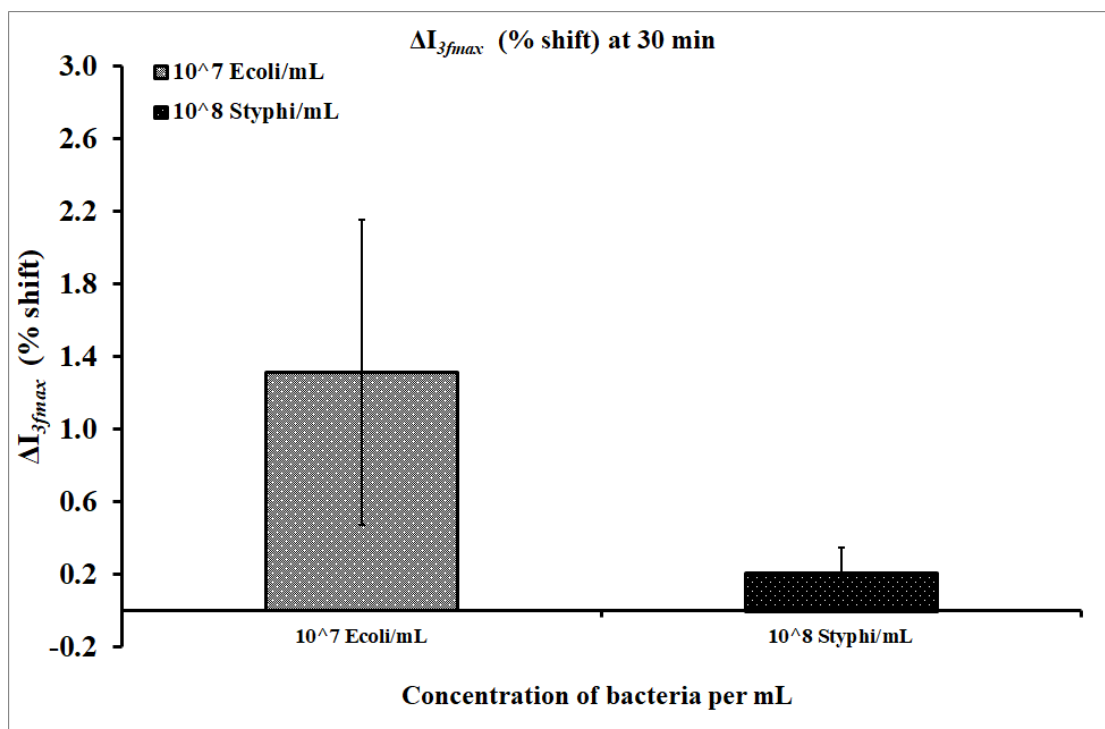


Fig. 5.13 - I_{3fmax} shift (%) at 30 mins with 10⁷ E.coli/mL and 10⁸ S.typhi/ over the surface functionalised with thiolated aptamer (shorter linker length).

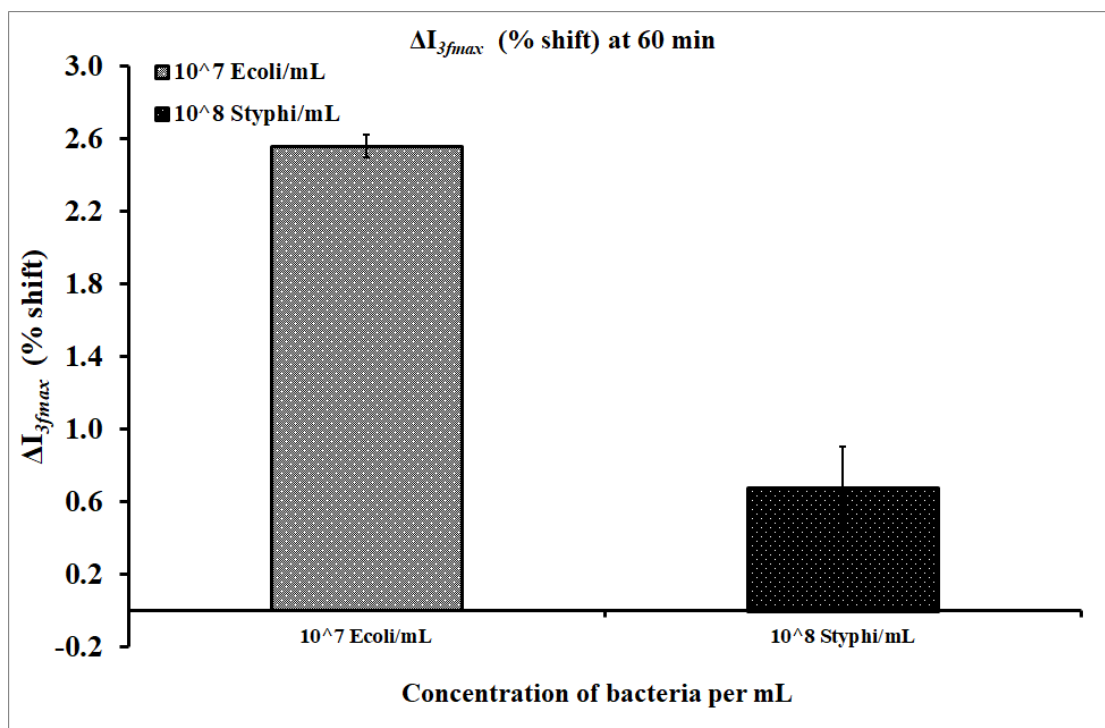


Fig. 5.14 - I_{3fmax} shift (%) at 60 mins with 10⁷ E.coli/mL and 10⁸ S.typhi/ over the surface functionalised with thiolated aptamer (shorter linker length).

Comparison of specificity

Mean values of the triplicate sets of experiments conducted with each concentration of *E.coli* bacteria (10^7 cells/mL) and *S.typhi* bacteria (10^8 cells/mL) recorded at 30 mins, were calculated and their ratios were compared. These ratios for ΔI_{3fmax} measurements are plotted in Fig. 5.15. For 10 times lower concentration of *E.coli* than *S.typhi* bacteria, the ratio values was 6.28. This value was found to be lower than that observed with longer linker (biotinylated aptamer) for same bacterial concentrations (please see Fig. 5.17).

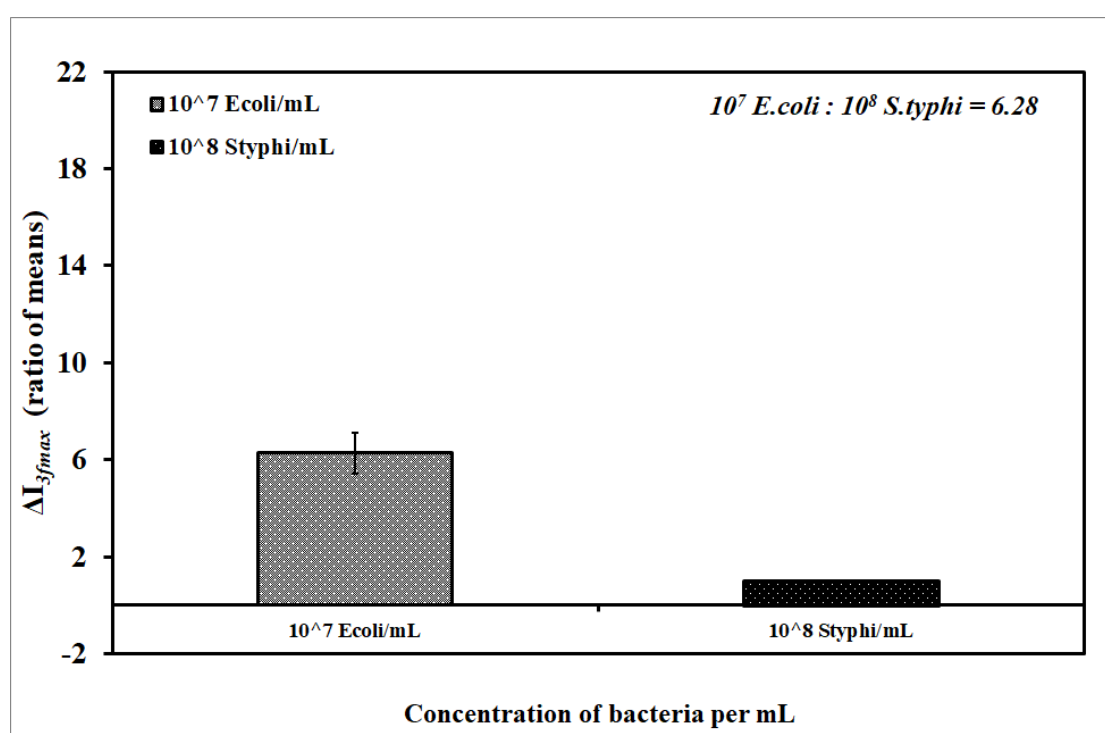


Fig. 5.15 - Comparison of specificity with short linker (thiolated aptamer): ratio of mean values of I_{3fmax} shift for 10^7 E.coli/mL and 10^8 S.typhi/mL.

5.11 Comparison of 3f signals with different bio-receptors

Comparison of sensitivity

Mean values of the triplicate sets of experiments conducted with each type of bio-molecular linker for concentration of *E.coli* bacteria (10^7 cells/mL) was recorded at 30 mins, were calculated and they are presented in Fig. 5.16. I_{3fmax} values were found to be highest for longer linker (biotinylated aptamer-

streptavidin-biotin thiol) about 2.06 units which was almost 1.6 times than that found for shorter linker (thiolated aptamer) and 5.8 times for pAbs (biotinylated antibody-streptavidin-biotin thiol). Thus, the assay with longer bio-molecular linker (biotinylated aptamer) had better sensitivity than with shorter linker and immunoassay.

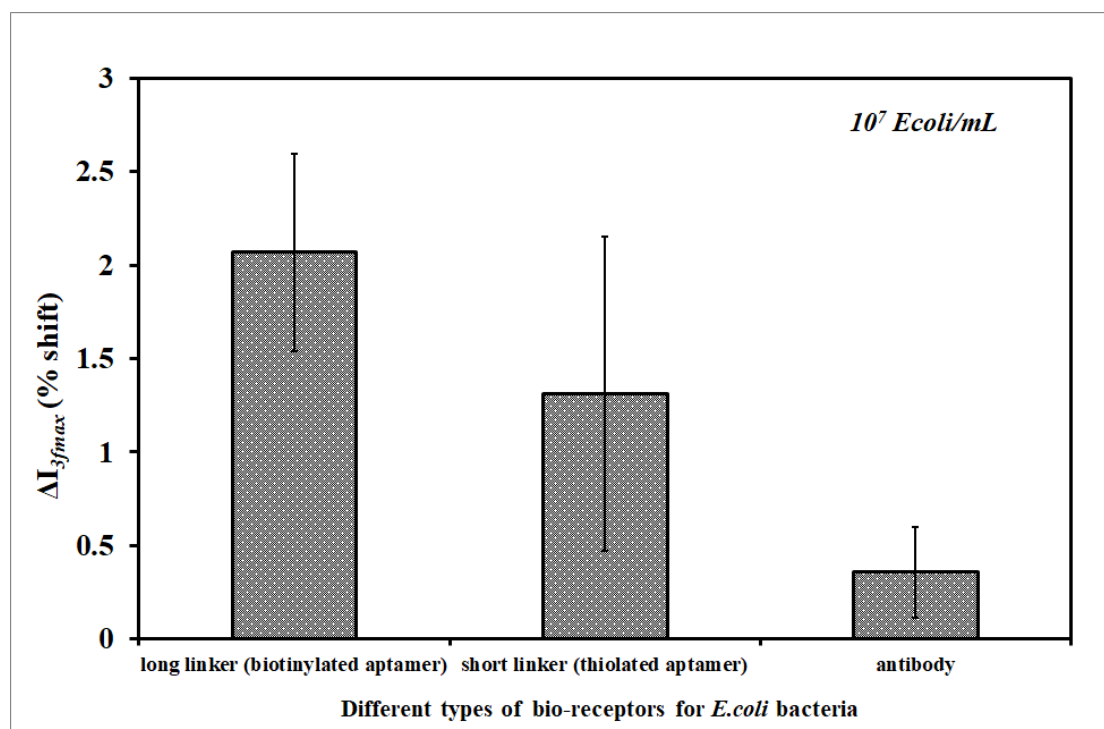


Fig. 5.16 - Comparison of sensitivity $-\Delta I_{3max}$ shift for 10^7 *E.coli*/mL with different bio-receptors: long linker (biotinylated aptamer), short linker (thiolated aptamer) and polyclonal antibody.

Comparison of specificity

Mean values of the triplicate sets of experiments conducted with each type of bio-molecular linker for concentration of *E.coli* bacteria (10^7 cells/mL) and *S.typhi* bacteria (10^8 cells/mL) recorded at 30 mins, were calculated and their ratios were compared. These ratios for ΔI_{3max} measurements are plotted in Fig. 5.17. I_{3max} values were found to be highest for longer linker (biotinylated aptamer-streptavidin-biotin thiol) about 12.6 which was almost 2 times than that found for shorter linker (thiolated aptamer) and 3.4 times for pAbs (biotinylated antibody-streptavidin-biotin thiol). Thus, the assay with longer

bio-molecular linker (biotinylated aptamer) had better specificity than with shorter linker and immunoassay.

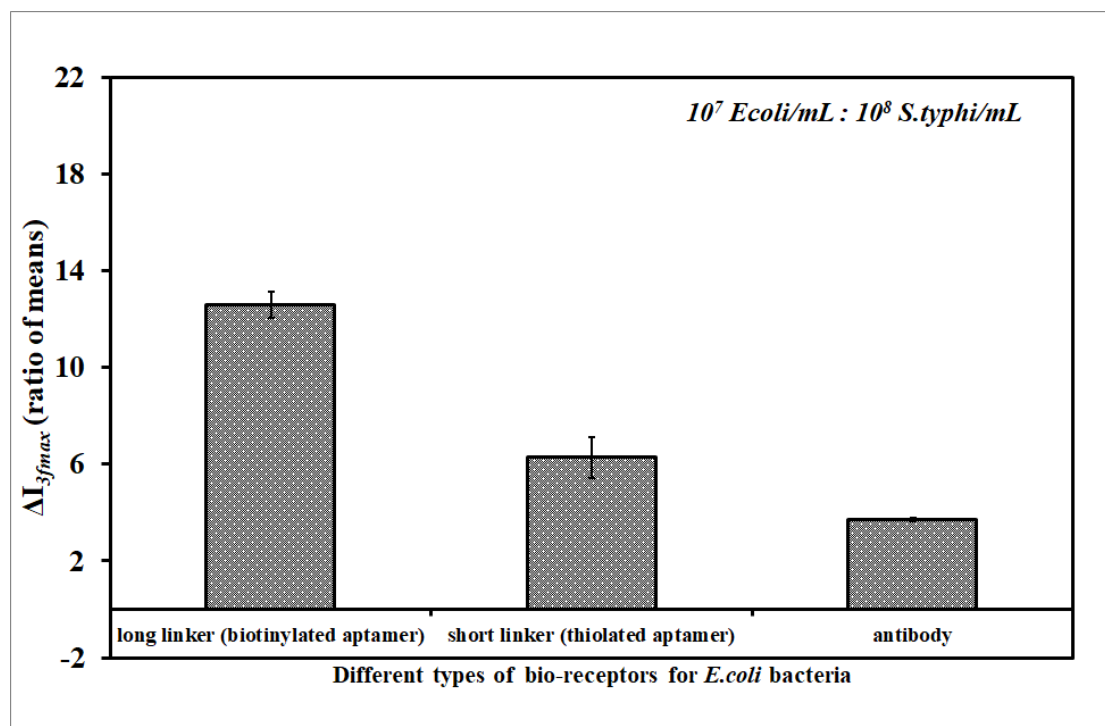


Fig. 5.17 - Comparison of specificity – ratio of mean values of I_{3fmax} shift for different concentrations of *E.coli*/mL and 10^8 *S.typhi*/mL with different bio-receptors – long linker (biotinylated aptamer), short linker (thiolated aptamer) and polyclonal antibody.

5.12 Summary

In the ADT technique, for a given drive frequency (f), the $3f$ signal is dependent on the force-extension characteristic of the molecular tether, its length, and also the size of the particles. Hence, to meet the objectives O.2.1 and O.2.2, in this chapter bio-receptor of different size i.e. anti-*E.coli* antibodies and different length i.e. thiolated *E.coli*-binding aptamer were investigated for detection of *E.coli* bacteria. It was found that the sensitivity and specificity of the assay with longer linker (biotinylated aptamer-streptavidin-biotin thiol) was highest for detection of *E.coli* bacteria as compared with shorter linker (thiolated aptamer) and biotinylated antibody assay. Bio-receptors with different linker lengths have been previously investigated, and it was found that with the longer linker the percentage

elongation is less and also the inclination is less, resulting in lower $3f$ response compared to a shorter linker. However, in this chapter, the response with shorter linker (thiolated linker) was found to be lower than longer linker in terms of both sensitivity and specificity. This could be due to saturation of the surface with 100% thiolated aptamers which might have affected its functionality by steric hindrance because of overcrowding. This can be potentially improved by co-immobilisation of the thiolated aptamer with MCH in a fixed combination rather than backfilling with MCH.

Chapter 6 Investigating novel mechanical designs of aptamer receptor for detection of bacteria using nonlinear acoustic biosensor

6.1 Introduction

Rapid point-of-care diagnostic tests need to be both sensitive and specific to play a significant role in stopping the spread of AMR. Sensitivity and specificity of a test is very crucial as a false-positive result can lead to unneeded interventions and treatment. In chapters 4 and 5, bio-receptors with different sizes and lengths were explored for detection of *E.coli* bacteria. Anharmonic acoustic aptasensor comprising of ADT as transducer and long bio-molecular linker with *E.coli*-binding aptamer as bio-receptor, demonstrated highest sensitivity and specificity. To further enhance the sensitivity and specificity of this system, novel mechanical structures were designed using the same *E.coli*-binding aptamer sequence such that the newly configured aptamer sequence along with the innovative structure would not only quantitatively detect bacteria, but also give a characteristic signal, highly specific for that interaction. Quartz crystal resonator (QCR) used to obtain this unique signal was operated in two modes: the first one measured the change in $3f$ signal (I_{3fmax}) caused by binding of *E.coli* bacteria to the immobilised modified aptamers, and the second one measured the characteristic signal as a results of introduction of the mechanical structure with designed nonlinearity into the stem of the *E.coli*-binding aptamer sequence.

6.2 Background

Aptamers are promising alternative bio-receptors that can substitute antibodies in various applications, as they offer several advantages, namely high binding affinity, high specificity and stability. Of all, the most important advantage is that aptamers can be chemically synthesised, whereas antibodies have to be obtained using less efficient biochemical or biological methods. In fact much of the success of nucleic acid aptamers is due to SELEX, a well-designed process by which aptamers can be generated for a given target (e.g., proteins, cells, etc.). Once aptamers are selected by this

SELEX process and their sequences are revealed, they can be chemically synthesised, thus, maintaining stable product quality. This also facilitates post-SELEX modifications, which can be made by precise introduction of labels or other modifications at defined positions in the aptamer sequence.^[239] The nucleic acid aptamers have also been previously modified for several reasons: to increase chemical diversity; to convey stability to enzymatic (endonuclease) degradation; to improve cellular uptake; to increase flexibility/rigidity and also to provide a means of measurement (e.g., incorporation of a fluorophore).^[240,241] Thus, as the aptamers are so versatile and adaptable, the *E.coli*-binding aptamers were also modified and applied in the bioassay.

The sensitivity and specificity of the bioassay depends on the affinity and strength of the ligand-receptor interaction. Intermolecular forces holding together ligand-receptor pairs are very important in biosensing, as these not only play important role in binding but they also provide stability to the intrinsic molecular structures. But, if the molecular structure of the receptor between the surface and the ligand is modified such that, it transiently becomes unsteady with the applied force, it can introduce potential non-linearity into the system and can give rise to unique signal, specific for that interaction. Therefore, the 'stem' of the *E.coli*-binding aptamer was modified to obtain a characteristic signal. A hairpin structure (comprising of DNA duplex) was added into the bio-molecular linker, such that depending on the positions of the receptor and biotin molecule on the arms of the hairpin structure, it would open up or stretch briefly due to the forces exerted by the oscillating resonator vibrating in thickness shear mode and opposing forces due to the inertia of the bound bacteria and the viscous forces of the liquid medium (as shown in figure 6.1). It was hypothesised that this transient unwinding can introduce momentary non-linearity in the dynamics and therefore the transduced characteristic electrical signal would enhance the specificity of the bioassay.

DNA duplex is a good candidate as it can be smartly incorporated into the aptamer sequence without affecting its function as a bio-receptor. Two force application geometries of dsDNA viz. unzipping and shearing have been exploited earlier.^[242-245] These were incorporated into the *E.coli*-binding

aptamer to give two configurations: unzip (weak) and shear (strong) (as depicted in Fig. 6.2). If the voltage is applied for very less impact time, in the weak configuration, the position of the biotin molecule (which then binds to streptavidin immobilised on the surface) on one arm of the hairpin structure is such that, it opens up under the pulling force, which does not happen for the strong configuration. Accordingly, two configurations are designed to establish that the distinct signal is due to the opening up of the hairpin structure and not just due to its presence. A numerical differentiation method is employed to a full complex $3f$ signal using Wolfram Mathematica software, to measure the resulting transient response due to the opening up of the designed hairpin structure. As square of the differentiated signal was taken, this method is named as ADT- D^2 i.e. ADT differentiated power. Energy of this signal was also calculated by integration and named as ADT-DI i.e. ADT differentiated energy.

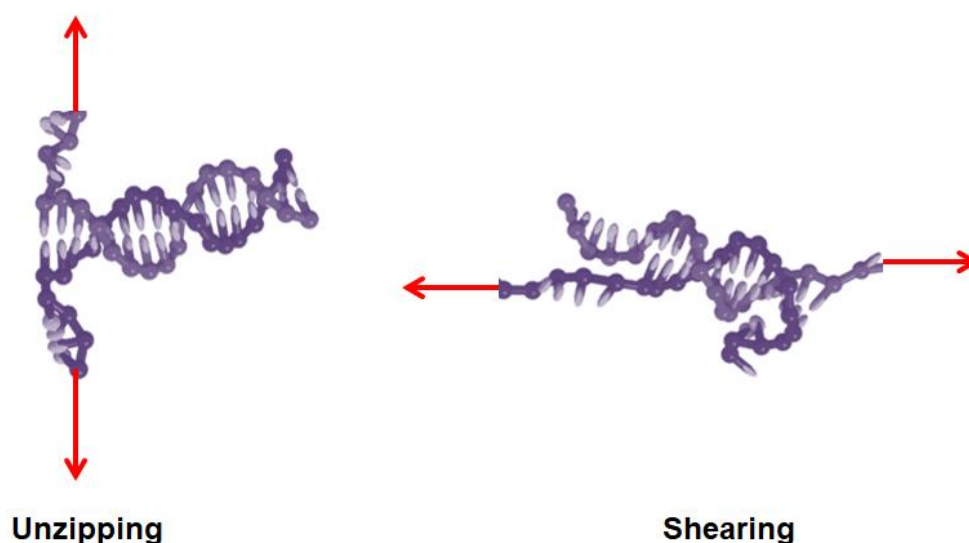


Fig. 6.1 – Two different force application geometries of DNA duplex: (a) Unzipping, and (b) Shearing mode. Adapted and modified from ^[241].

6.3 Modified aptamer sequences – novel mechanical designs

The fluorescein-labelled ssDNA *E.coli*-binding aptamers consisting of 88 bases were flanked with random sequence (named as, aptamer handle) of 21 bases to its 3' end, to make a longer sequence of total 109 bases (please see

table 6.1). This aptamer handle constituted one arm of the hairpin structure. Using Mfold software, binding was checked and it was found that ssDNA aptamer (88-mer) does not bind to aptamer handle (21-mer) or the total sequence consisting of 109 bases do not fold on itself. Complementary sequences to these 21 bases (added to 88 bases at 3' end) were procured with Biotin-TEG (triethylene glycol) attached to 5' end in aptamer configuration that would open in unzipping mode under the pulling force and to 3' end in aptamer configuration that would stretch in shear mode. The resultant two aptamer designs (configurations) are depicted in Fig. 6.2. Aptamer handles which constituted one arm of the hairpin structures of both the aptamer configurations (unzip and shear) were joined by hybridisation process to other arm of hairpin structure comprised of complementary 21 bases with Biotin-TEG at either end (5' or 3') and then introduced on the QCR surface coated with streptavidin (surface – 10% Biotin thiol / 90% methoxy thiol) (as shown in Fig. 6.3). Hybridisation was confirmed by measuring the frequency shift.

Fig. 6.2 - Modified aptamer configurations – unzip and shear mode

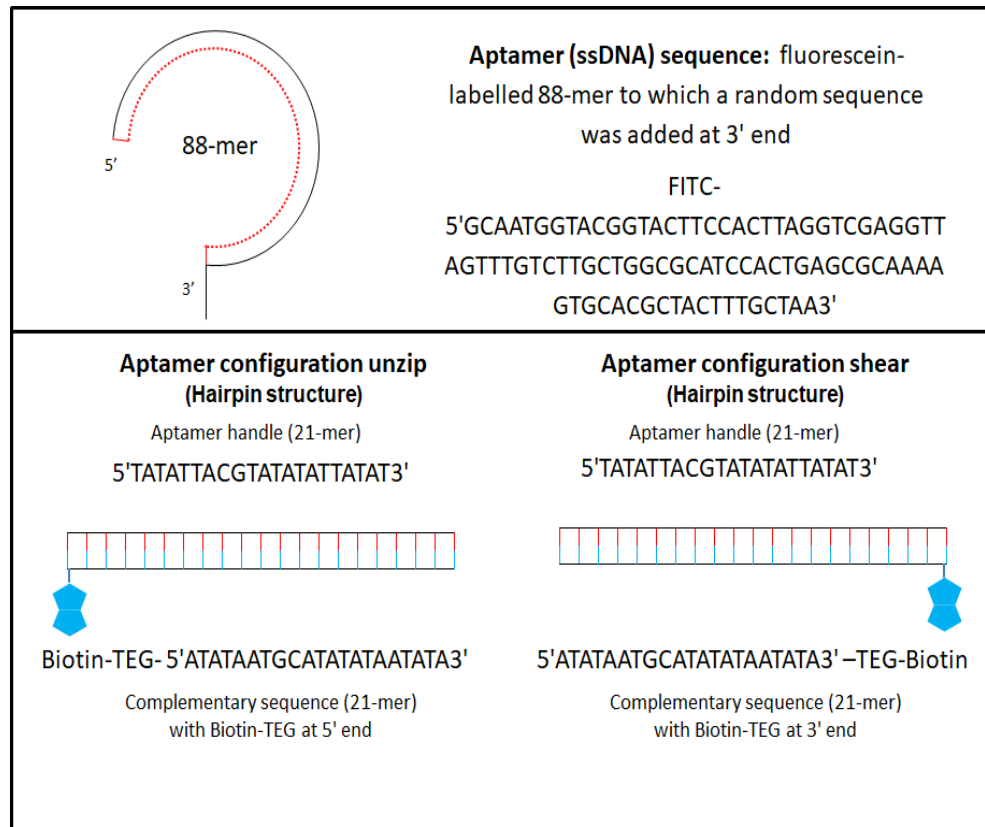


Table 6.1: Aptamer configurations		
Fluorescein-labelled ssDNA aptamer sequence: (88-mer)	FITC- 5'GCAATGGTACGGTACTTCCACTTAGGTCGAGGTTAGT TTGTCTTGCTGGCGCATCCACTGAGCGCAAAAGTGCAC GCTACTTTGCTAA3'	
Random sequence of aptamer handle (one arm of hairpin structure): 21-mer	5'TATATTACGTATATATTATAT3'	
Biotinylated sequence with complementary bases to aptamer handle (other arm of hairpin structure): 21-mer	Unzipping mode: Biotin TEG at 5' end	Biotin-TEG 5'ATATAATGCATATATA ATATA3'
	Shear mode: Biotin TEG at 3' end	5'ATATAATGCATATATA ATATA3'-TEG-Biotin
Aptamer configuration unzip	Fluorescein-labelled ssDNA aptamer sequence (88-mer) with aptamer handle (21-mer) hybridised to complementary sequence (21-mer) with Biotin TEG at its 5' end	
Aptamer configuration shear	Fluorescein-labelled ssDNA aptamer sequence (88-mer) with aptamer handle (21-mer) hybridised to complementary sequence (21-mer) with Biotin TEG at its 3' end	

6.4 Hybridisation of aptamer sequences

Hybridisation is a phenomenon in which single-stranded DNA or RNA molecules anneal to complementary DNA or RNA. Heating followed by cooling facilitates hybridisation. Heat 'breaks' all hydrogen bonds, thereby disrupting any secondary structure within each oligonucleotide. Slow cooling then facilitates hybridisation as new hydrogen bonds form between the complementary sequences.

E.coli-binding aptamers (88-mer) along with aptamer handles of both the aptamer configurations (unzip and shear) were annealed and joined by hybridisation process to complementary 21 bases with Biotin-TEG at either end (5' or 3') and then introduced on the QCR surface coated with streptavidin (surface – 10% Biotin thiol / 90% methoxy thiol) (as shown in Fig. 6.3).

Both the sequences i.e. fluorescein-labelled ssDNA *E.coli*-binding aptamer sequence plus aptamer handle (109-mer) and biotinylated complementary sequences (21-mer) to aptamer handle [with Biotin-TEG at either (5' or 3')] were re-suspended to the same molar concentration, using TE buffer.

Annealing was performed by mixing equal volumes of both the sequences (at equimolar concentration) in a 1.5 ml microfuge tube along with an appropriate volume of 10× annealing buffer and water to make the final concentration of each sequence to equal 50 μmol and 1× annealing buffer.

Then the tubes were placed in a standard heat block at 90–95°C for 3–5 minutes. Later, the heat block was removed from the apparatus and allowed to cool to room temperature (or at least below 30°C) on the workbench. Slow cooling to room temperature was done for 45–60 minutes. Thereafter, it was stored at 4°C until ready to use.

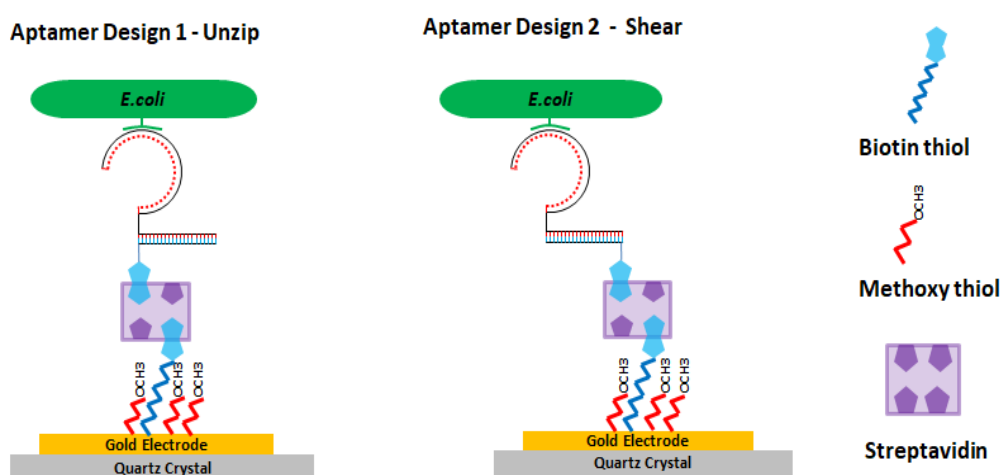


Fig. 6.3 – Modified aptamer designs (configurations): (1) Unzip mode, (2) Shear mode.

To confirm whether hybridisation occurred or not, frequency shifts were measured. Post-hybridisation, the gold surfaces of quartz crystals were rinsed with ultra-pure ethanol for removing the non-adsorbed thiol. After placing the crystal on cartridge and sealing with “O-ring” of flow-cell, about 6-8 mL of DI water was passed through for 10 mins; thus removing the ethanol. The gold surfaces were then rinsed with PBS solution. For functionalization, a solution of ~ 7 $\mu\text{g/ml}$ of streptavidin was flown over the surface. The excess streptavidin was removed by flowing PBS solution and then baseline measurements were taken. Thereafter, fluorescein-labelled ssDNA aptamer sequence plus aptamer handle (109-mer) with and without hybridised biotinylated complementary sequences (21-mer) to aptamer handle [with Biotin-TEG at either (5' or 3')] were flowed over the surface and resonance frequency shift was measured.

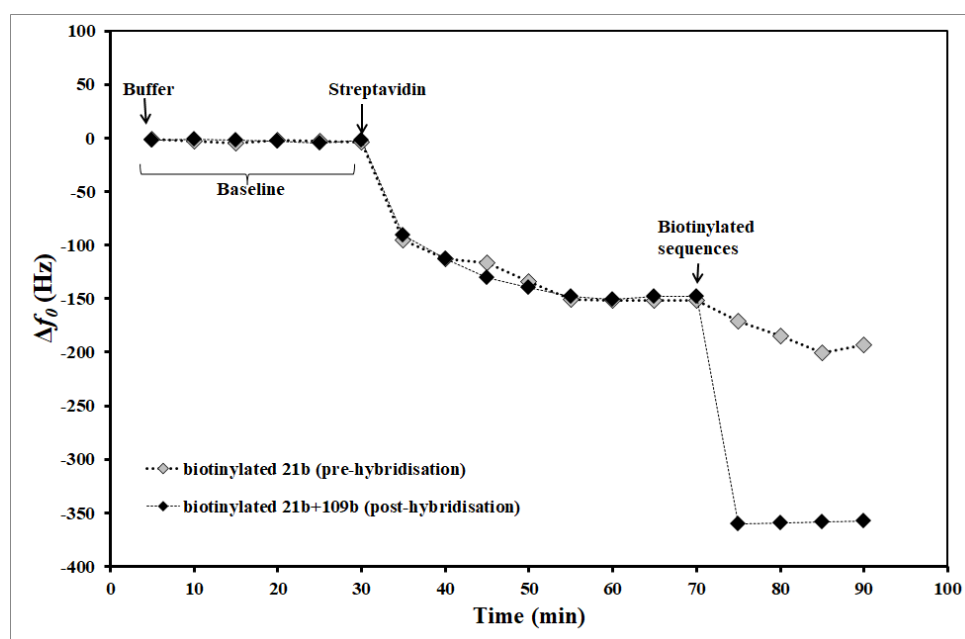


Fig. 6.4 – Frequency shift measured after immobilising: (a) biotinylated 21b (pre-hybridisation), and (b) biotinylated 21b+109b (post-hybridisation).

The frequency shift is reported in Hz as shown in the Fig. 6.4. When streptavidin is injected into the flow-cell, frequency shift of Δf (~ 150 Hz) was observed for both the experiments. Smaller shift Δf (~ 50 Hz) was observed during the immobilisation step of biotinylated 21-mer sequences and larger shift Δf (~ 210 Hz) due to the more mass going on the surface because of the

hybridised sequence. Following the binding of both the sequences, any unbound sequence was removed from the flow-cell by rinsing with PBS. Thus, for this experiment, it can be concluded that the hybridisation step was successful which resulted in larger frequency shift, as the biotin was attached only to the 21base sequence and not to the ssDNA *E.coli*-binding aptamer sequence with aptamer handle (109-mer).

X-ray photoelectron spectroscopy (XPS) measurements

XPS measurements were carried out with a Thermo Scientific K-Alpha spectrometer using a monochromatic Al K α X-ray source (Ion Gun Operating range: 100 eV - 4 keV) with a spot size of 400 μ m. The survey spectra were collected over a range of -10 to 1350 eV with pass energy of 200 eV. The high resolution spectra over the Au 4f, C1s, O1s, S2p, and N1s regions were acquired with pass energy of 50 eV.

Survey spectra especially over N1s and P2p (Fig. 6.5) demonstrated that the peaks were higher for substrates with biotinylated 21b+109b, indicating hybridisation of the complementary sequences.

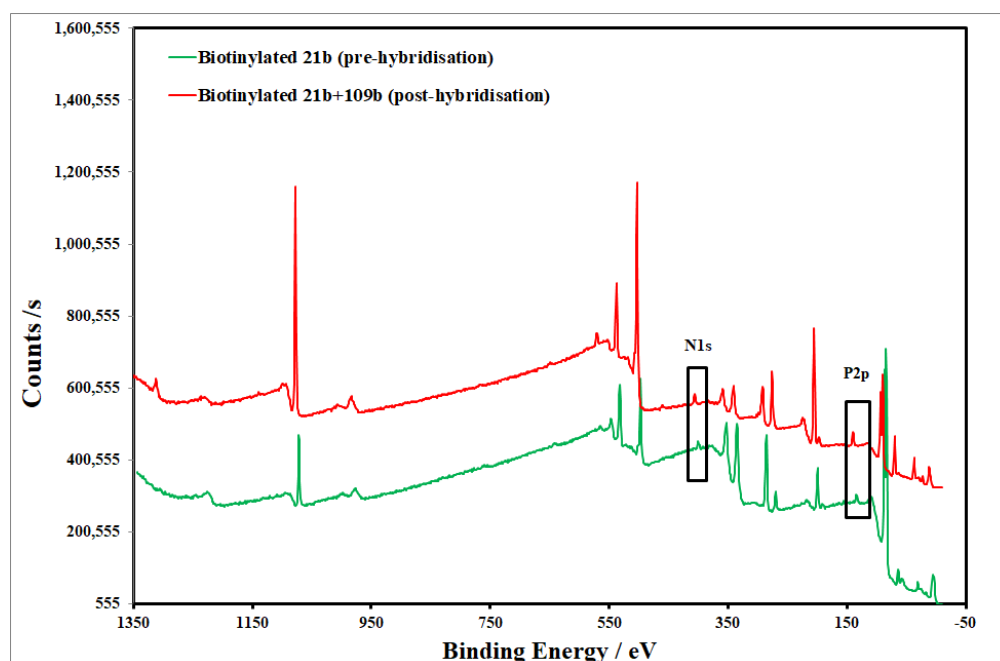


Fig. 6.5 – XPS spectra showing comparison of surveys for different substrates:
(a) Biotinylated 21b (pre-hybridisation) and (b) Biotinylated 21b+109b (post hybridisation)

6.5 Binding of the two modified aptamer configurations to *E.coli* bacteria

Post-hybridisation, binding of the fluorescein-labelled hybridised sequences (FITC-109b+21b-biotin) to *E.coli* bacteria strain (KCTC 2571) was validated through fluorescence assay.

Fluorescence assay

Microplate wells were first washed with 150 μ L of 5% BSA in PBS overnight at 4°C and next day washed with washing buffer (1 \times PBS and 0.05% [v/v] Tween 20). *E.coli* bacteria strain (KCTC 2571) was cultured in nutrient broth to middle growth phase (OD600 of 0.45) and centrifuged at 3,000 rpm for 10 mins to remove the media. This washing step was repeated 3 times. Subsequently, *E.coli* bacteria (10^7 /mL) were incubated with fluorescein-labelled hybridised sequences (FITC-109b+21b-biotin) (nM as final concentrations) in microplate wells for 45 mins at 25°C with mild shaking. Cells were then washed three times to remove unbound sequences from cells by centrifugation for 10 mins and were re-suspended in 150 μ L of washing buffer. Finally, the fluorescence intensity of each sample was measured with BMG FLUOstar Omega microplate reader (at excitation 485 nm and emission 520 nm wavelengths). The fluorescence intensity was compensated by subtraction with the fluorescence intensity of blank and then by division with respective gains.

Here, both the configurations as depicted in Fig. 6.1 (aptamer config. unzip and shear) exhibited a high affinity for the target *E.coli* strain. Fig. 6.6 & 6.7 show representative binding saturation curves obtained by fluorescence analysis for both the aptamer configurations, respectively. The dissociation constants (K_d) of both the aptamer configurations unzip and shear against *E.coli* (KCTC 2571) were estimated to be 22.8 and 25.9 nM, respectively, by nonlinear regression analysis. Thus, this confirmed the binding of the target *E.coli* strain to both the aptamer configurations post-hybridisation. Also, the values were close to the K_d value reported for the original aptamer sequence (88b) after binding to *E.coli* (KCTC 2571) bacteria.^[230]

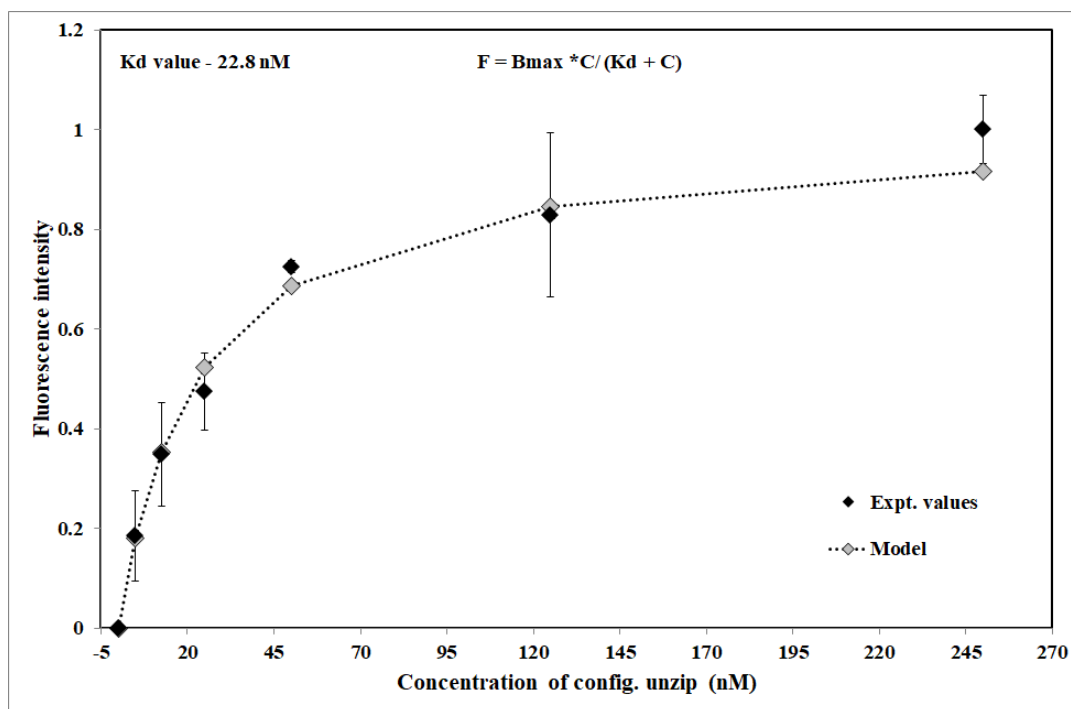


Fig. 6.6 – Binding saturation curves of aptamer configuration unzip to the target *E.coli* strain and estimation of their dissociation constants (K_d) value of 22.8 nM obtained by nonlinear regression analysis.

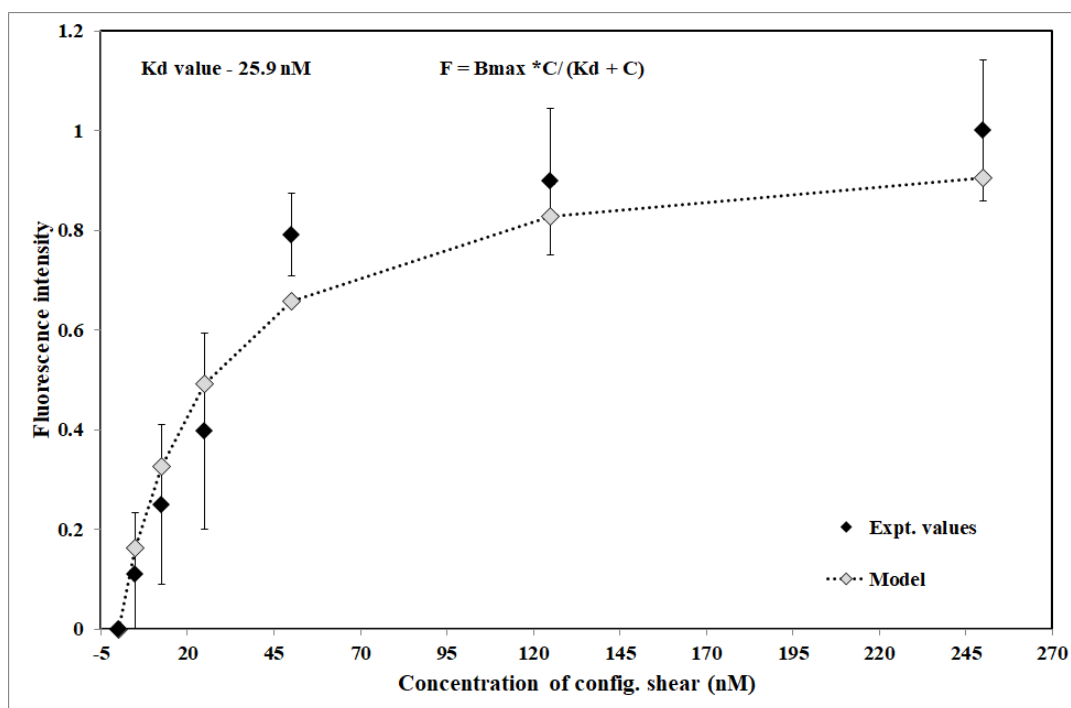


Fig. 6.7 – Binding saturation curves of aptamer configuration shear to the target *E.coli* strain and estimation of their dissociation constants (K_d) value of 25.9 nM obtained by nonlinear regression analysis.

6.6 Linking the modified aptamers to the QCR

6.6.1 Cleaning the surface of gold electrode

AT-cut stepped (non-uniform) quartz crystals were used with fundamental resonant frequency range of 14.23 -14.25 MHz (Lap-Tech Inc., Bowmansville, Ontario, Canada). The surfaces of gold electrodes of quartz crystals were cleaned with acetone for 5 mins and then with isopropanol (IPA) by ultra-sonication process for 5 mins. Then after drying with nitrogen gas, they were placed in plasma cleaner to remove impurities and contaminants from the surface using inert argon gas for 1 min in a Harrick Plasma cleaner. They were then stored in a well of clean 24-well tissue culture plate covered with plastic film.

6.6.2 Formation of self-assembled monolayer (SAM)

The cleaned quartz crystals were then immersed in about 250 μ l of 1mM ethanolic solution of mixture of thiols [biotin terminal group (10%), and methoxy terminal group (90%)] and left overnight for formation of a SAM. Thiols with biotin terminal group HS-C11-(EG)6-Biotin (th004-m11.n6-0.005) and methoxy terminal group HS-C11-(EG)3-OCH₃ (th006-n3) were obtained from Prochimia Surfaces, Poland. The following day, the gold surfaces of quartz crystals were rinsed three times with ultra-pure ethanol (Sigma-Aldrich, UK) for removing the non-adsorbed thiols and then both sides of crystal were dried with a stream of nitrogen gas. After making sure that the electrode on bottom side was completely dried, the crystal was mounted on PCB cartridge and sealed with "O-ring" of microfluidic flow-cell with only one face exposed to the solution. The gold surfaces were then rinsed with de-ionized (DI) water to remove ethanol followed by Phosphate buffer saline (PBS) with physiological pH 7.4.

6.6.3 Deposition of Streptavidin

PBS buffer solution (100 μ L) was then flowed over the substrate at the continuous flow rate of 10 μ L/min and baseline measurements were taken for 15 mins at 5 min interval. This was followed by about 150 μ l of Streptavidin

(10 µg/mL) for 15 mins at the flow rate of 10 µL/min; thus forming a strong bond with the biotin terminal group of the alkane thiol. Measurements were taken under flow for 15 mins at 5 min interval.

6.6.4 Immobilisation of bio-receptor on the gold electrode of QCR

After depositing streptavidin, PBS buffer solution (500 µL) was then flowed over the substrate at the continuous flow rate of 100 µL/min for 5 mins, to remove the unbound streptavidin. Then the surface was functionalised with aptamer configurations unzip and shear post-hybridisation (annealed to biotinylated-ssDNA sequence consisting of 21 bases), by passing over the surface for 15 mins. The excess of bio-receptors were removed by flowing PBS solution and then baseline measurements were taken every 5 minutes over 30 minutes under a continuous flow of PBS at flow rate of 5 µl/min.

After this, in order to detect *E. coli* (KCTC 2571) by direct assay, 10^7 cells/mL of bacteria were spiked into the sample (as final concentrations) over the prepared sensor surface at a flow rate of 5 µl/min for further 60 mins. A total of 3×10^6 bacterial cells are therefore injected over 60 mins.

Frequency scans were taken at 0.02 and 0.1 SU (0.1s period) to measure $3f$ signal and at 0.1 to 0.7 SU (1s period) to measure ADT-D² and ADT-DI signal. Δf and ΔD were simultaneously monitored in real time during streptavidin and aptamer immobilisation and *E.coli* detection using a quartz crystal nonlinear network analyser. All the measurements were taken in continuous flow mode.

6.7 Determination of drive amplitude

The surfaces of the QCR were functionalised with aptamer configurations unzip and shear, separately post-hybridisation step, and then rinsed with PBS buffer.

After taking baseline measurements, 10^7 *E.coli*/mL (as final concentrations) were spiked into the sample and passed over the both the prepared sensor surfaces at a flow rate of 5 µl/min for 60 mins.

Resonant frequency (f_0) was determined with frequency sweep and the sensor was then driven by a pure sinusoidal oscillation at f_0 in frequency mode scan, at different amplitudes ranging from 0.1 to 0.5 SU.

The complex values (in-phase and quadrature) of current and voltage were recorded at $1f$ and $3f$ simultaneously using the ADT machine. The percentage shift in the peak values of the corresponding $3f$ signal (I_{3fmax}) from baseline, are plotted at 60 mins (Fig. 6.8). Maximum shift was observed at 0.1 SU. The results were found consistent with the ones obtained with *E.coli* binding aptamers (unmodified), where the maximum shift in $3f$ signal was also observed at 0.1 SU.

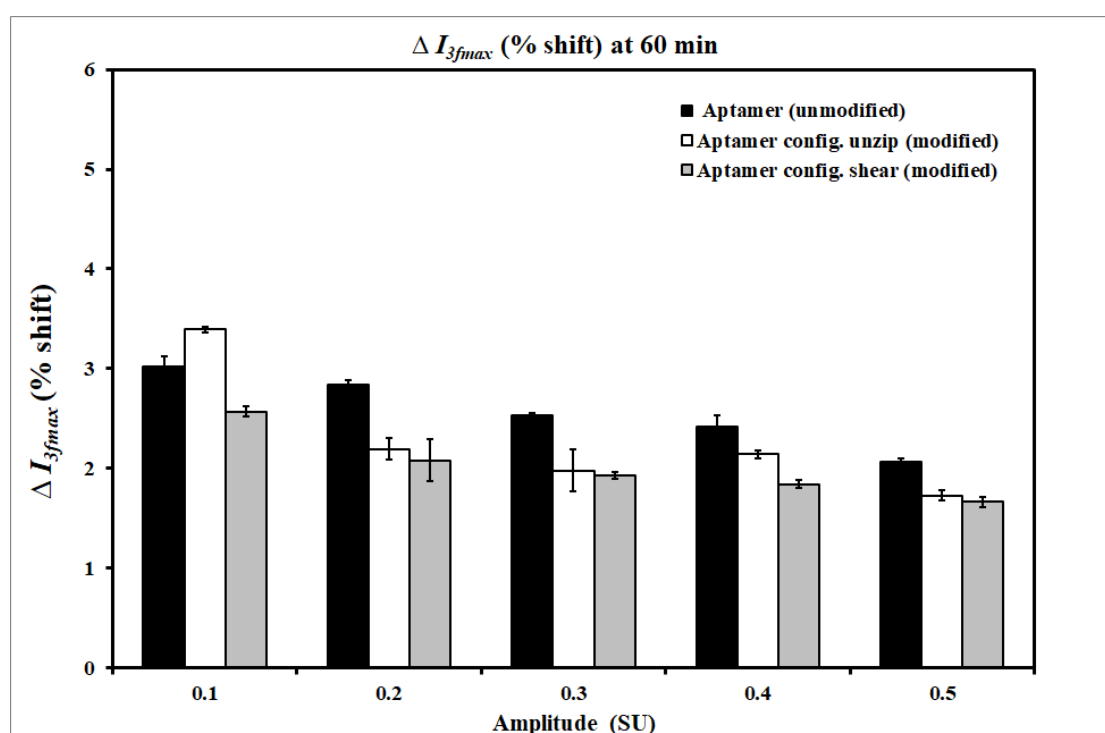


Fig. 6.8 - I_{3fmax} shift (%) measured at different amplitudes – 0.1 to 0.5 SU at 60 mins, after passing 10^7 *E.coli*/mL on the surface functionalised with: (a) Aptamer (unmodified); (b) Aptamer configuration unzip (modified), and (c) Aptamer configuration shear (modified)

6.9 Selection of aptamer configuration for *E.coli* detection

After functionalising the surfaces of the QCR with two different aptamer configurations (unzip and shear), baseline measurements were taken. To

obtain ADT-D² and ADT-DI signal, different amplitudes ranging from 0.1 to 0.7 SU were applied for 1s in frequency mode scan. Thereafter, 10⁷ *E.coli*/mL (as final concentrations) were spiked into the sample and passed over the both the prepared sensor surfaces at a flow rate of 5 μ l/min for 60 mins. At the end of the experiment, again different amplitudes were applied for 1s. Signals measured at 3rd harmonic ($3f_{\text{ADT-D}^2}$) and $3f_{\text{ADT-DI}}$ both were analysed. ADT-D² and ADT-DI analysis showed characteristic signals observed at 0.6 and 0.7 SU with aptamer configuration unzip but none with aptamer configuration shear mode) as shown in Fig. 6.9 and 6.11, respectively. As hypothesised, characteristic response was observed in unzipping mode due to transient unwinding of the DNA helix (aptamer hairpin structure) after *E.coli* binding. This could be due to opposing forces acting on the helix due to viscous drag after bacterial binding. In the shearing mode, unique signals were not observed, as the bond might have got only stretched but not unwound after *E.coli* binding (as shown in Fig. 6.10 and 6.12). Thus, aptamer configuration unzip was selected for further investigations.

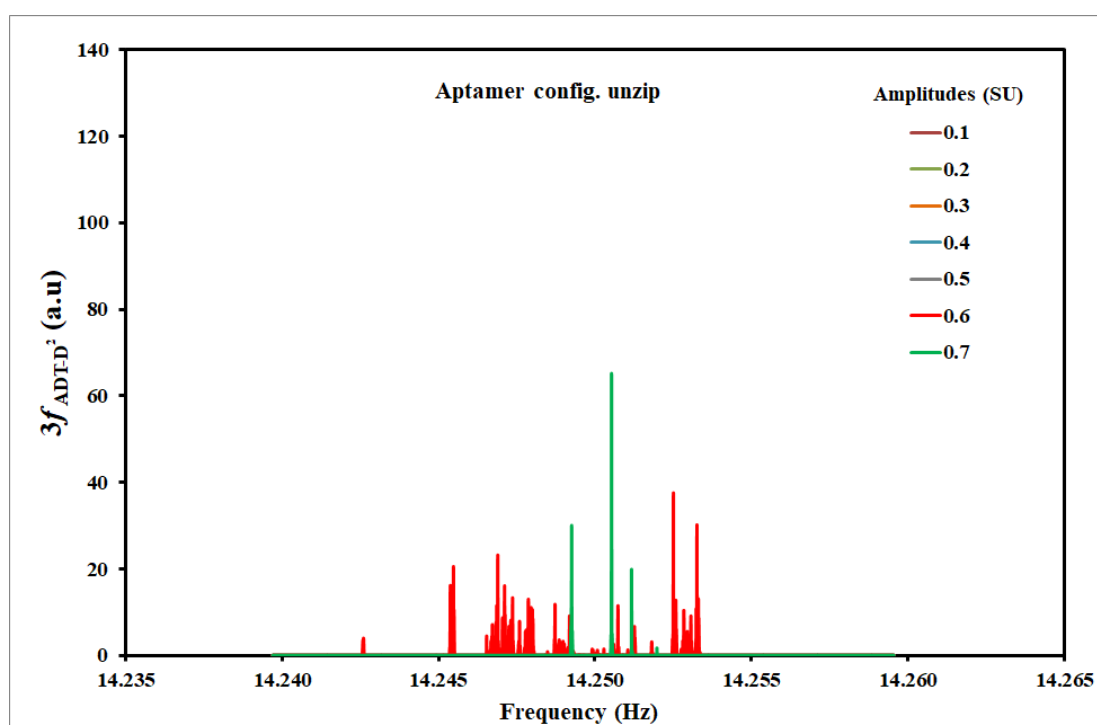


Fig. 6.9 - ADT-D² signal measured at 3rd harmonic ($3f_{\text{ADT-D}^2}$) after flowing 10⁷ *E.coli*/mL over surface functionalised with aptamer configuration unzip.

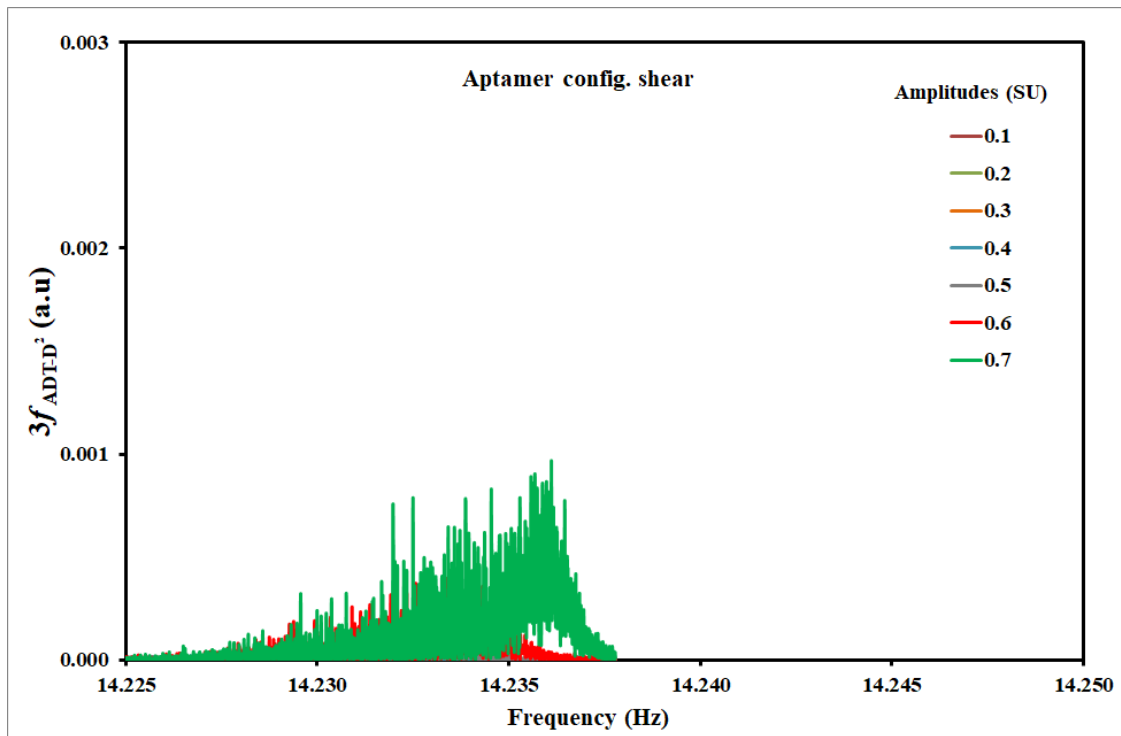


Fig. 6.10 - ADT-D² signal measured at 3rd harmonic ($3f_{AD^2}$) after flowing 10^7 E.coli/mL over surface functionalised with aptamer configuration shear.

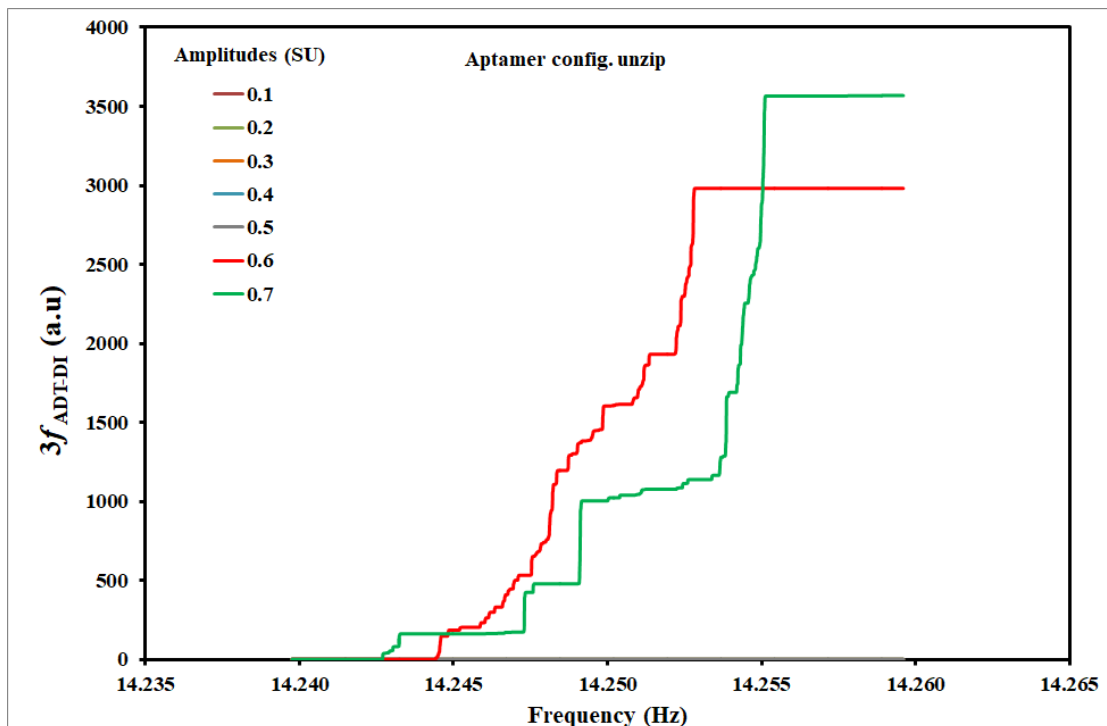


Fig. 6.11 - ADT-DI signal measured at 3rd harmonic ($3f_{AD-DI}$) after flowing 10^7 E.coli/mL over surface functionalised with aptamer configuration unzip.

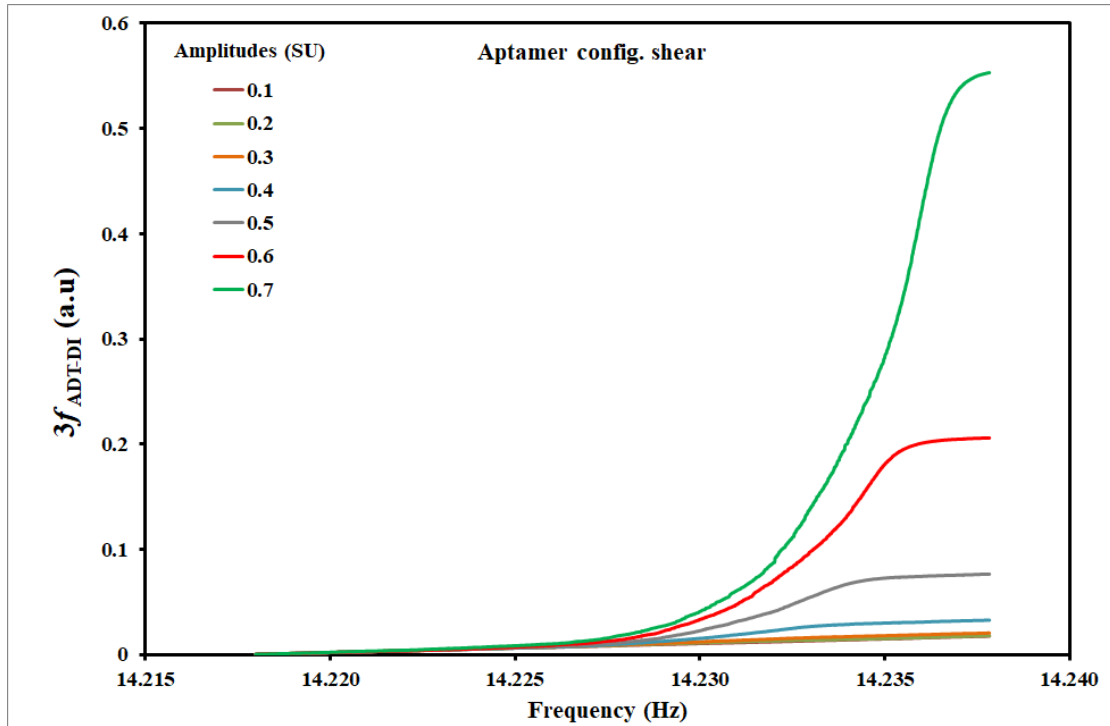


Fig. 6.12 - ADT-DI signal measured at 3rd harmonic ($3f_{\text{ADT-DI}}$) after flowing 10^7 *E.coli*/mL over surface functionalised with aptamer configuration shear.

6.10 Detection of *E.coli* bacteria using aptamer configuration unzip

Aptamer configuration unzip was selected for detection of *E.coli* bacteria as it not only gave characteristic signal due to transient DNA helix unwinding at 0.6 and 0.7 SU, but also the shift in $I_{3f_{\text{max}}}$ was observed maximum with this configuration.

In order to detect *E.coli* (KCTC 2571) by direct assay, bacteria were spiked into the sample (10^7 cells/mL as final concentrations) over the prepared sensor surface at a flow rate of 5 $\mu\text{l}/\text{min}$ for further 60 mins.

A total of 3×10^6 bacterial cells are therefore injected over 60 mins, respectively. The changes in resonant frequency and dissipation units were measured and also the shift in 3f signal ($I_{3f_{\text{max}}}$). The results were comparable to the ones obtained with *E.coli* binding aptamer (unmodified).

Relative decrease in peak values of $\Delta I_{3f_{\text{max}}}$ from baseline are plotted at 60 mins for which the *E.coli* bacteria were flowed over the sensor surface after

achieving the baselines, as shown in the Fig. 6.15. This relative decrease in $\Delta I_{3f_{max}}$ was compared with the increase in resonant frequency (Δf_0) and the relative increase in dissipation values ΔD . Fig. 6.13 and Fig. 6.14 depict the frequency shift and dissipation shift at 60 mins after introducing the *E.coli* bacteria over the surface functionalised with *E.coli*-binding aptamers.

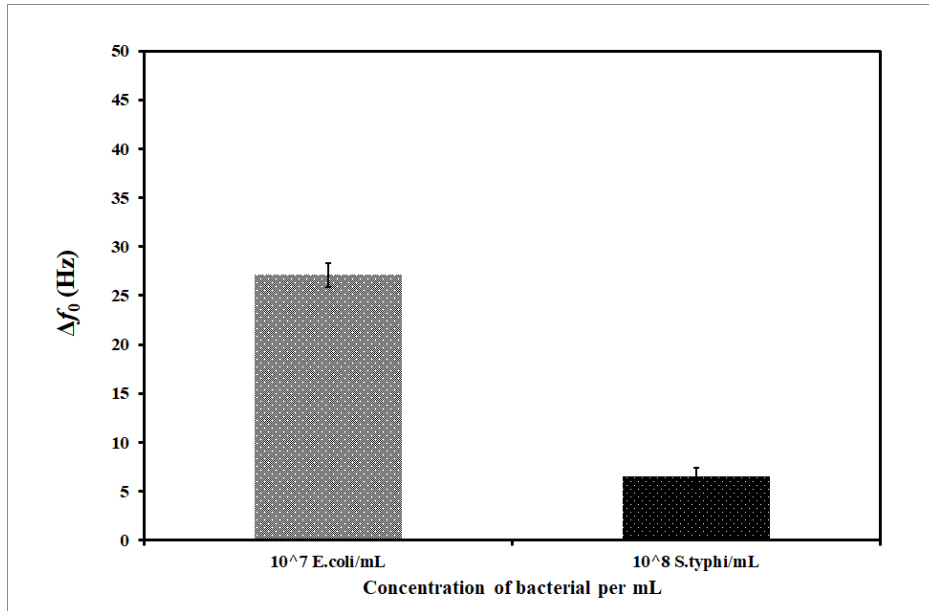


Fig. 6.13 - Frequency shift (Hz) at 60 mins with different bacterial suspensions flowed over the surface functionalised with aptamer configuration unzip.

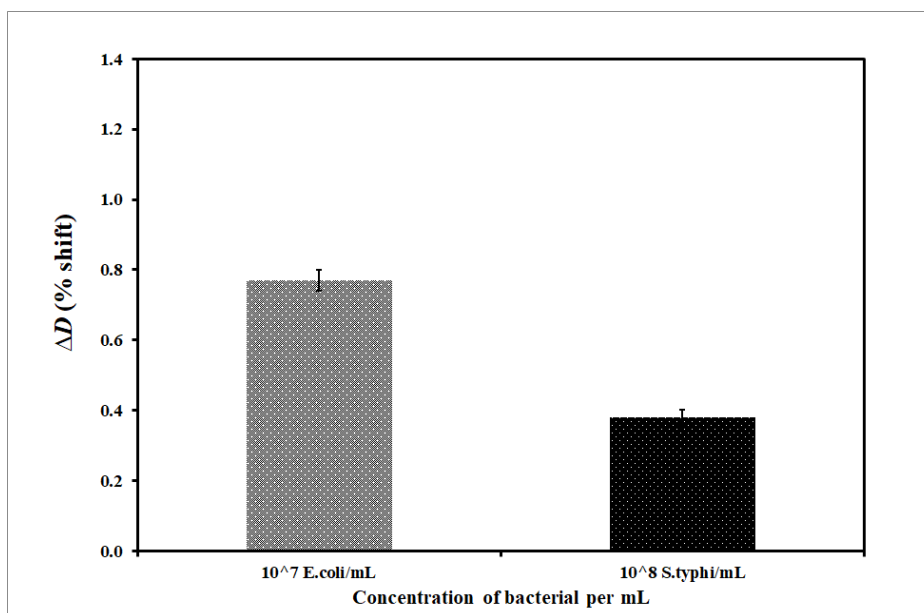


Fig. 6.14 - Dissipation shift (%) at 60 mins with different bacterial suspensions flowed over the surface functionalised with aptamer configuration unzip.

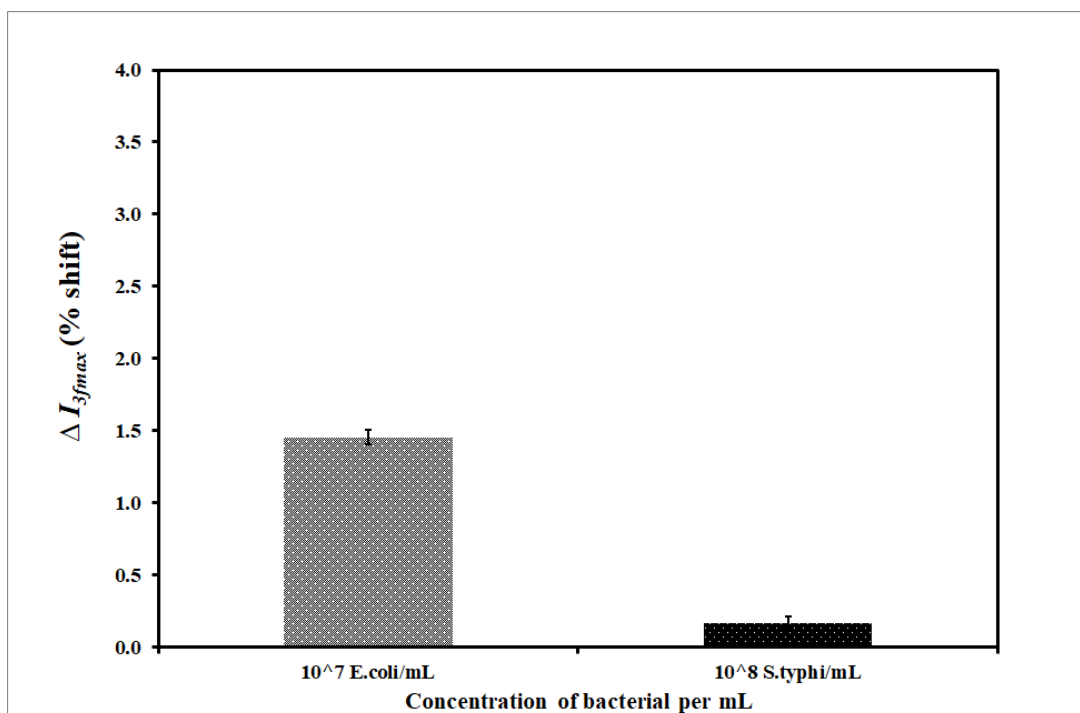


Fig. 6.15 – I_{3fmax} shift (%) at 60 mins with different bacterial suspensions flowed over the surface functionalised with aptamer configuration unzip.

6.11 Specificity analysis

For specificity analysis, ADT-D² and ADT-DI signals at 3rd harmonic were measured at 0.6 SU before and after flowing *E.coli* bacteria functionalised with aptamer configuration unzip. Three set of scans were taken each time to ensure reproducibility. Characteristic signals were obtained for 10^7 E.coli/mL but none for 10^8 S.typhi/mL. ADT-D² signal at 0.6 SU before and after *E.coli* bacteria are shown in Fig. 6.16 and 6.17. ADT-D² signal at 0.6 SU before and after *S.typhi* bacteria are shown in Fig. 6.18 and 6.19. Also, ADT-DI signal at 0.6 SU before and after *E.coli* bacteria are shown in Fig. 6.20 and 6.21 and for *S.typhi* bacteria in Fig. 6.22 and 6.23.

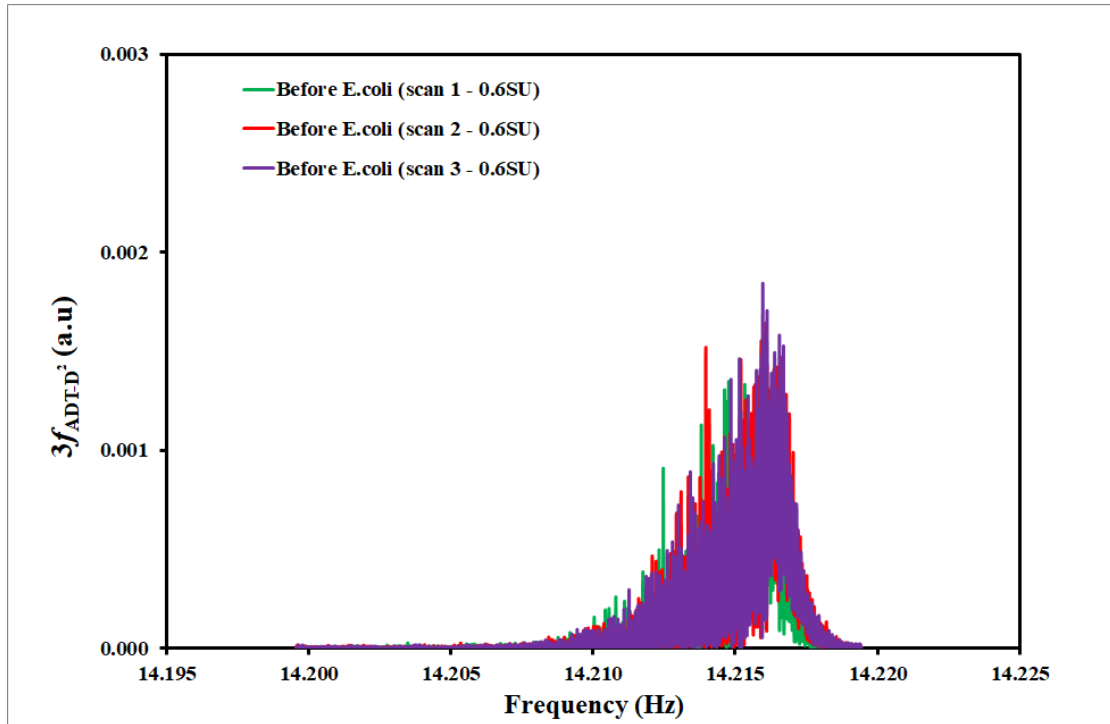


Fig. 6.16 – ADT-D² signal measured at 3rd harmonic ($3f_{\text{ADT-D}^2}$) before flowing 10^7 E.coli/mL over surface functionalised with aptamer config. unzip at 0.6 SU (ADT-D²_{max}: Mean = 0.0016, SD = 0.0002).

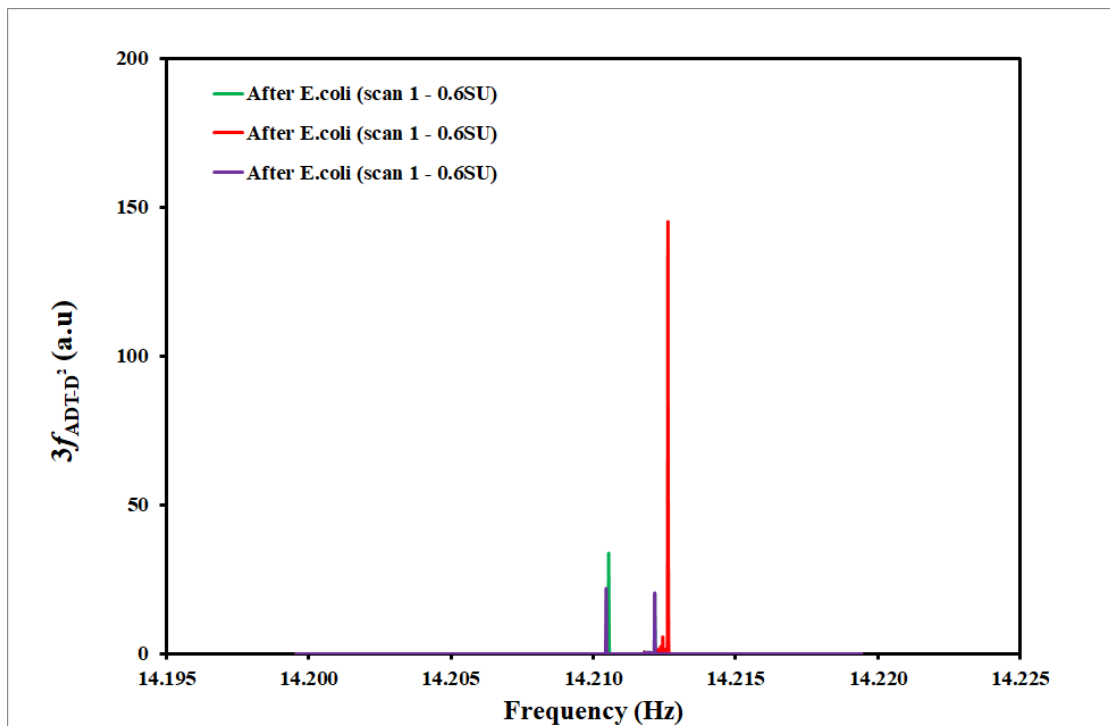


Fig. 6.17 - ADT-D² signal measured at 3rd harmonic ($3f_{\text{ADT-D}^2}$) after flowing 10^7 E.coli/mL over surface functionalised with aptamer config. unzip at 0.6 SU (ADT-D²_{max}: Mean = 66.8415, SD = 67.8378).

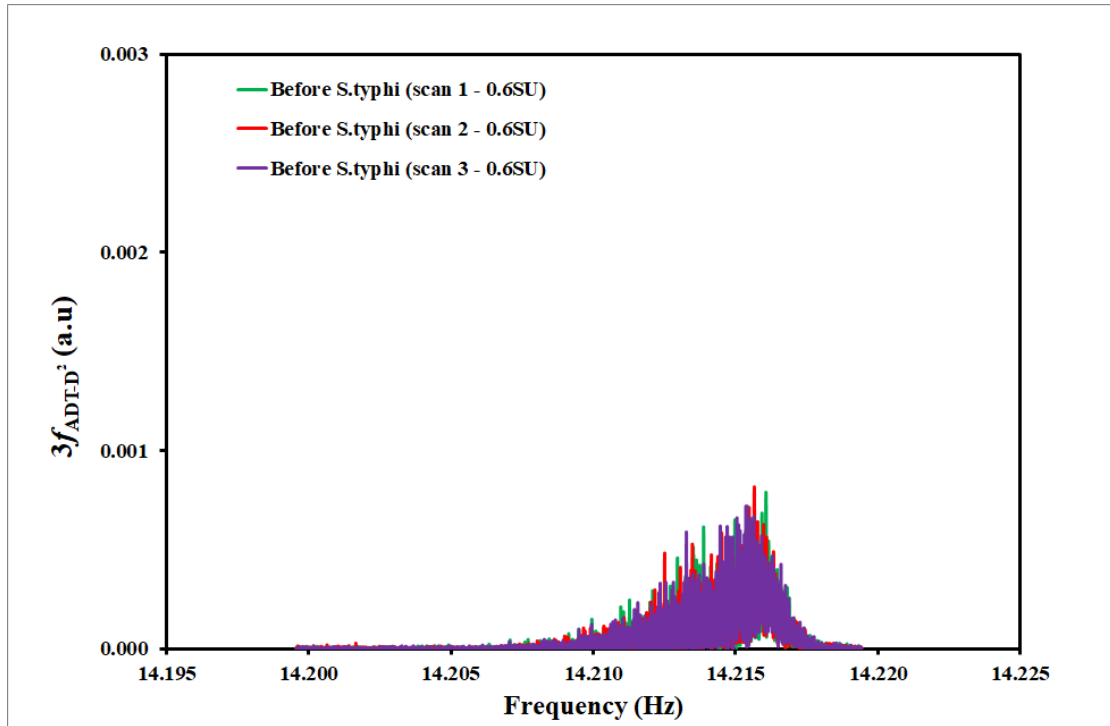


Fig. 6.18 - ADT-D² signal measured at 3rd harmonic ($3f_{ADT-D^2}$) before flowing 10^7 S.typhi/mL over surface functionalised with aptamer config. unzip at 0.6 SU (ADT-D²_{max}: Mean = 0.0007, SD = 0.00004).

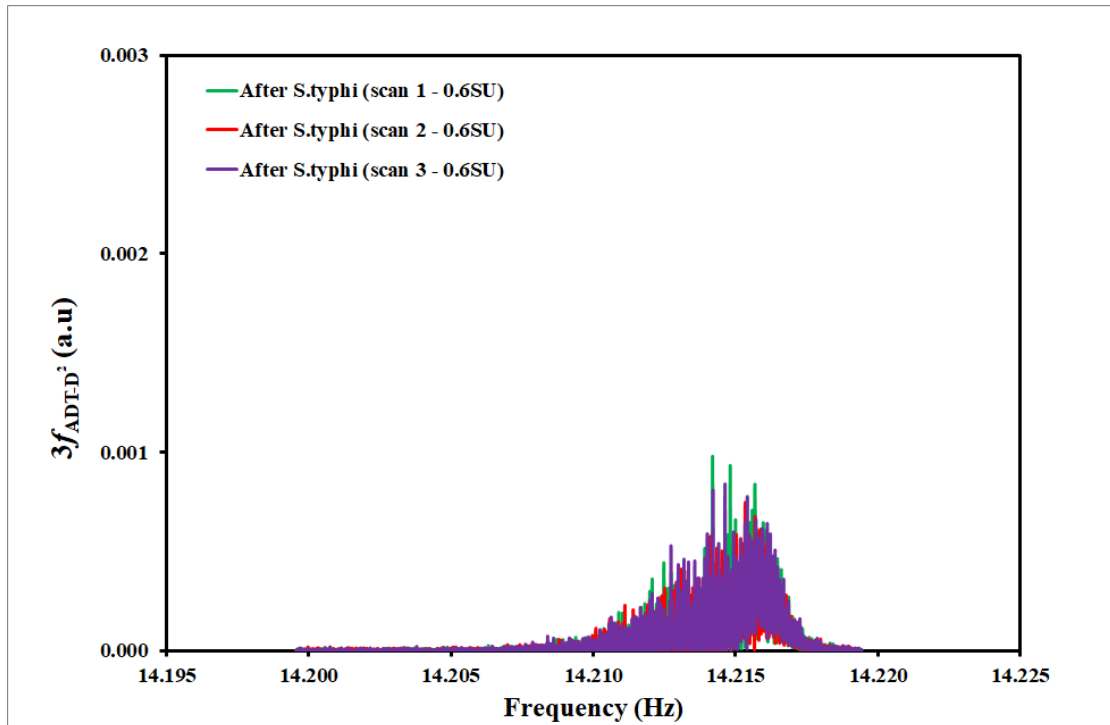


Fig. 6.19 - ADT-D² signal measured at 3rd harmonic ($3f_{ADT-D^2}$) after flowing 10^7 S.typhi/mL over surface functionalised with aptamer config. unzip at 0.6 SU (ADT-D²_{max}: Mean = 0.0008, SD = 0.0001).

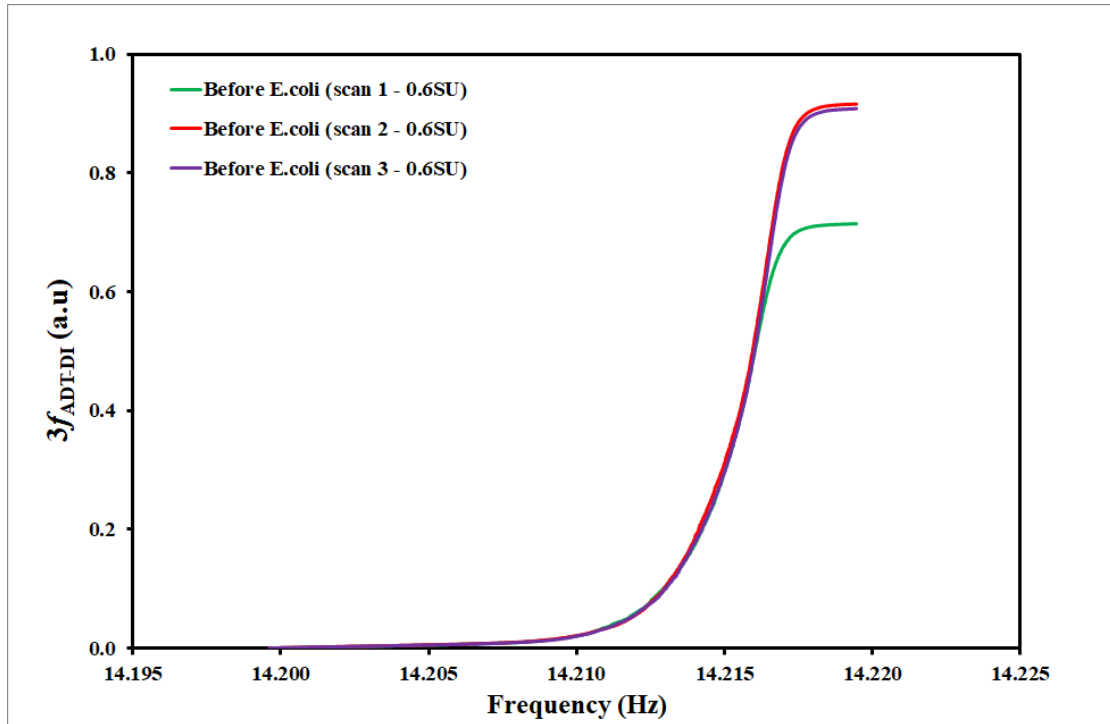


Fig. 6.20 - ADT-DI signal measured at 3rd harmonic ($3f_{ADT-DI}$) before flowing 10^7 E.coli/mL over surface functionalised with aptamer config. unzip at 0.6 SU ($ADT-DI_{max}$: Mean = 0.8460, SD = 0.1141).

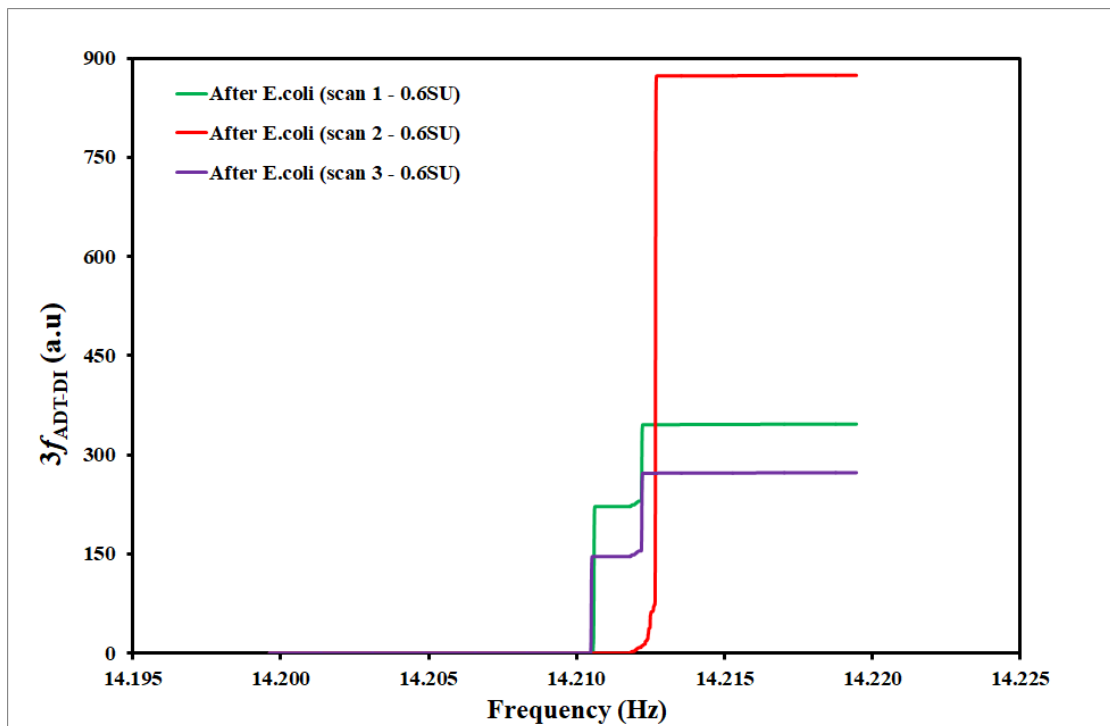


Fig. 6.21 - ADT-DI signal measured at 3rd harmonic ($3f_{ADT-DI}$) after flowing 10^7 E.coli/mL over surface functionalised with aptamer config. unzip at 0.6 SU ($ADT-DI_{max}$: Mean = 497.7650, SD = 327.8621).

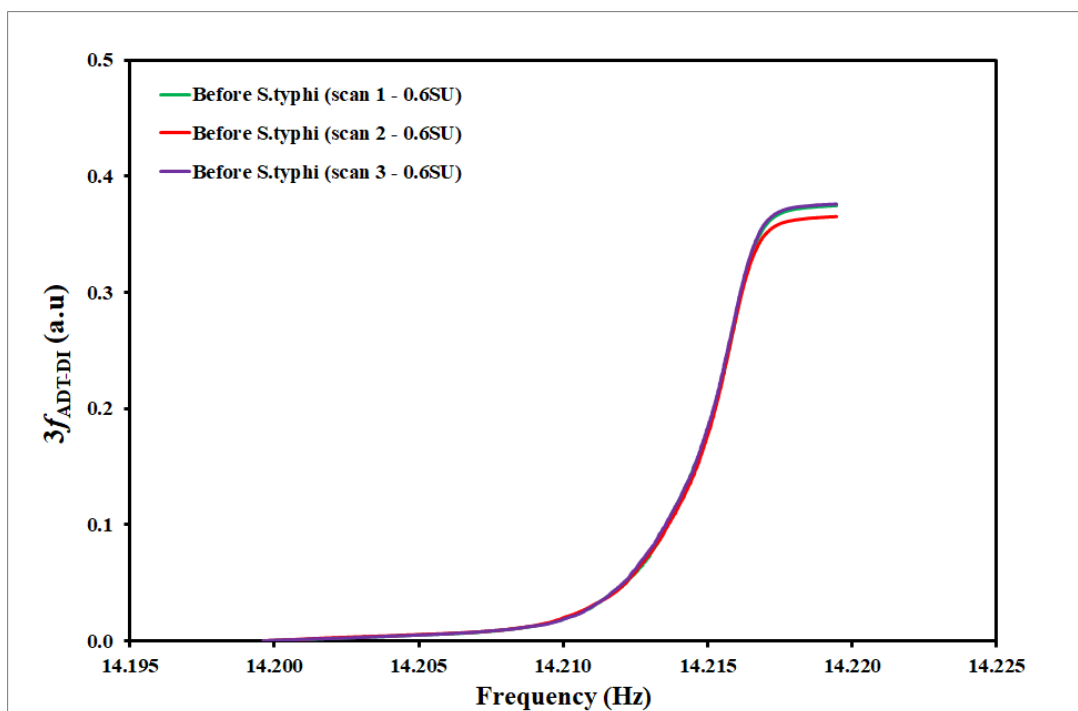


Fig. 6.22 - ADT-DI signal measured at 3rd harmonic ($3f_{\text{ADT-DI}}$) before flowing 10^7 S.typhi/mL over surface functionalised with aptamer config. unzip at 0.6 SU ($\text{ADT-DI}_{\text{max}}$: Mean = 0.3719, SD = 0.0058).

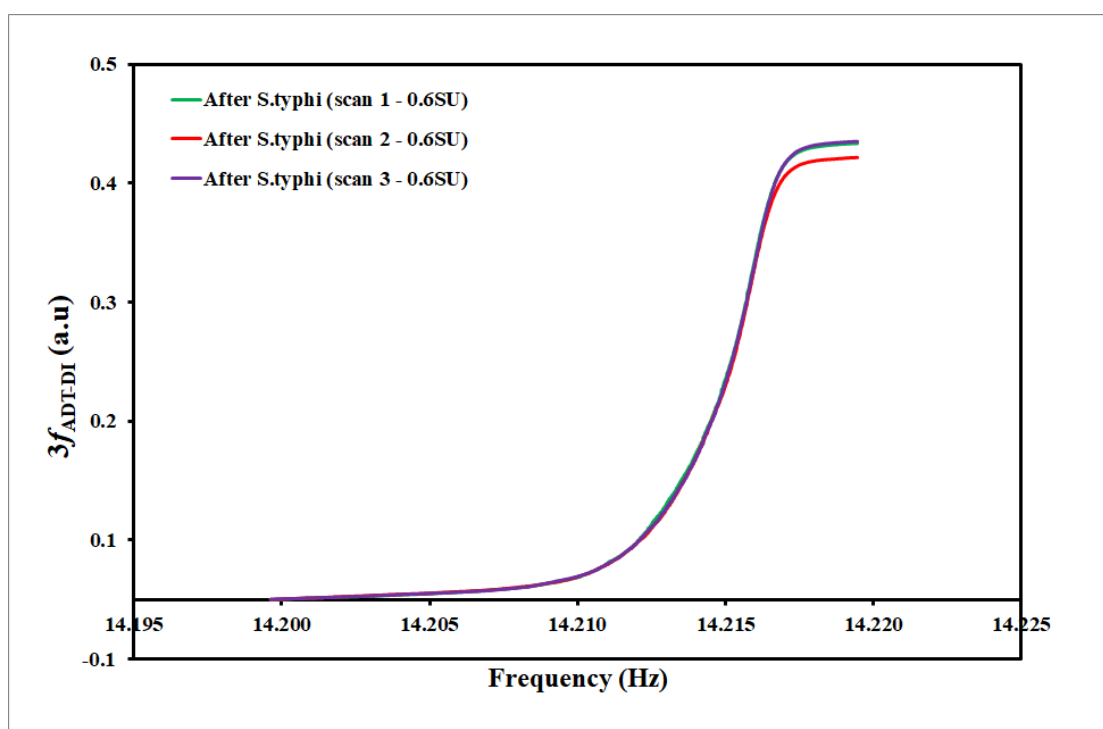


Fig. 6.23 - ADT-DI signal measured at 3rd harmonic ($3f_{\text{ADT-DI}}$) after flowing 10^7 S.typhi/mL over surface functionalised with aptamer config. unzip at 0.6 SU ($\text{ADT-DI}_{\text{max}}$: Mean = 0.3800, SD = 0.0073).

Comparison of specificity

Mean values of the triplicate set of scans conducted with each concentration of *E.coli* bacteria (10^7 cells/mL) and *S.typhi* bacteria (10^8 cells/mL) recorded at 60 mins, were calculated and their ratios were compared. These ratios for I_{3fmax} , $ADT-D^2_{max}$ and $ADT-DI_{max}$ measurements are plotted in Fig. 6.24. For 10 times lower concentration of *E.coli* (10^7 cells/mL) than *S.typhi* (10^8 cells/mL) bacteria, the ratio values were 8.59 for I_{3fmax} and 575.84 for $ADT-DI_{max}$. The ratio of means value for $ADT-D^2_{max}$ was found to be highest and about 4394.30 times that of I_{3fmax} and 65.55 times that of $ADT-DI_{max}$. Thus, this showed that addition of hairpin structure into the *E.coli*-binding aptamers introduced non-linearity into the system and the resultant unique unzipping signal dramatically increased the specificity of the sensor which could be determined by $ADT-D^2$ method of analysis.

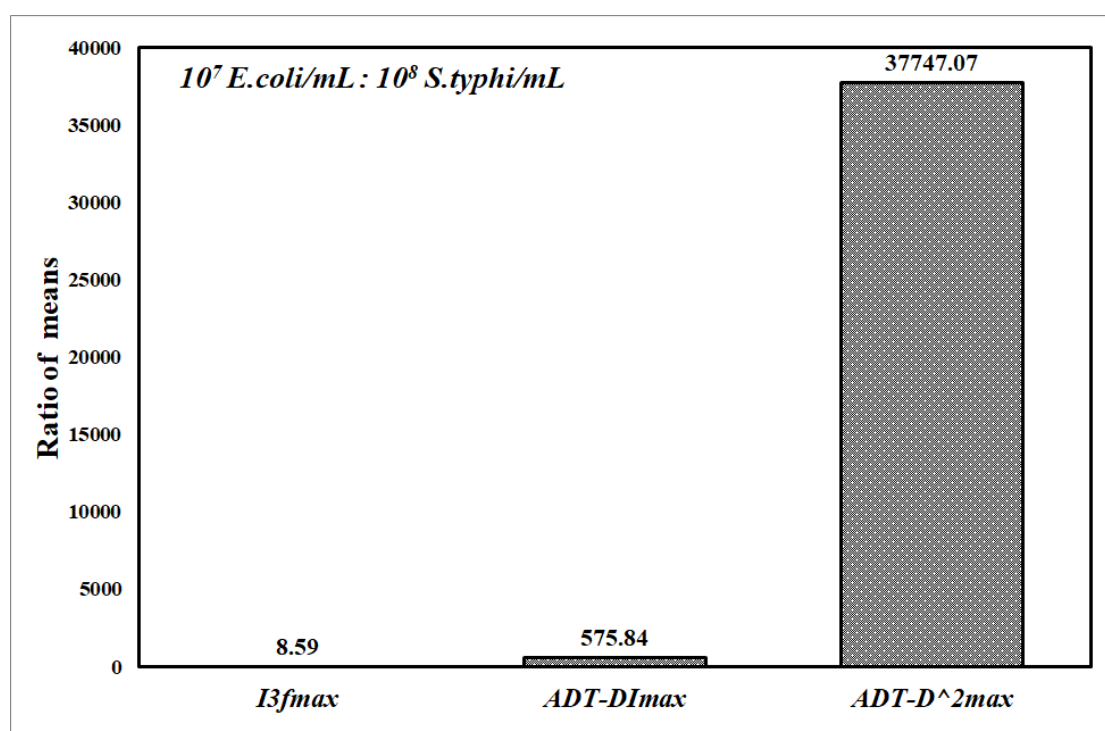


Fig. 6.24 - Comparison of specificity: ratio of mean values of I_{3fmax} shift, $ADT-DI_{max}$ shift and $ADT-D^2_{max}$ shift (10^7 E.coli/mL : 10^8 S.typhi/mL).

6.10 Summary

The focus of this chapter is to investigate the influence of structurally modified aptamers with designed nonlinearity in enhancing specificity of the anharmonic acoustic detection of *E.coli* bacteria. Two configurations were designed by introducing smart chemical moieties into the structure of the *E.coli*-binding aptamers operating in two different modes: (1) unzip, and (2) shear mode. Out of these two, unzip configuration gave characteristic signals when the sensor was driven at higher amplitudes (0.6 and 0.7 SU) due to transient unzipping response, while for the shear configuration no characteristic signal was observed, implying there was no unzipping of the hairpin structure. Unzipping is dependent not only on the amplitude of the drive but also on its duration. Unzipping signal was observed at higher amplitude as the scans of shorter duration were employed. However, for scans of longer duration, lower amplitude would be enough due to greater thermal assistance. This unzip configuration was further investigated to determine specificity of the anharmonic acoustic sensor. *S.typhi* bacteria were used as control sample.

Chapter 7 Summary of conclusions and Future work

7.1 Introduction

This chapter presents the summary, contributions and conclusions of this thesis and closes with a discussion of the limitations of the present research, and the proposal of a number of areas of further research to build upon the findings of this thesis.

7.2 Summary of contributions and conclusions of the work

This doctoral thesis was motivated by the global need for rapid diagnostic tests to control growing problem of infectious diseases especially, due to antimicrobial resistance (AMR). If rapid diagnostic tests are made available for pathogen identification and also determination of their susceptibility to antimicrobials; this will facilitate appropriate prescription and reduce the chances of development of drug-resistant or multidrug-resistant infectious diseases.

AMR is endangering the global health and needs to be tackled collectively on global scale. Therefore, the responses of various professional groups like Infectious Diseases Society of America (IDSA, US), Jim O'Neill's AMR review group (UK) and Presidential Advisory Council on Combating Antibiotic-Resistant Bacteria (PACCARB, US) were reviewed to identify the current key unmet needs regarding diagnostic testing.^[2] The review made it clear that an ideal rapid diagnostic test should be cheap and reliably deliver sensitive, specific and quantitative measurements and be suitable for integration onto a POC platform. The key features of POCTs that distinguish them from conventional laboratory tests are: they do not require specialised laboratory infrastructure or trained personnel to use them; they deliver a rapid (i.e. within 1 hour) diagnosis and they are more cost-effective than conventional tests.^[69]

Presently, bacterial identification (ID) and antibiotic susceptibility testing (AST) are the well-established diagnostic methodologies. Culture-dependent pathogen identification methods are very time-consuming and generally require 18 to 48 hours with further 8 to 48 hours to perform AST and report

the results. As it is unlikely to shorten the time required to conduct phenotypic AST, the initial pathogen detection and identification step needs to be reduced, to reduce the length of the diagnostic cycle. This will help clinicians to initiate appropriate treatments quickly. Thus, the initial literature survey explored all the currently available culture-independent rapid diagnostic methods viz. nucleic-acid based methods, immunological methods, mass-spectrometry-based methods and biosensor-based methods.

Detection of whole-cell bacteria is important so that they can be further utilised for subsequent AST. However, nucleic acid-based methods are genotypic tests and do not permit isolating pathogens for further use. Immunological tests can detect whole-cell bacteria but in these methods also, bacteria cannot be recovered for AST. Moreover, both these methods are also label-based and require laborious labelling processes, making them costly. Also, methods like PCR, ELISA or MALDI-TOF-MS are laborious and require specialised equipment and trained personnel to operate the system. Biosensor-based methods allow label-free detection of whole-cell bacteria, except for optical label-based biosensors. However, optical biosensors are bulky in size and the set-up method of electrochemical biosensors is very complicated, making them both difficult to be translated as POCT. Later flow immunoassays (LFIs) are cheap and can be employed at the point-of-care but it is difficult to integrate them with electronics and suffer from higher false-positive rates than PCR and ELISA. On the other hand, ADT could potentially address this problem because of its intrinsic ability to differentiate specific and non-specific interactions, making diagnosis more reliable and reproducible. Also, ADT is an easy-to-use, integrable, low-cost technology that can be miniaturised and applied as POCT. Moreover, it is also possible to maintain suitable temperature and grow bacteria within the microfluidic device integrated with ADT, to investigate antibiotic action on slow growing pathogens. Therefore, as potentially AST can be performed with ADT and it can be applied at the point-of-care for rapid, label-free, low-cost, detection with high specificity which is lacking in most of the other methods, this technology was selected to explore its use for whole-cell bacterial detection.

In biosensor-based diagnostic methods, it is vital to identify appropriate bio-receptor targeting bacteria, which can be then potentially coupled with the transducer. The right combination would then expedite diagnosis and thus decreasing the time between culture collections to specific antimicrobial treatment. Aptamers that are analogous to antibodies in their range of target recognition and variety of applications, they possess several key advantages over their protein counterparts. Therefore, in this thesis for the first time 'aptamer' as bio-recognition element, was coupled with anharmonic acoustic transduction technique for detection of target *E.coli* bacteria. The main aim of this thesis was to investigate the feasibility of this 'anharmonic acoustic aptasensor' platform for rapid point-of-care detection of whole-cell bacteria, which can be applied for rapid identification of the pathogen and subsequent determination of antimicrobial susceptibility. Following are the most important observations made from this research:

7.2.1. Addressed the experimental challenges with the integrated biosensor assay

E.coli-binding aptamer as bio-receptor was first time integrated with the ADT transduction technique and also the microfluidic flow-cell for detection of target *E.coli* (*KCTC 2571*) bacteria. To achieve high sensitivity and specificity with this integrated bioassay several experimental challenges were addressed around the transduction technique, microfluidic flow-cell, and the assay itself and the objective O.1.1 was achieved.

a. Increasing the sensitivity of the sensor through energy trapping

Energy trapping concept is well-known concept and have been previously explored by Efimov *et al.*, where they investigated the variation in sensitivity of QCR in response to energy trapping effect. They observed that the energy trapping effect not only suppresses the spurious modes but also increases the sensitivity of the QCR by confining the oscillations to the region of additional loading. Hence, this effect was further explored in terms of anharmonic acoustic detection technique and the electrode geometry was modified to stepped (non-uniform) crystals, by loading the gold electrodes of QCR with

central gold deposits. To demonstrate the energy trapping effect on the ADT signal, experiments were performed, where QCRs with the uniform and stepped electrodes were used to detect the streptavidin-coupled beads. It was observed that the sensitivity of the QCR ($3f$ signal) increased dramatically almost 3 times by loading it with central gold deposit (~ 65 nm height) and concentrating the oscillations to loaded area through energy trapping effect, in comparison to that of the uniform crystals. Thus, energy trapping effect increased the sensitivity of the nonlinear acoustic sensor.

b. Identification of optimal method of measurement of $3f$ signal

The two modes of scans used for ADT measurements were explored: frequency mode scan (FMS) and amplitude mode scan (AMS). It was found that for AMS scans, it is imperative to determine f_0 values before each scan to get maximum response. Consequently, real-time measurements are difficult to obtain with AMS mode scan, as the driving frequency needs to be reset to resonant frequency before each scan. Thus, it was concluded that FMS mode scan should be used for measuring $3f$ signal as it gives true shift and also allows real-time measurements as there is no need to reset the driving frequency to f_0 before each step. This was an important finding as it reduced the overall assay time, which is one of the important requirements for the diagnostic test for controlling AMR.

c. Selection of suitable bioassay format

The interface between the transducer and the bio-receptor plays important role, influencing the generation of anharmonic acoustic signal. Biotin-streptavidin bioassay format was selected to ensure optimum orientation of the bio-receptor, thereby, enhancing the performance of the biosensor assay.

d. Resolved the problem of bubble formation with the microfluidic flow-cell

Previous experiments with ADT machine done by Ghosh *et al.* ^[151, 152] were done using simple batch method, wherein a droplet of sample was placed on the sensor surface. However, in all the experiments for this PhD project, a

microfluidic flow-cell was used for sample delivery. The performance of this flow-cell was frequently challenged with the problem of bubble formation, which apparently affected the signal acquired. The problem was identified to be at the entry point of tubes into the flow-cell. This issue was resolved by increasing the diameter of both inlet and outlet and inserting small piece of softer tube having internal diameter same as the outer diameter of the harder tubes connected to sample reservoir (as shown in Fig. 3.21 (B) and (C)). Thus, this was a key solution as it ensured the reliability of the signal and also efficient exposure of the sample to the surface without any interference due to bubbles.

e. Achievement of baseline stability

For the comparability purposes, it is important that baseline is measured under the same conditions as that after passing analyte. Baseline values essentially represent the noise in the system. Therefore, baseline stability is important to get better signal-to-noise ratio (SNR) after introduction of the target analyte. Several ways were tried before a stable baseline could be achieved like, warming up the QCR half an hour before the experiments, ensuring proper clamping, removing bubbles (if any) from the system, etc. Of all the steps, the most critical and useful step was found to be acoustically clean the surface intermittently with constant amplitude scans. Given that ADT is very sensitive transduction technique, baseline stability was a very important achievement, as it reduced the noise and improved the SNR of the measurements.

7.2.2. Anharmonic acoustic aptasensor enables detection of E.coli bacteria

ADT transduction technique has been previously employed for detection of *Bacillus subtilis* spores in liquid, but not for live whole-cell bacteria. For the first time, the nonlinear acoustic response of QCR was probed with functionalised specific DNA aptamers that are multivalent and bind whole bacterial cell for direct detection and quantification of viable *E. coli* KCTC

2571 bacteria. This aptamer-based assay coupled with nonlinear acoustic sensor constituted the anharmonic acoustic aptasensor.

With this aptasensor, it is possible to detect the presence of viable surface-bound *E.coli* bacteria by measuring the maximum value of magnitude of the transduced $3f$ current (I_{3fmax}), which is referred to as the $3f$ or ADT signal. The fabricated 'anharmonic acoustic aptasensor' on gold surface of QCR electrodes was successful in rapid, sensitive, specific and quantitative detection of *E.coli* bacteria and met the objective O.1.

Enabling rapid and sensitive detection of viable whole-cell *E.coli* bacteria:

The response of this aptasensor was observed for the bacterial suspensions ranging from 10^5 - 10^8 cells/mL. The results show that the $3f$ signals (I_{3fmax}) allow rapid, sensitive and quantitative detection of 2.5×10^4 viable *E.coli* bacteria in 5 mins, as compared to standard frequency shift (Δf_0) and dissipation shift (ΔD) measurements.

Enabling quantitative detection of viable whole-cell *E.coli* bacteria:

Linear quantitative correlation could be reliably achieved with $3f$ signal (I_{3fmax}) ($R^2 = 0.984$) for four concentrations of *E.coli* bacteria (10^5 - 10^8 cells/mL), than with Δf_0 and ΔD . For the highest concentration of *E.coli* of 10^8 cells/mL, negative frequency and dissipation shifts were observed. This could be due to increase in mass going on the surface, highlighting the need for washing step with these methods. On the other hand, linear quantitative correlation could be achieved for *E.coli* concentrations with ΔI_{3fmax} without the washing step, as the $3f$ signal is additive since the motion of the flexibly bound bacteria is synchronous and their interaction with the surface is independent of each other.

Enabling specific detection of viable whole-cell *E.coli* bacteria:

This aptasensor also allowed detection of *E.coli* bacteria with high specificity. To determine specificity, *S.typhi* bacteria were used as control sample. For the same concentrations of *E.coli* and *S.typhi* bacteria (10^8 cells/mL), the ratio

values were, 1.01 for Δf_0 , 8.42 for ΔD and highest 19.02 for ΔI_{3fmax} . Thus, the increase in resonant frequency and the relative increase in dissipation were found to be lower by 18.83 and 2.26 times than the relative decrease in $3f$ signal (I_{3fmax}).

Enabling reproducible detection of viable whole-cell *E.coli* bacteria:

Triplicate set of experiments were performed to validate reproducibility after achieving stable baseline each time.

Accordingly, this anharmonic acoustic aptasensor which allows fast, sensitive quantitative detection of viable target bacteria with high specificity and reproducibility not only saves time but also allows subsequent AST by sparing intact bacteria for further characterisation. Thus, this sensor could be applied for rapid pathogen identification to reduce the overall length of the diagnostic cycle and prevent AMR.

7.2.3 Comparative performance of different bio-receptors integrated with ADT for detection of bacteria

In the ADT transduction technique, for a given drive frequency (f), the $3f$ signal is dependent on the force-extension characteristic of the molecular tether, its length, and also the size of the particles. Hence, to meet the objective O.2.1 and O.2.2, bio-receptors of different size i.e. anti-*E.coli* antibodies and different length i.e. thiolated *E.coli*-binding aptamer (shorter) were investigated for detection of *E.coli* bacteria, respectively.

It was found that the sensitivity and specificity of the assay with longer linker (biotinylated aptamer-streptavidin-biotin thiol) was highest for detection of *E.coli* bacteria as compared with shorter linker (thiolated aptamer) and biotinylated antibody assay. Bio-receptors with different linker lengths have been previously investigated, and it was found that with the longer linker the percentage elongation is less and also the inclination is less, resulting in lower $3f$ response compared to a shorter linker. However, the response with shorter linker (thiolated linker) was found to be lower than longer linker in terms of both sensitivity and specificity.

This could be due to saturation of the surface with 100% thiolated aptamers which might have affected its functionality by steric hindrance because of overcrowding. This can be potentially improved by co-immobilisation of the thiolated aptamer with MCH in a fixed combination rather than backfilling with MCH.

7.2.4 Novel aptamer configurations enabling highly specific detection of bacteria

The influence of structurally modified aptamers with designed nonlinearity was investigated in enhancing the sensitivity and specificity of the anharmonic acoustic detection of *E.coli* bacteria. Two configurations were designed by introducing smart chemical moieties into the structure of the *E.coli*-binding aptamers operating in two different modes: (1) unzip, and (2) shear mode. Out of these two, unzip configuration gave characteristic signals when the sensor was driven at higher amplitudes (0.6 and 0.7 SU) due to transient unzipping response, while for the shear configuration no characteristic signal was observed, implying there was no unzipping of the hairpin structure.

Unzipping is dependent not only on the amplitude of the drive but also on its duration. Unzipping signal was observed at higher amplitude as the scans of shorter duration were employed. However, for scans of longer duration, lower amplitude would be enough due to greater thermal assistance.

This unzip configuration was further investigated to determine specificity of the anharmonic acoustic aptasensor. *S.typhi* bacteria were used as control sample. Characteristic signals were obtained for 10^7 *E.coli*/mL but none for 10^8 *S.typhi*/mL.

This is again unique and novel for a biosensor assay. This enables detection of bacteria with high specificity by introduction of innovative mechanical structures in the stem of the *E.coli*-binding bacteria. This can be also applied for multiplex detection by employing aptamer designs with and without unzip configurations on the single sensor and differentiating the characteristic signals by varying driving amplitude and duration of scans. This is a novel direction for the research in terms of developing aptamer-based bioassay for

nonlinear acoustic sensor ADT to be used as POC device for infectious disease diagnosis.

7.3 Potential impact through future research

7.3.1 Exploring detection of other pathogens

It was possible to directly detect viable *E.coli* bacteria with the fabricated anharmonic acoustic aptasensor, but it will be interesting to explore direct detection of other pathogens of different sizes like, virus (smaller) and fungi (larger). Also, the *E.coli* (KCTC 2571) bacteria detected in this work are non-pathogenic. To apply this sensor for pathogen identification in real-world samples, a similar feasibility study needs to be carried out with pathogenic strains.

7.3.2 Exploring other diagnostic methods

The aptamer-based bioassay which constituted the bio-recognition element of the biosensor assay can be applied to other diagnostic methods too. It will be interesting to test this aptamer-based bioassay with the Lateral Flow Assays (LFAs) that are rapid, cheap and simple-to-use which can be applied easily at the point-of-care to control AMR.

7.3.3 Investigating QCRs with lower resonant frequency

For all the experiments TSM quartz crystal resonators were used with fundamental resonant frequency range of 14.275 -14.325 MHz. However, QCRs with lower resonant frequencies like 5 MHz could be integrated with aptamer-based assay and tested for detection of *E.coli* bacteria. QCRs with lower resonant frequencies will have greater amplitude of oscillations. This could cause greater distortion or stretching of the biomolecular linkers for given driving amplitude, thus a greater $3f$ signal.

7.3.4 Improving microfluidics for *in-situ* pathogen identification and AST

The anharmonic acoustic aptasensor allows a label-free direct phenotypic detection of live bacteria within a controlled microfluidic environment, which

can be maintained at a desired temperature. This means it is possible to culture bacteria within the microfluidic cell and measure the growth curve. Thus, it is possible to introduce antibiotic and to record any change in signal and thereby interpret the antibiotic susceptibility. My work has led to this current activity in Dr. Ghosh's lab. A successful outcome of the project will allow, “rapid identification of pathogens along with determination of phenotypic antibiotic susceptibility and minimum inhibitory concentration”, for the first time known. Also, this sensing system can be further applied for detection of pathogens in biological samples like blood, urine, food samples, etc. For this disposable cartridge with foil-based pressure sensors are being developed and investigated, as a part of another Enterprise Project.

7.3.5 Modification of the aptamers to enable multiplex detection

By introducing smart chemical structures in the *E.coli*-binding aptamer sequence, a characteristic signal was achieved which significantly enhanced the specificity of the biosensor. The novel mechanical hairpin structure introduced in the stem of the aptamer comprised of a short dsDNA helix (21b) with very low GC content, thus allowing unzipping easily. This can be further modified and several sequences can be tried with different AT or GC nucleic acid combinations and thus varying the corresponding signal, as the driving amplitude will differ depending on the nucleic acid composition. Also, instead of all complementary strands, sequences with mismatched based can be introduced to cause unzipping at a lower amplitude. Aptamer configurations thus modified having specific binding affinity for different bacteria can be employed on the same QCR and the different amplitudes could be determined for different configurations giving characteristic signals. Thus, this could be applied for multiplex detection of bacteria using single sensor platform.

7.4 Considerations for ‘Anharmonic acoustic aptasensor’ as POCT

Point-of-care (POC) biosensor systems can potentially improve patient care through real-time and remote health monitoring. It is expected that future POC diagnostic systems should support artificial intelligent algorithms through the use of decision support process, in order to provide accurate and efficient

diagnostic results in real-time. Decision support processing is a critical component of a POC system since they can assist new clinicians in their diagnostic and clinical judgement and thereby, help in controlling AMR.

Currently, Lateral Flow Assays (LFAs) that are fast, inexpensive and easy-to-use are applied at the point-of-care. Like LFAs, anharmonic acoustic aptasensor also has the potential to be applied at the POC. Anharmonic acoustic aptasensor is an analytical device consisting of three important elements: ADT along with QCR as transducer, microfluidic flow-cell for sample introduction and aptamers as bio-receptor. In order to apply anharmonic acoustic aptasensor as POCT, all these three elements need to be further improved.

The small size and simple construction of biosensor used for detection of biological agents are ideally suited for POC lab-on-a-chip systems. The currently used ADT machine for transduction is portable, but to be applied as lab-on-a-chip system, it needs to be further fabricated at micro- or nano-scale. Besides, it is also important to use materials having mechanical properties that enable improved sensitivity with low electrical losses.

Previous experiments with ADT machine were done by using simple batch method, wherein a droplet of sample was placed on the sensor surface. However, in all the experiments for this PhD project, a polycarbonate microfluidic flow-cell (Fig. 3.21) was used for sample delivery. The microscale features of the microfluidic flow-cell ensured laminar flow and very little mixing. But by using cheaper materials like Polydimethylsiloxane (PDMS) for fabrication, the cost of this microfluidic flow-cell can be further reduced. Currently, a lot of researchers use PDMS and soft lithography due to their easiness of use and fast process. This permits to build prototypes very quickly and test its applications, instead of wasting time in laborious fabrication protocols. Also, the soft lithography technique requires only a little bench space under a lab fume hood to place rapid PDMS prototyping instruments and to quickly assess microfluidic concepts. In the past, research efforts have been made to realise the rapid multiplexed detections using lab-on-a-chip devices with integrated microfluidic system. Therefore, in addition to the points

mentioned in the section 7.3.4, the microfluidic flow-cell should be further improved to address the issue of multiplexed detection at the POC. The microfluidic flow-cell with multiple channels can be designed to achieve multiplex detection. But this warrants use of syringe pump with multiple channels and with most precise flow rate and pressure control.

The *E.coli*-binding aptamers can be easily procured, as they can be replicated by simple chemical synthesis with very high fidelity once a useful DNA sequence of the aptamer is known. Aptamers are thus easily quantifiable and do not require re-evaluation before a new batch of aptamers comes into use. The regeneration of the crystals used is a key factor to be considered in the development of a real-world biosensor. Aptamer receptors can allow repeated affine layer regeneration after ligand binding and recycling of the biosensor with little loss of sensitivity. Aptamers can be denatured and renatured to their original conformations by changing the temperature and pH, thus can be reused for the subsequent capture assay. Another elution strategy is based on the usage of the chelating agent like ethylenediamine tetra-acetic acid (EDTA), which chelates the divalent ions that are important for the binding affinity of the aptamer against the target. Thus, aptamers have excellent reusability property and are suitable bio-receptors for bacterial detection.^[246-248]

Also, biosensors with wireless link capabilities are desirable because wireless sensing systems can monitor health conditions in real-time and also promote novel healthcare services, like real-time drug delivery.

In summary, by further improving all the three elements of the 'anharmonic acoustic aptasensor' with the help of advanced techniques, it is possible to apply it at the POC and thereby, control AMR.

References:

- [1] Cunningham, A., Daszak, P. and Wood, J. (2017). One Health, emerging infectious diseases and wildlife: two decades of progress? *Philosophical Transactions of the Royal Society B: Biological Sciences*, 372(1725), p.20160167.
- [2] Caliendo AM, Gilbert DN, Ginocchio CC, Hanson KE, May L, Quinn TC, Tenover FC, Alland D, Blaschke AJ, Bonomo RA, Carroll KC, Ferraro MJ, Hirschhorn LR, Joseph WP, Karchmer T, MacIntyre AT, Reller LB, Jackson AF; Infectious Diseases Society of America (IDSA). Better Tests, Better Care: Improved Diagnostics for Infectious Diseases. (2013). *Clinical Infectious Diseases*, 57(suppl_3), p.NP-NP.
- [3] World Health Organization. (2018). *Antimicrobial resistance*. [online] Available at: <http://www.who.int/mediacentre/factsheets/fs194/en/> [Accessed 10 Apr. 2018].
- [4] Akova, M. (2016). Epidemiology of antimicrobial resistance in bloodstream infections. *Virulence*, 7(3), pp.252-266.
- [5] McKie, R. (2017). 'Antibiotic apocalypse': doctors sound alarm over drug resistance. [online] the Guardian. Available at: <https://www.theguardian.com/society/2017/oct/08/world-faces-antibiotic-apocalypse-says-chief-medical-officer> [Accessed 10 Apr. 2018].
- [6] O'Neill J. (2016). *Amr-review.org*. [online] Available at: https://amr-review.org/sites/default/files/160525_Final%20paper_with%20cover.pdf [Accessed 10 Apr. 2018].
- [7] O'Neill J. (2014). *Amr-review.org*. [online] Available at: http://amr-review.org/sites/default/files/AMR%20Review%20Paper%20-%20Tackling%20a%20crisis%20for%20the%20health%20and%20wealth%20of%20nations_1.pdf [Accessed 10 Apr. 2018].
- [8] de Kraker M, Stewardson A, Harbarth S. Will 10 Million People Die a Year due to Antimicrobial Resistance by 2050?. *PLoS Med*. 2016;13(11):e1002184.

- [9] Centers for Disease Control and Prevention (2013). *Cdc.gov*. [online] Available at: <http://www.cdc.gov/drugresistance/threat-report-2013/pdf/ar-threats-2013-508.pdf> [Accessed 10 Apr. 2018].
- [10] ECDC/EMA Joint technical report. (2018). *Ecdc.europa.eu*. [online] Available at: https://ecdc.europa.eu/sites/portal/files/media/en/publications/Publications/0909_TER_The_Bacterial_Challenge_Time_to_React.pdf [Accessed 10 Apr. 2018].
- [11] World Bank Group Discussion Draft. (2016). *Pubdocs.worldbank.org*. [online] Available at: <http://pubdocs.worldbank.org/en/527731474225046104/AMR-Discussion-Draft-Sept18updated.pdf> [Accessed 10 Apr. 2018].
- [12] MacIntyre, C. and Bui, C. (2017). Pandemics, public health emergencies and antimicrobial resistance - putting the threat in an epidemiologic and risk analysis context. *Archives of Public Health*, 75(1).
- [13] Desai, R. Antimicrobial Resistance (2016) [online] Available at: <http://drrajivdesaimd.com/2016/11/20/antimicrobial-resistance-amr/> [Accessed 10 Apr. 2018].
- [14] Center for Disease Dynamics, Economics & Policy (CDDEP). (2018). *Countries reporting plasmid-mediated colistin resistance encoded by mcr-1 - Center for Disease Dynamics, Economics & Policy (CDDEP)*. [online] Available at: https://cddep.org/tool/countries_reporting_plasmid_mediated_colistin_resistance_encoded_mcr_1/ [Accessed 10 Apr. 2018].
- [15] Chen, L., Todd, R., Kiehlbauch, J., Walters, M. and Kallen, A. (2017). Notes from the Field: Pan-Resistant New Delhi Metallo-Beta-Lactamase-Producing *Klebsiella pneumoniae* — Washoe County, Nevada, 2016. *MMWR. Morbidity and Mortality Weekly Report*, 66(1), p.33.
- [16] ContagionLive. (2018). *Superbugs Equal Super Headlines for the Media: Public Health Watch Report*. [online] Available at: <http://www.contagionlive.com/news/superbugs-equal-super->

- headlines-for-the-media-public-health-watch-report [Accessed 10 Apr. 2018].
- [17] Aminov, R. (2010). A Brief History of the Antibiotic Era: Lessons Learned and Challenges for the Future. *Frontiers in Microbiology*, 1.
- [18] Sir Alexander Fleming. (1945). *Nobelprize.org*. [online] Available at: https://www.nobelprize.org/nobel_prizes/medicine/laureates/1945/fleming-lecture.pdf [Accessed 10 Apr. 2018].
- [19] Ventola CL. (2015). The Antibiotic Resistance Crisis: Part 1: Causes and Threats. *Pharmacy and Therapeutics*. 40(4): pp.277-283.
- [20] Sengupta, S., Chattopadhyay, M. and Grossart, H. (2013). The multifaceted roles of antibiotics and antibiotic resistance in nature. *Frontiers in Microbiology*, 4.
- [21] Chambers, H. and DeLeo, F. (2009). Waves of resistance: Staphylococcus aureus in the antibiotic era. *Nature Reviews Microbiology*, 7(9), pp.629-641.
- [22] Davies, J. and Davies, D. (2010). Origins and Evolution of Antibiotic Resistance. *Microbiology and Molecular Biology Reviews*, 74(3), pp.417-433.
- [23] WHO Antimicrobial Resistance: Global Report on Surveillance (2014). [online] *Apps.who.int*. Available at: http://apps.who.int/iris/bitstream/handle/10665/112642/9789241564748_eng.pdf;jsessionid=37C2FAAD396A7ABB754D6A215C76274D?sequence=1 [Accessed 10 Apr. 2018].
- [24] Silver, L. (2011). Challenges of Antibacterial Discovery. *Clinical Microbiology Reviews*, 24(1), pp.71-109.
- [25] Scorciapino, M., Acosta-Gutierrez, S., Benkerrou, D., D'Agostino, T., Mallocci, G., Samanta, S., Bodrenko, I. and Ceccarelli, M. (2017). Rationalizing the permeation of polar antibiotics into Gram-negative bacteria. *Journal of Physics: Condensed Matter*, 29(11), p.113001.
- [26] Castro-Sánchez, E., Moore, L., Husson, F. and Holmes, A. (2016). What are the factors driving antimicrobial resistance? *Perspectives from a public event in London, England. BMC Infectious Diseases*, 16(1).

- [27] Singer, A., Shaw, H., Rhodes, V. and Hart, A. (2016). Review of Antimicrobial Resistance in the Environment and Its Relevance to Environmental Regulators. *Frontiers in Microbiology*, 7.
- [28] Bartlett, J., Gilbert, D. and Spellberg, B. (2013). Seven Ways to Preserve the Miracle of Antibiotics. *Clinical Infectious Diseases*, 56(10), pp.1445-1450.
- [29] CDC. (2016). *CDC Press Releases*. [online] Available at: <https://www.cdc.gov/media/releases/2016/p0503-unnecessary-prescriptions.html> [Accessed 10 Apr. 2018].
- [30] Hollis, A. and Ahmed, Z. (2013). Preserving Antibiotics, Rationally. *New England Journal of Medicine*, 369(26), pp.2474-2476.
- [31] Van Boeckel, T., Brower, C., Gilbert, M., Grenfell, B., Levin, S., Robinson, T., Teillant, A. and Laxminarayan, R. (2015). Global trends in antimicrobial use in food animals. *Proceedings of the National Academy of Sciences*, 112(18), pp.5649-5654.
- [32] Goossens, H., Ferech, M., Vander Stichele, R. and Elseviers, M. (2005). Outpatient antibiotic use in Europe and association with resistance: a cross-national database study. *The Lancet*, 365(9459), pp.579-587.
- [33] Riedel, S., Beekmann, S., Heilmann, K., Richter, S., Garcia-de-Lomas, J., Ferech, M., Goosens, H. and Doern, G. (2007). Antimicrobial use in Europe and antimicrobial resistance in *Streptococcus pneumoniae*. *European Journal of Clinical Microbiology & Infectious Diseases*, 26(7), pp.485-490.
- [34] Butler, C., Rollnick, S., Pill, R., Maggs-Rapport, F. and Stott, N. (1998). Understanding the culture of prescribing: qualitative study of general practitioners' and patients' perceptions of antibiotics for sore throats. *BMJ*, 317(7159), pp.637-642.
- [35] Paredes, P., de la Peña, M., Flores-Guerra, E., Diaz, J. and Trostle, J. (1996). Factors influencing physicians' prescribing behaviour in the treatment of childhood diarrhoea: Knowledge may not be the clue. *Social Science & Medicine*, 42(8), pp.1141-1153.
- [36] Eccles, R. and Weber, O. (2009). Common cold. *Basel: Birkhäuser*. p. 234. ISBN 978-3-7643-9894-1.

- [37] Bartoloni, A., Cutts, F., Leoni, S., Austin, C., Mantella, A., Guglielmetti, P., Roselli, M., Salazar, E. and Paradisi, F. (1998). Patterns of antimicrobial use and antimicrobial resistance among healthy children in Bolivia. *Tropical Medicine and International Health*, 3(2), pp.116-123.
- [38] Leekha, S., Terrell, C. and Edson, R. (2011). General Principles of Antimicrobial Therapy. *Mayo Clinic Proceedings*, 86(2), pp.156-167.
- [39] Knobler, S. (2003). The Resistance phenomenon in microbes and infectious disease vectors. *Washington, D.C.: National Academies Press*.
- [40] FIND. Because diagnosis matters (2017) [online] <https://www.slideshare.net/SystemOneUS/2018-find-amr-strategy> [Accessed 10 Apr. 2018].
- [41] Shapiro, E. (2002). Injudicious antibiotic use: An unforeseen consequence of the emphasis on patient satisfaction? *Clinical Therapeutics*, 24(1), pp.197-204.
- [42] Van Duong, D., Binns, C. and Van Le, T. (1997). Availability of antibiotics as over-the-counter drugs in pharmacies: a threat to public health in Vietnam. *Tropical Medicine and International Health*, 2(12), pp.1133-1139.
- [43] McNulty, C., Boyle, P., Nichols, T., Clappison, P. and Davey, P. (2007). The public's attitudes to and compliance with antibiotics. *Journal of Antimicrobial Chemotherapy*, 60(suppl_1), pp.i63-i68.
- [44] Michael, C., Dominey-Howes, D. and Labbate, M. (2014). The Antimicrobial Resistance Crisis: Causes, Consequences, and Management. *Frontiers in Public Health*, 2.
- [45] Needham, D., Foster, S., Tomlinson, G. and Godfrey-Faussett, P. (2001). Socio-economic, gender and health services factors affecting diagnostic delay for tuberculosis patients in urban Zambia. *Tropical Medicine and International Health*, 6(4), pp.256-259.
- [46] Almuzaini, T., Choonara, I. and Sammons, H. (2013). Substandard and counterfeit medicines: a systematic review of the literature. *BMJ Open*, 3(8), p.e002923.

- [47] Nayyar, G., Fernandez, F., Herrington, J., Kendall, M., Attaran, A., Newton, P., Breman, J., Clark, J. and Culzoni, M. (2015). Responding to the Pandemic of Falsified Medicines. *The American Journal of Tropical Medicine and Hygiene*, 92(6_Suppl), pp.113-118.
- [48] Bassat, Q., Tanner, M., Guerin, P., Stricker, K. and Hamed, K. (2016). Combating poor-quality anti-malarial medicines: a call to action. *Malaria Journal*, 15(1).
- [49] Renschler, J., Walters, K., Newton, P. and Laxminarayan, R. (2015). Estimated Under-Five Deaths Associated with Poor-Quality Antimalarials in Sub-Saharan Africa. *The American Journal of Tropical Medicine and Hygiene*, 92(6_Suppl), pp.119-126.
- [50] The White House Press Office. (2015). *whitehouse.gov. FACT SHEET: President's 2016 Budget Proposes Historic Investment to Combat Antibiotic-Resistant Bacteria to Protect Public Health*. [online] Available at: <http://www.whitehouse.gov/the-press-office/2015/01/27/fact-sheet-president-s-2016-budget-proposes-historic-investment-combat-a> [Accessed 10 Apr. 2018].
- [51] IMI and AMR factsheet (2018). *Drive-ab.eu*. [online] Available at: http://drive-ab.eu/wp-content/uploads/2014/09/IMIandAMRfactsheet_Nov2015.pdf [Accessed 10 Apr. 2018].
- [52] WHO. Global action plan for antimicrobial resistance. *Who.int*. (2015). [online] Available at: http://www.who.int/drugresistance/global_action_plan/en/. [Accessed 10 Apr. 2018].
- [53] Wellcome trust files. Sustaining global action on AMR (2018). *Wellcome.ac.uk*. [online] Available at: <https://wellcome.ac.uk/sites/default/files/sustaining-global-action-on-antimicrobial-resistance.pdf> [Accessed 10 Apr. 2018].
- [54] Elanco. Jeff Simmons remarks to the Presidential Advisory Council on Combating Antibiotic-Resistant Bacteria. (2018). *Elanco.com*. [online] Available at: <https://www.elanco.com/news/> [Accessed 10 Apr. 2018].

- [55] Antibiotic resistance solutions initiative. Centers for disease control and prevention. (2018). *Cdc.gov*. What CDC is Doing: AR Solutions Initiative | Antibiotic/Antimicrobial Resistance | CDC. [online] Available at: <https://www.cdc.gov/drugresistance/solutions-initiative/index.html> [Accessed 10 Apr. 2018].
- [56] Barlam, T., Cosgrove, S., Abbo, L., MacDougall, C., Schuetz, A., Septimus, E., Srinivasan, A., Dellit, T., Falck-Ytter, Y., Fishman, N., Hamilton, C., Jenkins, T., Lipsett, P., Malani, P., May, L., Moran, G., Neuhauser, M., Newland, J., Ohl, C., Samore, M., Seo, S. and Trivedi, K. (2016). Executive Summary: Implementing an Antibiotic Stewardship Program: Guidelines by the Infectious Diseases Society of America and the Society for Healthcare Epidemiology of America. *Clinical Infectious Diseases*, 62(10), pp.1197-1202.
- [57] Messacar, K., Parker, S., Todd, J. and Dominguez, S. (2016). Implementation of Rapid Molecular Infectious Disease Diagnostics: the Role of Diagnostic and Antimicrobial Stewardship. *Journal of Clinical Microbiology*, 55(3), pp.715-723.
- [58] Tabah, A., Cotta, M., Garnacho-Montero, J., Schouten, J., Roberts, J., Lipman, J., Tacey, M., Timsit, J., Leone, M., Zahar, J. and De Waele, J. (2015). A Systematic Review of the Definitions, Determinants, and Clinical Outcomes of Antimicrobial De-escalation in the Intensive Care Unit. *Clinical Infectious Diseases*, 62(8), pp.1009-1017.
- [59] Kollef, M. and Micek, S. (2015). Editorial Commentary: Antimicrobial De-escalation: What's in a Name?. *Clinical Infectious Diseases*, 62(8), pp.1018-1020.
- [60] Doernberg, S. and Chambers, H. (2017). Antimicrobial Stewardship Approaches in the Intensive Care Unit. *Infectious Disease Clinics of North America*, 31(3), pp.513-534.
- [61] Bauer, K., Perez, K., Forrest, G. and Goff, D. (2014). Review of Rapid Diagnostic Tests Used by Antimicrobial Stewardship Programs. *Clinical Infectious Diseases*, 59(suppl_3), pp.S134-S145.
- [62] Goff, D., Kullar, R., Bauer, K. and File, T. (2017). Eight Habits of Highly Effective Antimicrobial Stewardship Programs to Meet the

- Joint Commission Standards for Hospitals. *Clinical Infectious Diseases*, 64(8), pp.1134-1139.
- [63] Daniel Markley, J., Bernard, S., Bearman, G. and Stevens, M. (2017). De-escalating Antibiotic Use in the Inpatient Setting: Strategies, Controversies, and Challenges. *Current Infectious Disease Reports*, 19(4).
- [64] Rapid Diagnostics Stopping Unnecessary Prescription (2015). *Amr-review.org*. [online] Available at: <https://amr-review.org/sites/default/files/Paper-Rapid-Diagnostics-Stopping-Unnecessary-Prescription-Low-Res.pdf> [Accessed 11 Apr. 2018].
- [65] PACCARB (2017). *Hhs.gov*. [online] Available at: <https://www.hhs.gov/sites/default/files/paccarb-final-incentives-report-sept-2017.pdf> [Accessed 11 Apr. 2018].
- [66] Woo PC, Chiu SS, Seto WH, Peiris M. (1997) Cost-effectiveness of rapid diagnosis of viral respiratory tract infections in pediatric patients. *Journal of Clinical Microbiology*. 35(6), pp.1579-1581.
- [67] Pai, N., Vadnais, C., Denkinger, C., Engel, N. and Pai, M. (2012). Point-of-Care Testing for Infectious Diseases: Diversity, Complexity, and Barriers in Low- And Middle-Income Countries. *PLoS Medicine*, 9(9), p.e1001306.
- [68] Price, C., St. John, A. and Hicks, J. (2004). Point-of-care testing. *Washington, DC: AACC Press*. ISBN 1-59425-012-X.
- [69] Price, C. (2001). Regular review: Point of care testing. *BMJ*, 322(7297), pp.1285-1288.
- [70] Bissonnette, L. and Bergeron, M. (2010). Diagnosing infections—current and anticipated technologies for point-of-care diagnostics and home-based testing. *Clinical Microbiology and Infection*, 16(8), pp.1044-1053.
- [71] Boehme, C., Nicol, M., Nabeta, P., Michael, J., Gotuzzo, E., Tahirli, R., Gler, M., Blakemore, R., Worodria, W., Gray, C., Huang, L., Caceres, T., Mehdiyev, R., Raymond, L., Whitelaw, A., Sagadevan, K., Alexander, H., Albert, H., Cobelens, F., Cox, H., Alland, D. and Perkins, M. (2011). Feasibility, diagnostic accuracy, and effectiveness

of decentralised use of the Xpert MTB/RIF test for diagnosis of tuberculosis and multidrug resistance: a multicentre implementation study. *The Lancet*, 377(9776), pp.1495-1505.

- [72] Hanafiah, K., Garcia, M. and Anderson, D. (2013). Point-of-care testing and the control of infectious diseases. *Biomarkers in Medicine*, 7(3), pp.333-347.
- [73] Bouricha, M., Samad, M., Levy, P., Raoult, D. and Drancourt, M. (2014). Point-of-Care Syndrome-Based, Rapid Diagnosis of Infections on Commercial Ships. *Journal of Travel Medicine*, 21(1), pp.12-16.
- [74] Holland, T., Woods, C. and Joyce, M. (2009). Antibacterial Susceptibility Testing in the Clinical Laboratory. *Infectious Disease Clinics of North America*, 23(4), pp.757-790.
- [75] American Thoracic Society. (2005). Guidelines for the Management of Adults with Hospital-acquired, Ventilator-associated, and Healthcare-associated Pneumonia. *American Journal of Respiratory and Critical Care Medicine*, 171(4), pp.388-416.
- [76] Kollef, M. (2008). Broad- Spectrum Antimicrobials and the Treatment of Serious Bacterial Infections: Getting It Right Up Front. *Clinical Infectious Diseases*, 47(S1), pp.S3-S13.
- [77] Morrell, M., Micek, S. and Kollef, M. (2009). The Management of Severe Sepsis and Septic Shock. *Infectious Disease Clinics of North America*, 23(3), pp.485-501.
- [78] Maurer, F., Christner, M., Hentschke, M. and Rohde, H. (2017). Advances in rapid identification and susceptibility testing of bacteria in the clinical microbiology laboratory: implications for patient care and antimicrobial stewardship programs. *Infectious Disease Reports*, 9(1).
- [79] Forbes, J., Knox, N., Ronholm, J., Pagotto, F. and Reimer, A. (2017). Metagenomics: The Next Culture-Independent Game Changer. *Frontiers in Microbiology*, 8.
- [80] Humphries, R. and Hindler, J. (2016). Emerging Resistance, New Antimicrobial Agents ... but No Tests! The Challenge of

- Antimicrobial Susceptibility Testing in the Current US Regulatory Landscape. *Clinical Infectious Diseases*, 63(1), pp.83-88.
- [81] Arena, F., Giani, T., Pollini, S., Viaggi, B., Pecile, P. and Rossolini, G. (2017). Molecular antibiogram in diagnostic clinical microbiology: advantages and challenges. *Future Microbiology*, 12(5), pp.361-364.
- [82] Li, Y., Yang, X. and Zhao, W. (2017). Emerging Microtechnologies and Automated Systems for Rapid Bacterial Identification and Antibiotic Susceptibility Testing. *SLAS TECHNOLOGY: Translating Life Sciences Innovation*, 22(6), pp.585-608.
- [83] Mandal, P., Biswas, A., Choi, K. and Pal, U. (2011). Methods for Rapid Detection of Foodborne Pathogens: An Overview. *American Journal of Food Technology*, 6(2), pp.87-102.
- [84] Zhao, X., Lin, C., Wang, J. and Oh, D. (2014). Advances in Rapid Detection Methods for Foodborne Pathogens. *Journal of Microbiology and Biotechnology*, 24(3), pp.297-312.
- [85] Lee, N., Kwon, K., Oh, S., Chang, H., Chun, H. and Choi, S. (2014). A Multiplex PCR Assay for Simultaneous Detection of *Escherichia coli* O157:H7, *Bacillus cereus*, *Vibrio parahaemolyticus*, *Salmonella* spp., *Listeria monocytogenes*, and *Staphylococcus aureus* in Korean Ready-to-Eat Food. *Foodborne Pathogens and Disease*, 11(7), pp.574-580.
- [86] Li, L., Mendis, N., Trigui, H., Oliver, J. and Faucher, S. (2014). The importance of the viable but non-culturable state in human bacterial pathogens. *Frontiers in Microbiology*, 5.
- [87] Wang, Y. and Salazar, J. (2015). Culture-Independent Rapid Detection Methods for Bacterial Pathogens and Toxins in Food Matrices. *Comprehensive Reviews in Food Science and Food Safety*, 15(1), pp.183-205.
- [88] Garibyan, L. and Avashia, N. (2013). Polymerase Chain Reaction. *Journal of Investigative Dermatology*, 133(3), pp.1-4.
- [89] Velusamy, V., Arshak, K., Korostynska, O., Oliwa, K. and Adley, C. (2010). An overview of foodborne pathogen detection: In the perspective of biosensors. *Biotechnology Advances*, 28(2), pp.232-254.

- [90] Pulido, M., Garcia-Quintanilla, M., Martin-Pena, R., Cisneros, J. and McConnell, M. (2013). Progress on the development of rapid methods for antimicrobial susceptibility testing. *Journal of Antimicrobial Chemotherapy*, 68(12), pp.2710-2717.
- [91] Diekema, D. and Pfaller, M. (2013). Rapid Detection of Antibiotic-Resistant Organism Carriage for Infection Prevention. *Clinical Infectious Diseases*, 56(11), pp.1614-1620.
- [92] Tenover, F., Canton, R., Kop, J., Chan, R., Ryan, J., Weir, F., Ruiz-Garbajosa, P., LaBombardi, V. and Persing, D. (2013). Detection of Colonization by Carbapenemase-Producing Gram-Negative Bacilli in Patients by Use of the Xpert MDRO Assay. *Journal of Clinical Microbiology*, 51(11), pp.3780-3787.
- [93] Nanosphere. Gram-negative Blood Culture (2018). [online] Available at: <http://www.nanosphere.us/product/gram-negative-blood-culture> [Accessed 10 Apr. 2018].
- [94] Curetis UNYVERO Pneumonia Application Guide (2018). [online] Available at: http://www.curetis.com/fileadmin/curetis/media/struktur/Products/Instructions/00118_Unyvero_Pneumonia_Application_Guide_V2_0.pdf [Accessed 11 Apr. 2018].
- [95] Blaschke, A., Heyrend, C., Byington, C., Fisher, M., Barker, E., Garrone, N., Thatcher, S., Pavia, A., Barney, T., Alger, G., Daly, J., Ririe, K., Ota, I. and Poritz, M. (2012). Rapid identification of pathogens from positive blood cultures by multiplex polymerase chain reaction using the FilmArray system. *Diagnostic Microbiology and Infectious Disease*, 74(4), pp.349-355.
- [96] Poritz, M., Blaschke, A., Byington, C., Meyers, L., Nilsson, K., Jones, D., Thatcher, S., Robbins, T., Lingenfelter, B., Amiott, E., Herbener, A., Daly, J., Dobrowolski, S., Teng, D. and Ririe, K. (2011). Correction: FilmArray, an Automated Nested Multiplex PCR System for Multi-Pathogen Detection: Development and Application to Respiratory Tract Infection. *PLoS ONE*, 6(11).
- [97] Fricker, M., Messelhauser, U., Busch, U., Scherer, S. and Ehling-Schulz, M. (2007). Diagnostic Real-Time PCR Assays for the

- Detection of Emetic *Bacillus cereus* Strains in Foods and Recent Food-Borne Outbreaks. *Applied and Environmental Microbiology*, 73(6), pp.1892-1898.
- [98] Maurer, J. (2011). Rapid Detection and Limitations of Molecular Techniques. *Annual Review of Food Science and Technology*, 2(1), pp.259-279.
- [99] Compton, J. (1991). Nucleic acid sequence-based amplification. *Nature*, 350(6313), pp.91-92.
- [100] Law, J., Ab Mutalib, N., Chan, K. and Lee, L. (2015). Rapid methods for the detection of foodborne bacterial pathogens: principles, applications, advantages and limitations. *Frontiers in Microbiology*, 5.
- [101] American Society for Microbiology (ASM). (2018). *Asm.org*. Multiplex White Paper: Clinical Utility of Multiplex Tests for Respiratory and Gastrointestinal Pathogens. [online] Available at: <https://www.asm.org/index.php/statements-and-testimony/item/6691-wp-multiplex> [Accessed 10 Apr. 2018].
- [102] Biswas, A., Kondaiah, N., Bheilegaonkar, K., Anjaneyulu, A., Mendiratta, S., Jana, C., Singh, H. and Kumar, R. (2008). Microbial profiles of frozen trimmings and silver sides prepared at Indian buffalo meat packing plants. *Meat Science*, 80(2), pp.418-422.
- [103] Vernozy-Rozand, C., Mazuy-Cruchaudet, C., Bavai, C. and Richard, Y. (2004). Comparison of three immunological methods for detecting staphylococcal enterotoxins from food. *Letters in Applied Microbiology*, 39(6), pp.490-494.
- [104] Zhang, G. (2013). Foodborne pathogenic bacteria detection: an evaluation of current and developing methods. *Meducator*, pp.1-15.
- [105] Yeni, F., Acar, S., Polat, Ö., Soyer, Y. and Alpas, H. (2014). Rapid and standardized methods for detection of foodborne pathogens and mycotoxins on fresh produce. *Food Control*, 40, pp.359-367.
- [106] Kumar, B., Raghunath, P., Devegowda, D., Deekshit, V., Venugopal, M., Karunasagar, I. and Karunasagar, I. (2011). Development of monoclonal antibody based sandwich ELISA for the rapid detection of pathogenic *Vibrio parahaemolyticus* in seafood. *International Journal of Food Microbiology*, 145(1), pp.244-249.

- [107] Bolton, F. J., Fritz, E., and Poynton, S. (2000). Rapid enzyme-linked immunoassay for the detection of Salmonella in food and feed products: performance testing program. *Journal of AOAC International*, 83, 299–304.
- [108] Glynn B., Lahiff S., Wernecke M., Barry T., Smith T. J., Maher M. (2006). Current and emerging molecular diagnostic technologies applicable to bacterial food safety. *International Journal of Dairy Technology*, 59(2), pp.126-139.
- [109] Ranjan, K., Minakshi, P. and Prasad, G. (2016). Application of Molecular and Serological Diagnostics in Veterinary Parasitology. *The Journal of Advances in Parasitology*, 2(4), pp.80-99.
- [110] Koczula, K. and Gallotta, A. (2016). Lateral flow assays. *Essays In Biochemistry*, 60(1), pp.111-120.
- [111] De Boer, S. and López, M. (2012). New Grower-Friendly Methods for Plant Pathogen Monitoring. *Annual Review of Phytopathology*, 50(1), pp.197-218.
- [112] Bohaychuk VM, Gensler GE, King R, Wu JT, McMullen LM. (2005). Evaluation of Detection Methods for Screening Meat and Poultry Products for the Presence of Foodborne Pathogens. *Journal of Food Protection*, 68(12), pp.2637-2647.
- [113] Chen, A. and Yang, S. (2015). Replacing antibodies with aptamers in lateral flow immunoassay. *Biosensors and Bioelectronics*, 71, pp.230-242.
- [114] Bahadır, E. and Sezgintürk, M. (2016). Lateral flow assays: Principles, designs and labels. *Trends in Analytical Chemistry*, 82, pp.286-306.
- [115] van Belkum, A. and Dunne, W. (2013). Next-Generation Antimicrobial Susceptibility Testing. *Journal of Clinical Microbiology*, 51(7), pp.2018-2024.
- [116] Perez, K., Olsen, R., Musick, W., Cernoch, P., Davis, J., Land, G., Peterson, L. and Musser, J. (2013). Integrating Rapid Pathogen Identification and Antimicrobial Stewardship Significantly Decreases Hospital Costs. *Archives of Pathology & Laboratory Medicine*, 137(9), pp.1247-1254.

- [117] Perez, K., Olsen, R., Musick, W., Cernoch, P., Davis, J., Peterson, L. and Musser, J. (2014). Integrating rapid diagnostics and antimicrobial stewardship improves outcomes in patients with antibiotic-resistant Gram-negative bacteremia. *Journal of Infection*, 69(3), pp.216-225.
- [118] Pusch, W., Flocco, M., Leung, S., Thiele, H., Kostrzewa, M. (2003). Mass spectrometry-based clinical proteomics. *Pharmacogenomics*, 4(4), pp.463-476.
- [119] Rushworth, J., Hirst, N., Goode, J., Pike, D., Ahmed, A. and Millner, P. (n.d.). Impedimetric biosensors for medical applications.
- [120] Ahmed, A., Rushworth, J., Hirst, N. and Millner, P. (2014). Biosensors for Whole-Cell Bacterial Detection. *Clinical Microbiology Reviews*, 27(3), pp.631-646.
- [121] McNaught, A., Wilkinson, A. and Jenkins, A. (2006). *IUPAC compendium of chemical terminology*. [Research Triangle Park, N.C.]: International Union of Pure and Applied Chemistry.
- [122] IUPAC, (1996). News and Market Update. Electrochemical biosensors: proposed definitions and classification. *Biosens. Bioelectron.* 11 (4), i-vi.
- [123] Shavanova, K., Bakakina, Y., Burkova, I., Shteplyuk, I., Viter, R., Ubelis, A., Beni, V., Starodub, N., Yakimova, R. and Khranovskyy, V. (2016). Application of 2D Non-Graphene Materials and 2D Oxide Nanostructures for Biosensing Technology. *Sensors*, 16(2), p.223.
- [124] Fan, X., White, I., Shopova, S., Zhu, H., Suter, J. and Sun, Y. (2008). Sensitive optical biosensors for unlabeled targets: A review. *Analytica Chimica Acta*, 620(1-2), pp.8-26.
- [125] Damborsky, P., vitel, J. and Katrlík, J. (2016). Optical biosensors. *Essays In Biochemistry*, 60(1), pp.91-100.
- [126] Mouffouk, F., Rosa da Costa, A., Martins, J., Zourob, M., Abu-Salah, K. and Alrokayan, S. (2011). Development of a highly sensitive bacteria detection assay using fluorescent pH-responsive polymeric micelles. *Biosensors and Bioelectronics*, 26(8), pp.3517-3523.
- [127] Cox, W. G., & Singer, V. L. (2004). Fluorescent DNA hybridization probe preparation using amine modification and reactive dye coupling, *BioTechniques* 36(1), pp.114-122.

- [128] Torun O, Boyaci IH, Temur E, Tamer U. (2012). Comparison of sensing strategies in SPR biosensor for rapid and sensitive enumeration of bacteria. *Biosens Bioelectron.* 37(1), pp.53–60.
- [129] Homola, J., Yee, S. S., Myszka, D.: Surface plasmon biosensors, in *Optical Biosensors: Today and Tomorrow*, editors F. S. Ligler, C. R. Taitt, *Elsevier*, (2008), s. 185-242.
- [130] Cheng Research Lab: Surface Plasmon Resonance Spectroscopy and Imaging. (2018). *Chenglab.ucr.edu*. [online] Available at: <http://chenglab.ucr.edu/spr.html> [Accessed 12 Apr. 2018].
- [131] Thévenot, D., Toth, K., Durst, R. and Wilson, G. (2001). Electrochemical biosensors: recommended definitions and classification1International Union of Pure and Applied Chemistry: Physical Chemistry Division, Commission I.7 (Biophysical Chemistry); Analytical Chemistry Division, Commission V.5 (Electroanalytical Chemistry).1. *Biosensors and Bioelectronics*, 16(1-2), pp.121-131.
- [132] Wan, Y., Zhang, D. and Hou, B. (2010). Selective and specific detection of sulfate-reducing bacteria using potentiometric stripping analysis. *Talanta*, 82(4), pp.1608-1611.
- [133] Korotchenkov, G. (2010). *Chemical sensors: fundamentals of sensor materials*. Vols 1-3. [New York, N.Y.] (222 East 46th Street, New York, NY 10017): Momentum Press.
- [134] Higson, S. (2012). *Biosensors for medical applications*. Oxford: Woodhead Pub.
- [135] Neufeld, T., Schwartz-Mittelmann, A., Biran, D., Ron, E. and Rishpon, J. (2003). Combined Phage Typing and Amperometric Detection of Released Enzymatic Activity for the Specific Identification and Quantification of Bacteria. *Analytical Chemistry*, 75(3), pp.580-585.
- [136] Qi, P., Wan, Y. and Zhang, D. (2013). Impedimetric biosensor based on cell-mediated bioimprinted films for bacterial detection. *Biosensors and Bioelectronics*, 39(1), pp.282-288.
- [137] Chan, K., Ye, W., Zhang, Y., Xiao, L., Leung, P., Li, Y. and Yang, M. (2013). Ultrasensitive detection of E. coli O157:H7 with biofunctional magnetic bead concentration via nanoporous membrane based

- electrochemical immunosensor. *Biosensors and Bioelectronics*, 41, pp.532-537.
- [138] Corcuera, IR De, & Cavalieri, RP (2003). *Biosensors EAFBE.pdf*. *Biosensor, Sensor*. [online] Available at: <https://www.scribd.com/document/334752457/Biosensors-EAFBE-pdf> [Accessed 11 Apr. 2018].
- [139] Benes, E., Groschl, M., Seifert, F. and Pohl, A. (1998). Comparison between BAW and SAW sensor principles. *IEEE Transactions on Ultrasonics, Ferroelectrics and Frequency Control*, 45(5), pp.1314-1330.
- [140] Sauerbrey, G. (1959) Use of quartz vibration for weighing thin films on a microbalance. *Physik Journal*, vol. 155, pp. 206–212.
- [141] Sauerbrey, G. (1959). Use of vibrating quartz for thin film weighing and microweighing (in German). *Z. Phys.*, 155, pp. 206 – 222
- [142] Latif, U., Can, S., Hayden, O., Grillberger, P. and Dickert, F. (2013). Sauerbrey and anti-Sauerbrey behavioral studies in QCM sensors—Detection of bioanalytes. *Sensors and Actuators B: Chemical*, 176, pp.825-830.
- [143] Casero, E., Vázquez, L., Parra-Alfambra, A. and Lorenzo, E. (2010). AFM, SECM and QCM as useful analytical tools in the characterization of enzyme-based bioanalytical platforms. *The Analyst*, 135(8), p.1878.
- [144] Pomorska, A., Shchukin, D., Hammond, R., Cooper, M., Grundmeier, G. and Johannsmann, D. (2010). Positive Frequency Shifts Observed Upon Adsorbing Micron-Sized Solid Objects to a Quartz Crystal Microbalance from the Liquid Phase. *Analytical Chemistry*, 82(6), pp.2237-2242.
- [145] Hirst, E., Yuan, Y., Xu, W. and Bronlund, J. (2008). Bond-rupture immunosensors—A review. *Biosensors and Bioelectronics*, 23(12), pp.1759-1768.
- [146] Ghosh, S., Ostanin, V. and Seshia, A. (2010). Anharmonic Interaction Signals for Acoustic Detection of Analyte. *Analytical Chemistry*, 82(9), pp.3929-3935.

- [147] Ghosh, S., Ostanin, V. and Seshia, A. (2011). Anharmonic Surface Interactions for Biomolecular Screening and Characterization. *Analytical Chemistry*, 83(2), pp.549-554.
- [148] Ghosh, S., Ostanin, V., Johnson, C., Lowe, C. and Seshia, A. (2011). Probing biomolecular interaction forces using an anharmonic acoustic technique for selective detection of bacterial spores. *Biosensors and Bioelectronics*, 29(1), pp.145-150.
- [149] Ghosh, S., Ostanin, V. and Seshia, A. (2013). Studying adsorbent dynamics on a quartz crystal resonator using its nonlinear electrical response. *Sensors and Actuators B: Chemical*, 176, pp.577-584.
- [150] Technical specifications on the harmonised monitoring and reporting of antimicrobial resistance in Salmonella, Campylobacter and indicator Escherichia coli and Enterococcus spp. bacteria transmitted through food. (2012). *EFSA Journal*, 10(6).
- [151] Tadesse, D., Zhao, S., Tong, E., Ayers, S., Singh, A., Bartholomew, M. and McDermott, P. (2012). Antimicrobial Drug Resistance in Escherichia coli from Humans and Food Animals, United States, 1950–2002. *Emerging Infectious Diseases*, 18(5), pp.741-749.
- [152] *E.coli: A Model Organism from Theodor Escherich's Legacy*. (2018). *Emlab.com*. [online] Available at: <https://www.emlab.com/resources/education/environmental-reporter/e-coli-a-model-organism-from-theodor-escherichs-legacy/> [Accessed 10 Apr. 2018].
- [153] Kanazawa, K.K. and Gordon, J.G. (1985). The oscillation frequency of a quartz resonator in contact with liquid. *Analytica Chimica Acta*, 175, pp.99-105.
- [154] Martin, S., Granstaff, V. and Frye, G. (1991). Characterization of a quartz crystal microbalance with simultaneous mass and liquid loading. *Analytical Chemistry*, 63(20), pp.2272-2281.
- [155] Shockley, W., Curran, D. and Koneval, D. (1967). Trapped-Energy Modes in Quartz Filter Crystals. *The Journal of the Acoustical Society of America*, 41(4B), pp.981-993.
- [156] Mortley, W. (1951). F.M.Q., *Wireless World*, 57, pp 399 – 403.

- [157] Mortley, W. (1957). Frequency-modulated quartz oscillators for broadcasting equipment. *Proceedings of the IEE - Part B: Radio and Electronic Engineering*, 104(15), pp.239-249.
- [158] Mortley, W. (1966). Priority in energy trapping. *Physics Today*, 19(12), pp.11-12.
- [159] Efimov, I., Hillman, A. and Walter Schultze, J. (2006). Sensitivity variation of the electrochemical quartz crystal microbalance in response to energy trapping. *Electrochimica Acta*, 51(12), pp.2572-2577.
- [160] Dulama, I., Cimpoca, G., Radulescu, C., Popescu, I., Bancuta, I., Cimpoca, M., Cernica, I. (2010) Analysis of liquids and viscoelastic films by quartz crystal microbalance, *Proceedings of the International Semiconductor Conference, CAS 1*, pp. 225-228.
- [161] Gooding, J. and Ciampi, S. (2011). The molecular level modification of surfaces: from self-assembled monolayers to complex molecular assemblies. *Chemical Society Reviews*, 40(5), p.2704.
- [162] Liedberg, B & Cooper, J. (1998). Bioanalytical applications of self-assembled monolayers. Immobilized biomolecules in analysis: A practical approach", (Eds: Cass, T. & Lieger, F.S.). Oxford University Press, pp. 55-78.
- [163] Bertilsson, L. and Liedberg, B. (1993). Infrared study of thiol monolayer assemblies on gold: preparation, characterization, and functionalization of mixed monolayers. *Langmuir*, 9(1), pp.141-149.
- [164] Ishida, T., Tsuneda, S., Nishida, N., Hara, M., Sasabe, H. and Knoll, W. (1997). Surface-Conditioning Effect of Gold Substrates on Octadecanethiol Self-Assembled Monolayer Growth. *Langmuir*, 13(17), pp.4638-4643.
- [165] Zhang, Y., Terrill, R. and Bohn, P. (1999). Ultraviolet Photochemistry and ex Situ Ozonolysis of Alkanethiol Self-Assembled Monolayers on Gold. *Chemistry of Materials*, 11(8), pp.2191-2198.
- [166] Tate, J., Rogers, J., Jones, C., Vyas, B., Murphy, D., Li, W., Bao, Z., Slusher, R., Dodabalapur, A. and Katz, H. (2000). Anodization and Microcontact Printing on Electroless Silver: Solution-Based

- Fabrication Procedures for Low-Voltage Electronic Systems with Organic Active Components. *Langmuir*, 16(14), pp.6054-6060.
- [167] Contact Angle of Water on Smooth Surfaces and Wettability. (2018). *Uskino.com. Contact Angle of Water on Smooth Surfaces and Wettability_USA KINO Industry Co., Ltd.* [online] Available at: <http://www.uskino.com/news/66.html> [Accessed 11 Apr. 2018].
- [168] Cognard, J. (1984). Adhesion to gold: A review. *Gold Bulletin*, 17(4), pp.131-139.
- [169] Alassi, A., Benammar, M. and Brett, D. (2017). Quartz Crystal Microbalance Electronic Interfacing Systems: A Review. *Sensors*, 17(12), p.2799.
- [170] Love, J., Estroff, L., Kriebel, J., Nuzzo, R. and Whitesides, G. (2005). Self-Assembled Monolayers of Thiolates on Metals as a Form of Nanotechnology. *ChemInform*, 36(32).
- [171] Tanaka, M., Hayashi, T. and Morita, S. (2013). The roles of water molecules at the biointerface of medical polymers. *Polymer Journal*, 45(7), pp.701-710.
- [172] Vericat, C., Vela, M., Benitez, G., Carro, P. and Salvarezza, R. (2010). Self-assembled monolayers of thiols and dithiols on gold: new challenges for a well-known system. *Chemical Society Reviews*, 39(5), p.1805.
- [173] González M., Bagatolli L., Echabe I., Arrondo J., Argaraña C., Cantor C. (1997). Interaction of Biotin with Streptavidin. *Journal of Biological Chemistry*, 272(17), pp.11288-11294.
- [174] Lazcka, O., Campo, F. and Muñoz, F. (2007). Pathogen detection: A perspective of traditional methods and biosensors. *Biosensors and Bioelectronics*, 22(7), pp.1205-1217.
- [175] Eaton, B., Gold, L. and Zichi, D. (1995). Let's get specific: the relationship between specificity and affinity. *Chemistry & Biology*, 2(10), pp.633-638.
- [176] Zichi, D., Eaton, B., Singer, B. and Gold, L. (2008). Proteomics and diagnostics: Let's Get Specific, again. *Current Opinion in Chemical Biology*, 12(1), pp.78-85.

- [177] Sharma, T. (2014). Nucleic Acid Aptamers as an Emerging Diagnostic Tool for Animal Pathogens. *Advances in Animal and Veterinary Sciences*, 2(1).
- [178] Ohuchi, S. (2012). Cell-SELEX Technology. *BioResearch Open Access*, 1(6), pp.265-272.
- [179] Sampson, T. (2003). Aptamers and SELEX: the technology. *World Patent Information*, 25(2), pp.123-129.
- [180] James W. (2000). (In: Mayers R A, editor). Aptamers. "Encyclopaedia of analytical chemistry", pp. 4848–71.
- [181] de-los-Santos-Álvarez, N., Lobo-Castañón, M., Miranda-Ordieres, A. and Tuñón-Blanco, P. (2008). Aptamers as recognition elements for label-free analytical devices. *TrAC Trends in Analytical Chemistry*, 27(5), pp.437-446.
- [182] Sun, H. and Zu, Y. (2015). A Highlight of Recent Advances in Aptamer Technology and Its Application. *Molecules*, 20(7), pp.11959-11980.
- [183] Proske, D., Blank, M., Buhmann, R. and Resch, A. (2005). Aptamers—basic research, drug development, and clinical applications. *Applied Microbiology and Biotechnology*, 69(4), pp.367-374.
- [184] Wilson, D. and Szostak, J. (1999). In Vitro Selection of Functional Nucleic Acids. *Annual Review of Biochemistry*, 68(1), pp.611-647.
- [185] Stoltenburg, R., Reinemann, C. and Strehlitz, B. (2007). SELEX—A (r)evolutionary method to generate high-affinity nucleic acid ligands. *Biomolecular Engineering*, 24(4), pp.381-403.
- [186] Ellington, A. and Szostak, J. (1990). In vitro selection of RNA molecules that bind specific ligands. *Nature*, 346(6287), pp.818-822.
- [187] Lato, S. (2002). Boron-containing aptamers to ATP. *Nucleic Acids Research*, 30(6), pp.1401-1407.
- [188] Kawakami, J., Imanaka, H., Yokota, Y. and Sugimoto, N. (2000). In vitro selection of aptamers that act with Zn²⁺. *Journal of Inorganic Biochemistry*, 82(1-4), pp.197-206.
- [189] Çalık, P., Balcı, O. and Özdamar, T. (2010). Human growth hormone-specific aptamer identification using improved oligonucleotide ligand

- evolution method. *Protein Expression and Purification*, 69(1), pp.21-28.
- [190] Stevenson, R., Baxter, H., Aitken, A., Brown, T. and Baxter, R. (2008). Binding of 14-3-3 proteins to a single stranded oligodeoxynucleotide aptamer. *Bioorganic Chemistry*, 36(5), pp.215-219.
- [191] Wochner, A., Menger, M., Orgel, D., Cech, B., Rimmelé, M., Erdmann, V. and Glökler, J. (2008). A DNA aptamer with high affinity and specificity for therapeutic anthracyclines. *Analytical Biochemistry*, 373(1), pp.34-42.
- [192] Yoshida, Y., Sakai, N., Masuda, H., Furuichi, M., Nishikawa, F., Nishikawa, S., Mizuno, H. and Waga, I. (2008). Rabbit antibody detection with RNA aptamers. *Analytical Biochemistry*, 375(2), pp.217-222.
- [193] Boiziau, C., Dausse, E., Yurchenko, L. and Toulmé, J. (1999). DNA Aptamers Selected Against the HIV-1trans-Activation-responsive RNA Element Form RNA-DNA Kissing Complexes. *Journal of Biological Chemistry*, 274(18), pp.12730-12737.
- [194] Cheng, C., Dong, J., Yao, L., Chen, A., Jia, R., Huan, L., Guo, J., Shu, Y. and Zhang, Z. (2008). Potent inhibition of human influenza H5N1 virus by oligonucleotides derived by SELEX. *Biochemical and Biophysical Research Communications*, 366(3), pp.670-674.
- [195] Gopinath, S. (2006). An RNA aptamer that distinguishes between closely related human influenza viruses and inhibits haemagglutinin-mediated membrane fusion. *Journal of General Virology*, 87(3), pp.479-487.
- [196] Patel, D., Suri, A., Jiang, F., Jiang, L., Fan, P., Kumar, R. and Nonin, S. (1997). Structure, recognition and adaptive binding in RNA aptamer complexes. *Journal of Molecular Biology*, 272(5), pp.645-664.
- [197] Potty, A., Kourentzi, K., Fang, H., Schuck, P. and Willson, R. (2011). Biophysical characterization of DNA and RNA aptamer interactions with hen egg lysozyme. *International Journal of Biological Macromolecules*, 48(3), pp.392-397.

- [198] Grosjean, H., Benne, R. (1998). Modification and Editing of RNA. *American Society for Microbiology*, Washington DC.
- [199] Orava, E., Cicmil, N. and Gariépy, J. (2010). Delivering cargoes into cancer cells using DNA aptamers targeting internalized surface portals. *Biochimica et Biophysica Acta (BBA) - Biomembranes*, 1798(12), pp.2190-2200.
- [200] de-los-Santos-Álvarez, N., Lobo-Castañón, M., Miranda-Ordieres, A. and Tuñón-Blanco, P. (2007). Modified-RNA Aptamer-Based Sensor for Competitive Impedimetric Assay of Neomycin B. *Journal of the American Chemical Society*, 129(13), pp.3808-3809.
- [201] Cui, Y., Ulrich, H. and Hess, G. (2004). Selection of 2'-Fluoro-modified RNA Aptamers for Alleviation of Cocaine and MK-801 Inhibition of the Nicotinic Acetylcholine Receptor. *The Journal of Membrane Biology*, 202(3), pp.137-149.
- [202] You, K., Lee, S., Im, A. and Lee, S. (2003). Aptamers as functional nucleic acids: In vitro selection and biotechnological applications. *Biotechnology and Bioprocess Engineering*, 8(2), pp.64-75.
- [203] Jayasena, S. (1999). Aptamers: An Emerging Class of Molecules That Rival Antibodies in Diagnostics. *Clinical Chemistry*, 45(9), pp. 1628-1650
- [204] Gopinath, S. and Kumar, P. (2013). Aptamers that bind to the hemagglutinin of the recent pandemic influenza virus H1N1 and efficiently inhibit agglutination. *Acta Biomaterialia*, 9(11), pp.8932-8941.
- [205] Cho, E., Lee, J. and Ellington, A. (2009). Applications of Aptamers as Sensors. *Annual Review of Analytical Chemistry*, 2(1), pp.241-264.
- [206] Famulok, M. (2002). Bringing picomolar protein detection into proximity. *Nature Biotechnology*, 20(5), pp.448-449.
- [207] Luzi, E., Minunni, M., Tombelli, S., Mascini, M. (2003). New trends in affinity sensing: aptamers for ligand binding. *Trends Anal. Chem.* 22(11), 810–818.

- [208] Geiger, A. (1996). RNA aptamers that bind L-arginine with sub-micromolar dissociation constants and high enantioselectivity. *Nucleic Acids Research*, 24(6), pp.1029-1036.
- [209] Haller, A. and Sarnow, P. (1997). In vitro selection of a 7-methyl-guanosine binding RNA that inhibits translation of capped mRNA molecules. *Proceedings of the National Academy of Sciences*, 94(16), pp.8521-8526.
- [210] Han, K., Liang, Z. and Zhou, N. (2010). Design Strategies for Aptamer-Based Biosensors. *Sensors*, 10(5), pp.4541-4557.
- [211] Dong, Y., Xu, Y., Yong, W., Chu, X. and Wang, D. (2014). Aptamer and Its Potential Applications for Food Safety. *Critical Reviews in Food Science and Nutrition*, 54(12), pp.1548-1561.
- [212] Santosh, B. and Yadava, P. (2014). Nucleic Acid Aptamers: Research Tools in Disease Diagnostics and Therapeutics. *BioMed Research International*, 2014, pp.1-13.
- [213] Wang, A. and Farokhzad, O. (2014). Current Progress of Aptamer-Based Molecular Imaging. *Journal of Nuclear Medicine*, 55(3), pp.353-356.
- [214] Wu, J., Zhu, Y., Xue, F., Mei, Z., Yao, L., Wang, X., Zheng, L., Liu, J., Liu, G., Peng, C. and Chen, W. (2014). Recent trends in SELEX technique and its application to food safety monitoring. *Microchimica Acta*, 181(5-6), pp.479-491.
- [215] Shen, Q., Xu, L., Zhao, L., Wu, D., Fan, Y., Zhou, Y., OuYang, W., Xu, X., Zhang, Z., Song, M., Lee, T., Garcia, M., Xiong, B., Hou, S., Tseng, H. and Fang, X. (2013). Specific Capture and Release of Circulating Tumor Cells Using Aptamer-Modified Nanosubstrates. *Advanced Materials*, 25(16), pp.2368-2373.
- [216] Bai, Y., Feng, F., Zhao, L., Wang, C., Wang, H., Tian, M., Qin, J., Duan, Y. and He, X. (2013). Aptamer/thrombin/aptamer-AuNPs sandwich enhanced surface plasmon resonance sensor for the detection of subnanomolar thrombin. *Biosensors and Bioelectronics*, 47, pp.265-270.

- [217] Tombelli, S., Minunni, M., Luzi, E. and Mascini, M. (2005). Aptamer-based biosensors for the detection of HIV-1 Tat protein. *Bioelectrochemistry*, 67(2), pp.135-141.
- [218] Bai, X., Hou, H., Zhang, B., Tang, J. (2014). Label-free detection of kanamycin using aptamer-based cantilever array sensor. *Biosens. Bioelectron.* 56, 112–116.
- [219] Yang Choon Lim, Kouzani, A., Wei Duan, Dai, X., Kaynak, A. and Mair, D. (2014). A Surface-Stress-Based Microcantilever Aptasensor. *IEEE Transactions on Biomedical Circuits and Systems*, 8(1), pp.15-24.
- [220] Song, S., Wang, L., Li, J., Fan, C. and Zhao, J. (2008). Aptamer-based biosensors. *Trends in Analytical Chemistry*, 27(2), pp.108-117.
- [221] Cui, Y., Ulrich, H. and Hess, G. (2004). Selection of 2'-Fluoro-modified RNA Aptamers for Alleviation of Cocaine and MK-801 Inhibition of the Nicotinic Acetylcholine Receptor. *The Journal of Membrane Biology*, 202(3), pp.137-149.
- [222] Peng, Z., Ling, M., Ning, Y. and Deng, L. (2014). Rapid Fluorescent Detection of Escherichia coli K88 Based on DNA Aptamer Library as Direct and Specific Reporter Combined With Immuno-Magnetic Separation. *Journal of Fluorescence*, 24(4), pp.1159-1168.
- [223] Li, H., Ding, X., Peng, Z., Deng, L., Wang, D., Chen, H. and He, Q. (2011). Aptamer selection for the detection of Escherichia coli K88. *Canadian Journal of Microbiology*, 57(6), pp.453-459.
- [224] Bruno, J., Carrillo, M. and Phillips, T. (2008). In Vitro antibacterial effects of antilipopolysaccharide DNA aptamer-C1qrs complexes. *Folia Microbiologica*, 53(4), pp.295-302.
- [225] Bruno, J., Carrillo, M., Phillips, T. and Andrews, C. (2010). A Novel Screening Method for Competitive FRET-Aptamers Applied to E. coli Assay Development. *Journal of Fluorescence*, 20(6), pp.1211-1223.
- [226] Savory, N., Nzakizwanayo, J., Abe, K., Yoshida, W., Ferri, S., Dedi, C., Jones, B. and Ikebukuro, K. (2014). Selection of DNA aptamers against uropathogenic Escherichia coli NSM59 by quantitative PCR controlled Cell-SELEX. *Journal of Microbiological Methods*, 104, pp.94-100.

- [227] Wu, W., Li, M., Wang, Y., Ouyang, H., Wang, L., Li, C., Cao, Y., Meng, Q. and Lu, J. (2012). Aptasensors for rapid detection of *Escherichia coli* O157:H7 and *Salmonella typhimurium*. *Nanoscale Research Letters*, 7(1), p.658.
- [228] Hong, K. and Sooter, L. (2015). Single-Stranded DNA Aptamers against Pathogens and Toxins: Identification and Biosensing Applications. *BioMed Research International*, 2015, pp.1-31.
- [229] Cao, X., Li, S., Chen, L., Ding, H., Xu, H., Huang, Y., Li, J., Liu, N., Cao, W., Zhu, Y., Shen, B. and Shao, N. (2009). Combining use of a panel of ssDNA aptamers in the detection of *Staphylococcus aureus*. *Nucleic Acids Research*, 37(14), pp.4621-4628.
- [230] Kim, Y., Song, M., Jurng, J. and Kim, B. (2013). Isolation and characterization of DNA aptamers against *Escherichia coli* using a bacterial cell–systematic evolution of ligands by exponential enrichment approach. *Analytical Biochemistry*, 436(1), pp.22-28.
- [231] Olsen, E., Pathirana, S., Samoylov, A., Barbaree, J., Chin, B., Neely, W. and Vodyanoy, V. (2003). Specific and selective biosensor for *Salmonella* and its detection in the environment. *Journal of Microbiological Methods*, 53(2), pp.273-285.
- [232] Pomorska, A., Shchukin, D., Hammond, R., Cooper, M., Grundmeier, G. and Johannsmann, D. (2010). Positive Frequency Shifts Observed Upon Adsorbing Micron-Sized Solid Objects to a Quartz Crystal Microbalance from the Liquid Phase. *Analytical Chemistry*, 82(6), pp.2237-2242.
- [233] Edvardsson, M., Rodahl, M., Kasemo, B. and Höök, F. (2005). A Dual-Frequency QCM-D Setup Operating at Elevated Oscillation Amplitudes. *Analytical Chemistry*, 77(15), pp.4918-4926.
- [234] Johannsmann, D. and Heim, L. (2006). A simple equation predicting the amplitude of motion of quartz crystal resonators. *Journal of Applied Physics*, 100(9), p.094505.
- [235] Leenaars, M. and Hendriksen, C. (2005). Critical Steps in the Production of Polyclonal and Monoclonal Antibodies: Evaluation and Recommendations. *ILAR Journal*, 46(3), pp.269-279.

- [236] Ricci, F., Volpe, G., Micheli, L. and Palleschi, G. (2007). A review on novel developments and applications of immunosensors in food analysis. *Analytica Chimica Acta*, 605(2), pp.111-129.
- [237] Hegner, M., Wagner, P. and Semenza, G. (1993). Immobilizing DNA on gold via thiol modification for atomic force microscopy imaging in buffer solutions. *FEBS Letters*, 336(3), pp.452-456.
- [238] Walter, J., Kökpinar, O., Friehs, K., Stahl, F. and Scheper, T. (2008). Systematic Investigation of Optimal Aptamer Immobilization for Protein–Microarray Applications. *Analytical Chemistry*, 80(19), pp.7372-7378.
- [239] Urmann, K., Modrejewski, J., Scheper, T. and Walter, J. (2016). Aptamer-modified nanomaterials: principles and applications. *BioNanoMaterials*, 18(1-2).
- [240] Ni, S., Yao, H., Wang, L., Lu, J., Jiang, F., Lu, A. and Zhang, G. (2017). Chemical Modifications of Nucleic Acid Aptamers for Therapeutic Purposes. *International Journal of Molecular Sciences*, 18(8), p.1683.
- [241] Nucleic acid aptamers. (2018). *Atdbio.com*. [online] Available at: <https://www.atdbio.com/content/61/Nucleic-acid-aptamers> [Accessed 12 Apr. 2018].
- [242] Dultsev, F. and Kolosovsky, E. (2014). Forces affecting nanoparticles in fluid, and the shape of the acoustic signal accompanying particle detachment from QCM surface. *Sensors and Actuators B: Chemical*, 202, pp.454-460.
- [243] Albrecht, C. (2003). DNA: A Programmable Force Sensor. *Science*, 301(5631), pp.367-370.
- [244] Wang, X. and Ha, T. (2013). Defining Single Molecular Forces Required to Activate Integrin and Notch Signaling. *Science*, 340(6135), pp.991-994.
- [245] Mosayebi, M., Louis, A.A., Doye, J.P., Ouldrige, T.E. (2015). Force-Induced Rupture of a DNA Duplex: From Fundamentals to Force Sensors. *ACS Nano*, 9(12), pp.11993-12003.
- [246] Bilibana, M., Citartan, M., Yeoh, T., Rozhdestvensky, T. and Tang, T. (2017). Aptamers as the Agent in Decontamination Assays (Apta-

Decontamination Assays): From the Environment to the Potential Application In Vivo. *Journal of Nucleic Acids*, 2017, pp.1-12.

- [247] Vasan, A. (2013). Point-of-care biosensor system. *Frontiers in Bioscience*, S5(1), pp.39-71.
- [248] Yao, C., Zhu, T., Qi, Y., Zhao, Y., Xia, H. and Fu, W. (2010). Development of a Quartz Crystal Microbalance Biosensor with Aptamers as Bio-recognition Element. *Sensors*, 10(6), pp.5859-5871.